UNIVERSITÀ
DEGLI STUDI
FIRENZE

DOTTORATO DI RICERCA IN
SCIENZE AGRARIE E AMBIENTALI

CICLO XXIX

COORDINATORE Prof. Simone Orlandini

# Anti-infective environmentally friendly molecules against plant pathogenic Gram-negative bacteria

Settore Scientifico Disciplinare AGR/12


**Dottoranda**
Dott.ssa Biancalani Carola

**Tutore**
Prof.ssa Tegli Stefania

**Co-tutore**
Prof. Biricolti Stefano

**Coordinatore**
Prof. Orlandini Simone


Anni 2013/2016

**PhD coordinator:**
Prof. Simone Orlandini

Università degli Studi di Firenze
Dipartimento di Scienze delle produzioni Agroalimentari e dell'Ambiente (DISPAA)
Sez-Agronomia e coltivazioni erbacee
Piazzale delle Cascine, 18 50144 Firenze

**Tutor:**
Prof.ssa Stefania Tegli

Università degli Studi di Firenze
Dipartimento di Scienze delle produzioni Agroalimentari e dell'Ambiente (DISPAA)
Sez-Patologia vegetale
Via della Lastruccia, 10 50019 Sesto Fiorentino

**Co-tutor:**
Prof. Stefano Biricolti

Università degli Studi di Firenze
Dipartimento di Scienze delle produzioni Agroalimentari e dell'Ambiente (DISPAA)
Sez- Arboricoltura generale e coltivazioni arboree
Viale delle Idee, 30 50019 Sesto Fiorentino

## Work concerning the topics of the Thesis:

### *Papers:*

Biancalani C, Cerboneschi M, Tadini-Buoninsegni F, Campo M, Scardigli A, Romani A, Tegli S. (2016) Global Analysis of Type Three Secretion System and Quorum Sensing Inhibition of *Pseudomonas savastanoi* by Polyphenols Extracts from Vegetable Residues. *PLoS ONE* 11(9): e0163357. doi:10.1371/journal.pone.0163357

Cerboneschi M, Decorosi F, Biancalani C, Ortenzi MV, Macconi S, Giovannetti L, Viti C, Campanella B, Onor M, Bramanti E, Tegli S. (2016) Indole-3-acetic acid in plant-pathogen interactions: a key molecule for *in planta* bacterial virulence and fitness. *Res Microbiol*. doi: 10.1016/j.resmic.2016.09.002

### *Oral presentations in national and international conferences:*

Biancalani C, Cerboneschi M, Macconi S, Moncelli MR, Smeazzetto S, Biricolti S, Bogani P, Tegli S. "Peptides as inhibitors of Type Three Secretion System for eco-friendly control of bacterial diseases of plants". National Congress Italian Society for Plant Pathology Pisa, 22-24 September 2014.

Tegli S, Cerboneschi M, Biancalani C, Macconi S, Tadini-BuoninsegniF, Sacconi A, Smeazzetto S, Moncelli MR, Bogani P, Biricolti S. "Virulence inhibiting peptides for the environmentally friendly control of plant diseases caused by *Pseudomonas syringae"*. 9th International Conference on *Pseudomonas syringae* and Related Pathogens Malaga, 2-5 June 2015.

Cerboneschi M, Biancalani C, Ortenzi MV, Macconi S, Bogani P, Biricolti S, Smeazzetto S, Tadini-Buoninsegni F, Moncelli MR, Tegli S. "Virulence inhibiting peptides: an environmentally friendly and effective alternative to copper for the control of plant pathogenic bacteria". 4th International workshop on Expression, Structure, and Function of Membrane Protein. Florence, 28June-2July, 2015.

### *Poster presentations in national and international conferences:*

Cerboneschi M, Maiullari S, Biancalani C, Bogani P, Tegli S, Biricolti S. "Transgenic transient expression as a tool to assess the efficacy of short peptides to control bacterial diseases". National Congress Italian Society for Plant Pathology Pisa, 22-24 September 2014.

Biancalani C, Macconi S, Ortenzi MV, Cerboneschi M, Campo M, Pinelli P, Romani A, Tegli S. "Epigallocatechin gallate and other polyphenols extracts from plants biomass for environment-friendly control of *Pseudomonas syringae* diseases". 9th International Conference on *Pseudomonas syringae* and Related Pathogens Malaga, 2-5 June 2015.

Cerboneschi M, Bogani P, Biricolti S, Biancalani C, Macconi S, Ortenzi MV, Tegli S. "Over-expression of virulence inhibiting peptides in *Nicotiana tabacum* plants as a tool to control *P. syringae* pv. *tabaci* ". 9th International Conference on *Pseudomonas syringae* and Related Pathogens Malaga, 2-5 June 2015.

Cerboneschi M, Decorosi F, Biancalani C, Ortenzi MV, Macconi S, Viti C, Giovannetti L, Tegli S. "Indole-3-acetic acid production by *Pseudomonas savastanoi* and its involvement in resistance to plant toxic compounds". Phenotype MicroArray Analysis in Cells. Florence, September 10-12, 2015.

Romani A, Campo M, Scardigli A, Biancalani C, Cerboneschi M, Tegli S. "Natural standardized polyphenolic fractions for innovative green formulations in agronomics." XXVIIIth International Conference on Polyphenols Vienna, July11-15, 2016.

### *Drafting of the final manual for the LIFE project AFTER Cu - LIFE12 ENV/IT/000336*

Tegli S, Cerboneschi M, Biancalani C. (2016) "Innovazione nella difesa delle colture da batteri fitopatogeni" DISPAA-University of Florence.

## Work concerning related topics:

Macconi S, Sereni E, Calistri E, Biancalani C, Cerboneschi M, Biricolti S, Bogani P, Tegli S. "*Nicotiana langsdorffii* transgenic plants with modified hormonal metabolism as model system for the study of phytopatogenic bacteria-plants interaction." National Congress Italian Society for Plant Pathology Pisa, 22-24 September 2014.

Macconi S, Bogani P, Ortenzi MV, Biancalani C, Cerboneschi M, Biricolti S, Tegli S. "Far beyond HopQ1 in the interaction between *Nicotiana spp*. and *Pseudomonas syringae sensu lato*." 9th International Conference on *Pseudomonas syringae* and Related Pathogens Malaga, 2-5 June 2015.

Bracalini M, Cerboneschi M, Croci F, Panzavolta T, Tiberi R, Biancalani C, Macconi S, Tegli S. (2015) "Alian pest molecular diagnostics: can DNA traces be exploited to assess the damage caused by the western conifer seed bug on stone pine fructification? *Bulletin of Insectology*, vol.68, pp 51-60, ISSN:1721-8861.

# TABLE OF CONTENTS

## Riassunto

**Parole chiave:** batteri Gram-negativi, malattie delle piante, estratti polifenolici, peptidi anti-virulenza, peptidi anti-microbici, Sistema di Secrezione di Tipo III, proteina HrpA, Quorum Sensing, pompe di efflusso.

**Obiettivi:** Analizzare possibili alternative ecocompatibili rispetto a quelle attualmente disponibili da applicare nella lotta alle malattie delle piante causate da batteri fitopatogeni Gram-negativi. Lo studio è articolato in modo da perseguire i seguenti obiettivi principali: I) analizzare i sistemi di patogenicità e virulenza dei batteri fitopatogeni Gram-negativi come il Sistema di Secrezione di Tipo III (TTSS) e in particolare la proteina strutturale del pilus HrpA, quali bersagli ideali contro i quali allestire molecole in grado di bloccare la patogenicità/virulenza di tali batteri senza interferire con la loro vitalità; II) verificare l'efficacia *in vitro* and *in vivo* di potenziali molecole anti-infettive, quali piccoli oligopeptidi ed estratti vegetali ad alto contenuto in polifenoli ottenuti in un contesto di economia circolare, nel limitare o bloccare lo sviluppo dei sintomi legati a malattie delle piante ad eziologia batterica; infine, come obiettivo futuro è stato posto quello di analizzare una possibile correlazione fra sistemi di virulenza, fitness e pompe implicate nell'efflusso di composti xenobiotici nei batteri fitopatogeni per individuare bersagli, ancora poco esplorati, contro i quali allestire molecole innovative.

**Metodi e risultati:** La ricerca è stata effettuata utilizzando come sistemi modelli batteri appartenenti al gruppo di *Pseudomonas syringae* quali; *P. savastanoi* pv.*nerii* (*Psn*), *P. syringae* pv.*tabaci* (*Ptab*) e pv.*actinidiae* (*Psa*) insieme alle relative piante ospiti *Nerium oleander, Nicotiana tabacum* and *Actinidia chinensis.* La prima fase della ricerca ha permesso di rilevare la presenza di un "punto debole" nel pilus del Sistema di Secrezione di Tipo III dove poter disegnare e progettare oligopeptidi in grado di bloccare la formazione di questo condotto indispensabile nei batteri Gram-negativi per espletare la loro azione di patogenicità e virulenza. Il "punto debole" di tale condotto è stato identificato nella proteina strutturale del pilus denominata HrpA dei batteri appartenenti al gruppo di *P. syringae,* i cui monomeri interagiscono gli uni con gli altri attraverso interazioni di tipo coiled-coils. Dalle analisi *in silico* attraverso specifici strumenti bioinformatici è stato possibile evidenziare in posizione C-terminale della proteina HrpA la presenza di amminoacidi fondamentali per l'instaurarsi di tali interazioni e la loro importanza è stata confermata da prove di mutagenesi sito-specifica, dove è stato rilevato un fenotipo non patogeno o ipovirulento dei mutanti batterici allestiti. Un protocollo per la sintesi biotecnologica della proteina HrpA è stato messo a punto su scala di laboratorio ed utilizzato nella fase di scale-up per la produzione dell'anticorpo primario utilizzato nei saggi immunoenzimatici appositamente allestiti. Sulla base di questi primi risultati sono stati progettati una serie di piccoli oligopeptidi (17-27 amminoacidi) in grado di impedire il legame fra i singoli monomeri della proteina HrpA, impedendone di fatto l'assemblaggio del pilus stesso. L'assenza di un effetto fitotossico aspecifico così come la capacità di inibire la risposta ipersensibile (HR) da parte di questi oligopeptidi sono state preventivamente accertate mediante infiltrazioni artificiali su foglie di Tabacco. L'assenza di un effetto battericida è stato valutato attraverso misure spettrofotometriche del batterio in coltura liquida addizionato a concentrazioni calibrate dell'oligopeptide. Infine, la specificità

di azione di tali oligopeptidi diretta contro il TTSS è stata analizzata e confermata attraverso saggi molecolari *in vitro* basati su misure di fluorescenza mediante l'utilizzo di batteri trasformati con vettori contenenti il gene reporter per la *green fluorescent protein* (*gfp*), saggio di colorazione con il Congo red e allestimento di mutanti "auto-produttori" in grado di sintetizzare in maniera endogena l'oligopeptide. L'efficacia di tali molecole nel ridurre o sopprimere lo sviluppo della malattia è stata accertata *in vivo* attraverso la produzione di piante in grado di esprimere in maniera transiente l'oligopeptide ed infine saggi di patogenicità su piante ospiti. Il peptide con maggior attività anti-infettiva, denominato AP17, è stato inserito all'interno del vettore d'espressione pCAMBIA1305.2 e per il tramite di *Agrobacterium tumefaciens* veicolato a livello dell'apoplasto della cellula vegetale di *N.tabacum* come confermato dal saggio istochimico GUS (attività β-glucuronidasica). Tali piante transgeniche infettate con *P. syringae* pv. *tabaci* si sono rivelate molto più resistenti rispetto alle piante di controllo. Saggi *in vitro* ed *in vivo* sono stati effettuati anche con il peptide denominato Psa21, progettato e disegnato sul dominio coiled-coil identificato nella sequenza amminoacidica della proteina HrpA di *Psa*, con risultati positivi. Un protocollo di trasformazione genetica su piante generalmente recalcitanti alla trasformazione come quelle legnose/arboree è stato sviluppato sulla varietà di kiwi Hayward trasformate con il peptide Psa21. Con lo stesso approccio adottato per gli oligopeptidi è stata valutata l'attività anti-infettiva ed esclusa un'attività antimicrobica di estratti polifenolici prototipati ottenuti da residui vegetali di *Olea europaea, Vitis vinifera* e *Cynara scolymus* in un contesto di economia circolare. Attraverso saggi appositamente progettati quali Congo red, ELISA e analisi di espressione genica mediante real time PCR è stato possibile evidenziare come tali estratti esercitino un'azione inibitoria altamente specifica nei confronti del TTSS e parziale nei confronti del Quorum Sensing. La loro efficacia nel contrastare lo sviluppo della malattia è stata valutata attraverso inoculazioni artificiali su sezioni di piante adulte. Infine, l'assenza di tossicità a livello delle membrane cellulari così come a livello di bersagli subcellulari universalmente presenti in organismi e microrganismi (come la pompa $Ca^{2+}$-ATPase) è stata dimostrata attraverso specifiche analisi bioelettrochimiche.

C**onclusioni:** Lo studio bioinformatico condotto sulla proteina HrpA di *P. syringae* ha permesso di rilevare la presenza di un motivo coiled-coil rilevatosi fondamentale per l'assemblaggio del pilus del TTSS nei batteri utilizzati come sistemi modello nella presente ricerca quali *P. savastanoi* pv. *nerii*, *P. syringae* pv. *tabaci* e pv. *actinidiae*. Su queste regioni sono stati progettati dei piccoli oligopeptidi in grado di ostacolare l'assemblaggio del pilus e dunque la patogenicità e virulenza di tali batteri sulle relative piante ospiti. L'efficacia anti-infettiva dei peptidi e degli estratti polifenolici verificata *in vitro* e *in vivo* sui sistemi modello utilizzati nella presente tesi di dottorato, insieme al carattere ecocompatibile e all'assenza di tossicità, depone fortemente a favore di una possibile applicazione di tali molecole nel settore fitoiatrico. La loro specificità di azione diretta contro sistemi non deputati alla vitalità batterica e conservati fra i patogeni Gram-negativi, non solo di piante ma anche di umani e animali, fa presupporre una scarsa se non assente pressione selettiva nella popolazione batterica garantendo una loro efficacia a più lungo termine.

**Significato ed impatto dello studio:** La globalizzazione dei mercati agroalimentari da una parte insieme ai cambiamenti climatici in atto stanno contribuendo in maniera sostanziale alla

possibile e rapida diffusione di fitopatogeni alieni ed invasivi in aree dalle quali finora erano assenti, oppure aggravando l'incidenza e la severità di quelli endemici, contribuendo in maniera sostanziale ad aumentare le possibili minacce per il settore agricolo. Del resto la scarsa disponibilità di efficaci presidi fitosanitari alternativi ai composti rameici, i cui effetti negativi sia sulla salute umana che sulla salvaguardia ambientale da troppo tempo trascurati, insieme alla necessità di adeguamento alla legislazione Europea, ha portato gli operatori nel settore fitoiatrico a riflettere sulla urgente necessità di mettere in atto una rivoluzione culturale nella quale sono richiesti importanti sforzi di innovazione. È proprio in questo contesto che il lavoro svolto nella presente tesi di dottorato apre delle prospettive significative di lotta verso i batteri Gram-negativi ed in particolare del genere *Pseudomonas* agenti di malattie di numerose specie di interesse agrario, che meritano di essere ulteriormente approfondite.

## Summary

**Key words:** Gram-negative bacteria, plant diseases, polyphenolic extracts, anti-virulence peptides, anti-microbial peptides, Type Three Secretion System, HrpA protein, Quorum Sensing, efflux pumps.

**Objectives:** Analysing environmentally friendly alternatives that could be applied in plant disease control caused by phytopathogenic Gram-negative bacteria. The study was carried out in order to achieve the following main aims: I) analysing pathogenic and virulence systems of phytopathogenic Gram-negative bacteria such as the Type Three Secretion System (TTSS), and in particular the main structural protein of TTSS pilus, *i.e.* "HrpA", in order to design molecules able to block the pathogenicity and virulence of these bacteria without undermining their viability; II) verifying the *in vitro* and *in vivo* efficacy of anti-infective molecules, such as small oligopeptides and polyphenolic extracts obtained in a circular economy framework, to reduce or to block symptoms development caused by plant pathogenic bacteria; finally, as a future objective to analyse a possible correlation among virulence systems, fitness and efflux pumps related to xenobiotic compounds extrusion in phytopathogenic bacteria, in order to identify underdeveloped targets, against which innovative molecules can be designed.

**Methods and Results:** The research was carried out with bacteria model systems belonging to *P. syringae* complex, such as *P. savastanoi* pv. *nerii* (*Psn*), *P. syringae* pv. *tabaci* (*Ptab*) *and* pv. *actinidiae (Psa)* together with the corresponding host plants *Nerium oleander, Nicotiana tabacum* and *Actinidia chinensis.* First of all, we have identified a "weak point" in TTSS pilus, which represents a pivotal device for pathogenicity and virulence of Gram-negative plant bacteria. This "weak point" was identified with the main structural protein called "HrpA" in bacteria belonging to *P. syringae* complex, whose monomers are linked through coiled-coil interactions. The *in silico* analysis, performed with specific bioinformatic tools, has identified in C-terminus portion of the HrpA protein several fundamental amino acids for coiled-coil interactions. Their essential role was confirmed by site-directed mutagenesis experiments, where a non pathogenic or ipovirulent phenotype of bacterial mutants was detected. An experimental protocol for the biotechnological synthesis of the HrpA protein was set up and then used in a scale-up phase for primary antibody production employed in immunoenzymatic assays. Based on these results a set of small oligopeptides (17-27 amino acids) were designed to prevent the TTSS pilus assembly. The absence of any phytotoxic effect as well as the ability to inhibit the hypersensitive response (HR) of these peptides were previously evaluated through artificial infiltration into mesophyll of tobacco leaves. The absence of any antibiotic activity was verified by spectrophotometric measurements of bacterial liquid cultures mixed with known concentrations of these peptides. Finally, the specific action of these peptides against TTSS was analysed and confirmed by *in vitro* molecular assays based on spectrophotometric measurements on transformed bacteria with vectors expressing the reporter gene for the *green fluorescent protein* (*gfp*), Congo red assay, and bacterial mutants able to endogenously synthesise these peptides. The efficacy of these molecules to reduce or abolish symptom development was evaluated *in vivo* through their transgenic transient expression directly in plants and by pathogenicity tests on host

plants. The peptide with the highest anti-infective activity, *i.e.* AP17, was cloned in the binary vector pCAMBIA 1305.2 and delivered by *A. tumefaciens* into the apoplastic space of *N. tabacum* plant cells as confirmed by GUS histochemical assay. These transgenic plants, after inoculation with *P. syringae* pv. *tabaci*, were more resistant than control plants. *In vivo* and *in vitro* assays were performed with the peptide Psa21, designed on coiled-coil motif of HrpA protein of *Psa*, with positive results. An experimental protocol for transgenic plants, which are usually refractory to genetic transformation such as woody plants, was developed on kiwi Hayward transformed with Psa21 peptide. Using the same approach adopted for the oligopeptides, the anti-infective activity was evaluated and the antibacterial activity was excluded for standardized polyphenolic extracts obtained from vegetable wastes of *Olea europaea*, *Vitis vinifera* and *Cynara scolymus*. These extracts specifically inhibit the TTSS and partially the Quorum Sensing as highlighted by specific assays such as Congo red dye absorption, ELISA, expression gene by real time PCR. Their effectiveness against disease development was verified by artificial inoculations on adult plants. Finally, the absence of any toxicity against the cell membranes as well as subcellular targets conserved both in organisms and microorganisms (*e.g.* $Ca^{2+}$-ATPase) was demonstrated by specific bioelectrochemical tests.

**Conclusions:** The bioinformatic analysis performed on the HrpA protein of bacteria belonging to *P. syringae* complex has detected a coiled-coil domain in its C-terminus portion. These motifs were essential for TTSS pilus assembly in bacteria used as model systems, such as *P. savastanoi* pv. *nerii*, *P. syringae* pv. *tabaci* and *P. syringae* pv. *actinidiae*. Using these regions a set of small peptides were designed to prevent pilus assembly, and to disarm the pathogenicity and virulence of such bacteria. The anti-infective activity of these peptides as well as of the polyphenolic extracts, verified *in vitro* and *in vivo* on model systems, together with the ecofriendly aspect and the absence of toxicity, support their possible application in plant protection. Their specific activity against systems not related to bacterial viability and conserved among Gram-negative pathogens, not only of plants but also of humans and animals, suggests that a poor or absent selective pressure may develop in the bacterial population, thus providing a longer efficacy.

**Significance and Impact of the Study:** The market globalisation and the climate change are contributing substantially to the possible and rapid spread of alien and invasive plant pathogens in areas where they were previously absent, or are intensifying the incidence and severity of endemic pathogens, thus contributing significantly to increase the possible threats to the agricultural sector. Moreover, the lack of effective alternative molecules to copper compounds in plant protection, whose negative effects on both human health and environmental protection, have been neglected for far too long, and the need to adapt to European legislation, have led the operators in plant protection sector to reflect about the urgent need to implement a cultural revolution in which major innovation efforts are required. In the scenario described above the work performed in this PhD thesis suggests significant perspectives in plant disease protection against Gram-negative bacteria and in particular of bacteria belonging to *Pseudomonas* genus, acting as pathogenic agents of a large number of important agronomic species, which deserve to be further investigated.

**Abstract**

The control and management of bacterial diseases of plants still rely mainly on applications of copper salts and antibiotics, the latter not allowed in European Member States. Moreover, copper-based treatments against phytopathogenic bacteria are also strictly regulated and temporarily limited within European Union. Heavy negative effects have been reported following copper applications, both on different ecosystems and several biological processes.

In this PhD thesis, the anti-infective activity of small peptides and polyphenolic extracts has been verified using as model systems bacteria belonging to *P. syringae* complex such as *P. savastanoi* pv. *nerii*, *P. syringae* pv. *tabaci* and *P. syringae* pv. *actinidiae* together with their corresponding host plants *Nerium oleander, Nicotiana tabacum* and *Actinidia chinensis.*

Some of these molecules inhibit specifically the Type Three Secretion System (TTSS) and partially the Quorum Sensing (QS), without undermining bacterial viability and without any toxic effect. Additionally, the secondary structure of the putative HrpA protein, the main component of the TTSS translocating pilus in phytopathogenic bacteria belonging to the *P. syringae* group was also examined. In particular, it was shown that C-terminus portion of HrpA protein is characterised by a coiled-coil motif essential for TTSS pilus assembly.

The work performed in this PhD thesis is presented and organised in six chapters. Chapter 1 provides a brief overview of bacterial virulence mechanisms belonging to *P. syringae* group and of alternative strategies to control bacterial plant disease, including a short focus on advantages and disadvantages of antimicrobial peptides and drawbacks of copper treatments. In chapter 2, the design and development of anti-virulence peptides are addressed together with the study of the HrpA protein. Moreover, the *in vivo* and *in vitro* efficacy of anti-virulence peptides to inhibit the development of *P. syringae* disease is verified. In chapter 3, the role of *Nicotiana tabacum* transgenic plants expressing the anti-virulence peptides as a tool to assess the peptides' efficacy to confer resistance towards *P. syringae* pv. *tabaci* is investigated. In chapter 4, polyphenolic extracts from vegetable no food/feed residues of typical Mediterranean crops are obtained and their inhibitory activity on TTSS and QS of *P. savastanoi* pv. *nerii* is also assessed. In chapter 5, the functional links between IAA (indol-3-acetic acid) metabolism, TTSS and drug efflux pumps in *P. savastanoi* pv. *nerii* are analysed in order to obtain information and to identify new ideal targets that could be useful in the near future for the development of alternative strategies for the control of plant pathogenic bacteria. Finally, chapter 6 provides an overall concluding discussion about the results obtained in this PhD thesis.

# *Chapter 1*

# General Introduction

## 1.1 Plant bacteria diseases

Phytopathogenic bacteria are responsible to affect a very large number of plants, especially those with agronomic importance, such as horticultural plants and fruit trees, causing severe financial losses. The known plant bacteria are about 5000 species and approximately 130 species are pathogenic (Jackson RW, 2009). Among these, Gram-negative bacteria belonging to the genera *Erwinia, Pseudomonas, Xanthomonas, Ralstonia* and *Xylella* are the etiological agents of the most widespread and destructive plant diseases around the world. In this scenario, bacteria referred to *Pseudomonas syringae* complex are responsible for diseases on a broad range of crops, some of these are widely distributed in the Mediterranean basin such as olive and citrus (Lamichhane JR *et al.,* 2015, Bull CT *et al.,* 2010).

Although an exception rather than the rule, the disease event is the result of a close interaction between the pathogen and the host plant, even at the molecular level. When a phytopathogenic bacterium interacts with a plant, two different reactions may occur: a "compatible" interaction, which is characterized by pathogen proliferation and disease development, or an "incompatible" interaction with no-host or resistant plant, where plant resistance can trigger a hypersensitive response (HR), characterised by a rapid and localised collapse and necrosis of tissue near the entry of the pathogen (Felix and Boller, 2003; Melotto *et al*., 2006).

The biological characteristics of the plant pathogenic bacteria, such as the ability to survive epiphytically also on seeds, multiply and move endophytically, make their control very difficult. Currently, the only means available and effective for the control of plant bacterial diseases are the preventive treatments based on copper salts. An overview of the available and under development tools for the control of diseases caused by bacteria belonging to *P. syringae* complex is presented in the next section.

## 1.2 *P. syringae* disease control

The strategies for minimising plant disease progression can be summarised into the following three categories: I) exclusion, elimination or reduction of pathogen inoculum, II) promotion of genetic diversity in the crop and III) inhibition of pathogen virulence mechanisms (Strange and Scott, 2005). However, these methods should not be used in exclusion, rather than they are combined together an integrated management approach. The management strategies rely on preventive methods, *e.g*. pathogen-free seeds and on good cultural practices (*e.g.* crop rotation) can be an effective means to reduce inoculum or to limit proliferation, together, when possible at the employment of resistant cultivars. During the last few decades, there has been a growing interest in adopting biological control measures, based on application to foliar or root tissues of non–pathogenic or pathogenically attenuated microorganisms, saprophytic bacteria and plant-growth promoting rhizobacteria (PGPRs) as well (Filho *et al.,* 2013; Hert

2007; Ji *et al.*, 2006). These strategies aim to suppress pathogen populations or induce systemic acquired resistance or a similar response in the plant that reduces the ability of the pathogen to colonise the plant and cause disease. However, also for biological control the best results can be achieved through combined treatments, in a view of integrated control and in any case taking into account the specific conditions that you have in the field rather than in a controlled testing environment. Another form of biological control, which has been successful for managing disease caused by *P. syringae,* although strictly limited to annual plants such as tomato, is the use of bacteriophages (Jones *et al*., 2007, 2012; Flaherty *et al.,* 2000). Selected bacteriophages have been demonstrated to be effective under greenhouse and field conditions for control of different bacterial diseases of annual plants but not of woody plants, because *P. syringae* etiological agents of vascular disease grew into cankers, resulting protected by all biological control agents (Lamichane *et al*., 2014; Jones *et al*., 2012). As emerged at the time, phage therapy has still to overcome several challenges before becoming effective. Moreover, in recent years, several studies showed the efficacy of natural extracts, obtained from different plants or plant parts, such as *Ficus carica, Allium sativum* and *Punica granatum* to control disease caused by *P. syringae*, such as *P. syringae* pv. *tomato* on tomato plants (Balestra *et al*., 2009). However, the only effective control methods used in plant protection are still based almost exclusively on chemical compounds. Although chemical control represents a strategy used for centuries in plant disease management, only a few bactericides, essentially antibiotics and copper salts, have been developed and commercially available. In recent decades, different chemical products like inducers of systemic acquired resistance such as acibenzolar-S-methyl (ASM) and benzothiadiazoleand (BTH) (Louws *et al*., 2001; Wilson *et al.,* 2002) have been used, although with limit results (Romero *et al.,* 2001). Another product of increasing use is chitosan, a natural biodegradable polymer with antimicrobial and plant-immunity eliciting properties (Xing *et al*., 2015). Chitosan is applied against a range of plant pathogens, including strains belonging to *P. syringae* group, although some limits have been reported (Mansilla *et al.,* 2013). As previously mentioned, within chemical treatments, there are also antibiotics, their large-scale application is restricted in many countries and their use in plant protection is strictly forbidden in some countries, including those in the European Union due to concern over their contribution to the emergence of antibiotic resistance in human pathogens (Casewell *et al.,* 2003; Lipsitch *et al.,* 2002). Finally, among the few effective and commercially available chemicals, there are copper compounds. However, many studies in recent time, have demonstrated that its massive use can lead to a range of undesired effects that are discussed in the following section.

### 1.3 Copper in plant protection: problems and current European legislation

Copper is an essential microelement whose presence in the soil is variable, according to the specific characteristics of the different soils *e.g*. sandy or clayey soils, with acid or basic pH. Some factors such as leaching, run off and uptake by microorganisms and plants combine with physical and biological processes occurring in the terrestrial environments, strongly influence copper bioavailability, which is defined as the portion of copper in the soil that is available for uptake by soil microorganisms/organisms and plants (Hinojosa *et al.,* 2010).

Copper in the soil is almost exclusively in the ionic divalent form ($Cu^{2+}$), and it is naturally attracted by negatively charged clay minerals, anionic salts and organic matter producing several metal-coordination compounds (Maier *et al*., 2000). A specific adsorption of copper to carbonates, phyllosilicates, and hydrous oxides of Al, Fe, and Mn was reported, where an antagonistic effect was observed between copper and N, P, Mo, Zn and Mn. In this scenario, it is noteworthy that the complete decomposition and mineralization of organic matter is indirectly prevented by copper, causing severe ecological imbalances in nutrient recycling (Parat *et al.,* 2002). When bound, copper loses its bioavailability and mainly this occurs in environments with high cation exchange capacity, high organic matter content and high pH (Maier *et al.*, 2000, Selim and Amacher 2001). On the contrary, soils displaying low pH values and cation exchange capacity, and/or poorly loaded with organic matter, content, make copper more mobile and bioavailable (Hinojosa *et al.*, 2010, Selim and Amcher 2001). The biological activity of cooper is strictly dependent on its ability to exist in a "free" or "ionic" state. In the latter condition copper is very reactive against a broad spectrum of plant pathogenic fungi and bacteria. The amount of copper in the ionic state, greatly increases at pH values lower than 6.5, this state makes a crucial contribution at its mobility, as well as its fungicidal and bactericidal activity, although this reactivity is also responsible for the phytotoxicity.

The normal amount of copper concentration in soils generally ranges between 5 and 20 mg/Kg of soil, unless copper is present in parent rock and natural minerals; in this case copper concentrations as much as 100 mg/Kg of soil are reached (Wightwick *et al.,* 2006). Conversely, when the copper levels range from 100 to up 1,280mg/Kg of soil and mainly accumulates in the topsoil, decreasing with depth in non sandy soils, and eventually returning to natural levels at about 40-60 cm unless, we are facing a contaminated agro-systems (Mirlean *et al.,* 2007; Rusjan *et al.,* 2007).

As reported, copper is a micronutrient metal necessary for many organisms and microorganisms, taking part in numerous physiological processes and it is also as an essential cofactor for many metalloproteins. However, high concentrations of copper salts dangerously affect physiological and biochemical processes in microorganisms and higher organisms. In humans dramatic toxic reactions are observed in cases of excessively elevated intake (Jaishankar M *et al.,* 2014).

In this frame a great concern is given by the residual copper in vegetables and fruits for human consumption. On environmental scale, copper accumulation in soils is toxic for resident plants, animals and microorganisms; it is also deleterious for many ecosystem processes, with a dramatic impact on soil biology. High copper content reduces soil fertility, induces plant stress and abiotic diseases, such as impaired root growth, atrophy, chlorosis, necrosis and leaf wilting (Moolenaar 1998; Magalhaes *et al.,* 1985). These deleterious effects are particularly damaging to plants when exposed to high temperatures and in acid soils, conditions which favour copper mobility and bioavailability. Moreover, the functional diversity of the soil microbial community is negatively affected by copper toxicity (Maier *et al.,* 2000; Hinojosa *et al.,* 2010). High copper concentrations in soil, kill naturally occurring beneficial microorganisms, as well as those applied as biocontrols including *Bacillus* and *Trichoderma* (Maier *et al.,* 2000). High copper levels (ca. 200 mg/Kg of soil) were also demonstrated to suppress nitrogen fixation by symbiotic bacteria belonging to the genus *Rhizobium* (Tindwa

*et al.,* 2014). Additionally, copper compounds heavily affect earthworms, which accumulate copper in their tissues and deleterious effects were also observed on bees and on fish fauna wildlife as well (Hinojosa *et al.,* 2010; Eijsackers *et al.,* 2005).

Another important aspect of copper accumulation, having huge consequences for human health, is the increase, in polluted copper environments, of antibiotic-resistance bacteria. It was demonstrated that copper-polluted soil induces the selection of copper-resistant bacteria, and further indirectly induces a co-selection for antibiotic resistance, because both these resistance genes are located on the same bacterial plasmids (Berg *et al.,* 2004, Baker *et al.,* 2006, Hu *et al.,* 2016). It is noteworthy that copper often causes the selection of bacteria resistant to vancomycin, which is among the last resort for antibiotic treatment of resistant staphylococcal infections in humans (Rincón *et al.,* 2014).

Since the antibacterial effects of copper sulfate preparations, in the form of "Bordeaux mixture" (Pierre-Marie Alexis Millardet, France 1880) were discovered, the production of fungicides/bactericides based on copper salts has reached its wide spread and several copper based compounds were synthesised and available on the market. Consequently, many thousands of tons of copper compounds were and are still now used annually in agricultural practices worldwide. Despite its negative eco-toxicological profile, the use of copper is still tolerated for its properties as wide-spectrum fungicide and bactericide and it is the only chemical compound allowed also in organic agriculture. The over-accumulation of copper in the soil reaching toxic levels, mainly due to agronomic practices, prompted the European Union (EU) and the governments of European Countries to restrict and control the use of copper compounds. Its maximum residue levels (MRLs) in and on food and feed, both of plant and animal origin, were defined in regulation 396/2005/EC and have been recently amended by Commission Regulation 149/2008/EC. New MRLs for pesticides with copper as the active ingredient in and on several fruit and vegetables are now fixed at 5mg/Kg.

Within the EU, limits to the use of copper compounds in organic production were introduced by the European Commission Regulation 473/2002/EC. Copper use is allowed up to 6Kg/ha/year, as specified in Regulation 889/2008/EC, detailing the rules for the implementation of Council Regulation 834/2007/EC on organic production. These limits were applied by most European countries, including Italy, France and Spain. In Germany, Austria, and Switzerland, copper application has been further restricted to 3-4 Kg/ha/year, while copper has been banned completely in Netherland and Denmark (Tamm *et al.,* 2004; Wightwick *et al.,* 2008).

Hence, treatments with copper derivatives against plant pathogenic bacteria and fungi contribute to its accumulation in soils more than any other agricultural activity, posing a serious threat to a wide range of organisms and microorganisms, and to terrestrial and aquatic ecosystems. In fact high concentrations of copper dangerously affect physiological and biochemical processes in microorganisms, algae and higher organisms. In addition to its negative ecotoxicological profile, a great concern is given by the residual copper in vegetables and fruits for human consumption. The restrictions imposed within the European Union on copper applications for plant disease control in agriculture stimulated the development of strategies to lower copper load into the topsoil, the optimisation of copper use, and the research

of realistic and efficient alternative strategies. Some of the most significant approaches, developed in recent years, are discussed in the following paragraphs.

### 1.4 AntiMicrobial Peptides (AMPs)

According to recent regulation to reduce the use of chemicals, AntiMicrobial Peptides (AMPs) have gained popularity for human and plant disease control during the past decade and are attractive alternatives to conventional antibiotics. These molecules distributed throughout the animal and plant kingdom are critical for the successful evolution of complex multicellular organisms and are effective weapons that higher organisms (including plants) have, among other defence strategies, to fight a great variety of pathogens (Table 2) (Boman 2003; Zasloff 2002; Guilhelmelli *et al.*, 2013).

In general, AMPs consist of less than 50 amino acids, possess an overall net positive charge and amphipathic topology (Ebenhan *et al.*, 2014; Yeaman and Yount 2003). The amphipathic topology creates clusters of hydrophilic and hydrophobic amino acids spatially separated from each other within the molecular selective antibacterial action through specific targeting of bacterial membranes having a high density of anionic lipids. Many bacterial membranes contain negatively charged components like hydroxylated phospholipids and lipopolysaccharides that are therefore major targets for AMPs. The hydrophobic regions of the AMPs support incorporation of the peptides into the membranes, leading to pore formation and permeabilisation. Basically, three models have been proposed for peptide insertion: the "barrel-stave model", the "carpet model", and the "toroidal-pore model" (Figure1) (Epand and Vogel 1999; Hancock and Diamond 2000; Lai and Gallo 2009).

The "barrel-stave model" (Figure1A) explains its name as the peptide helices form a bundle in the membrane with a central lumen, much like a barrel composed of helical peptides as the staves.

The orientation of the peptides forming the pore is so that the hydrophobic regions of the peptide align with the lipid core region, and the hydrophilic ones form the interior region of the pore. In the "carpet model" (Figure1B) peptides accumulate orienting by parallel to the surface of the lipid bilayer, because electrostatically attracted to the anionic phospholipid head groups, forming an extensive carpet. As the peptide concentration increases, the peptides are thought to disrupt the bilayer in a detergent-like manner, leading to the formation of micelles after disruption of the bilayer curvature.

In the "toroidal-pore model" (Figure1C), the polar faces of the peptides are associated with the polar head of the lipids, so that the pore is lined both by the peptides and the lipid head groups.

For their mode of action, namely targeting fundamental features of microbial cell membranes, AMPs have attracted the interest of researchers for many years. However, increasing hypothesis suggest that the effects such as formation of ion channels, transmembrane pores, and extensive membrane rupture, which surely leads to the lysis of microbial cells, are not the only mechanisms of microbial killing. In fact, other mechanisms may be involved, such as intracellular targets, that can alter the cytoplasmic membrane septum formation, inhibit cell-wall synthesis and inhibit enzymatic activity (Brogden 2005; Hancock and Sahl 2006; Yeaman and Yount 2003). Moreover, the difference in prokaryotic and eukaryotic membrane

architecture has imparted selectivity of AMPs for bacteria and fungi, thus reducing toxic side effects against cells of higher organisms (Alan and Earle 2002; Montesinos 2007; Montesinos and Bardaji, 2008; Nawrot *et al*., 2014). For these reasons the diversity of mechanisms of action has led to believe that the frequency of resistance emergence to AMPs should be low (Brogden 2005; Peschel and Sahl 2006).

**Table 2: Representative antimicrobial peptides (Jung *et al.*, 2014)**

| Type | AMPs | Size | Characteristic | Origin | Activity | Reference |
|---|---|---|---|---|---|---|
| α-helical peptides of Lack in cysteine | Magainin | ~2.5 kDa, 23 amio acid (aa) | Lys rich | analog of frogs | Gram positive/negative bacteria, fungi, parasite | Gesell *et al.* 1997 |
| | Cecropins | ~4 kDa, 30~45 aa | Lys rich, Amidation of C-terminal | Blood of insects | Gram positive/negative bacteria | Holak *et al.* 1988 |
| | Cepropin P1 | ~4 kDa, 30~45 aa | Amidation of C-terminal | paneth cell from small intestine of pigs | Gram negative bacteria | Sipos *et al.* 1992 |
| | Buforin | 39 aa | Similarity to C-terminal of Histone IIa | Stomach of American Bull Frog | Gram positive/negative bacteria, fungi, | Yi *et al.* 1996 |
| | hCAP18/ LL-37 | 18 kDa, 37 aa | Helical C-terminal | humans | Gram positive/negative bacteria, fungi, | Gudmundsson *et al.* 1996 |
| Cationic peptide enriched for specific amino acid | Bac5, Bac7 | 43 or 59 aa | Lack in cysteine residue, rich in proline, arginine, phenylalanine, glycine, tryptophan | Neutrophils of cattle | Gram positive/negative bacteria | Scocchi *et al.* 1994 |
| | PR39 | 39 aa | | small intestine of pigs | | Agerberth *et al.* 1991 |
| | Indolicidin | 13 aa | | Neutrophils of cattle | | Selsted *et al.* 1992 |
| β-hairpin or loop due to the presence of a single disulfide bond | Dodecapeptide | 12 aa | and/or cyclization of the peptide chain | Neutrophils of cattle | Gram positive/negative bacteria | Romeo *et al.* 1988 |
| | Brevinins | 20'34 aa | | amphibians | | Conlon *et al.* 1999 |
| | Raqnalexin | 20 aa | | amphibians | | Clark *et al.* 1994 |
| β-sheet peptides due to the presence of 2 or more disulfide bonds | Defensins | ~4 kDa, 29~45 aa | Arg-rich, salt or iron sensitive activity | Neutrophils of rabbits and humans | Gram positive/negative bacteria, fungi, cytotoxicity | Pardi *et al.* 1992 |
| | β-Defensin | 38~42 aa | | Bovine leukocytes | | Zimmermann *et al.* 1995 |
| | Protegrin | 16~18 aa | S-S bond | Porcine leukocytes | | Fahrner *et al.* 1996 |

In plants several families of natural AMPs have been identified, such as thionins, defensins, lipid transfer proteins, hevein-and knottin-like proteins and snakins, differing in structure, size and cysteine content (Tam *et al.*, 2005). AMPs from animals were also analysed for their plant protecting potential. For example magainin (from frog), cecropin (from silkmoth) and modified or chimeric forms of these two peptides were used mainly in *vitro* or *ex vivo* (*i.e.* detached leaves or fruits) studies against plant pathogens (Alan and Earle, 2002; Coca *et al.*, 2006).

As previously reported AMPs are widely recognised as promising candidates and substitutes of antibiotics, although naturally occurring sequences present drawbacks that limit their development, such as susceptibility to protease degradation and low bioavailability (Choi *et al.*, 2014). Overcome these limitations, a rational design of new AMPs, in order to find shorter and more stable peptides, maintaining or increasing the activity with a low cytotoxicity has been carried out (Zhang and Fall 2006; Hancock and Sahl 2006). A brief summary of the advantages and disadvantages of AMPs is reported in Table 3.

**Figure 1: Schematic representation of some action mechanisms of membrane-active AMPs. (A) Barrel-stave model. AMP molecules insert themselves into the membrane perpendicularly. (B) Carper model. Small areas of the membrane are coated with AMP molecules with hydrophobic sides facing inward, leaving pores behind in the membrane. (C) Toroidal pore model. This model resembles the Barrel-stave model, but AMPs are always in contact with phospholipid head groups of the membrane. The blue colour represents the hydrophobic portions of AMPs, while the red colour represents the hydrophilic parts of the AMPs (Bahar and Ron, 2013).**

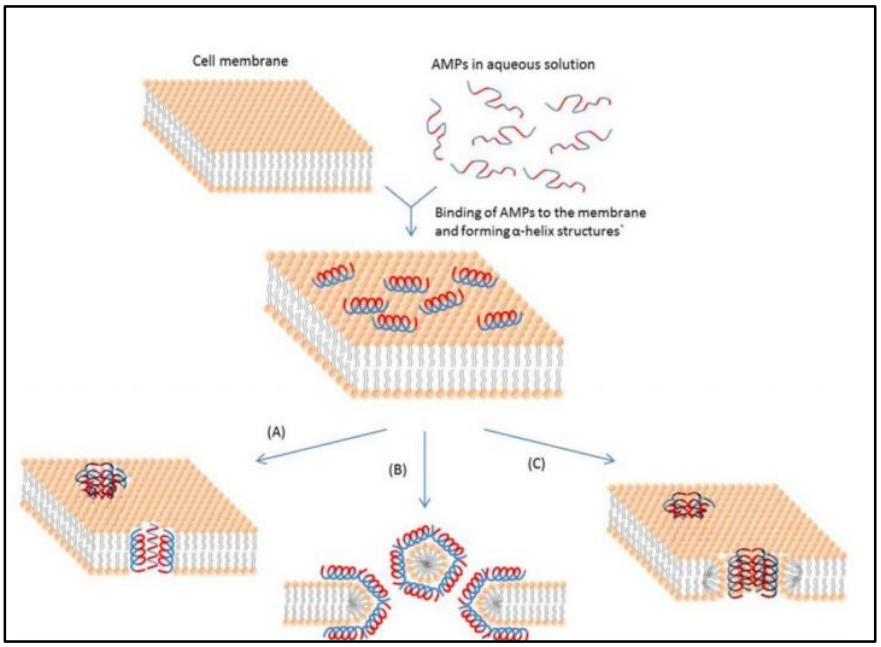


For example the synthetic peptide BP100 was found to be effective at micromolar concentration against *Xanthomonas axonopodis* pv. *vesicatoria* in pepper, *Erwinia amylovora* in apple, pear and *Pseudomonas syringae* pv. *syringae* (Badosa *et al.*, 2007).
However, the process involved in the development of AntiMicrobial Peptides is time-consuming and limited by the number of individual compounds that can be synthesised. For these reasons, molecules able to block pathogenicity and virulence systems of pathogenic bacteria have been suggested as an alternative strategy (Silva *et al.*, 2016).

**Table 3. Advantages and disadvantages of AntiMicrobial Peptides (Gordon *et al.*, 2005)**

| Advantages | Disadvantages |
|---|---|
| Broad-spectrum activity (antibacterial, antiviral, antifungal)<br>Rapid onset of killing<br>Cidal activity<br>Potentially low levels of induced resistance<br>Concomitant broad anti-inflammatory activities | Discovery costs of synthesis and screening<br>Patent exclusivity for economic viability<br>Systemic and local toxicity<br>Reduced activity based on salt, serum, and pH sensitivity<br>Susceptibility to proteolysis<br>Pharmacokinetic and pharmacodynamic issues<br>Sensitization and allergy after repeated application<br>Natural resistance (*e.g.*, *Serratia marcescens*)<br>Confounding biological functions (*e.g.*, angiogenesis)<br>High manufacturing costs |

## 1.5 Bacterial Virulence mechanisms: Quorum Sensing and Type Three Secretion System

Among the ideal targets against which set up alternative control methods, based on anti-virulence activity molecules, there should be mechanisms that pathogenic bacteria use in the early stage of interaction and presiding over their pathogenicity and virulence (Figure 2). Among the main known strategies used by pathogenic bacteria to communicate each other and with the potential host, there are:

i) The ability to synchronize the population behaviour in response both to density and specific external stimuli which indicate the plant host presence;

ii) The ability to secrete directly into the cytoplasm of the potential host cell, molecules known as effectors, responsible for pathogenicity and virulence of pathogenic bacteria.

In particular, these systems are the Quorum Sensing (QS) and the Type Three Secretion System (TTSS).

### 1.5.1 Quorum Sensing

The Quorum Sensing, discovered for the first time in the bioluminescent bacterium *Vibrio fischeri*, is an important universal mechanism, considered the "master switch" that regulates the bacteria virulence and allows to such class of microorganisms belonging to the same species and sometimes even to different species, to communicate through molecules, called autoinducers, which are generally omoserin-acyl-lactone (AHL) in Gram-negative bacteria and oligopeptides in Gram-positive bacteria (Waters and Bassler 2005; Galloway *et al.*, 2011; Rutherford and Bassler 2012). This mechanism enables the bacteria to act as a coordinated community in the regulation of their gene expression. In fact, the QS regulates motility phenomena, bioluminescence, synthesis of virulence factors and/or related to the host colonisation (Castillo-Juárez, 2015). The communication can be interrupted by the opposite phenomenon called Quorum Quenching (QQ), which bacteria possess as a mechanism to control QS.

**Figure 2: Bacterial virulence factor targets for antivirulence agents (Silva *et al.*, 2016)**

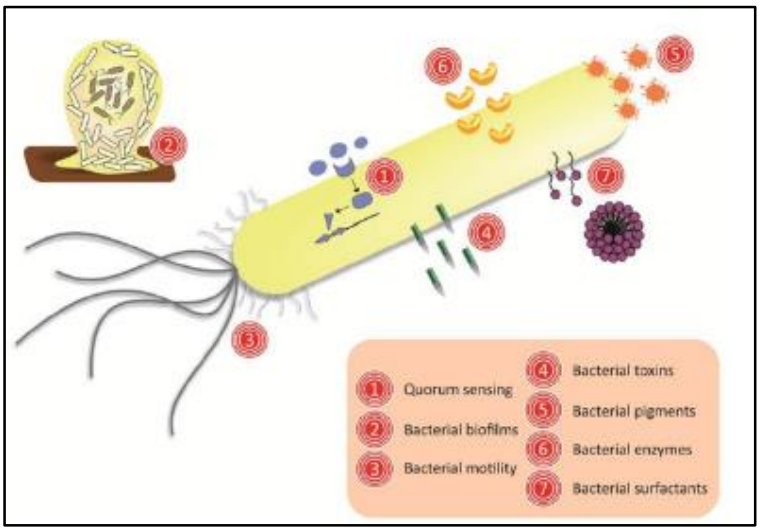


Fundamentally, in this regard, three mechanisms can be identified (Brackman and Coenye 2015; Rutherford and Bassler 2002):
i) inhibition of the biosynthesis of the molecules directly involved in the QS through the inactivation of the enzymes responsible for the synthesis of the acyl chain,
ii) degradation by enzymes as lattonasi acylase of these molecules to the purpose of preventing their accumulation,
iii) inhibition of the interaction between these molecules and their specific receptors
The existence in nature of the QQ phenomenon has been exploited in disease protection in order to find molecules able to block the QS and therefore the communication between bacteria, essential for their coordination during plant-bacteria interaction.
Moreover, this mechanism provides a lower risk of developing resistance, since it has not generally effect both growth and bacteria fitness. This phenomenon represents a strategy with interesting practical implications and with significant therapeutic potential, as to be already widely studied to limit the bacterial infection (Koh *et al*., 2013).
In addition to synthesis compounds, some natural molecules are able to determine the QQ, such as halogenated furanones produced by the marine red alga *Delisea pulchra,* which interfere the N-acylated homoserine lactone (AHL) regulatory system in several Gram-negative bacteria (Bauer and Teplitski 2001; Kjelleberg *et al.*, 1997).
In recent years, the discovery of QS antagonists of bacterial and non-bacterial origin has increased considerably. For example, it was reported that certain bacteria possess the ability to quench QS through the synthesis of specific enzymes such as AiiA (an N-acylhomoserine (AHL) lactonase enzyme) from *Bacillus sp*., able to hydrolyze the lactone bond of the AHL signalling compound and PON (the paraoxonase enzymes) in human airway epithelial cells (Dong *et al.*, 2001; Chun *et al.*, 2004). However, as reported by Koh *et al.*, 2013 the most of the antagonists, to date found, have been discovered in plant extracts and are active against human pathogenic bacteria.

### 1.5.2 The Type Three Secretion System

The Type Three Secretion System is a molecular device, through which the bacterial pathogens inject effector proteins able to subvert eukaryotic cellular processes enabling the invasion. This structure, similar to a needle, consisting of more than 20 proteins that can be divided into three domains: the cytoplasmatic, the transmembrane, and the extracellular domain. The core *hrp/hrc* encodes the actual TTSS apparatus and it is composed of 27 genes, most of which are arrayed in four major operons (Alfano *et al.*, 2000). Flanking the core *hrp/hrc* cluster are the Conserved Effector Locus (CEL) and the Exchangeable Effector Locus (EEL), which primarily contain a range of TTSS effectors, selfish elements and uncharacterised ORFs (Charity *et al.*, 2003).

The basal body, resembling the structure of the flagellum, is made up of the cytoplasmic and the transmembrane domains. The extracellular domain is composed of a needle-like structure, build by multiple copies of a single protein which acquires a superstructure helical-like forming a conduit, and a translocon complex which span the membrane of the host forming a pore (Figure 3). These regions allow the direct contact with the host cell and to secrete directly into the cytoplasm effectors of pathogenicity and virulence, which are the basis of onset of disease symptoms. In fact the transcription of genes related to such system is in response to different environmental conditions and after contact with the host cell. Although TTSSs have been identified in many bacterial species, quite limited number of TTSSs has been extensively investigated. Until now, five animal pathogens (*Salmonella, Shigella flexneri*, *Pseudomonas aeruginosa*, *Yersinia*, *Escherichia coli*, and *Chlamydia spp.*) and two plant pathogens (*Pseudomonas* and *Xanthomonas*) have been well studied for their TTSSs (He *et al.*, 2004) .

**Figure 3: Schematic representation of the TTSS from plant pathogenic bacteria. The secretion apparatus spans both bacterial membranes and is associated with a cytoplasmic ATPase. The TTSS from plant pathogenic bacteria is connected to an extracellular pilus that presumably spans the plant cell wall. IM, Inner membrane; OM, outer membrane; PM, plasma membrane (Buttner and He, 2009).**

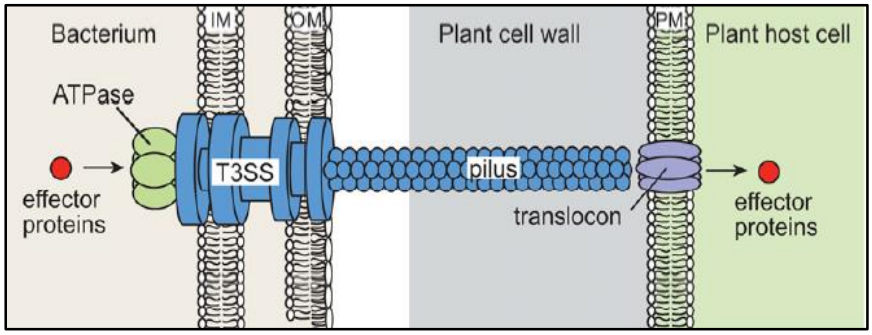


In plant pathogens, both structural and effector genes are coregulated, possessing the same "hrp box" regulatory motif. This means that the secretion of effectors happens at the same time of the assembly of the TTSS and the newly synthesised proteins will be recovered near the tip, depending on the hypothesised "conduit model" (He *et al*., 2004). On the contrary, the other model hypothesised "the guiding filament/conveyor model" suggested that the effectors

were carried inside the Hrp pilus during its growth, and therefore the newly synthesised effectors would have been recovered near the base of the pilus (He *et al*., 2004).
Moreover, such apparatus consists of structural proteins, among these the HrpA protein is the most important component in the structuring pilus of the TTSS of plant pathogenic Gram-negative bacteria belonging to *P. syringae* complex.
Some evidences show as the TTSS is crucial for successful pathogenesis and that bacteria with a TTSS not fully functional are no more pathogenic or extremely reduced in virulence (Alfano and Block 2011; Dean 2011). The proteins constituting the Hrp pili tend to be quite diverse in sequence homology among different species, and even within each species among different strains (He and Buttner 2009; Weber and Koebnik 2005). However, despite this, they share a considerable number of physicochemical features: they are small and predicted to be constituted almost exclusively of α-helices. Additionally, some of these proteins (HrpE from *Xanthomonas campestris*, HrpA from *Pseudomonas syringae* group, and HrpY from *Ralstonia solanacearum*) show very similar hydrophobicity profiles and resemble each other in their instability and aliphatic indices (Weber and Koebnik, 2005).
Given its good conservation of both structural and physiological in all pathogenic Gram-negative bacteria, the TTSS is considered the ideal target, for excellence, against which set up innovative anti-bacterial molecules.

## 1.6 References

**Jackson RW** (2009). Plant Pathogenic Bacteria: Genomics and Molecular Biology. *Caister Academic Press.* ISBN 978-1-904455-37-0

**Lamichhane JR**, Messèan A, Morris CE. (2015) Insights into epidemiology and control of diseases of annual plants caused by the *Pseudomonas syringae* species complex. *J Gen Plant Pathol.*

**Bull CT**, De Boer SH, Denny TP, Firrao G, Saux FL, Saddler M, Scortichini M, Stead DE and Takikawa Y. (2010) Comprehensive list of names of plant pathogenic bacteria, 1980–2007. J. *Plant Pathol*. 92, 551–592

**Felix G**, Boller T. 2003. Molecular sensing of bacteria in plants. The highly conserved RNA-binding motif RNP-1 of bacterial cold shock proteins is recognized as an elicitor signal in tobacco. *J. Biological Chemistry* 278, 6201–6208

**Melotto M**., Underwood W., Koczan J., Nomura K., Yang He S. (2016) Plant Stomata Function in Innate Immunity against Bacterial Invasion Cell, Volume 126, Issue 5, 8 September 2006, Pages 969-980

**Strange RN**, Scott PR. (2005) Plant disease: a threat to global food security. *Annu. Rev. Phytopathol*. 43, 83–116

**Filho RL**, de Souza RM, Ferreira A, Quecine MC, Alves E, de Azevedo JL. (2013) Biocontrol activity of Bacillus against a GFP-marked *Pseudomonas syringae* pv.*tomato* on tomato phylloplane. *Australas Plant Pathol* 42:643–651

**Hert AP**. (2007) Evaluation of bacteriocins in *Xanthomonas* perforans for use in biological control of *Xanthomonas euvesicatoria*. PhD thesis, University of Florida, Gainesville

**Ji P**, Campbell HL, Kloepper JW, Jones JB, Suslow TV, Wilson M. (2006) Integrated biological control of bacterial speck and spot of tomato under field conditions using foliar biological control agents and plant growth-promoting rhizobacteria. *Biol Control* 36:358–367

**Jones JB**, Jackson LE, Balogh B, Obradovic A, Iriarte FB, Momol MT. (2007) Bacteriophages for plant disease control. *Annu Rev Phytopathol* 45:245–262

**Jones JB**, Vallad GE, Iriarte FB, Obradovic A, Wernsing MH, Jackson LE *et al.* (2012) Considerations for using bacteriophages for plant disease control. *Bacteriophage* 2:208–214

**Flaherty JE**, Jones JB, Harbaugh BK, Jackson LE. (2000) Control of bacterial spot on tomato in the greenhouse and field with H-mutant bacteriophages. *Hort Science* 35:882–884

**Lamichhane JR**, Varvaro L, Parisi L, Audergon J-M, Morris CE. (2014) Disease and frost damage of woody plants caused by *Pseudomonas syringe*: seeing the forest for the trees. *Adv Agron* 126:235–295

**Jones JB**, Vallad GE, Iriarte FB, Obradovic A, Wernsing MH, Jackson LE, Balogh B *et al.* (2012) Considerations for using bacteriophages for plant disease control. *Bacteriophage* 2:208–214

**Balestra GM**, Heydari A, Ceccarelli D, Ovidi E, Quattricci A (2009) Antibacterial effect of *Allium sativum* and *Ficus carica* extracts on tomato bacterial pathogens. *Crop Prot* 28:807–811

**Louws FJ**, Wilson M, Campbell HL, Cuppels DA, Jones JB, Shoemaker PB, Sahin F *et al*. (2001) Field control of bacterial spot and bacterial speck of tomato using a plant activator. *Plant Dis* 85:481–488

**Wilson M**, Campbell HL, Ji P, Campbell HL, Cuppels DA, Louws FJ, Miller SA *et al.* (2002) Biological control of bacterial speck of tomato under field conditions at several locations in North America. *Phytopathology* 92:284–1292

**Romero AM**, Kousik CS, Ritchie DF. (2001) Resistance to bacterial spot in bell pepper induced by acibenzolar-S-methyl. *Plant Dis* 85:189–194

**Mansilla AY**, Albertengo L, Rodrìguez MS, Debbaudt A, Zuniga A, Casalongue CA. (2013) Evidence on antimicrobial properties and mode of action of a chitosan obtained from crustacean exoskeletons on *Pseudomonas syringae* pv.*tomato* DC3000. *Appl Microbiol Biotechnol* 97:6957–6966

**Casewell M**, Friis C, Marco E, McMullin P, Phillips. (2003) The European ban on growth-promoting antibiotics and emerging consequences for human and animal health. *J Antimic Chemother* 52:159–161

**Xing K**, Zhu X, Peng X, Qin S. (2015) Chitosan antimicrobial and eliciting properties for pest control in agriculture: a review. *Agronomy for Sustainable Development* April 2015, Volume 35, Issue 2, pp 569–588

**Lipsitch M**, Singer RS, Levin BR. (2002) Antibiotics in agriculture: when is it time to close the barn door? *Proc Natl Acad Sci* USA 99:5572–5574

**Hinojosa MB**, Garcia-Ruiz R, Carreira JA. (2010) Utilizing microbial community structure and function to evaluate the health of heavy metal polluted oils. *Soil Heavy Metals* 19, 185–224

**Maier R**, Pepper I, Gerba C. (2000) Environmental Microbiology. *Academic Press*, San Diego

**Parat C**, Chaussod R, Leveque J, Dousset S, Andreux F. (2002) The relationship between copper accumulated in vineyard calcareous soils and soil organic matter and iron. European *Journal of Soil Science*. 10.1046/j.1365-2389.2002.00478

**Selim HME**, Amacher MC. (2001) Sorption and release of heavy metals in soils: non-linear kinetics. In: Selim HME, Sparks D (eds) Heavy metals release in soils. *Lewis Publishers*, Boca Raton, pp 1–30

**Wightwick A**, Mollah M, Smith J, MacGregor A. (2006) Sampling considerations for surveying copper concentrations in Australian vineyard soils. *Australian Journal of Soil Research* 44(7) 711-717 http://dx.doi.org/10.1071/SR05135

**Mirlean N**, Baisch P, Medeanic S. (2009) Copper Bioavailability and Fractionation in Copper-Contaminated Sandy Soils in the Wet Subtropics (Southern Brazil) *Bull Environ Contam Toxicol* 82: 373

**Rusjan D**, Strlič M, Pucko D, Korošec-Koruza Z. (2007) Copper accumulation regarding the soil characteristics in SubMediterranean vineyards of Slovenian. *Geoderma* 141, 111-118

**Jaishankar M**, Tseten T, Anbalagan N, Mathew B, Beeregowda KN. (2014) Toxicity, mechanism and health effects of some heavy metals. *Interdiscip Toxicol.* Jun; 7(2): 60–72. Published online 2014 Nov 15. Doi: 10.2478/intox-2014-0009

**Moolenaar SW**, Temminghoff EJW, De Haan F.(1998)Modelling dynamic copper balances for a contaminated sandy soil following land use change from agriculture to forestry.*Environ. Pollut*.117–125

**Magalhaes MJ**, Sequeira EM, Lucas MD. (1985) Copper and zinc in vineyards of central Portugal. *Water, Air and Soil Pollution* 26: 1-17

**Hinojosa M**, Garcia-Ruiz R, Carreira J, Karaca A, Cetin S, Turgay O. (2010) *Soil Biology:* Soil Heavy Metals. Springer, Berlin

**Tindwa H**, Semu E, Msumali GP. (2014) Effect of elevated copper levels on biological nitrogen fixation and occurrence of rhizobia in a Tanzanian coffee-cropped soil. *J. Agric. Sci. Appl*. Volume 3, Issue 1 Mar. 2014 PP. 13-19 DOI: 10.14511/jasa.2014.030103

**Eijsackers H**, Beneke P, Maboeta M, Louw JP, Reinecke AJ. (2005) The implications of copper fungicide usage in vineyards for earthworm activity and resulting sustainable soil quality. *Ecotoxicol Environ Saf.* 2005 Sep; 62(1):99-111

**Berg J**, Tom-Petersen A, Nybroe O. (2004) Copper amendment of agricultural soil selects for bacterial antibiotic resistance in the field. *Letters in Applied Microbiology*. DOI: 10.1111/j.1472-765X.2004.01650.x

**Baker-Austin C**, Wright MS, Stepanauskas R, McArthur JV. (2006) Co-selection of antibiotic and metal resistance. *TRENDS in Microbiology* Vol.14 No.4 DOI:10.1016/j.tim.2006.02.006

**Hu HW**, Wang JT, Li J, Li JJ, Ma YB, Chen D, He JZ. (2016) Field-based evidence for copper contamination induced changes of antibiotic resistance in agricultural soils. *Environmental microbiology*. DOI: 10.1111/1462-2920.13370

**Rincón S**, Panesso D, Díaz L, Carvajal LP, Reyes J, Munita JM, Arias CA. (2014) Resistance to "last resort" antibiotics in Gram-positive cocci: The post-vancomycin era. *Biomedica*. Suppl 1:191-208. DOI: 10.1590/S0120-41572014000500022

**Tamm L**, Smit AB, Hospers M, Janssens SRM, Buurma JS, Mølgaard JP, Lærke PE, Hansen HH, Bodker L, Bertrand C, Lambion J, Finckh MR, Schüler C, Lammerts van Bueren E, Ruissen T, Nielsen BJ, Solberg S, Speiser B, Wolfe MS, Phillips S, Wilcoxon SJ, Leifert C. (2004) Assessment of the Socio economic impact of late blight and state of the art. *Management in European Potato Production Systems*. Research Institute of Organic Agriculture FiBL, Frick, Switzerland

**Wightwick A**, Mollah M, Partington D, Allinson G. (2008) Copper fungicide residues in Australian vineyard soils. *Journal of Agricultural and Food Chemistry*, 56, 2457–2464

**Boman HG**. (2003) Antibacterial peptides: basic facts and emerging concepts. *J Intern Med*. Sep; 254(3):197–215

**Zasloff M**. (2002) Antimicrobial peptides of multicellular organisms *Nature* Vol 415-2002

**Guilhelmelli F**, Vilela N, Albuquerquel P, S.Derengowski L, Silvia-Pereira I, M-Kyaw C. (2013) Antibiotic development challenges: the various mechanisms of action of antimicrobial peptides and of bacterial resistance. *Frontiers in Microbiology* doi: 10.3389/fmicb.2013.00353

**Ebenhan T**, Gheysens O, Kruger HG, Zeevaat JR, Sathekge MM. (2014) Antimicrobial peptides: their role as infection-selective tracers for molecular imaging. *Biomed Res Int*; 867381. Doi: 10.1155/2014/867381
**Yeaman MR**, Yount NY. (2003) Mechanisms of antimicrobial peptide action and resistance. *Pharmacological Reviews*; 55 (1):27–55
**Epand RM** and Vogel JH. (1999) Diversity of antimicrobial peptides and their mechanisms of action Biochimica et Biophysica Acta (BBA) – *Biomembranes*- Volume 1462, Issues 1–2, 15 December 1999, Pages 11–28
**Hancock RE** and Diamond G. (2000) The role of cationic antimicrobial peptides in innate host defences. *Trends Microbiol*. 2000 Sep; 8(9):402-10
**Lai Y** and Gallo LR. (2009) AMPed up immunity: how antimicrobial peptides have multiple roles in immune defense *Trends Immunol*. 30(3): 131–141. Doi: 10.1016/j.it.2008.12.003
**Brogden KA**. (2005) Antimicrobial peptides: pore formers or metabolic inhibitors in bacteria? *Nat. Rev.Microbiol*. (3)238-25010.1038/nrmicro1098
**Hancock REW**, Sahl HG. (2006) Antimicrobial and host defense peptides as new anti-infective therapeutic strategies. *Nat Biotechnol* 24:1551–7
**Yeaman MR**, Yount NY. (2003) Mechanisms of antimicrobial peptide action and resistance. *Pharmacol Rev* 55:27–55
**Alan AR**, Earle ED. (2002) Sensitivity of bacterial and fungal plant pathogens to the lytic peptides, MSI-99, magainin II, and cecropin B. *Mol Plant Microbe Interact*. 15: 701–708. Doi: 10.1094/mpmi.2002.15.7.701
**Montesinos E**. (2007) Antimicrobial peptides and plant disease control. FEMS *Microbiol Lett* 270:1–11
**Montesinos E**, Bardaji E.(2008) Synthetic antimicrobial peptides as agricultural pesticides for plant-disease control. *Chem Biodivers* 5: 1225–1237
**Nawrot R**, Barylski J, Nowicki G, Broniarczyk J, Buchwald W, Goździcka-Józefiak A. (2014) Plant antimicrobial peptides Folia *Microbiol* (Praha). 2014; 59(3): 181–196. Doi: 10.1007/s12223-013-0280-4
**Brogden KA**. (2005) Antimicrobial peptides: pore formers or metabolic inhibitors in bacteria? *Nat. Rev.Microbiol*. (3)238-25010.1038/nrmicro1098
**Peschel A**, Sahl HG. (2006) The co-evolution of host cationic antimicrobial peptides and microbial resistance. *Nat RevMicrobiol* 4:529–36
**Tam JP**, Wang S, Wong KH, Tan WL. (2015) Antimicrobial peptides from plants. *Pharmaceuticals* (Basel). 2015 Dec; 8(4): 711–757. Doi: 10.3390/ph8040711
**Alan AR** and Earle ED. (2002) Sensitivity of bacterial and fungal plant pathogens to the lytic peptides, MSI-99, magainin II, and cecropin B. *Mol Plant-Microbe Interact* 15:701–708
**Coca M**, Penas G, Gomez J, Campo S, Bortolotti C, *et al*. (2006) Enhanced resistance to the rice blast fungus Magnaporthe grisea conferred by expression of a cecropin A gene in transgenic rice. *Planta* 223: 392–406. Doi: 10.1007/s00425-005-0069
**Choi N**, Soler M, Güell I, Badosa E, Cabrefiga J, Bardaji E, Montesinos E, Planas M, Feliu L. (2014) Antimicrobial peptides incorporating non-structural amino acids as agents for plant protection. *Protein Pept Lett*. 2014 Apr; 21(4):357-67
**Zhang L**, Falla TJ. (2006) Antimicrobial peptides: therapeutic potential. *Expert Opin Pharmac*7:653–63
**Hancock REW**, Sahl HG. (2006) Antimicrobial and host defense peptides as new anti-infective therapeutic strategies. *Nat Biotechnol* 24:1551–7
**Badosa E**, Ferre R, Planas M, Feliu L, Besalu E, Cabrefiga J, Bardajì E, Montesinos E. (2007) A library of linear undecapeptides with bactericidal activity against phytopathogenic bacteria. Peptides Volume 28, Issue 12, December 2007, pages 2276–2285
**Silva LN**, Zimmer KR, Macedo AJ, Trentin DS. (2016) Plant Natural Products Targeting Bacterial Virulence Factors. *Chemical Reviews* DOI: 10.1021/acs.chemrev.6b00184
**Waters CM**, Bassler BL. (2005) Quorum Sensing: Cell-to-Cell Communication in Bacteria. *Annu. Rev. Cell Dev. Biol.* 21 (1), 319−346
**Galloway WR**, Hodgkinson JT, Bowden SD, Welch M, Spring DR. (2011) Quorum sensing in Gram-negative bacteria: smallmolecule modulation of AHL and AI-2 quorum sensing pathways. *Chem. Rev.* 111 (1), 28−67

**Rutherford ST**, Bassler BL. (2012) Bacterial quorum sensing: its role in virulence and possibilities for its control. Cold Spring Harbor Perspect. *Med*. 2 (11), a012427

**Castillo-Juárez I**, Maeda T, Mandujano-Tinoco EA, Tomás M, Pérez-Eretza B, García-Contreras SJ,Wood TK, García-Contreras R. (2015) Role of quorum sensing in bacterial infections. *World J Clin Cases*.16; 3(7): 575–598. Doi:10.12998/wjcc.v3.i7.575

**Brackman G**.; Coenye T. (2015) Quorum sensing inhibitors as antibiofilm agents. *Curr. Pharm. Des*. 21 (1), 5−11

**Koh CL**, Sam CK, Yin WF, Tan LY, Krishnan T, Chong YM, Chan KC. (2013) Plant-Derived Natural Products as Sources of Anti-Quorum Sensing Compounds Sensors 13, 6217-6228; doi:10.3390/s130506217

**Bauer WD**, Teplitski M. (2001) Can plants manipulate bacterial quorum sensing? *Funct. Plant Biol*. 28, 913–921

**Kjelleberg S**, Steinberg P, Givskov M, Gram L, Manefield M, de Nys R. (1997) Do marine natural products interfere with prokaryotic AHL regulatory systems? *Aquat. Microbial. Ecol*. 13, 85–93

**Dong YH**, Wang LH, Xu JL, Zhang HB, Zhang XF, Zhang LH. (2001) Quenching quorum-sensing-dependent bacterial infection by an N-acyl homoserine lactonase. *Nature* 411, 813–817

**Chun CK**, Ozer EA, Welsh MJ, Zabner J, Greenberg EP. (2004) Inactivation of a *Pseudomonas aeruginosa* quorum-sensing signal by human airway epithelia. *Proc. Natl. Acad.Sci*. USA 2004, 101, 3587–3590

**Koh CL,** Sam CK, Yin WF, Tan LY, Krishnan, Chong YM, Chan KG. (2013) Plant-Derived Natural roducts as Sources of Anti-Quorum Sensing Compounds. *Sensors*. 2013 May; 13(5): 6217–6228.

**Alfano JR**, Charkowski AO, Deng WL, Badel JL, PetnickiOcwieja T, van Dijk K and Collmer A. (2000) The Pseudomonas syringae Hrp pathogenicity island has a tripartite mosaic structure composed of a cluster of type III secretion genes bounded by exchangeable effector and conserved effector loci that contribute to parasitic fitness and pathogenicity in plants. *Proc. Natl Acad. Sci*. USA, 97, 4856–4861

**Charity JC**, Pak K, Delwiche CF, Hutcheson SW. (2003) Novel exchangeable effector loci associated with the Pseudomonas syringae hrp pathogenicity island: evidence for Integron-like assembly from transposed agene cassettesi. *Mol. Plant-Microbe Interact*. 16, 495–507

**He SY**, Nomura K, Whittam CT. (2004) Type III protein secretion mechanism in mammalian and plant pathogens. *Molecular Cell Research*.Volume 1694, Issues 1-3, 11 November 2004, Pagesd 181-206.

**Block A**, Alfano JR. (2011) Plant targets for *Pseudomonas syringae* Type III effectors: virulence targets or guarded decoys? *Curr Opin Microbiol*. Feb;14(1):39-46. Doi: 10.1016/j.mib.2010.12.011

**Dean P**. (2011) Functional domains and motifs of bacterial type III effector proteins and their roles in infection. *FEMS Microbiol Rev*; 1–26

**He SY** and Buttner D. (2009) Type III Protein Secretion in Plant Pathogenic Bacteria. *Plant Physiol*. 2009 Aug; 150(4): 1656–1664

**Weber E**, Koebnik R. (2005) Domain Structure of HrpE, the Hrp Pilus Subunit of *Xanthomonas campestris* pv. *vesicatoria*. *J.Bacteriol.* Sept. 2005, p. 6175–6186 Vol. 187, No. 17 0021-9193/05/$08.00 0 doi:10.1128/JB.187.17.6175–6186.2005

### 1.7 Interest and aims of the study

Bacteria plant pathogens cause serious diseases around the word resulting in significant crop losses. Among the critical issues that may impact both on yields and on food safety, it should be taken into account the effects of climate change, which are reflected in the diffusion of several plant pathogens and in the greater frequency of their reproductive cycles. In addition, the globalization of food markets also contributes to a rapid spread of alien and invasive plant pathogens in areas where they were previously absent, through the trade of infected and asymptomatic plant material, with devastating consequences both in productive and ecological sectors. The phytoiactric sector is still based on chemical treatment with compounds such as copper salts and antibiotics, the latter not allowed in European Member States. However, copper-based treatments are strictly regulated and temporarily limited within the European Union. Extensive applications of copper-based compounds, such as fungicides and bactericides, have contributed to the development of copper-resistant bacteria, making these compounds completely ineffective in phytoiatric sector. Similarly, the copper stored in the soil determines an alarming increase in multi-drug resistant bacteria in the agro-ecosystems, which provide a source of antibiotic resistance genes, easily transmissible also to human and animal pathogenic bacteria, through cross-resistance phenomena. This scenario undermines prophylactic and therapeutic effectiveness of these substances both in human and animal medicine, generating a general concern.
Recently, the scientific community has addressed this issue and several approaches to identify and develop new ecofriendly alternative for plant protection are under study.
Many efforts have been made to identify inhibitors of natural or synthetic origin, which are able to target structures and/or systems related to pathogenicity and virulence of pathogenic bacteria such as Quorum Sensing and even more the Type Three Secretion System. Furthermore, recent scientific evidence indicates that Multi Drug Efflux Pumps (MATE) may contribute to both intrinsic and acquired resistance to toxic compounds in several life forms, and therefore represent a potential target for innovative molecules.

In this scenario, the main objective of this PhD thesis has been to develop and test innovative strategies to be applied in plant protection. In particular, the research aimed at controlling bacterial disease progression in host plants using bacteria belonging to *P. syringae* complex. The main objective has been achieved through the following specific actions:

- To analyse the structural protein HrpA of *P. syringae*, essential in the Type Three Secretion System pilus assembly, and to verify the efficacy *in vitro* and *in vivo* of small anti-infective peptides towards Gram-negative plant pathogenic bacteria in a very specific manner without undermining their viability.

- To assess the peptides' efficacy to confer resistance towards *P. syringae* pv. *tabaci* into *Nicotiana tabacum* transgenic plants.

- To identify new sources rich in polyphenols using no food/feed vegetable residues of typical Mediterranean crops and to verify the inhibitory activity of polyphenolic compounds on master virulence systems of Gram-negative phytopatogenic bacterium *P. savastanoi* pv. *nerii*.

- To study the interaction among determinants of pathogenicity and virulence such as IAA, TTSS and MATE in *P. savastanoi* and to identify unexplored ideal targets to develop innovative molecules that can fight plant pathogenic bacteria.

# *Chapter 2*

# Peptides as inhibitors of the Type Three Secretion System for environmentally friendly control of plant disease caused by *P. syringae*

## 2.1 Abstract

The control and management of bacterial diseases of plants still rely mainly on applications of copper salts and antibiotics. In European Member States, antibiotics are not allowed for plant protection, while copper is among the very few chemicals still authorised in organic agriculture. Furthermore, it has been demonstrated that repeated copper-based treatments cause a dramatic increase of antibiotic-resistant bacteria into agroecosystems, due to a cross-selection mechanism, with risks for human and animal health.
Promising alternative options to copper are not yet available for the control of Gram-negative plant pathogenic bacteria including those belonging to the *Pseudomonas syringae* group.
For these reasons, based on secondary structure of the putative HrpA protein of *P. savastanoi* pv. *nerii* and confirmed by site-directed mutagenesis experiments, we identified and discovered the pivotal role that coiled-coil domains practice on the proper TTSS pilus assembly. From this finding, we designed a set of small peptides targeting the translocation of bacterial pathogenicity and virulence effectors by the Type Three Secretion System (TTSS), highly conserved and essential for the pathogenicity of Gram-negative bacteria, both of plants and of mammalian hosts including humans.
As a result of their distinguishing hallmark, these Virulence Inhibiting Peptides (VIPs) compromise the TTSS injection of Type Three Effectors (TTEs) into plant cells, instead of bacterial viability, thus to avoid or decrease the risk to develop any VIPs resistance. This innovative strategy based on these VIPs, using *P. savastanoi* pv. *nerii* as model system, has demonstrated a compromise *in vitro* and *in vivo* bacterial pathogenicity on hosts, and HR on Tobacco. VIPs-induced inhibition of the TTSS assembly was confirmed by Congo Red assay. Finally, no negative side-effects on model membranes and $Ca^{2+}$-ATPase were found.

**Key words:** Virulence Inhibiting Peptides; coiled-coil; Gram-negative bacteria; Type Three Secretion System; *P. syringae;* plant protection;

Biancalani C., Cerboneschi M., Biricolti S., Bogani P., Tadini-Buoninsegni F., Smeazzetto S., Tegli S. Peptides as inhibitors of the Type Three Secretion System for environmentally friendly control of plant disease caused by *P. syringae. Manuscript in preparation.*

## 2.2 Introduction

The most common strategy for controlling diseases caused by plant pathogenic bacteria is still based on application of bactericides, as it was decades ago. Formulations active in the control of phytopathogenic bacteria mainly include a variety of copper compounds, or other heavy metals, with or without pest-control chemicals added. Antibiotics and other organic bactericides are or have also been used, but to a lesser extent. In particular the use of antibiotics (*e.g.*, streptomycin) against plant pathogenic bacteria is not allowed all over Eureopean Union, while still are in USA and other Countries outside Europe such as Japan, Mexico and Israel: although the amount of antibiotics used on plants could be considered negligible when compared to that medical and veterinary uses (Perry and Wright, 2013; Smillie *et al*., 2011). Among the main undesirable effects observed either for the environment or for human and animal health, there is the selection in agroecosystems and agrosoils of bacteria resistant to antibiotics, which increase the frequency in the environment of antibiotic resistance genes that can be eventually transferred into medically relevant bacteria (Martinez and Baquero, 2014). In fact, the development and spread of resistance bacteria both copper and antibiotic in bacterial populations is strictly dependent and regulated by transmission of several genes and by several mechanisms, such as horizontal gene transfer, through conjugation of plasmids or transposable elements. These circumstances strongly undermine the effectiveness of these treatments (Mellanoù and Cooksey 1988; Gutirrez-Barranquero *et al*., 2013; Behlau *et al*., 2011). When a plant pathogenic acquires a resistance against these chemicals, the frequency of resistant strains into bacterial population could increase, resulting a less effective disease control. Different strategies have been introduced to fight this phenomenon, such as the use of health seed, the biological control by antagonistic microorganisms, the soil solarization, and the use of natural-occuring antibacterial compounds, in a frame of a sustainable agriculture where the use of chemicals is gradually decreasing (Lamichhane *et al*., 2015). Advances in the studies on bacterial pathogenicity and virulence factors have provided mounting evidences about the essential role of the Type Three Secretion System (TTSS) for the pathogenicity of a broad spectrum of Gram-negative bacteria, which infect both plant and mammalian hosts including humans (He *et al.*, 2004; Mota and Cornelis, 2005).

Genes required for Hrp pilus production are encoded by a distinct gene cluster called "hypersensitive reaction and pathogenicity" (*hrp*), which is present in the genomes of Gram-negative plant pathogens, including *Pseudomonas*, *Xanthomonas*, *Ralstonia* and *Erwinia* (Alfano and Collmer, 1997). The TTSS is a macromolecular complex of about 20 unique proteins extending from the bacterial cytosol across three membranes to the eukaryotic cytosol (Hueck, 1998). Until now, this syringe-like apparatus has been found and deeply studied in over two dozen of Gram-negative phytopathogenic bacteria, where it was shown to be very well conserved both structurally and functionally. Basically, TTSS is essential to cause disease into host plants by injecting pathogenicity and virulence effector proteins (named "Type Three Effectors", TTEs), that are highly specific of the host-pathogen interaction, directly into the cytosol of host cells. Among the structural proteins forming the TTSS apparatus, it is worth to mention the so-called "HrpA protein", which is the main component of the translocating pilus in the phytopathogenic bacteria belonging to the *Pseudomonas syringae* group. It was

demonstrated that in-frame deletion mutations in the chromosomal *hrpA* gene are able to abolish *P. syringae* pathogenicity on host plants, as well as induction of Hypersensitive Response on non-host plants such as Tobacco, and pilus production (Roine *et al*., 1997a; Roine *et al*., 1997b; Lee *et al.,* 2005). In other words, *hrpA* deletion mutants are defective both in type III secretion and in the elicitation of any TTSS-mediated host response (Wei *et al.*, 2000; Lee *at al*., 2005). Currently, it is known that HrpA protein from *P. syringae* pv. *tomato* DC3000 is a hydrophilic 11KDa protein encoded by the *hrpA* gene, but little is known about its molecular features for transporting effector proteins and only a few molecular details are known about subunit-subunit interaction during the TTSS needle assembly (Preston *et al*., 1995; Lee *et al*.,2005).

From the bioinformatic analysis of amino acid sequence corresponding to the putative HrpA protein of *P. savastanoi* pv. *nerii,* we found that the carboxy terminus of this protein comprises an α-helical region which demonstrates *heptad* periodicity, that is the basis of coiled-coils (Mason and Arndt, 2004). Site-directed mutagenesis of HrpA *heptad* residues, without altering α-helices secondary structure, generated HrpA mutants defective in the TTSS pilus assembly. The abolition of such coiled-coil domain without altering α-helix secondary structure generates HrpA mutant bacteria with a no-pathogenic or hypovirulent phenotype. Using these evidences, we designed a novel set of Virulence Inhibiting Peptides targeting coiled-coil domains of the HrpA protein and their possible use in plant protection has here depicted.

## 2.3 Materials and Methods

### Bacterial strains, media and growth conditions

The *P. savastanoi* pv.*nerii* (*Psn23*) and its mutants including *Agrobacterium tumefaciens* (EHA105) used in this study are listed in Table 1.

*Psn23* strains were routinely grown at 26°C as liquid or solid cultures, in King's B (KB) (King *et al.*, 1954) or in *hrp*-inducing Minimal Medium (MM) (Huynh *et al*., 1989), while *A. tumefaciens* EHA105 was grown and maintained on liquid or solid YEP medium at 28°C in the dark (An *et al*., 1988). Bacterial growth was monitored by determining the culture optical density at 600nm ($OD_{600}$) at different times during incubation, and bacterial concentrations were estimated by serial dilutions and plate counts. For long term storage bacteria were maintained at -20°C and -80°C in 40% (v/v) glycerol. *Escherichia coli* strains TOP10 and ER2925 were grown in Luria–Bertani (LB) liquid or agarised medium (Miller, 1972). Antibiotics, when required, were added into the medium at the following concentrations: 20 µg/ml streptomycin, 50 µg/ml nitrofurantoin, 10 µg/ml gentamicin, 50 µg/ml kanamycin and 40 µg/ml rifampicin.

**Table 1: Bacterial strains and plasmids used in this study.**

| Strain/Plasmid | Relevant characteristics | Reference/Source^ |
|---|---|---|
| **Strain** | | |
| *E. coli* TOP10 | F-, *mcr*A, Δ(*mrr-hsd*RMS-*mcr*BC) Φ80 *lac*ZΔM15 Δ*lac*X74 *rec*A1 *araD139* Δ(*araleu*)7697 *gal*U *gal*K *rps*L (StrR) *end*A1 *nup*G | Invitrogen, Carlsbad, USA |
| *E. coli* ER2925 | *ara*-14 *leu*B6 *fhu*A31 *lac*Y1 *tsx*78 *gln*V44 *gal*K2 *gal*T22 *mcr*A *dcm*-6 *his*G4 *rfb*D1 R(*zgb*210::*Tn*10)*Tet*S *end*A1 *rps*L136 *dam*13::*Tn*9 *xyl*A-5 *mtl*-1 *thi*-1 *mcr*B1 *hsd*R2 | NEB, Hertfordshire, UK |
| *P. savastanoi pv. nerii (Psn23)* | Wild type | LPVM collection |
| Δ*hrpA* | *hrpA* in-frame deletion mutant of *Psn23* | Chapter 5<br>This study |
| PF5αα | *hrpA* site-directed mutagenesis mutant of *Psn23* | This study |
| PF3αα | *hrpA* site-directed mutagenesis mutant of *Psn23* | |
| PF2αα | *hrpA* site-directed mutagenesis mutant of *Psn23* | This study |
| *A.tumefaciens*(EHA105) | C58 pTiBo542; T-region::aph, kan; derivative of EHA101 | Hood *et al.*, 1993 |
| **Plasmid** | | |
| pLPVM_T3A | $Gm^R$, lacz, mcs,*hrpA* promoter+*gfp* | Chapter 4 |
| pLPVM_T3A_AP17 | $Gm^R$, lacz, mcs,*hrpA* promoter+*ap17* | This study |
| pLPVM_T3A_LI27 | $Gm^R$, lacz, mcs,*hrpA* promoter+*li27* | This study |
| pK18mobsacB | sacB, lacZa, Km, mcs mobilizable vector | Schafer *et al.* 1994 |
| pK18- PF5αα | pK18mobsacB derivative, site-directed mutagenesis of the *hrpA* gene | This study |
| pK18- PF3αα | pK18mobsacB derivative, site-directed mutagenesis of the *hrpA* gene | This study |
| pK18- PF3αα | pK18mobsacB derivative, site-directed mutagenesis of the *hrpA* gene | This study |
| pCAMBIA1305.2 | $Gm^R$, $kan^R$, GUSPlus™, signal peptide | CAMBIA Labs, Austrialia |
| pCAMBIA1305.2*Δgus* | $Gm^R$, $kan^R$, *Δgus,* signal peptide | This study |
| pCAMBIA1305.2::AP17 | $Gm^R$, $kan^R$, *Δgus, ap17*, signal peptide | This study |
| pCAMBIA1305.2::LI27 | $Gm^R$, $kan^R$, *Δgus, li27*, signal peptide | This study |

^LPVM collection Laboratorio di Patologia Vegetale Molecolare (University of Florence)

### Molecular techniques

PCR, restriction digestion, ligation, DNA electrophoresis, and transformations were performed as described by standard procedure (Sambrook *et al*., 1989). The plasmids used and those generated in this study are listed in Table 1. Genomic DNA from *P. savastanoi* strains was extracted from single bacterial colonies using thermal lysis (Sambrook *et al*., 1989), or from bacterial cultures ($OD_{600}$=0.8), using Puregene® Genomic DNA Purification

Kit (Gentra Systems Inc., Minneapolis, MN, USA) according to manufacturers' instructions. DNA concentration was evaluated both spectrophotometrically, with NanoDrop™ ND-1000 (NanoDrop Technologies Inc., DE, USA), and visually by standard agarose gel electrophoresis [1% agarose (w/v) in TBE 1×] (Sambrook *et al.*, 1989). For plasmid DNA extraction, NucleoSpin® Plasmid (Macherey-Nagel GmbH and Co. KG, Düren, Germany) was used according to the manufacturer's protocol. Amplicons were purified from agarose gel with NucleoSpin® Gel and PCR clean-up (Macherey-Nagel GmbH and Co. KG, Düren, Germany) and double-strand sequenced at Eurofins Genomics (Ebersberg, Germany). Multiple sequence alignments and comparisons were performed using the computer package CLUSTALW (version 2, http://www.ebi.ac.uk/Tools/clustalw2) (Thompson *et al.*, 1994), and by means of Basic Local Alignment Search Tool (BLAST, http://www.ncbi.nlm.nih.gov/blast). Primers were designed using Beacon Designer 7.7 software (Premier Biosoft International, Palo Alto, CA, USA) (Table 2).

**Table 2: Primers used in this study.**

| Primer name | Primer sequence (5'-3') | Tm°C |
|---|---|---|
| Aa_hrpA_XbaI_For | TTTTCTAGAATCTGTACTTTCGCCTTAACG | 57 |
| Aa_hrpA_EcoRI_Rev | TTTGAATTCGGAAGTTATCTTCCTTGAGTTC | 57 |
| hrpA_CrossREVx2 | TTGGAAAGGGCTTCTTTCTTGTCTTCGAAGCCCGCGCGTTTGCTCGT | 62 |
| hrpA_CrossFORx2 | AAGACAAGAAAGAAGCCCTTTCCAACCAAATCGTTGCGAGCAAGATCCGG | 61 |
| hrpA_CrossREVx3 | TTGGAGCAGGCTTCTTTCTTGTCTTCGAAGCCCGCCAGCATGCTCGT | 62 |
| hrpA_CrossFORx3 | AAGACAAGAAAGAAGCCTGCTCCAACCAAGAAGACGCGAGCAAGATCCGG | 63 |
| hrpA_CrossREVx5 | TTGGAGCACATGGCTTCTTTCTTGTCTTCGAAGCCCGCCAGCATGCTCGT | 62 |
| hrpA_CrossFORx5 | AAGACAAGAAAGAAGCATCGTTGGCCTCCAACCAAGAAGACGCGAGCAAGATCCGG | 63 |
| Li27F_BamHI | TTTGGATCCCTGCTGCGTGAGACGAG | 59 |
| Li27R_KpnI | TTTGGTACCTCAGATCTTGCTCGCAACGATTT | 57 |
| Ap17F_BamHI | TTTGGATCCATGCTGGCGGGCTTCGAA | 60 |
| Ap17R_KpnI | TTTGGTACCAACGATTTGGTTGGAAAGGGC | 59 |
| CAMBIA_FOR | CTACTACTAAGCATTTGG | 51 |
| CAMBIA_REV | AACCCATCTCATAAATAAC | 51 |
| AP17_CAMBIA_FOR | TTTAGATCTATGCTGGCGGGCTTC | 55 |
| AP17_CAMBIA_REV | TTTCACGTGTCAAACGATTTGGTTGGAAAGGG | 58 |
| Li27_CAMBIA_FOR | TTTAGATCTCTGCTGCGTGAGACGAG | 59 |
| Li27_CAMBIA_REV | TTTAGATCTTCAGATCTTGCTCGCAACGATTT | 58 |

## Quantification of bacterial IAA synthesis

Indole quantification was conducted using Salkowski assay (Ehmann, 1977) (Chapter 5). Bacteria were grown on MM supplied with 250µM tryptophan, and indole production was measured after 24, and 48 h of growth. To this aim, bacterial suspensions were centrifuged at 5,000*g* for 15 min at 4°C, and 1 ml of supernatant was added to Salkowski's reagent. The reaction was incubated for 15 minutes at room temperature in the dark, and then the absorbance was measured using the spectrophotometer Infinite® M200PRO Quad4 Monochromators™-based (TECAN, Switzerland).

**Pathogenicity tests on oleander plants**

*In vitro* micropropagated oleander *(Nerium oleander* L.) (Vitroplant Italia s.r.l., Cesena, Italy), with red double flowers, were grown for 3 weeks at 26°C on MS (Murashige and Skoog, 1962) without addition of phytohormones, with a photoperiod of 16 h/light-8 h/dark. Then, plants were wounded on the stem at the second internode, using a 1 ml syringe needle, and immediately inoculated with 1 µl of a bacterial suspension in sterile physiological solution (SPS, NaCl 0.85% in distilled water), with an $OD_{600}$=0.5 (about $0.5\times10^8$ Colony Forming Unit/ml; CFU/ml). Negative control plants were inoculated with SPS alone. When required, the peptides were mixed at 60µM with bacterial suspension ($OD_{600}$ = 0.5) and inoculated direclty into wounded stem. Plants were then incubated at 26°C, and a 16 h/light-8 h/dark photoperiod, periodically monitored for symptoms appearance and photographic records were made at 7, 14 and 21 days and the bacterial growth was estimated in time course. Three independent experiments were performed, and nine plants for each *P. savastanoi* strains were used in each run.

**Hypersensitive response assay**

Hypersensitive Response (HR) assay was performed on *Nicotiana tabacum* (var. Burley White), grown at 24°C, with a relative humidity of 75% and a photoperiod of 16/8-h light/dark. Bacterial cultures were grown overnight in KB medium at 26°C, resuspended in SPS to an $OD_{600}$ of 0.5, and bacterial cell concentration was confirmed by a serial dilution plating method. When required the peptides were diluted up to 60 µM in sterile distilled water and co-infiltrated with *Psn23* $OD_{600}$ = 0.5, (approximately $0.5x10^8$ CFU/ml). Using a 2 ml blunt-end syringe, approximately 100 µl of bacterial suspension was injected into abaxial mesophyll of fully expanded leaves of three tobacco plants (Baker, 1987), with six replicates for each strain tested, and for each of the three independent experiments carried out. The development of HR was assessed according to the macroscopic tissue collapse at 24 and 48 h post-inoculation, taking photographic record of the results obtained.

**Spectrophotometric and fluorometric analysis**

*In vitro* growth analysis was performed for *Psn23* wild type and its mutants inoculated on MM and KB medium supplemented or not with anti-virulence peptides herein tested. Antibiotic activity of AP17 and LI27 peptides was evaluated *in vitro* by monitoring the bacterial growth as optical density at 600 nm ($OD_{600}$), at different times during 24h incubation with these peptides using the spectrophotometer Infinite® M200PRO Quad4 Monochromators™-based (TECAN, Switzerland). Bacterial cells were cultured in KB medium at 26°C overnight, and after two washes in sterile physiological solution (SPS, 0.85% NaCl in distilled water) the bacterial pellet was resuspended adjusting to a final $OD_{600}$ = 0.5 in MM or KB, supplemented or not with the anti-virulence peptides at concentrations ranging from 10 to 60 µM.

To verifiy the *hrpA* promoter inhibition by AP17 and LI27 peptides, *Psn23* bacterial cells carrying the promoter-probe plasmids pLPVM_T3A (Table 1) were cultured overnight on KB medium at 26°C. Then their pellet was washed twice with SPS, and inoculated in MM (final $OD_{600}$ = 0.5) supplemented with AP17 or LI27 at concentrations ranging from 10 to 60 µM. Wild type *Psn23* carrying the empty vector was used as control. The experiments were carried

out into 24 multiwell plates (BIOFIL®, Guangzhou, China) at different time during 24h of incubation. The promoter activity of *hrpA* was then analyzed and quantitatively assessed, using the multimode microplate reader Infinite®M200PRO Quad4 Monochromators™-based (TECAN), by simultaneously measuring the GFP intensity and the bacterial growth.

**Congo Red assay**

*Psn23* cells were grown on MM liquid medium ($OD_{600}$ = 0.2), supplemented or not with the anti-virulence peptides here examined at 60 μM, and incubated at 18°C for 24 h with continuous shaking (100rpm). After 24 h incubation, the concentration of bacterial cultures was evaluated as $OD_{600}$, and then the dye Congo red (SIGMA-Aldrich Co.) was added (10 μg/ml), followed by a further incubation at 18°C for 1h, under shaking. Bacterial cells were removed by centrifugation (5000*g* for 10min.), and 1 ml supernatant for each sample was then aliquoted into 24 multiwell plates (BIOFIL®). The absorbance value at 490 nm ($OD_{490}$) was recorded by spectrofluorimetry using Infinite® M200PRO (TECAN). Data analysis were performed as reported in Chapter 4.

**Generation of PF5αα, PF3αα and PF2αα *Psn23* mutants by site-directed mutagenesis**

The *Psn23* PF5αα, PF3αα and PF2αα mutants were constructed by site-directed mutagenesis of *hrpA* gene from *Psn23* wild type genome (Table 1), using marker exchange mutagenesis (Yang *et al*., 2002). Copies mutated by substitution in specific amino acids of *hrpA* nucleotide sequence, were generated by primers reported in Table 2. PF5αα, PF3αα and PF2αα final constructs were generated by overlap extension PCR, using the primers reported in Table 2. The plasmids generated in this study to obtained final genomic mutants are based on *pK18mobsacB*, a suicide vector for *P. syringae sensu lato* allowing for SacB counterselection (Hagen *et al*., 2002; Zazìmalovà *et al*., 2007), and are listed in Table 1. The intermediate vectors were first transferred by electroporation with Gene Pulser XCell™ (Bio-Rad Laboratories Inc., Hercules, CA, USA) into *E.coli* TOP10 cells then into *E.coli* ER2925, which mimicks the methylation profile of *Psn23*, finally into electrocompetent *P. savastanoi* pv. *nerii* cells that were obtained as previously described (Pèrez-Martìnez *et al*., 2010). $Suc^R$ colonies were screened by PCR, and the marked deletions were then confirmed by sequencing.

**Transgenic transient expression of AP17 and LI27 peptides**

Agroinfiltration experiments were performed on *in vitro* micropropagated oleander (*Nerium oleander* L.) (Vitroplant Italia s.r.l., Cesena, Italy), with red double flowers. Plants were grown for 3 weeks at 26°C on MS (Murashige and Skoog, 1962) without addition of phytohormones, in a chamber with a photoperiod of 16 h/light-8 h/dark before infiltration. Binary vectors in *A. tumefaciens* EHA105 strain transformed bacteria were obtained from pCAMBIA1305.2, after double digestion with BglII and PmlI to remuove GUSplus™ sequence and to obtain the intermediate pCAMBIA1305.2*Δgus* vector. After double digestion with BglII and PmlI, the nucleotide sequences corresponding to AP17 and LI27 were inserted in pCAMBIA1305.2*Δgus*, downstream the GRP signal sequence using the primers reported in Table 2 and the final vectors named pCAMBIA1305.2::AP17 and pCAMBIA1305.2::LI27

were obtained. Intermediate vectors were first transferred by electroporation with Gene Pulser XCell™ (Bio-Rad Laboratories Inc., Hercules, CA, USA) into *E.coli* TOP10 cells and then electroporated into *A. tumefaciens* EHA105.
Transformed *A. tumefaciens* cultures were grown in a shaker overnight at 24°C at 200 rpm in YEP media (An *et al*., 1988) (1% peptone, 1% yeast extract, and 0.5% NaCl) (3 ml) containing 50 mg/l rifampicin and 50 mg/l kanamycin to select for transformed *Agrobacterium* cells. Optical density at 600 nm was taken on starter cultures by spectrofluorimetry using Infinite® M200PRO (TECAN). Starter cultures were used to inoculate two 25 ml cultures to an $OD_{600}$ of 0.004 and grown overnight. Infiltration suspensions for each vector were brought to $OD_{600}$ of 0.5 x $10^{\wedge 6}$ CFU. The co-infiltration inoculum was prepered at different concentration of *Psn23* wild type bacteria ranging from 0.5 x $10^{\wedge 6}$ CFU to 0.5 x $10^{\wedge 4}$ CFU and fixed concentration of *A. tumefaciens* transformed with pCAMBIA1305.2::AP17 or pCAMBIA1305.2::LI27 (0.5 x $10^{\wedge 6}$ CFU). *In vitro* oleander plants were wounded on the stem at the second internode, using a 1 ml syringe needle, and immediately inoculated with 1 µl of bacterial suspension mixtures. After infiltration, plants were placed back into the growth chamber and at 7 days post-infiltration (dpi) monitored for symptoms development and used to evaluate *in planta* bacterial multiplication.

**Biomimetic membrane analysis**
The anti-virulence peptides here examined were investigated for their effects both on $Ca^{2+}$-ATPase and on synthetic bilayer lipid membranes (BLMs).
Current measurements were carried out on sarcoplasmic reticulum (SR) vesicles containing $Ca^{2+}$-ATPase adsorbed onto a hybrid alkanethiol/phospholipid bilayer anchored to a gold electrode (the so-called Solid Supported Membrane, SSM) (Tadini-Buoninsegni *et al.,* 2006). The experiment, including SR vesicles preparation and reagents were performed as reported in Chapter 4. To investigate the effects of anti-virulence peptides on current signals generated by $Ca^{2+}$-ATPase, the required concentration of each compound was added to both the non-activating and activating solutions. The ATP-induced current signal observed in the presence of AP17 and LI27 was compared to the control measurement obtained in the absence of the compound. To prevent $Ca^{2+}$ accumulation into the vesicles, 1 µM calcium ionophore A23187 (calcimycin) was used. The concentration jump experiments were performed by the $SURFE^2R^{One}$ device (Nanion Technologies, Münich, Germany). The temperature was maintained at 22–23°C for all the experiments. To verify the reproducibility of the current signals on the same SSM, each single measurement was repeated six times, and then averaged to improve the signal to noise ratio. Standard deviations did not exceed 5%. Moreover, each set of measurements was reproduced using two different SSM sensors.
BLMs experiments were conducted in 250 mM KCl, 10 mM MOPS in Tris buffer pH 7, in both the chambers (1.3 mL per chamber) in a set up instruments constituted by Axon digidata 1322A and Axopatch 200B amplifier. The lipid utilized was diphytanoylphosphatidylcholine (DPhPC) (Avanti Polar Lipids, Alabaster, AL) suspended in pentane 10 mg/mL. The final amount of lipids used to form the bilayer was 100 µg per chamber; the pore connecting the two chambers corresponded to an area of around 78.5 $\mu m^2$. The formation of the lipid bilayer was accomplished through the folding method and the typical change in colour was visibibly

evaluated through a stereomicroscope and through the current recorded after the imposition of a square potential excitement.
Through a voltage clamp protocol (step protocol:-120mV-+120mV) we recorded the response of the system in terms of current (pA). Before the addition of the peptides, the bilayer conductance was continuously recorded for 1h in order to exclude artefacts from contamination. Signals were recorded with Clampex Softwere 10.2 (Elecrophysiology Data Acquisition & Analysis).

**Bioinformatic analysis**

Several bioinformatic analysis were carried out through open source software described below. SignalP 4.1 server (http://www.cbs.dtu.dk/services/SignalP) was consulted to predict the presence and location of signal peptide in amino acid sequence of the putative HrpA protein, while CELLO v2.5: subCellular Localization (http://cello.life.nctu.edu.tw) and TMHMM-2.0 (http://www.cbs.dtu.dk/services/TMHMM-2.0) to predict transmembrane protein topology. Secondary structure of HrpA protein was predicted by the Predict Protein server (https://www.predictprotein.org/). The coiled-coil interactions were identified by Paircoil2 (http://groups.csail.mit.edu/cb/paircoil2) and COILS (http://embnet.vital-it.ch/software/COILS_form.html) statistical analysis programs. The secondary structure prediction of HrpA wild type and PF5αα, PF3αα and PF2αα mutants was performed by YASPIN (http://www.ibi.vu.nl/programs/yaspinwww) and COILS. For peptide sequence characterisation, including hydrophobicity profile was used INNOVAGEN bioinformatics tool (http://www.innovagen.se/custom-peptide-synthesis/peptide-property-calculator/peptide-property-calculator.asp).

**Statistical analysis**

All the experiments in this study were performed in triplicate and repeated three times, unless otherwise stated. The data were presented as the means ± standard deviation (SD) and subjected to one-way analysis of variance (ANOVA) using PAST software (Version 3.11, Øyvind Hammer, Natural History Museum, University of Oslo). When ANOVA indicated a significant difference ($P < 0.05$), a Tukey-Kramer post-test was performed.

## 2.4 Results

### C-terminal portion of the HrpA protein is characterised by a coiled-coil motif

The organization of the TTSS cluster in *P. savastanoi* pathovars appears to be highly conserved, it is 23,835 bp long and it is composed of twenty-seven genes, most of which arranged in five operons organized in two main blocks having convergent genes transcription (Tegli *et al*., 2011). The *hrpA* gene is located in this cluster together with other genes codifying for the proteins of the TTSS. This gene is 327 bp long, codifying for a protein of 108 amino acids (about 11 kDa) and the gene locus is preceded by a typical *hrp box* (Frederick *et al*., 2001; Wei and Beer, 1995).

From these evidences, the amino acid sequence of the putative HrpA protein of *P. savastanoi* pv. *nerii* was obtained and bioinformatic analyses were performed in order to achieve specific information on this protein. At the N-terminus position of the HrpA protein, from 1 to 10 amino acids (aa), a signal peptide was predicted by SignalP4.1 (Figure S1A). The protein localisation outside cellular membrane, with hight score for periplasmatic space, was confirmed based on physic-chemical composition by two different bioinformatics tools CELLO v2.5 and TMHMM (Yu *et al.*, 2006; Krogh *et al.*, 2001) (Figure S1B). The secondary structure of the HrpA protein was predicted with Protein server (Rost *et al.*, 2004) (Figure S2). The C-terminal portion (from 69 to 101 aa) was constituted by an α-helices region, which demonstrates heptad periodicity and where positions *a* and *d* in the *heptad* repeat unit *abcdefg* are occupied by hydrophobic residues, while *e* and *g* are occupied by polar and charged residues indicating a propensity for coiled-coil domain (Figure 1). This evidence was completely confirmed using Paircoil2 and COILS statistical analysis programs (McDonnell *et al*., 2006), where in correspondence of α-helix region a very hight score for coiled-coil was recorded (Figure S2).

**Figure 1: A) C-terminal amino acid sequences of putative HrpA protein of *P. savastanoi* pv. *nerii* and PF mutants. In yellow (from 75 to 102 AA) is indicated the α-helices region with heptad periodicity "*abcdefg*", positions "*a*" and "*d*" are occupied by hydrophobic residues, while *e* and *g* are occupied by polar and charged residues. Bold letters in the amino acid sequences indicate amino acid substitutions. B) Amino acid sequence of LI27 (bold red colour) and AP17 (bold blue colour), long 27 and 17 aa respectively.**

**A)**

```
                                abcdefgabcdefgabcdefgabcdefg
hrpA          KSSELDGTANEENGLLRETSMLAGFEDKKEALSNQIVASKIRNSVVQF
PF5aa         KSSELDGTANEENGLLRETSKRAGFEDKKEACSNQEDASKIRNSVVQF
PF3aa         KSSELDGTANEENGLLRETSMLAGFEDKKEACSNQEDASKIRNSVVQF
PF2aa         KSSELDGTANEENGLLRETSKRAGFEDKKEALSNQIVASKIRNSVVQF
```

**B)**

```
Li27                          LLRETSMLAGFEDKKEALSNQIVASKI
AP17                               MLAGFEDKKEALSNQIV
```

**Bacterial mutants impaired in coiled-coil domain show a non pathogenic phenotype**

To confirm what we have found by *in silico* analysis on the HrpA protein and to better understand the importance of such interactions on the TTSS pilus assembly, we have set up three bacterial mutants by site-directed mutagenesis on *hrpA* nucleotide sequence (Accession Number GeneBank FR717897.2). These bacterial mutants denominated PF5αα, PF3αα and PF2αα (PF mutants) (Table 1) have mutated five, three and two amino acids compared to the wild type HrpA sequence, respectively. The introduced amino acid substitutions, starting from the nucleotide sequence of HrpA and respecting the codon usage of *P. savastanoi* have been chosen as reported in Figure 1A. In particular, PF5αα mutant presents five substitutions at 81, 82, 92, 96 and 97 position, where the hydrophobic amino acids, methionine (M), leucine (L), leucine (L), isoleucine (I) and valine (V), have been replaced by polar and charges amino acids such as lysine (K), arginine (R), cysteine (C), glutamic acid (E) and aspartic acid (D), respectively. PF3αα mutant presents three substitutions at 92, 96 and 97 position with amino acids cysteine (C), glutamic acid (E) and aspartic acid (D) and PF2αα mutant have substitutions at 81 and 82 position with amino acids lysine (K) and arginine (R). These mutations have been chosen in such a way to eliminate the coiled-coil interactions without altering the α-helices secondary structure as verified and confirmed by bioinformatic analyses (Figures 2 and 3). Results obtained show that the substitutions at 81 and 82 positions do not modify the coiled-coil interaction, while amino acids at 92 and 96 positions appear to be fundamental and directly involved in the coiled-coil interaction. It is important to highlight that the coiled-coil motif in PF5αα mutant is completely abolished, while in PF2αα, in which the amino acids at 92 and 96 positions are not substituted, the coiled-coil region is almost completely restored (Figure 3).

**Figure 2: Output obtained by YASPIN for wild type HrpA and PF5αα, PF3αα PF2αα mutants. α-helix structure is preserved in all four cases, shown in yellow. The amino acids mutated are shown in red colour.**

```
*   AA: Target sequence
* Pred: Predicted secondary structure (H=helix, E=strand, -=coil)
* Conf: Confidence (0=low, 9=high)
*Hconf: Confidence of helix  predictions
*Econf: Confidence of strand predictions
*Cconf: Confidence of coil   predictions
```

**HrpA**

```
AA:   MSIISSLTNAGRGVVNTVGGAAQGINSVKSSADRNIALTKNTGSTDSIDATRSSISKGDA
Pred: ----HHHHH---EEEE----HHHHHHHHHHHHHH---EEE-------HHHHHHHHHH---
Conf: 9311102520123312243121110102331644111213426765126277841036 77

Hconf: 000087999720000000039788747998999930100000000049999999999000
Econf: 023300000000998000001000000000000022989000000000000000000000
Cconf: 976612000278000199960001142001000066601099999950000000000999

AA:   KSSELDGTANEENGLLRETSMLAGFEDKKEALSNQIVASKIRNSVVQF
Pred: ---HHHHHHHHHHHHHHHHHHHHHHHHHHHHHHHHHHHHHH-EEE-
Conf: 64201111544000024458686564231120010236787111124 9

Hconf: 011488899999247999999999999989986599999999820000
Econf: 000201000000000000000000000000000000000000009990
Cconf: 987300000000752000000000000010013400000000160009
```

**PF5αα**

```
AA: MSIISSLTNAGRGVVNTVGGAAQGINSVKSSADRNIALTKNTGSTDSIDATRSSISKGDA
 Pred: ----HHHHH---EEEE----HHHHHHHHHHHHHH---EEE-------HHHHHHHHHH---
 Conf: 92110023203243122331211203133316431101133267651363778420367 7

Hconf: 000075999500000001039898988998999930000000000049999999999000
Econf: 024400000001999900000000000000000004599900000000000000000000
Cconf: 974513000498000098950001011001000065400099999950000000000999

   AA: KSSELDGTANEENGLLRETSKRAGFEDKKEACSNQEDASKIRNSVVQF
 Pred: ---HHHHHHHHHHHHHHHHHHHHHHHHHHHHHHHHHHHHHH-EEE-
 Conf: 631011214440000245486864642311121212358872101249

Hconf: 012488899999258999999999999998988329999999840000
Econf: 000100000000000000000000000000000000000000009890
Cconf: 987400000000741000000000000010116700000000150009
```

**PF3αα**

```
AA: MSIISSLTNAGRGVVNTVGGAAQGINSVKSSADRNIALTKNTGSTDSIDATRSSISKGDA
 Pred: ----HHHHH---EEEE----HHHHHHHHHHHHHH---EEE-------HHHHHHHHHH---
 Conf: 93111024203243122331211203133216431101133267651363778420367 7

Hconf: 000086999600000001039898988998999930000000000049999999999000
Econf: 024300000001999900000000000000000003499900000000000000000000
Cconf: 975512000388000098950001011001000065400099999950000000000999

   AA: KSSELDGTANEENGLLRETSMLAGFEDKKEACSNQEDASKIRNSVVQF
 Pred: ---HHHHHHHHHHHHHHHHHHHHHHHHHHHHHHHHHHHHHH-EEE-
 Conf: 642001114440001245586865642311121112358872101249

Hconf: 011388899999258999999999999998988329999999840000
Econf: 000100000000000000000000000000000000000000009890
Cconf: 988410100000741000000000000010116700000000150009
```

**PF2αα**

```
   AA: MSIISSLTNAGRGVVNTVGGAAQGINSVKSSADRNIALTKNTGSTDSIDATRSSISKGDA
 Pred: ----HHHHH---EEEE----HHHHHHHHHHHHHH---EEE-------HHHHHHHHHH---
 Conf: 9311102420224312233121110213331643110113436765126277841036 77

Hconf: 000086999610000001049898978998999930000000000049999999999000
Econf: 024300000001999900000000000000000003499900000000000000000000
Cconf: 975512000388000098950000021001000065500099999950000000000999

   AA: KSSELDGTANEENGLLRETSKRAGFEDKKEALSNQIVASKIRNSVVQF
 Pred: ---HHHHHHHHHHHHHHHHHHHHHHHHHHHHHHHHHHHHHH-EEE-
 Conf: 642001114440001355486864642311200102367871111249

Hconf: 001488899999358999999999999998998659999999820000
Econf: 000101000000000000000000000000000000000000009990
Cconf: 998300000000641000000000000010013400000000170009
```

**Figure 3: Output obtained by COILS service. Colour lines indicate coiled-coil motifs, which are present in HrpA and PF2αα, while in PF5αα and PF3αα are completely or partially removed.**

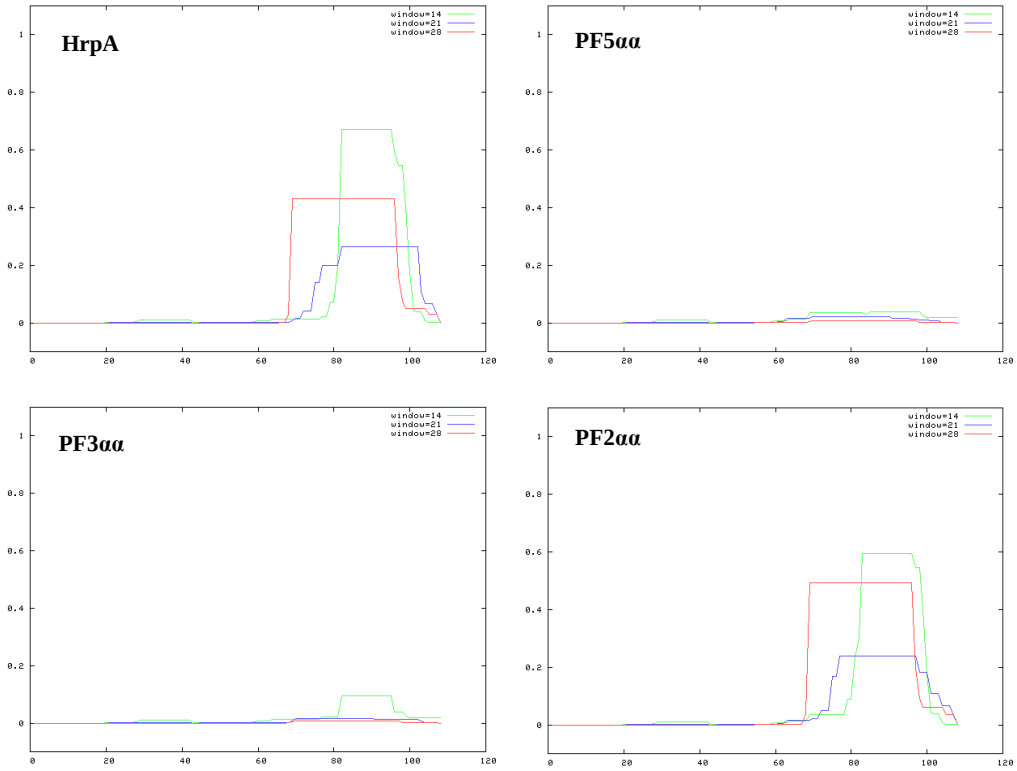


As reported in Chapter 4, to quantitatively evaluate variations in the TTSS pilus assembly a Congo red-based assay was performed on PF5αα, PF3αα, and PF2αα bacterial mutant cultures. Data obtained are consistent with bioinformatic analysis, in fact, PF5αα, PF3αα and PF2αα bacterial mutants show a percentage of dye adsorption of 18%, 35% and 75%, respectively (Figure 4). The direct involvement of these mutations on correct functionality of the TTSS pilus was confirmed following infiltration of PF bacterial mutants on Tobacco leaves. PF5αα and PF3αα strongly reduce HR response comparable to Δ*hrpA* mutant included as positive control, while PF2αα shows only a slight reduction (Figure 5).

**Figure 4: Percentage of Congo red dye absorption of PF5*αα*, PF3*αα* and PF2*αα* bacterial cultures, grown in MM. The data were calculated according to the formula: $[(X_{unk}-X_{\Delta hrpA}) / (X_{WT}-X_{\Delta hrpA})] *100$ where $X_{WT}$ and $X_{\Delta hrpA}$are the ratio $OD_{490}/OD_{600}$ for *Psn23* and *ΔhrpA* respectively. The data represent the means ± SD of three replicates. Results obtained are statistically significant (*P* <0.05).**

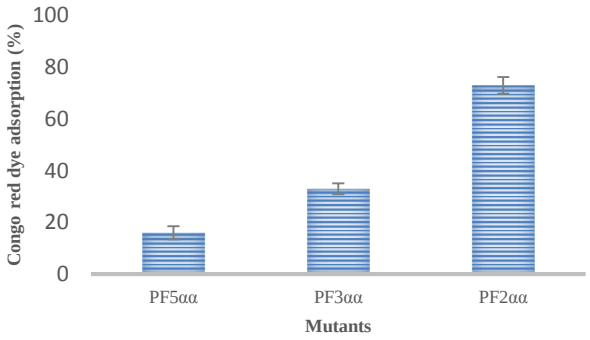


**Figure 5: Hypersensitive Response assay on Tobacco leaves at 48h after infiltration of *Psn23* wild type bacteria (WT), PF5*αα*, PF3*αα* and PF2*αα*. As control, sterile physiological solution (FS) and Δ*hrpA* mutant were used.**

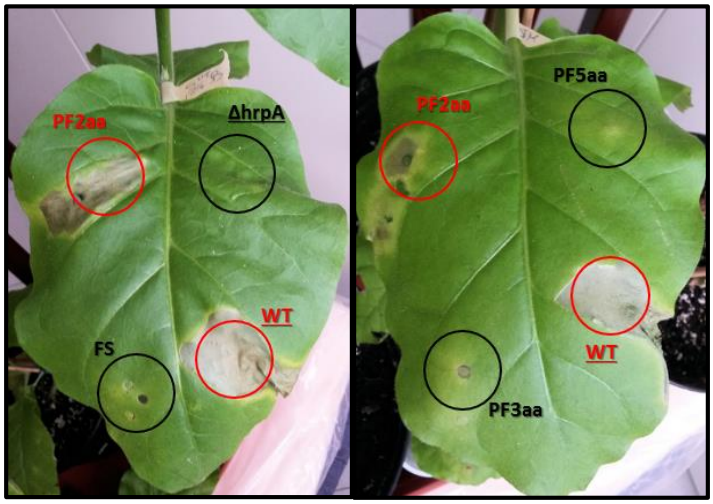


Finally, to establish the PF mutants' phenotype, pathogenicity trials on *in vitro* oleander plants were performed. As shown in Figure 6 plants inoculated with PF5αα and PF3αα show an absent or very little gall formation comparable to Δ*hrpA* (positive control), while plants inoculated with PF2αα show a reduced gall in comparison to *Psn23* wild type bacteria. Moreover, *in planta* bacterial growth rate at 7, 14, 21 dpi (days post inoculation) confirm a strong decrease of bacterial multiplication following inoculation with PF5αα and PF3αα, respectively (Figure 6).

**Figure 6: on the top) Pathogenicity trials of micropropagated oleander plants conducted using *Psn23* and its mutants Δ*hrpA*, PF5αα, PF3αα and PF2αα at 14 and 21 days post inoculation (dpi). On the bottom) *In planta* bacterial growth at 7, 14 and 21 (dpi), in blu colour (*Psn23* wild type), in red (PF5αα), in green (PF3αα), in violet (PF2αα) and in yellow (Δ*hrpA*) as positive control. Values are the mean of three independent experiments with nine replicates for each strain ± standard deviation (SD). ANOVA revealed statistically significant differences ($p<0.05$), comparison using the Tukey post-test are indicated by letters, where different letters indicate statistically significant differences.**

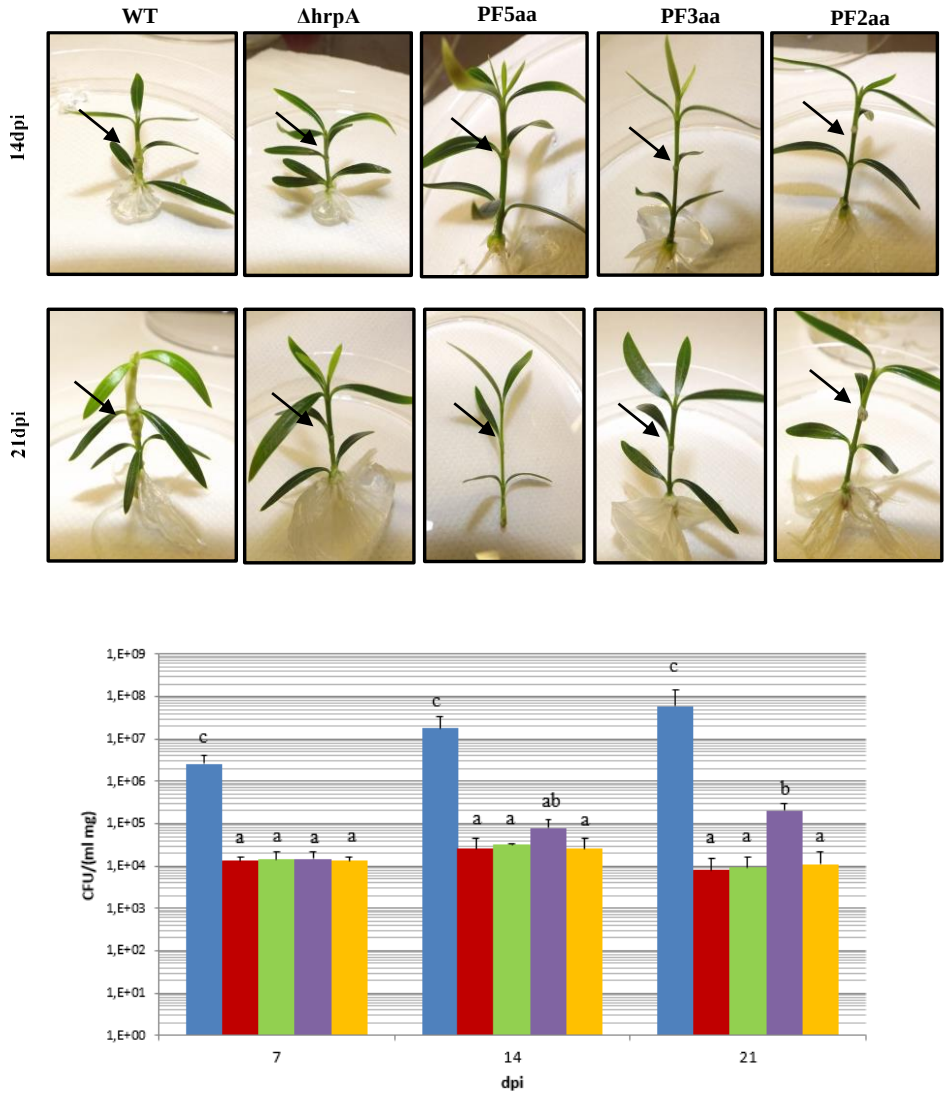


To rule out any variations in growth and IAA (acid-3-indol acetic) metabolism in PF5αα, PF3αα, and PF2αα mutants, we have analysed *in vitro* the bacterial growth rate and indole production. The bacterial growth was measured both in minimal and in rich medium. The indole production was recorded at 24 and 48 h by Salkowski assay on MM supplied with tryptophan, precursor to IAA (closely involved in *Psn23* hyperplastic gall formation)(Rodríguez-Moreno *et al.*, 2008; Quesada *et al.*, 2012), without recorded any fluctuation compared to wild type bacterial cells (Figures 7 and 8).

**Figure 7: *In vitro* bacterial growth rate in KB medium (A) and MM medium (B). Green line indicates PF5αα mutant; orange line PF3αα mutant; blu line PF2αα mutant and red line *Psn23* wild type.**

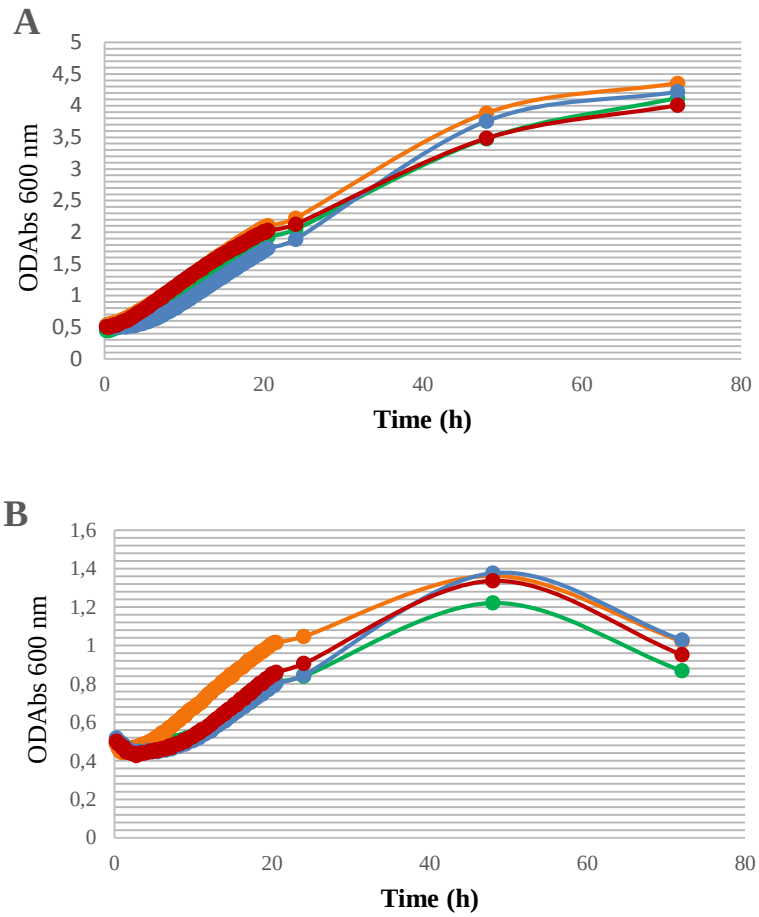


**Figure 8: Quantification of IAA production using the Salkowski assay for *Psn23* and its PF5αα, PF3αα, and PF2αα mutant supernatants at 24 (green) and 48 h (blue) post-inoculation on MM supplemented with L-Trp (250 µM). The data are expressed as the average of three replicates ± standard deviation (SD). Statistically significant differences are represented by different letters above the bars (ANOVA and the Tukey test, p<0.05).**

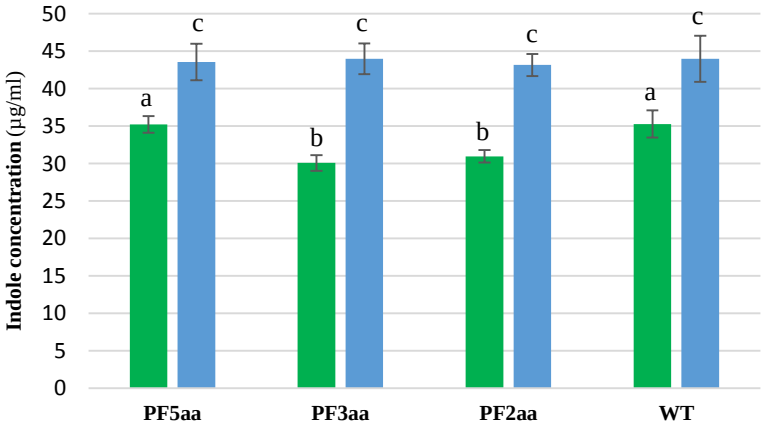

**Design and performance of Virulence Inhibiting Peptides (VIPs)**

Based on obtained results we have hypothesised that single monomers of HrpA protein interact each other through hydrophobic bonding between *a / d* position residues at the interface of the helical bundle, which provides the driving force for the interaction and influences the oligomerisation state of the coiled-coil to form the entire translocation pilus.

Thus, according to amino acid residues present in the hydrophobic surface of HrpA protein, supposed to be involved in the TTSS pilus assembly, and as suggested by phenotypic analysis carried out on PF5αα, PF3αα, PF2αα mutants, two different peptides were designed and their chemically synthesis obtained by Proteogenix (Oberhausbergen, France). These small peptides, named AP17 and LI27, are 17 and 27 amino acids long, respectively. Their sequences are perfectly homologous at a portion on HrpA protein, from 81 to 97 aa for AP17, and from 75 to 101 aa for LI27. Their physical-chemical profile was analysed by INNOVAGEN bioinformatic tool, AP17 shows a higher hydrophobicity profile than LI27 (Figure S3). Preliminary tests were conducted to ascertain their applicability, excluding their antibiotic effect and verifying their specific activity against the TTSS pilus assembly. As preliminary verified these peptide do not trigger any plant defense responses and to exclude any phytotoxic effect, AP17 and LI27 were infiltrated into the mesophyll of Tobacco leaves until 60 µM, without observing any unspecific phytotoxicity (data not shown). Moreover, when AP17 and LI27 were co-infiltrated with *Psn23* wild type cells, a strong reduction in HR symptoms was found at 60 µM for AP17, while only a significant reduction was recorded for LI27 (Figure 9). To further demonstrate the highly specific effect of AP17 and LI27 on the TTSS machinery, we investigated their impact on the TTSS pilus assembly through a Congo red-based assay to quantitatively evaluate variation in dye adsorption in *Psn23* cells after treatment with these Virulence Inhibiting Peptides (Table 3). Finally, we have evaluated their effect on *hrpA* promoter by using the *gfp*-reporter fusion construct pLPVM_T3A and we have excluded any bacterial growth inhibition after treatment with these peptides by monitoring *in vitro* bacterial growth (Table 3). As previously reported *hrpA* gene is situated downstream of TTSS regulation pathway, and presumably the HrpA protein acts upstream stimulating TTSS genes expression (Tang *et al.,* 2006). For this reason, it was highlighted a possible involvement of the HrpA protein in a positive feedback regulation, although still not entirely clarified (Wei *et al*., 2000). Under inducing conditions, the HrpA protein activates the transcription of the upstream genes, carrying out a fundamental role in the transcriptional activation of TTSS genes. The fluorescent signal inhibition corresponding to a down activation of *hrpA* promoter could be related indirectly to this regulation where the HrpA protein is involved. The effect obtained on *hrpA* promoter activity after application of AP17 peptide was thus in frame with previous reports (Table 3). It could be hypothesised that AP17 peptide binds to HrpA monomer, sequestering this protein and making it less available as trascriptional activator of TTSS pathway, resulting in a total or partial block of this system.

Therefore, data obtained confirm the inhibitory activity of these peptides both *in vitro* and *in planta* against *Psn23* and in all analyses performed AP17 has shown a better performance than LI27.

**Figure 9: Hypersensitive response after infiltration of *Psn23* wild type with different concentration of LI27 and AP17 (30 and 60µM), respectively. FS indicates infiltration with only physiological solution (control).**

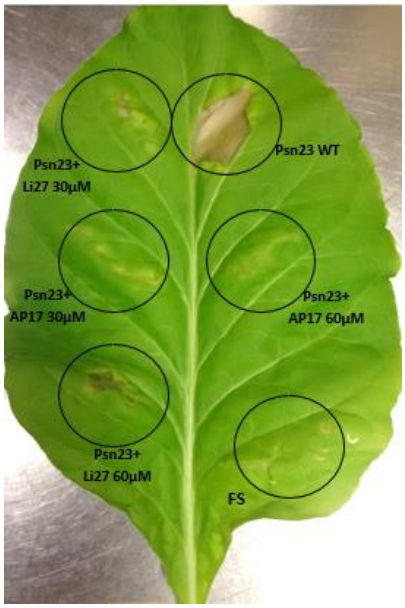


**Table 3: Effect on bacterial growth in MM and KB, on the trans-activation of *hrpA* promoter and on TTSS pilus assembly of the AP17 and LI27 peptides tested in this study. Common letters indicate differences not statistically significant at p<0.05 according to Tukey's test.**

| VIPs | Bacterial growth in MM ($OD_{600}$) | Bacterial growth in KB ($OD_{600}$) | *hrpA* promoter* | Congo red dye§ adsorption % |
|---|---|---|---|---|
| **LI27** | $0.95 \pm 0.18^a$ | $1.15 \pm 0.18^a$ | $0.92 \pm 0.11^a$ | $75 \pm 1.8^a$ |
| **AP17** | $1.00 \pm 0.11^a$ | $1.05 \pm 0.16^a$ | $0.64 \pm 0.12^a$ | $12 \pm 1.5^b$ |
| **Kanamycin** | $0.45 \pm 0.16^b$ | $0.39 \pm 0.19^b$ | $0.23 \pm 0.15^b$ | - |

* $OD_{600}$ was recorded after 24h growth and data are calculated as GFP Abs $_{(Ex.485nm;\ Em.535nm)}$ / Abs $_{(600nm)}$ ± SD, and as normalized fold versus untreated bacterial cultures.

§ $[(X_{unk}-X_{\Delta hrpA})/(X_{WT}-X_{\Delta hrpA})]*100$ where:
$X_{WT}$ and $X_{\Delta hrpA}$ are the ratio $OD_{490}/OD_{600}$ for *Psn23* and *ΔhrpA* respectively.

## Virulence inhibiting peptides-expressing *Psn23* mutants

To further confirm our results we have generated bacterial mutants able to synthesize these peptides into their cytoplasm under *hrpA* promoter control, in order to obtain an instrument where the TTSS pilus assembly and peptides synthesis can take place in the same time and under the same stimuli. For this purpose we have transformed *Psn23* wild type bacteria with the expression vectors pLPVM_T3A+AP17 and pLPVM_T3A+LI27, respectively. The obtained mutants have been identified as T3A_AP17 and T3A_LI27, respectively. Their phenotype was analysed both by pathogenicity tests (Figure 10) and by assays directed on the TTSS functionality such as HR and Congo red (Figure 11), confirming their inhibitory effect.

**Figure 10: A) Pathogenicity test on micropropagated oleander plants with *Psn23* T3A_AP17 (left side) and *Psn23* T3A_LI27 (right side), below with PF5αα as positive control. B) Bacterial growth rate at 7, 14 and 21days post-inoculation (dpi), in blu color (*Psn23* wild type), in red (PF5αα) as positive control, in green (T3A_AP17) and in violet (T3A_LI27). Values are the mean of three independent experiments with nine replicates for each strain ± standard deviation (SD). ANOVA revealed statistically significant differences (p<0.05), comparison using the Tukey post-test are indicated by letters, where different letters indicate statistically significant differences.**

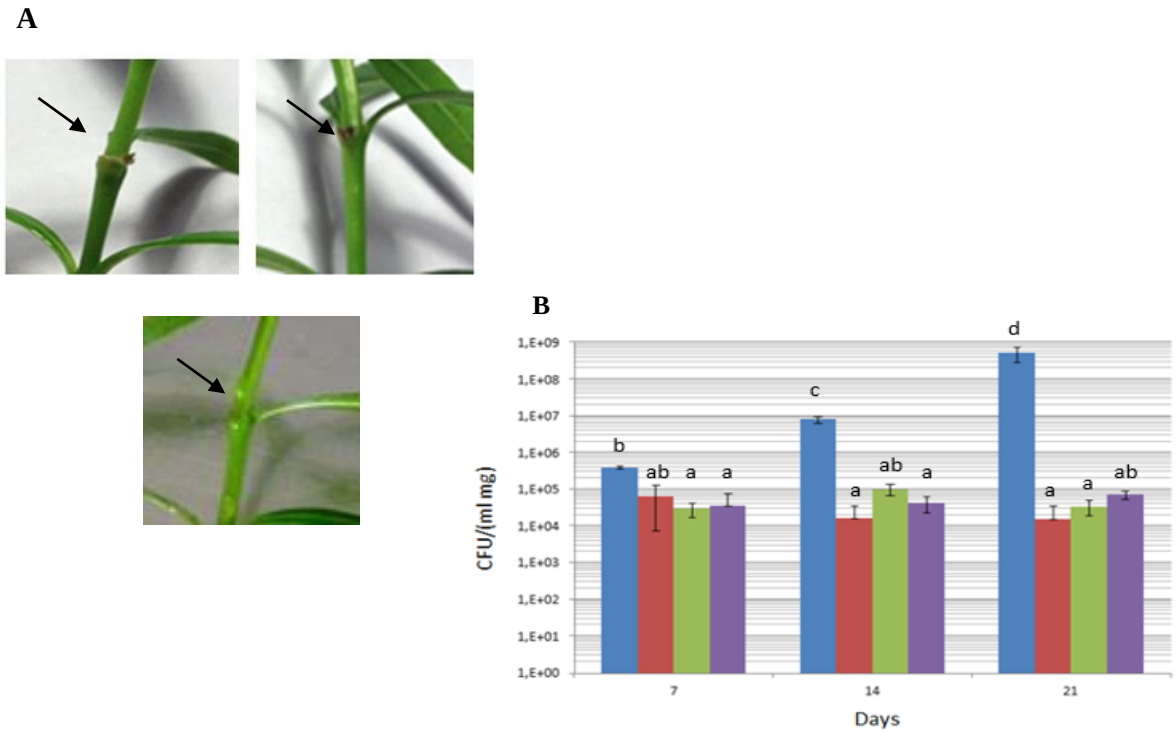


As shown in Figure 10, especially T3A+AP17 mutant results severely impaired in its pathogenicity and virulence on oleander plants.

Therefore, we would assume that VIPs produced endogenously and under the control of *hrpA* promoter may act in concert with HrpA protein by competing each other through coiled-coil interactions.

**Figure 11: Percentage of Congo red dye absorption of T3A+AP17 (here named pT3-AP17) and T3A+LI27 (here named pT3-Li27) bacterial cultures, grown in MM. The data were calculated according to the formula: $[(X_{unk}-X_{\Delta hrpA})/(X_{WT}-X_{\Delta hrpA})]*100$ where $X_{WT}$ and $X_{\Delta hrpA}$ are the ratio $OD_{490}/OD_{600}$ for *Psn23* and Δ*hrpA* respectively. The data represent the means ± SD of three replicates. Results obtained are statistically significant (P <0.05).**

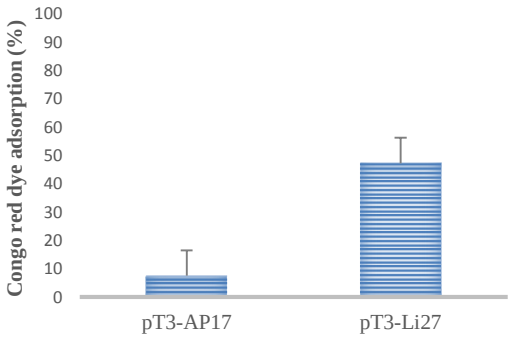

Finally, in order to indirectly follow the peptide fate endogenously produced we have carried out a set of co-inoculation experiments. T3A_AP17 and T3A_LI27 bacterial mutants and *Psn23* wild type cultures were inoculated together, at two different concentrations ($OD_{600}$=0.25 and/or 0.50). T3A_AP17 mutant was able to strongly reduce the typical hyperplastic gall compared to both *Psn23* wild type and T3A_LI27 mutant (Figure 12).

**Figure 12: Pathogenicity test on *in vitro* oleander plants at 21dpi with (a) *Psn23* wild type bacteria (wt) at $OD_{600}$=0.5; (b) *Psn23* wt ($OD_{600}$=0.25) + T3A_AP17 ($OD_{600}$=0.25), (c) *Psn23* wt ($OD_{600}$=0.50) + T3A_AP17 ($OD_{600}$=0.50); (d) *Psn23* wt ($OD_{600}$=0.25) + T3A_LI27 ($OD_{600}$=0.25); (e) *Psn23* wt ($OD_{600}$=0.50) + T3A_LI27 ($OD_{600}$=0.50).**

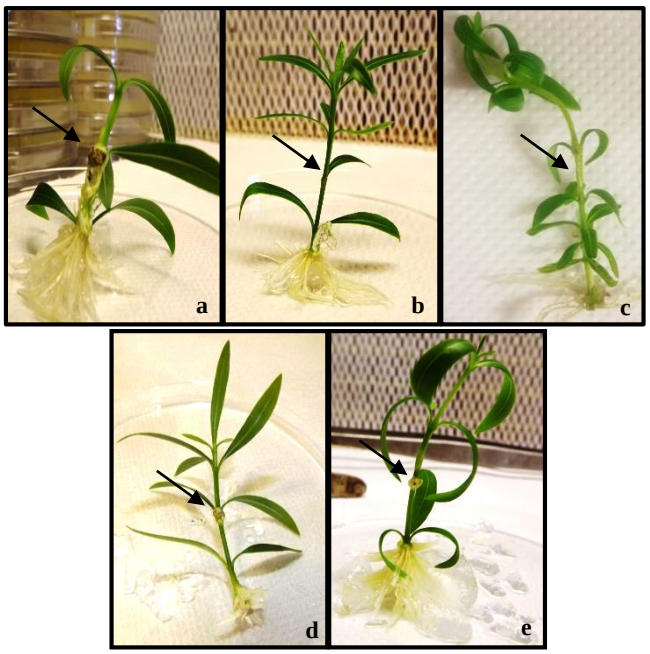


**VIPs transiently expressing plants by Agro-infiltration**

The use of transient expression through infiltration of *Agrobacterium tumefaciens* (agroinfiltration) harbouring the transgene of interest should substantially decrease the time required to test candidate resistance genes and might provide a better platform to assess the potential of the gene products (Leckie and Stewart, 2011).

To this purpose and to further verify the effectiveness of VIPs strategy we have used *A. tumefaciens* EHA105 transformed to specific binary vectors, named pCAMBIA1305.2::AP17 and pCAMBIA1305.2::LI27 (Table 1), and used in agroinfiltration experiments. pCAMBIA1305.2 vector is characterised by a GRP signal peptide upstream *gus* gene replaced in the final vectors with the sequence corresponding to AP17 and LI27 respectively, to target peptide delivery to the apoplast of plant cells as monitored by histochemical GUS assay (Chapter 3).

The efficacy of VIPs transiently expressed by *A. tumefaciens*EHA105 into micropropagated oleander plants was verified at different concentration of *Psn23* wild type bacteria used in co-inoculation (from 0.5 x $10^{\wedge 6}$ to 0.5 x $10^{\wedge 4}$ CFU) and fixed concentration of *A. tumefaciens* transformed with pCAMBIA1305.2::AP17 or pCAMBIA1305.2::LI27(0.5 x $10^{\wedge 6}$ CFU) (Figure 13).

**Figure 13: A) Agroinfiltration on *in vitro* oleander plants at 7dpi. On the top, inoculation with *Psn23* (control) at different concentration ($10^{\wedge 6}$; $10^{\wedge 5}$ and $10^{\wedge 4}$), where the gall formation at inoculation site is well visible. In the middle, co-infiltration with *Psn23* and *A. tumefaciens* transformed with pCAMBIA 1305.2::LI27. On the bottom, inoculation with *Psn23* and *A. tumefaciens* transformed with pCAMBIA 1305.2::AP17. In correspondence of inoculation sites (circled), a reduction in gall formation can be observed in comparison to inoculation with *Psn23* alone. B) Bacterial growth rate monitored at 14dpi. *A. tumefaciens* pCAMBIA indicates *A. tumefacies* trasformed with the native vector, used as control. (Histogram colour legend: blue =0.5 x $10^{\wedge 6}$; red=0.5 x $10^{\wedge 5}$ and green=0.5 x $10^{\wedge 4}$ CFU). Values are the mean of three independent experiments with nine replicates for each strain ± standard deviation (SD). ANOVA revealed statistically significant differences ($p<0.05$), comparison using the Tukey post-test are indicated by letters, where different letters indicate statistically significant differences.**

**A**

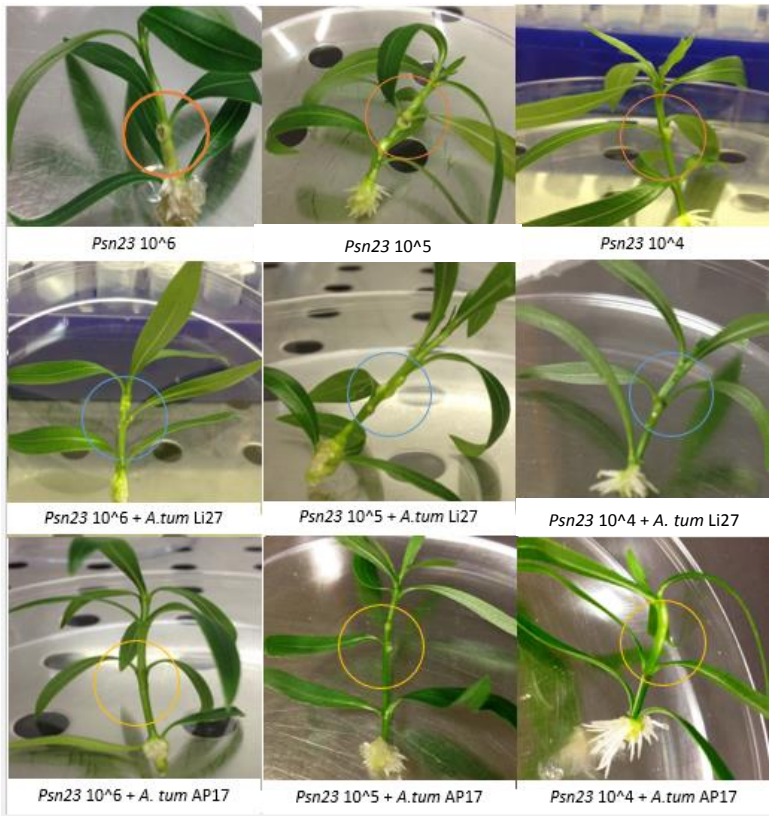


**B**

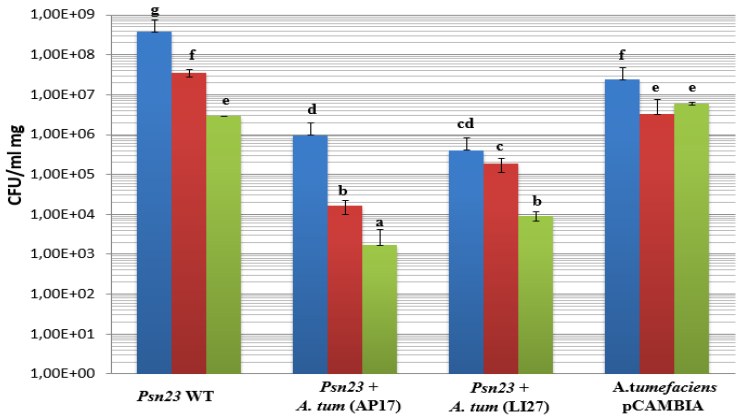

**VIPs strongly reduce disease symptoms development on host plant**

Finally, we proceed with co-inoculation of *Psn23* wild type mixed with synthetic peptides, to mimic as much possible the VIPs effect into plant. Preliminary data have shown that the minimal ihnibitory concentration of these peptides without any phytotoxic side effects was 60 µM.

Pathogenicity trials were performed at this VIPs concentration and their exogenous application mixed at *Psn23* wild type bacterial cells ($OD_{600}$=0.5, approximately $0.5x10^8$ Colony Forming Unit/ml; CFU/ml) has greatly reduced gall formation at inoculation side and has drastically decreased bacterial growth *in planta* both at 7 and 14 dpi. Thus, in particular AP17 peptide blocks both pathogenicity and virulence of *Psn23* wild type bacteria comparably to Δ*hrpA* mutant bacteria (Figure 14).

**Figure 14: A) Pathogenicity test on oleander plants at 14 dpi. When *Psn23* wild type is mixed with AP17 or LI27 peptides (at 60µM) the gall formation is strongly impaired. B) *In planta* bacterial multiplication at 7 and 14 dpi. (Histogram colour legend: blue=*Psn23* wild type; red=*Psn23* mixed with AP17 (60 µM); green =*Psn23* mixed with LI27 (60 µM); violet histogram=Δ*hrpA* mutant). Data represent the means ± SD of three runs with nine replicates for each strain. Statistically significant differences are represented by different letters above the bars (ANOVA and Tukey's test, *P* < 0.05).**

**A**

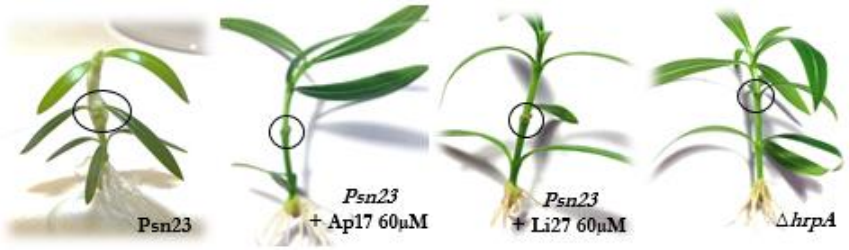


**B**

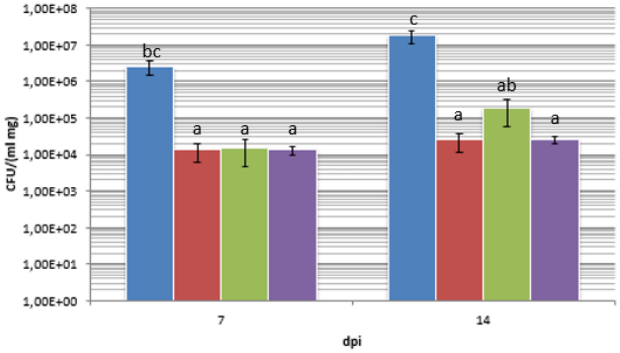

**VIPs do not have any toxicity effect on cellular membranes and $Ca^{2+}$ ATPase**

The anti-virulence peptides here examined were investigated for their effects on $Ca^{2+}$-ATPase, taken as a model of the ubiquitous molecular ion pumps P-type ATPases, known to be targets for many toxic compounds. Moreover, since the majority of anti-microbial peptide are known to penetrate the lipid membrane through hydrophobic interaction resulting in pore formation, we analysed the effect of AP17 and LI27 on synthetic bilayer lipid membrane (BLMs) to rule out this unwanted effect.

The SR $Ca^{2+}$ -ATPase belongs to the highly- conserved P-type ATPase family. P-type ATPases are a large, ubiquitous and varied family of membrane proteins that are involved in many transport processes in virtually all living organisms (Bublitz *et al.*, 2011). A number of heavy metal ions, *e.g.* $Cd^{2+}$, $Hg^{2+}$, $Pb^{2+}$, $Zn^{2+}$ and $Cu^{2+}$, were found to inhibit $Ca^{2+}$ -ATPase activity in different types of membranes (Gramigni *et al*., 2009). Such inhibition typically causes a sudden increase in the cytosolic concentration of calcium ions, endoplasmic reticulum stress, and eventual cell death through apoptosis.

To exclude the inhibitory effect of these VIPs on $Ca^{2+}$ -ATPase, we investigated their interaction on $Ca^{2+}$ -ATPase, and we analysed these results with the effect reported for $Cu^{2+}$ ions (Chapter 4). In this experiment we compared the current signals generated by the ATPase following 100 µM ATP concentration jumps in the absence of the peptide (control measurement) and in the presence of AP17 (Figure 15D). Notably, we found no effect of AP17 and LI27 on the ATP-induced current signal and related charge over a concentration range from 1 to 30 µM (inset of Figure 15C and D). Thus, this result indicated that the peptide AP17 does not affect ATP-dependent translocation of calcium ions by $Ca^{2+}$ -ATPase.

While, we found that $Cu^{2+}$ ions suppress the ATP-induced current signal and the associated displaced charge both at 0.1 µM and 1 µM concentration (inset of Figure 15C and D). Therefore, we may conclude that sub-micromolar copper exerts a strong inhibitory effect on $Ca^{2+}$ -ATPase by interfering with ATP-dependent calcium translocation through the enzyme.

Since the majority of the peptides are known to penetrate the lipid membrane we analysed the lipid-peptide interactions by BLMs experiment, associated to bioelectrical characterization and current recording.

After the BLM formation, and once checked its stability, we started adding the AP17 and LI27 peptides. Through several micromolar additions, we increased the peptide concentration from 5 µM to 60 µM, the concentration which resulted to be active *in vivo*, and we left the system overnight. No change in current was recorded indicating any toxic effect on cellular membranes (Figure 15 A and B).

**Figure 15: On the left side: effect of AP17 (A) and LI27 (B) on synthetic bilayer lipid membranes (BLMs). Current measurements carried out at different potentials (-80, -60,-40, +40, +60, +80mV), in presence or not of AP17 and LI27 (5 µM, 30 µM and 60 µM) in symmetrical conditions with 250 mM KCl in 10 mM MOPS (pH=7) buffer. On the right side: effect of copper ions and AP17 on ATP-dependent current signals generated by $Ca^{2+}$-ATPase. Current signals induced by 100 µM concentration jumps in the presence of 10 µM $CaCl_2$ and in the absence (black curve, control measurement or in the presence of 1 µM $CuCl_2$ (red curve). The inset shows the charges related to ATP-induced current signals in the presence of different $CuCl_2$ concentrations. Charges are normalized with respect to the value measured in the absence of copper ions (control measurement). Data represent the mean ± SE of three independent measurements. D) Current signals induced by 100 µM ATP concentration jumps in the presence of 10 µM $CaCl_2$ and in the absence (black curve, control measurement) or in the presence of 30 µM AP17 (red curve). The inset shows the charges related to ATP-induced current signals in the presence of different concentrations of the peptide AP17. Charges are normalized with respect to the value measured in the absence of AP17 (control measurement). Data represent the mean ± SE of three independent measurements.**

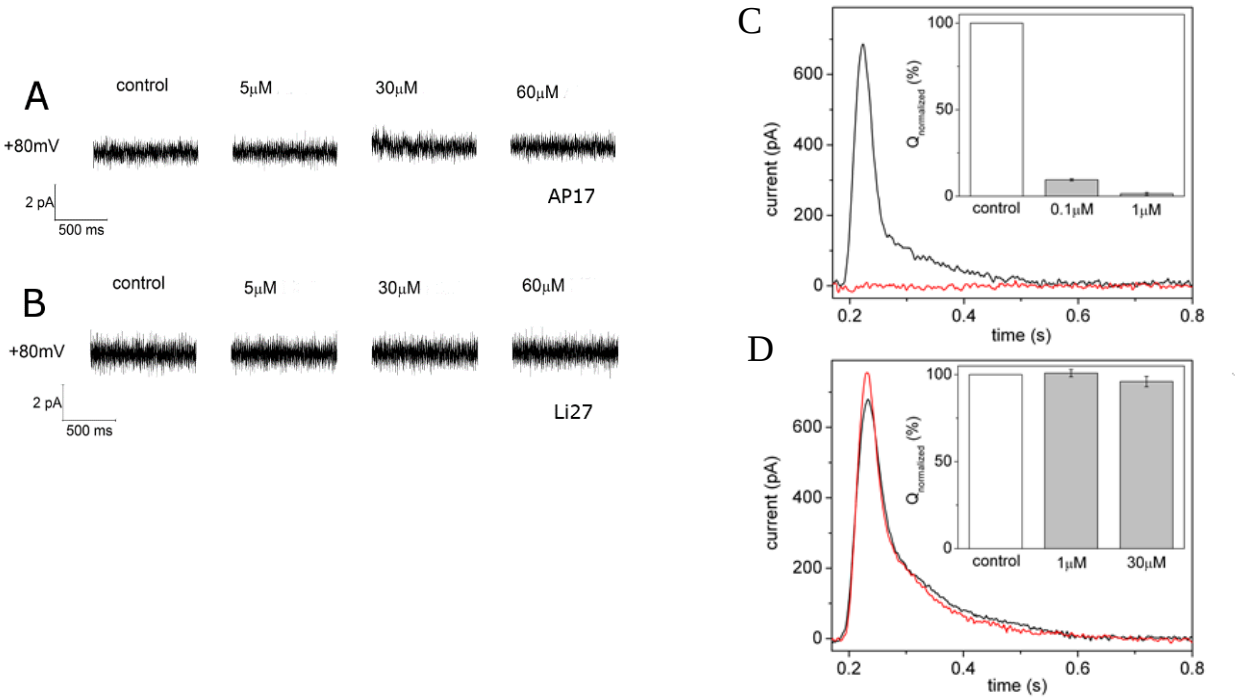

## 2.5 Discussion

The need to develop innovative anti-bacterial molecules is an urgent issue not only in human medicine but also in plant protection as a result of the worldwide spreading of antibiotics and copper resistance.
The most cutting-edge approaches focus on searching of bioactive molecules which acting on the pathogenicity and the virulence of pathogenic bacteria, without affecting their viability, in order to decrease the selective pressure applied on bacteria populations and thus the consequent development of resistance phenomena.
Among the ideal targets for this kind of innovative antibacterials, there is the Type Three Secretion System that is the highly conserved molecular syringe through which Gram-negative bacterial pathogens inject their effectors into the host cells.
Firstly, several critical amino acids residues were identified at the C-terminus portion of the HrpA protein, which is the main component of *P. syringae* TTSS pilus, supposed to be involved in coiled-coil interaction among HrpA subunits during the assembly of the Type Three injectisome.
The bioinformatic analysis of the amino acid sequence corresponding to the putative HrpA protein of *P. savastanoi* pv. *nerii* has found that this protein is characterized by an α-helix region with a seven-residue repeat recurring in the coiled-coils motif. These domains are generally involved in protein-protein interaction, particularly in molecular recognition phenomena and in the formation of multimeric proteic complexes (Daniell *et al*., 2001; Wall and Kaiser, 1999). An experimental evidence about the role of coiled-coil domains in the assembly of the TTSS translocator protein EspA in the enteropathogenic bacteria *Escherichia coli* was reported, although about nothing is still known about the molecular details of subunit-subunit interactions during filament assembly (Larzabal *et al*., 2010). Non-conservative amino acid substitution of specific EspA *heptad* residues generated *E.coli* defective in EspA filament assembly, indicating that coiled-coil interactions are involved in assembly or stability of the EspA filament-associated type III translocon (Delahay *et al*., 1999). Moreover, coiled-coil domains are found in high frequency amongst structural and effector proteins of the Type Three Secretion System of *Yersinia spp., Salmonella spp., E.coli* and *Shigella spp*.(Costa *et al*., 2012; Knodler *et al*., 2011; Zoetewey *et al*., 2003; Barta *et al*., 2012) but until now, to the best of our knowledge, they have never been reported in the TTSS structural proteins of plant pathogenic bacteria. *P. savastanoi* pv. *nerii* mutants replaced in five, three and two amino acids among those hypothesized to be involved in HrpA coiled-coil interactions were produced and named PF5αα, PF3αα and PF2αα, respectively. When their behaviour was compared with the knock-out mutant *Psn23* Δ*hrpA* (which retains 8,3% of amino acids sequence of wild type protein), carrying an in frame deletion in *hrpA* gene, only PF5αα and with minor extent PF3αα were unable to induce HR on *N. tabacum* leaves, and to cause disease and to properly grow on oleander micropropagated plants. As far as PF5αα was concerned, these results could have been determined by the replacement of those residues critical for HrpA subunits assembly or for the correct HrpA folding. The potential of these results in the frame to develop innovative anti-bacterial peptides was further investigated by comparing the PF5αα behaviour *in planta* with that of several other *Psn23* mutants. According to these

results, it could be concluded that the TTSS pilus is an ideal target for innovative anti-bacterial molecules, for the control of bacteria diseases of plants. Therefore, small peptides were designed and synthesized, allowing them to hinder HrpA-HrpA interactions, and therefore halt both the TTSS assembly and the delivering of virulence factors from the pathogens into the host cells. Two different peptides, named AP17 and LI27 were planned, each of them designed according to HrpA sequence, with the feature of contain the amino acid sequence corresponding to the coiled-coil domain and with the only difference in their length.
When co-infiltrated with *Psn23* wild type into *N. tabacum* mesophyll and on oleander micropropagated plants, AP17 and LI27 (with minor extent) were demonstrated both able to suppress HR, pilus assembly by Congo red assay and unable to cause typical hypertrophic symptoms, respectively. Moreover, the activity of these Virulence Inhibiting Peptides on the activation of the promoter driving the transcription of *hrpA* operon was also investigated. To this purpose it was utilised a reporter system, where *gfp* was under the control of *hrpA* promoter, named T3A. The analysis was performed on Minimal Medium, mimicking the apoplastic condition in which the bacteria are located previous to the infection, with or without anti-infective peptides added (Tang *et al.*, 2006). The results of GFP fluorescence assays showed that, in particular the AP17 peptide was also active on the *hrpA* promoter at 60 μM, and a strong decrease in the GFP fluorescence was observed in respect to the control condition. The endogenous production of AP17 and LI27 peptides by T3A+AP17 and T3A+LI27 mutants under the *hrpA* promoter control has allowed to detect both a direct competition between HrpA monomers and the peptides expressed into bacterial cytoplasm and an indirect regulatory role of HrpA protein in the TTSS cluster, that it is still not entirely outlined (Wei *et al.*, 2000). The co-inoculation *in planta* of *Psn23* wild type bacterial cells and these mutants respectively, has shown a strong reduction in gall formation demonstrating as these peptides block disease symptoms development acting outside bacterial membrane until wild type bacterial wall. However, it should nevertheless point out that this hypothesis requires further confirmations. The peptides transiently expressed in oleander plant cells by *A. tumefaciens* carrying a binary vector pCAMBIA1305.2::AP17, have been able to reduce the gall formation. This important result shows that the peptides expressed into the periplasmatic space compete with HrpA proteins in the same cell compartment where the TTSS pilus assembly was previously hypothesised to occur (Busch and Waksman, 2012). Altogether these results detect the efficacy of VIPs strategy, the absence of any toxic effect of these peptides both on targets and preserved structures of cell membranes highlight their applicability.
In conclusion, in this study, we have discovered and analysed the pivotal role of coiled-coil interactions in the TTSS pilus assembly of *P. savastanoi* pv. *nerii*.
The simplest explanation about the present of this kind of domains in HrpA protein can be indicated in the homo or hetero oligomeric interaction between the HrpA monomers. Our hypothesis can be indirectly confirmed because until now no high-resolution x-ray crystal structure of a type III conduit protein in the final conformation has been reported, due to the technical problem concerning the propensity of these proteins to form multimeric superstructures rather than three-dimensional crystals (Roine *et al.*, 1997 a and b; Lee *et al.*, 2005).

## 2.6 References

**Perry JA** and Wright GD. (2013) The antibiotic resistance "mobilome": searching for the link between environment and clinic. *Front Microbial*. 4, 138

**Smillie CS**, Smith MB, Friedman J, Cordero OX, David LA, Alm EJ. (2011) Ecology drivers a global network of gene exchange connecting the human microbiome. *Nature*, 480, 241-244

**Martinez JL** and Baquero F. (2014) Emergence and spread of antibiotic resistance: setting a parameter space.*Ups J Med Sci*. 2014 May; 119(2): 68–77

**Mellano MA** and Cooksey DA. (1988) Nucleotide sequence and organization of copper resistance genes from *Pseudomonas syringae* pv. *tomato. J. Bacteriol*. 170, 2879–2883

**Gutierrez-Barranquero JA**, de Vicente A, Carrion VJ, Sundin GW and Cazorla FM. (2013) Recruitment and rearrangement of three different genetic determinants into a conjugative plasmid increase copper resistance in *Pseudomonas syringae*. *Appl. Environ. Microbiol*. 79, 1028–1033

**Behlau F**, Canteros BI, Minsavage GV, Jones JB and Graham JH. (2011) Molecular characterization of copper resistance genes from *Xanthomonas citri* subsp. *citri* and *Xanthomonas alfalfae* subsp. *citrumelonis*. *Appl. Environ. Microbiol*.77, 4089–4096

**Lamichhane JR**, Messèan A, Morris CE. (2015) Insights into epidemiology and control of diseases of annual plants caused by the *Pseudomonas syringae* species complex. *J Gen Plant Pathol*. September 2015, Volume 81, Issue 5, pp 331–350

**He SY**, Nomura K, Whittam TS. (2004) Type III protein secretion mechanism in mammalian and plant pathogens. *Biochem. Biophys. Acta*, 1696, 181-206

**Mota LJ** and Cornelis GR. (2005) The bacterial injection kit: type III secretion systems. *Ann. Med*. 37:234-249

**Alfano JR** and Collmer A. (1997) The type III (Hrp) secretion pathway of plant pathogenic bacteria: trafficking harpins, Avr proteins, and death. *J Bacterial* 179:5655-5662

**Hueck CJ.** (1998) Type III protein secretion system in bacterial pathogens of animals and plants. *Microbiol. Mol. Biol. Rev.* 62, 379-433

**Roine E**, Saarinen J, Kalkkinen N, Romantschuk M. (1997a) Purified HrpA of *Pseudomonas syringae* pv. *tomato* DC3000 reassembles into pili. *FEBS Letters* 417(1997) 168-172

**Roine E**, Wei W, Yuan J, Nurmiaho-Lassila EL, Kalkkinen N, Romantschuk M, He SY. (1997) Hrp pilus: an hrp-dependent bacterial surface appendage produced by *Pseudomonas syringae* pv. *tomato* DC3000. *Proc Natl Acad Sci USA*. 1997 Apr 1;94(7):3459-64

**Lee YH**, Kolade OO, Nomura K, Arvidson DN, He SY. (2005) Use of Dominant-negative HrpA Mutants to Dissect Hrp Pilus Assembly and Type III Secretion in *Pseudomonas syringae* pv. *tomato. The Journal of Biological Chemistry*. 280, 21409-21417

**Wei W**, Plovanich Jones A, Deng WL, Collmer A, Huang HC, He SY. (2000) The gene coding for the Hrp pilus structural protein is required for type III secretion of Hrp and Avr proteins in *Pseudomonas syringae* pv. *tomato*. *Proc. Natl. Acad. Sci*. USA 97, 2247-2252

**Mason JM** and Arndt KM. (2004) Coiled Coil Domains: Stability, Specificity, and Biological Implications. *ChemBioChem* 2004, 5, 170 ± 176

**King EO**, Ward MK, Raney DE. (1954) Two simple media for the determination of pyocianine and fluorescein. *J Lab Clin Med*. 1954; 44: 301–307

**Huynh TV**, Dahlbeck D, Staskawicz BJ. (1989) Bacterial blight of soybean: Regulation of a pathogen gene determining host cultivar specificity. *Science*. 1989; 245: 1374–1377

**An G**, Evert PR, Mitra A, Ha SB (1988) In: Gelvin SB, Schilperoot RA (eds) Plant Molecular Biology Manual, *Kluwer Academic Publishers*, Dordrecht, Netherlands., pp 1-19

**Miller H**. (1972) Experiments in molecular genetics. Cold Spring Harbor Laboratory, *Cold Spring Harbor*: New York, 1972

**Sambrook J**, Fritsch EF, Maniatis TA. (1989) Molecular cloning: a laboratory manual. 2nd ed. New York, NY, USA: *Cold Spring Harbor Laboratory Press*; 1989

**Thompson JD**, Higgins DG, Gibson TJ. (1994) CLUSTALW: improving the sensitivity of progressive multiple sequence alignment through sequence weighting, position-specific gap penalties and weight matrix choice. *Nucleic Acids Res* 1994;22:4673e80

**Ehmann A**. (1977) The Van Urk-Salkowski reagent - A sensitive and specific chromogenic reagent for silica gel thin-layer chromatographic detection and identification of indole derivatives. *J Chromatogr* 1977; 132:267-76

**Murashige T**, SKOOG F. (1962) A revised medium for rapid growth and bioassays with tobacco tissue cultures. *Physiol Plant* 1962; 15:473–97

**Baker CJ**, Atkinson MM, Collmer A. (1987) Concurrent Loss in Tn5 Mutants of *Pseudomonas syringae* pv. *syringae* of the ability to induce the hypersensitive response and host plasma membrane K+/H+ exchange in Tobacco. *Phytopathotogy.* 1987; 77: 1268-1272

**Biancalani C**, Cerboneschi M, Tadini-Buoninsegni F, Campo M, Scardigli A, Romani A, Tegli S. (2016) Global Analysis of Type Three Secretion System and Quorum Sensing Inhibition of *Pseudomonas savastanoi* by Polyphenols Extracts from Vegetable Residues. PLoSONE 11(9): e0163357. doi: 10.1371/journal.pone.0163357

**Yang CH**, Gavilanes-Ruiz M, Okinaka Y, Vedel R, Berthuy I, Boccara M, et al. (2002) hrp genes of *Erwinia chrysanthemi* 3937 are important virulence factors. *Mol Plant Microbe In* 2002; 15:472–80

**Hagen G**, Guilfoyle T. (2002) Auxin-responsive gene expression: genes, promoters and regulatory factors. *Plant Mol Biol* 2002; 49:373-85

**Zazímalová E**, Krecek P, Skůpa P, Hoyerová K, Petrásek J. (2007) Polar transport of the plant hormone auxin – the role of PIN-FORMED (PIN) proteins. *Cell Mol Life Sci*. 2007; 64:1621-37

**Pérez-Martínez I**, Rodríguez-Moreno L, Lambertsen L, Matas MI, Murillo J, Tegli S, et al. (2010) Fate of a *Pseudomonas savastanoi* pv. *savastanoi* type III secretion system mutant in olive plants (*Olea europaea* L.). *App Environ Microbiol* 2010; 76:3611-19

**Tadini-Buoninsegni F**, Bartolommei G, Moncelli MR, Guidelli R, Inesi G. (2006) Pre-steady state electrogenic events of $Ca^{2+}/H^{+}$ exchange and transport by the $Ca^{2+}$-ATPase. *J Biol Chem*. 2006; 281: 37720-37727

**Tegli S**, Gori A, Cerboneschi M, Cipriani MG, Sisto A. Type Three Secretion System in *Pseudomonas savastanoi* pathovars: Does timing matter? Genes. 2011; 2: 957–979. doi: 10.3390/genes2040957. pmid:24710300

**Frederick RD**, Ahmad M, Majerczak DR, Arroyo-Rodríguez AS, Manulis S, Coplin DL. (2001). Genetic organization of the *Pantoea stewartii* subsp. *stewartii hrp* Gene Cluster and Sequence Analysis of the *hrpA*, *hrpC*, *hrpN*, and *wtsE* Operons. *Molecular Plant Microbe Interactions*. October 2001, Volume 14, Number 10, Pages 1213-1222

**Wei ZM**, and Beer SV. (1995) *hrpL* activates *Erwinia amylovora* hrp gene transcription and is a member of the ECF subfamily of sigma factors. *J. Bacteriol*. 177:6201-6210

**Yu CS**, Chen YC, Lu CH, Hwang JK. (2006) Prediction of protein subcellular localization. *Proteins: Structure, Function and Bioinformatics* 2006, 64:643-651

**Krogh A**, Larsson B, von Heijne G, Sonnhammer EL. (2001) Predicting transmembrane protein topology with a hidden Markov model: application to complete genomes. *J Mol Biol*. 2001 Jan 19;305(3):567-80

**Rost B**, Yachdav G, Liu J. (2004) The PredictProtein server. *Nucleic Acids Res*. 2004 Jul 1;32 (Web Server issue): W321-6.

**McDonnell AV**, Jiang T, Keating AE, Berger B. (2006) Paircoil2: improved prediction of coiled coils from sequence. *Bioinformatics.* Volume 22, Issue 3, pp 356-358

**Rodríguez-Moreno L**, Barceló-Muñoz A, Ramos C. (2008) *In vitro* analysis of the interaction of *Pseudomonas savastanoi* pvs. *savastanoi* and *nerii* with micropropagated olive plants. *Phytopathology. 2008 Jul; 98(7):815-22.*

**Quesada JM**, Penyalver R, López MM. (2012) Epidemiology and control of plant diseases caused by phytopathogenic bacteria: the case of olive knot disease caused by *Pseudomonas savastanoi* pv. *savastanoi*," in *Plant Pathology*, ed. Cumagun C. J., editor

**Leckie BM** and Stewart CN. (2011) Agroinfiltration as a technique for rapid assays for evaluating candidate insect resistance transgenes in plants. *Jr Plant Cell Rep* (2011) 30:325–334 DOI 10.1007/s00299-010-0961-2

**Bublitz M**, Morth JP, Nissen P. (2011) P-type ATPases at a glance. *J Cell Sci*. 2011; 124: 2515-2519

**Gramigni E**, Tadini-Buoninsegni F, Bartolommei G, Santini G, Chelazzi G, Moncelli MR. (2009) Inhibitory effect of $Pb^{2+}$ on the transport cycle of the $Na^+$, $K^+$-ATPase. *Chem Res Toxicol*. 2009; 22: 1699-1704

**Daniell SJ**, Delahay RM, Shaw RK, Hartland EL, Pallen MJ. (2001) Coiled-coil domain of enteropathogenic Escherichia coli type III secreted protein EspD is involved in EspA filament-mediated cell attachment and hemolysis. *Infect Immun* 60:4055-64

**Wall D** and Kaiser D. (1999) Type IV pili and cell motility. *Mol Microbiol* 32: 1–10

**Larzabal M**, Mercado EC, Vilte DA, Salazar-Gonzalez H, Cataldi A, Navarro-Garcia F.(2010) Designed Coiled-coil Peptides inhibit the Type Three Secretion System in Enteropathogenic Escherichia coli. *Plos One* 5(2):e9046

**Delahay RM**, Knutton S, Shaw RK, Hartland EL, Pallen MJ, *et al*. (1999) The coiled-coil domain of EspA is essential for the assembly of the type III secretion translocon on the surface of enteropathogenic *Escherichia coli*. *J Biol Chem* 274: 35969–74

**Costa TR**, Amer AA, Fällman M, Fahlgren A, Francis MS. (2012) Coiled-coils in the YopD translocator family: a predicted structure unique to the YopD N-terminus contributes to full virulence of Yersinia pseudotuberculosis. *Infect Genet Evol.* 2012 Dec;12(8):1729-42. doi: 10.1016/j.meegid.2012.07.016. Epub 2012 Aug 11

**Knodler LA**, Ibarra JA, Pérez-Rueda E, Yip CK, Steele-Mortimer O. (2011) Coiled-coil domains enhance the membrane association of Salmonella type III effectors. *Cell Microbiol.* 2011 Oct;13(10):1497-517. doi: 10.1111/j.1462-5822.2011.01635.x. Epub 2011 Jul 11

**Zoetewey DL**, Tripet BP, Kutateladze TG, Overduin MJ, Wood JM, Hodges RS. (2003) Solution structure of the C-terminal antiparallel coiled-coil domain from *Escherichia coli* osmosensor ProP. *J Mol Biol*. 2003 Dec 12;334(5):1063-76

**Barta ML**, Dickenson NE, Patil M, Keightley A, Wyckoff GJ, Picking WD, Picking WL, Geisbrecht BV.(2012) The structures of coiled-coil domains from type III secretion system translocators reveal homology to pore-forming toxins. *J Mol Biol*. 2012 Apr 13;417(5):395-405. doi: 10.1016/j.jmb.2012.01.026. Epub 2012 Feb 1

**Tang X**, Xiao Y, Zhou JM. (2006) Regulation of the type III secretion system in phytopathogenic bacteria. *Mol Plant Microbe Interact*. 2006; 19: 1159-1166

**Wei W**, Plovanich Jones A, Deng WL, Collmer A, Huang HC, He SY. (2000) The gene coding for the Hrp pilus structural protein is required for type III secretion of Hrp and Avr proteins in *Pseudomonas syringae* pv. *tomato*. *Proc. Natl. Acad. Sci*. USA 97, 2247-2252

**Busch A** and Waksman G. (2012) Chaperone-usher pathways: diversity and pilus assembly mechanism. *Philos Trans R Soc Lond B Biol Sci*. 2012 Apr 19; 367(1592): 1112–1122. doi: 10.1098/rstb.2011.0206

**Roine E**, Saarinen J, Kalkkinen N, Romantschuk M. (1997a) Purified HrpA of *Pseudomonas syringae* pv *tomato* DC3000 reassembles into pili. *FEBS Letters* 417(1997) 168-172.

**Roine E**, Wei W, Yuan J, Nurmiaho-Lassila EL, Kalkkinen N, Romantschuk M, He SY. (1997b) Hrp pilus: an hrp-dependent bacterial surface appendage produced by *Pseudomonas syringae* pv *tomato* DC3000. *Proc Natl Acad Sci USA*. 1997 Apr 1;94(7):3459-64

**Lee YH**, Kolade OO, Nomura K, Arvidson DN, He SY. (2005) Use of dominant-negative HrpA mutants to dissect Hrp pilus assembly and type III secretion in *Pseudomonas syringae* pv *tomato*. *J Biol Chem.* 2005 Jun 3;280(22):21409-17. Epub 2005 Mar 29

## 2.7 Supporting Information

**S1 Figure: A) Output obtained by SignalP 4.1 service. Signal peptide of the HrpA protein was predicted from 1 to 10 amino acids. B) Output obtained by TMHMM service. Based on physico-chemical composition and on present of signal peptide the HrpA protein shows a localisation outside cellular membrane.**

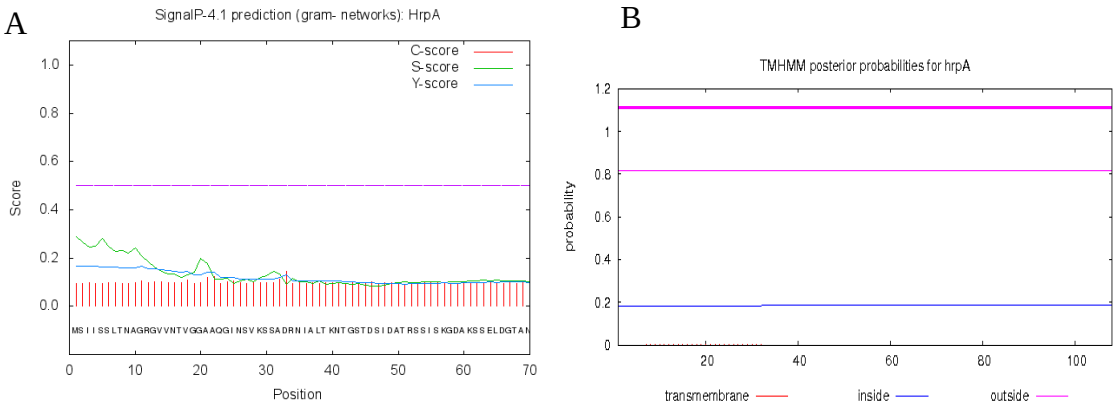


**S2 Figure: Output obtained by Predict Protein service. A considerable region (from 69 to 101 aa) of the HrpA protein shows a secondary structure rich in α-helix.**

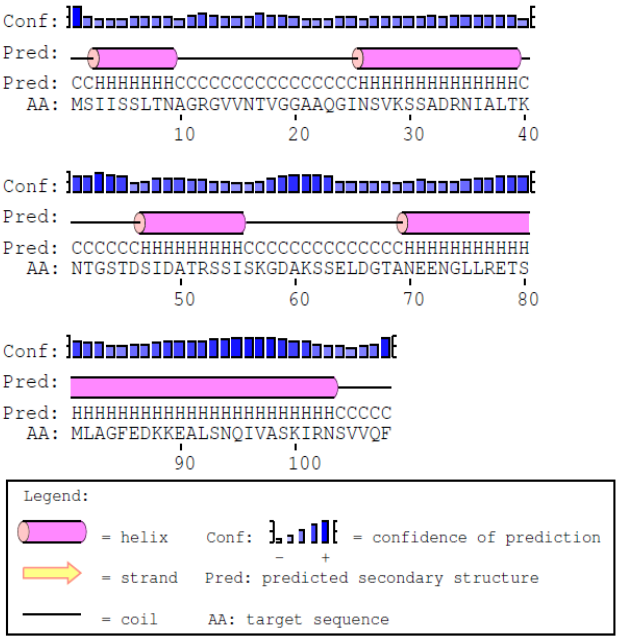

**S3 Figure: Amino acids sequence of AP17 and LI27 characterized by INNOVAGEN bioinformatic tool http://www.innovagen.se/custom-peptide-synthesis/peptide-property-calculator/peptide-property-calculator.asp**

>**LI27** 2.99kD pH 6.62

**LLRETSMLAGFEDKKEALSNQIVASKI**

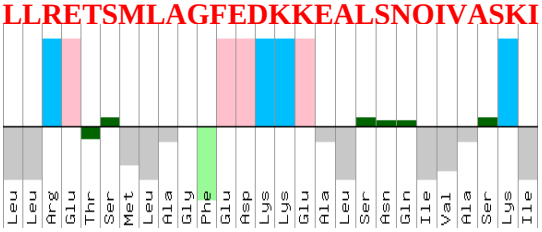


>**AP17** 1.89kD pH 4.44

**MLAGFEDKKEALSNQIV**

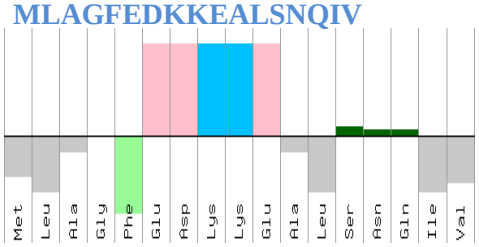


**Color legend:** Acidic Aromatic Basic Aliphatic Polar

**Hydrophilicity Analysis:**

| Peptide | Charge | Attribute |
|---|---|---|
| LLRETSMLAGFEDKKEALSNQIVASKI | 0 | neutral |

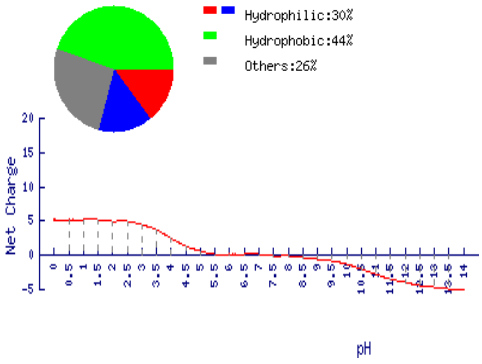


| Peptide | Charge | Attribute |
|---|---|---|
| MLAGFEDKKEALSNQIV | -1 | acidic |

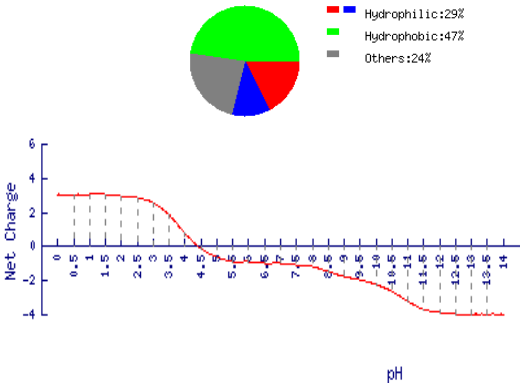

## 2.8 Annex 1:

**HrpA protein synthesis by recombinant DNA-based technology**

In this section it was reported the experimental protocol for the biotechnological synthesis of the HrpA protein of *P. savastanoi* pv. *nerii*. This protocol was set up at laboratory scale and successively used in scale-up phase for primary antibody production employed in immunoenzymatic assays.

The experimental approach is based on the pET200 D-TOPO expression vector and ProBond™ purification system (Invitrogen, Life Technologies, USA). HisTrap™ 1ml purification column (GE Healthcare, Uppsala, Sweden) was used in scale-up phase according to the manufacturer's instructions. Briefly, *hrpA* genes from *Psn23* was cloned into pET200D-TOPO (Invitrogen, Life Technologies, USA) expression vector, using the primers A_RIC FOR 5' CACCATGAGCATCATAAGTTCTCTG (Tm=62°C) and A_RIC_REV 5' CAGAACTGGACGACC (Tm=64°C). After having successfully assessed the correct insertion of this sequence into the cloning vector, the recombinant plasmid was used in transformation experiments by electroporation, using several *E. coli* strains as recipients (BL21 from Invitrogen, USA, and C41 from Novagen). A single positive colony from the selection plate was inoculated in 20 ml LB liquid media containing 50 μg/ml kanamycin. The culture was incubated overnight with shaking at 37°C, and then transferred to a larger-scale LB media (10 ml culture was transferred into 90 ml fresh LB). The optimisation of the expression protocol was set up on pET200D-TOPO+*hrpA* expression, varying several fundamental parameters such as IPTG Isopropyl β-D-1- thiogalactopyranoside concentration (0.5; 0.75; 1mM), $OD_{Abs\ 600nm}$ (0.5; 0.8), time post-induction (2; 4; 6; overnight - on); temperature post-induction (37; 26 °C). Finally, the expression of the target protein was induced by 1mM IPTG when $OD_{600}$ of the culture reached 0.8. Cells were harvested by centrifugation after grown for an additional 6 h at 28°C.

After IPTG induction, expression of HrpA protein was assessed both on whole cell lysate and culture filtrates, by traditional electrophoretic methods. The expected size was approximately 16KDa.

The results obtained by gel electrophoresis, using *E. coli* C41 as recipients are reported in Figure 1A. The correct expression was confirmed by Western blotting using Anti-Xpress™ antibody (Invitrogen, Life Technologies, USA) according to the manufacturer's instructions (Figure 1B).

On the samples with significant levels of recombinant protein expression, purification was carried out under native condition through ProBond™ Nickel-Chelating Resin (Invitrogen, Life Technologies, USA), using the N-terminal Hys-tag added to the recombinant protein by pET200D-TOPO (Invitrogen, Life Technologies, USA) and in scale-up phase through HisTrap™ 1ml (GE Healthcare, Uppsala, Sweden) according to the manufacturer's instructions.

The obtained results concerning the HrpA protein elution are reported in Figure 2A, where in line 4 it is shown a conspicuous band corresponding to the HrpA protein (16KDa). On the same purification Nickel-Chelating Resin column, the digestion to eliminate from HrpA protein the polyhistidine–tag was also performed using the enterokinase enzyme. In Figure 2B, the results obtained are shown, after the enzymatic reaction performed at 25°C, overnight

and with 7u of EK Max™ (Invitrogen, Life Technologies, USA) to digest the Hys tag and obtained the purified HrpA protein approximately of 11 KDa.

**Figure 1: A) SDS-PAGE analysis of C41 *E. coli* supernatants at 4, 6, and overnight hours post-induction (1mM IPTG); 1-3-5 lines: induced samples; 2-4-6 lines: no-induced samples; M: proteins standard B) Western blotting analysis, in line 1 the HrpA protein expressed and detected by antibody.**

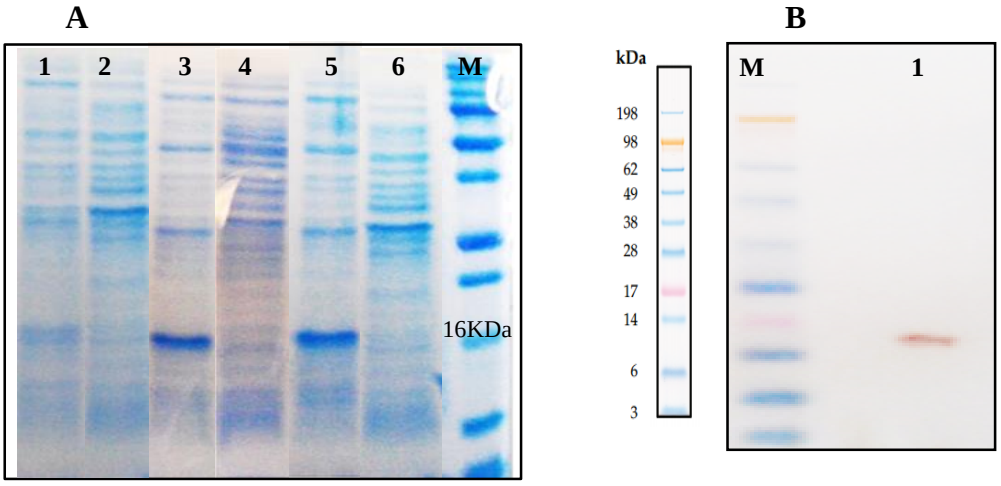


**Figure 2: A) SDS-PAGE analysis of the fractions recovered from purification steps by using HisTrap™ 1ml column system (GE Healthcare, Uppsala, Sweden). Line 1: binding step, 2: wash 20mM imidazole, 3: 50mM imidazole, 4: elution HrpA protein. B) SDS-PAGE analysis in line 1 purified HrpA protein under native conditions; line 2 last elution step, M) proteins standard.**

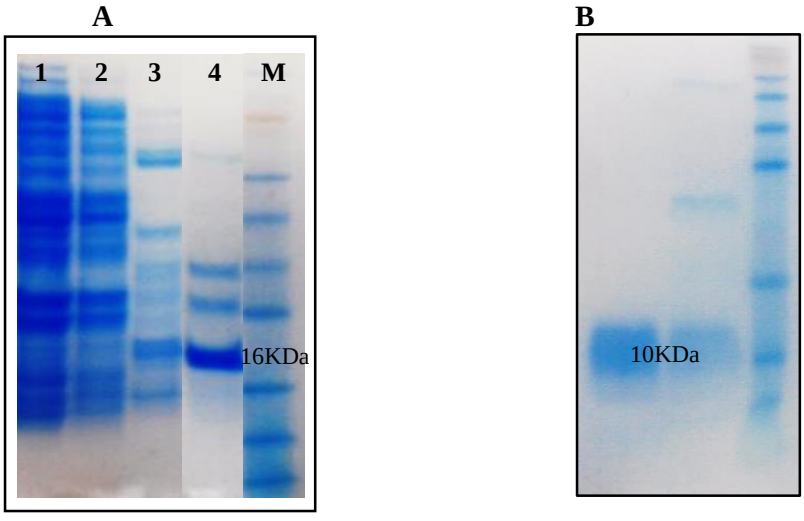


The final yield obtained of purified HrpA protein from recombinant technology was no more than 1 mg of proteins starting from a 100 ml of *E. coli* culture enriched in HrpA protein and measured through absorbance at 280 nm (NanoDrop™ ND-1000 (NanoDrop Technologies Inc., DE, USA).

Finally, the experimental protocol used in the HrpA protein purification was further improvement to get the needed yields for antibody anti-HrpA production obtained from Primm srl (Milano-Italy), following immunisation of two rabbits with recombinant protein HrpA (Figure 3) and used in immunoenzymatic assays performed in this PhD thesis.

**Figure 3: line 1 SDS-PAGE analysis of the HrpA protein obtained from recombinant technology and in line 2 Western blot performed with anti-HrpA antibody obtained from Primm srl (Milano-Italy).**

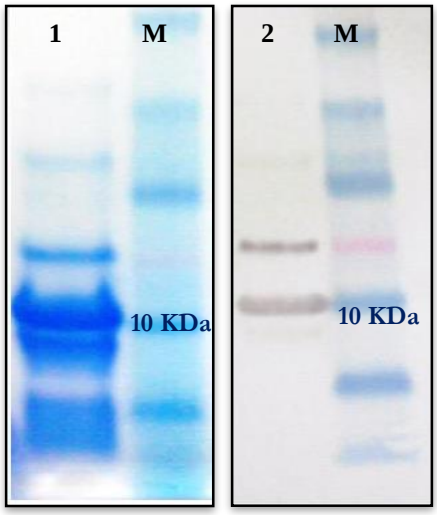

## 2.9 Annex 2:

### *P. syringae* pv. *actinidiae* and the anti-infective peptide Psa21

In this section it was reported the study performed on amino acid sequence of HrpA protein (113 AA) of *P. syringae* pv. *actinidiae.* Moreover, the efficacy *in vitro* and *in vivo* of the corresponding peptide Psa21 was also verified using the same methodological approach reported in Chapter 2.

The C-terminus portion of HrpA amino acid sequence of *Psa* as reported for *Psn23* (Chapter 2) is characterised by a coiled-coil motif (from 57 to 92 AA). The Psa21 peptide was designed on this domain from 70 to 91 AA and it is 21 amino acid long (Figure 1A).

The coiled-coil motif was verified through bioinformatic analysis (Material and Methods see Chapter 2). The result obtained with Paircoil (http://groups.csail.mit.edu/cb/paircoil2) is reported in Figure 1B.

**Figure 1: A) C- terminal amino acid sequence corresponding of putative HrpA protein of *P. syringae* pv. *actinidiae* rich in α-helices. In bold red color is indicated the amino acid sequence of Psa21 peptide. B) Output of the analysis performed with Paircoil.**

**A)**

*Psa*ICMP ESDANGAKLI**AMQAQETMKKQTMDVLNAIQA**GKEDSSNKKISATATNAKGISY

**B)**

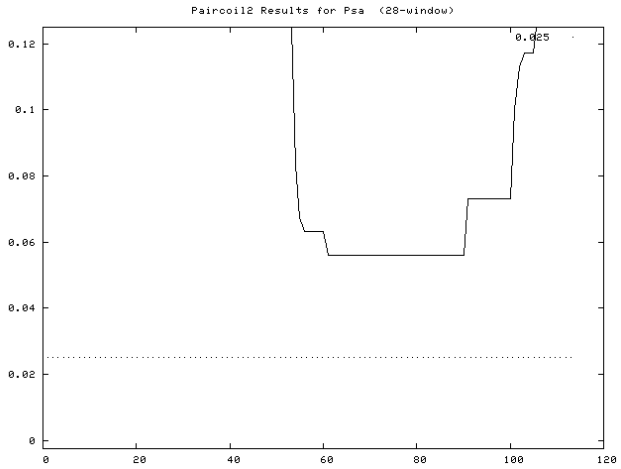


To ascertain the pivotal role of the HrpA protein in the TTSS pilus assembly, we have generated as reported for *Psn23* (Chapter 5), the *hrpA* in-frame deletion mutant, named Δ*hrpA* using the primers in Table 1 and following the methodological approach reported in the section Material and Methods (Chapter 5).

The peptide activity on both structure and functionality of TTSS was verified *in vitro* and *in vivo* by several tests performed also in Chapter 2 for the peptides AP17 and LI27 (Material and Methods see Chapter 2).

**Table 1. Primers used in this study.**

| Primer name | Primer sequence (5'-3') | Tm°C |
|---|---|---|
| HrpA_XbaI_For | TTTTCTAGATGACACTCAAGCTTCCGC | 56.9 |
| HrpA_EcoRI_Rev | TTTGAATTCCACTCGGTGTCAGCAGATC | 56.1 |
| Cross_BamHI_Rev | CCGGATCCAAACCTATTAAACTCCTGCAAATGCGACCAT | 59.5 |
| Cross_BamHI_For | GTTTAATAGGTTTGGATCCGGCAGTTACTAATTATTTCTGATTGC | 57.2 |
| Psa21_BglII_For | AAAAGATCTGCGATGCAGGCTCAGGAAAC | 59.0 |
| Psa21_PmlI_Rev | TTTCACGTGTTAGGCCTGGATGGCGTTGAG | 59.0 |

Firstly, we have verified the activity of this peptide on the TTSS functionality throught co-infiltration of *Psa* wild type cells with Psa21 peptide at 60µM and a strong reduction in HR symptoms was found after infiltration with Psa21 comparable to Δ*hrpA* bacterial mutant (Figure 2).

**Figure 2: Hypersensitive response after infiltration of *Psa* wild type with 60µM of Psa21. FS indicates infiltration with only physiological solution (control) and *Psa* Δ*hrpA* is used as positive control.**

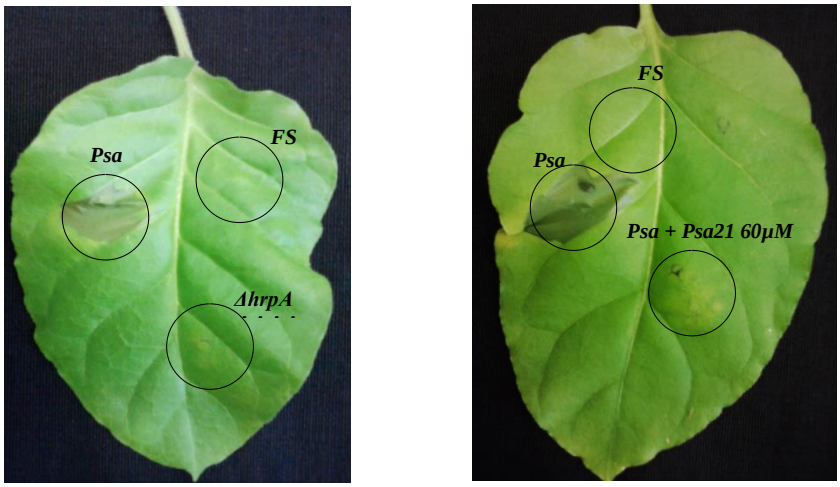


To further demonstrate the highly specific effect of Psa21 on the TTSS machinery, we investigated its impact on the TTSS pilus assembly through a Congo red-based assay to quantitatively evaluate variation in dye adsorption in *Psa* cells after treatment with this Virulence Inhibiting Peptide (Table 3). Moreover, we have evaluated the effect of Psa21 peptide on *hrpA* promoter by using the *gfp*-reporter fusion construct pLPVM_T3A and we have excluded any bacterial growth inhibition after treatment with this peptide by monitoring *in vitro* bacterial growth (Table 3). Data obtained confirm the inhibitory activity of this peptide both *in vitro* and *in planta* against *Psa* (Material and Methods see Chapter 4).

**Table 3: Effect on bacterial growth in MM and KB, on the trans-activation of *hrpA* promoter and on TTSS pilus assembly of the Psa21 peptide tested in this study. Common letters indicate differences not statistically significant at p<0.05 according to Tukey's test.**

| VIP | Bacterial growth in MM ($OD_{600}$) | Bacterial growth in KB ($OD_{600}$) | *hrpA* promoter* | Congo red dye§ adsorption % |
|---|---|---|---|---|
| **Psa21** | $0.98 \pm 0.13^{a}$ | $1.05 \pm 0.18^{a}$ | $0.68 \pm 0.12^{a}$ | $28 \pm 1.5$ |
| **Kanamycin** | $0.45 \pm 0.16^{b}$ | $0.39 \pm 0.19^{b}$ | $0.23 \pm 0.15^{b}$ | - |

* $OD_{600}$ was recorded after 24h growth and data are calculated as GFP Abs $_{(Ex.485nm;\ Em.535nm)}$ / Abs $_{(600nm)}$ ± SD, and as normalized fold versus untreated bacterial cultures.

§ $[(X_{unk}-X_{\Delta hrpA})/(X_{WT}-X_{\Delta hrpA})]*100$ where:
$X_{WT}$ and $X_{\Delta hrpA}$ are the ratio $OD_{490}/OD_{600}$ for *Psa* and *ΔhrpA* respectively.

Finally, we proceed with co-inoculation of *Psa* wild type mixed with synthetic peptide, to mimic as much possible the peptide effect into plant. Preliminary data have shown that the minimal inhibitory concentration of this peptide without any phytotoxic side effect was 60 µM.

Pathogenicity trials were performed at this concentration and their exogenous application mixed at *Psa* wild type bacterial cells ($OD_{600}$=0.5, approximately $0.5x10^8$ Colony Forming Unit/ml; CFU/ml) has greatly reduced the necrotic spots on *A. chinensis* leaves and has drastically decreased bacterial growth *in planta* until 20 dpi (days post inoculations). Thus, this peptide blocks both pathogenicity and virulence of *Psa* wild type bacteria comparably to Δ*hrpA* bacterial mutant (Figure 3).

**Figure 3: A) Pathogenicity tests on *in vitro A. chinensis* plants by anti-infective peptide Psa21 at 10 and 20 dpi; a) *Psa* wild type, b) *Psa* + 60µM Psa21, c) *Psa* Δ*hrpA* bacterial mutant (positive control). B) *In planta* bacterial multiplication at 20 dpi. Data represent the means ± SD of three runs with nine replicates for each strain. Statistically significant differences are represented by different letters above the bars (ANOVA and Tukey's test, *P* < 0.05).**

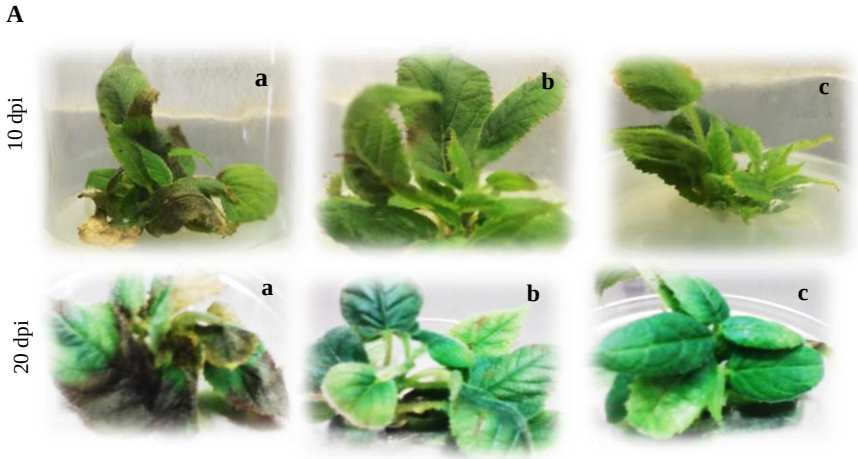

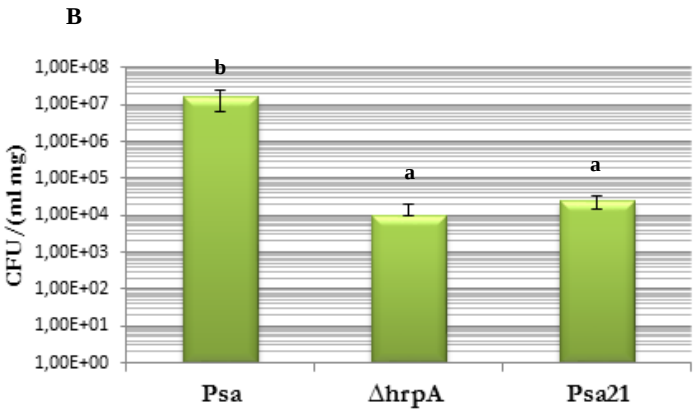


Considering the promising performance of Psa21 peptide, we have set up an experimental protocol for genetic transformation of kiwi Hayward *A. tumefaciens*-mediated using the binary vector pCAMBIA 1305.2 (Material and Methods see Chapter 2). The primers used are reported in Table 1.

*In vitro* micropropagated *A. chinensis* (*var.* Hayward) (Vitroplant Italia s.r.l., Cesena, Italy) plants were maintained on MS medium (Murashige and Skoog, 1962) containing salts and vitamins, 1.5 mg/l 6-Benzylaminopurine (BAP), 0.01 mg/l Naphthaleneacetic acid (NAA), 0.1 mg/l Gibberellic acid ($GA_3$). The pH of the medium was adjusted to 5.8 prior to autoclaving. The *in vitro* plants were grown for 3 weeks at 26°C, with a photoperiod of 16 h/light-8 h/dark.

The binary vector pCAMBIA1305.2_Psa21 was transformed into *A. tumefaciens* EHA105 by electroporation (Chapter 2). Single colonies from YEP medium (Chapter 2) plates containing kanamycin (50 µg/ml), were used to initiate 5ml YEP medium starter cultures. After 6 h shaking at 200rpm at 28°C, this suspension was used to inoculate a 20 ml YEP medium containing kanamycin (50 µg/ml) and rifampicin (10µg/ml), and grown overnight on a shaking platform at 200rpm to reach an $OD_{600}$ of 1.0. Bacterial culture was centrifuged at 2500 rpm for 15 min and pellet was re-suspended in liquid MS20 medium (MS + sucrose 20g/l; pH =5.2) supplemented with 0.1M acetosyringone and 1M betaine chloride (Sigma-Aldrich Co.-St. Louis, MO, USA) and grow further for 5 h at 20°C with shaking at 100 rpm. The optical density ($OD_{600}$) of culture was checked and adjusted to 0.5. The bacterial suspension was used for transformation experiments. About 500 leaf discs of kiwi *var.* Hayward were immersed in bacterial suspension and gentle shaking at 45 rpm for 20 min at room temperature. After inoculation, leaf discs were blotted on sterile paper towels and co-cultivated for 3 days under dark condition at 28°C, in petri dishes containing MS medium supplemented with 0.1mg/l (NAA) and 2mg/l thioridazine (TDZ). About 400 leaf discs were used in each experiments and transformation efficiency was compared with *A. tumefaciens* EHA105 strain used as control (about 100 leaf discs) (Figure 4).

**Figure 4: Hayward leaf discs after co-cultivation with *A. tumefaciens* EHA105 harboring the binary vector pCAMBIA1305.2_Psa21.**

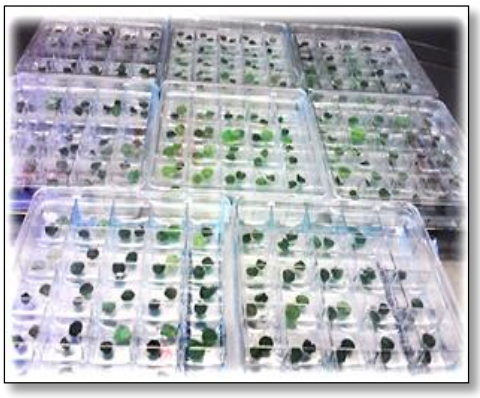

Following co-cultivation, the leaf discs were rinsed once in the washing solution (MS20 supplemented with 0.1M acetosyringone, 1M betaine chloride 200mg/l cefotaxime and 500mg/l amoxicillin) for 5h at 20°C with shaking at 100rpm. After that, leaf discs were blotted dry on sterile filter paper and placed onto MS20 selective medium supplemented with 0.1mg/l (NAA), 2mg/l thioridazine, 200mg/l cefotaxime and 10mg/l hygromycin for approximately 1 month at 28°C 16/8h photoperiod (Figure 5A). The regenerated shoots from each leaf disc were separeted and transferred to MS20 medium supplemented with 200mg/l cefotaxime and 10mg/l hygromycin (Figure 5B). The percentage of regenerated discs was about 11% (46/400 regenerated leaf discs and 2,5 shoots for regenerated leaf discs).

**Figure 5: A) Hayward leaf discs after one month on selective medium; B) Regenerated shoots from Hayward leaf discs.**

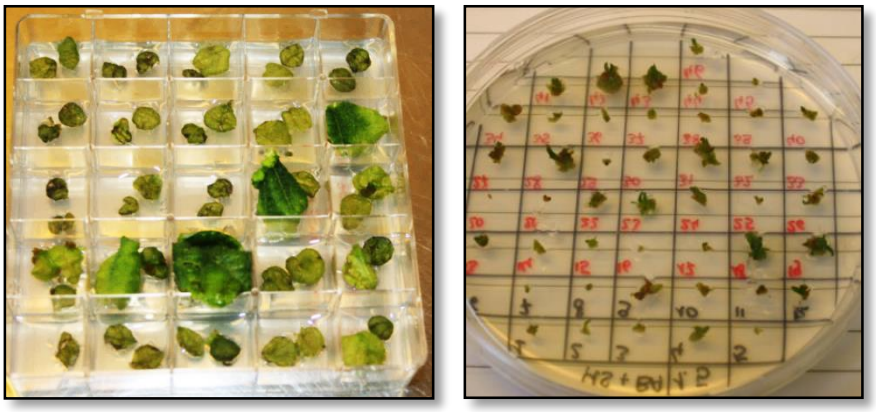

# *Chapter 3*

## The expression of short anti-infective peptides targeting Type Three Secretion System (TTSS) confers improved resistance to *Pseudomonas syringae* pv.*tabaci* in tobacco transgenic plants

### 3.1 Abstract

In this study, we used the pCAMBIA1305.2 binary vector, in which a sequence coding for a short oligopeptide (namely AP17), targeting the HrpA protein of the Type Three Secretion System (TTSS) of *Pseudomonas syringae* pv.*tabaci* replaces native GUSPlus™ gene. The vector electroporated into *Agrobacterium* EHA105, has been used to transform *Nicotiana tabacum* L.cv Xanthi. The peptide sequence was cloned in the vector downstream of the signal peptide GRP to target peptide delivery to the apoplast of plant cells. Bacterial suspensions containing *A. tumefaciens* EHA105/pCAMBIA 1305.2 native vector were also used to transform tobacco as transgenic control to rule out any transformation effect on resistance to *Pseudomonas syringae* pv. *tabaci* and to demonstrate apoplastic expression of GUS protein monitored by histochemical GUS assay. The integration of the peptide sequence was confirmed by polymerase chain reaction (PCR) and the expression was evaluated by RT-PCR and reverse transcription quantitative PCR. ELISA tests using polyclonal antibody against HrpA, were used to detect its presence in transgenic plants. Transgenic plants expressing high levels of peptide were selected, and then *in vitro* inoculated with *P. syringae* pv. *tabaci* strain ATCC 11528. While untransformed control and transgenic control plants carrying GUSPlus™ were severely affected by *Pseudomonas* infection, AP17 transgenic plants showed faint symptoms, and the bacterial growth was severely inhibited in few days after inoculation. This data denote a proof of principle that constitutively expressed virulence-inhibiting peptides could represent a successful strategy to control bacterial diseases of plants.

**Keywords:** Anti-infective peptides; AP17; HrpA; *Nicotiana tabacum; Pseudomonas syringae* pv. *tabaci*;

---

Bogani P., Biricolti S., Biancalani C., Cerboneschi M., Tegli S. The expression of short anti-infective peptides targeting Type Three Secretion System (TTSS) confers improved resistance to *Pseudomonas syringae* pv.*tabaci* in tobacco transgenic plants. *Manuscript in preparation.*

## 3.2 Introduction

Phytopathogens are the major problem in the agricultural sector around the world, causing substantial declines in yields with huge economic losses. Plant protection and resistance against pathogens have been traditionally and are still currently addressed with chemicals and breeding programs. However, both agrochemicals methods and conventional breeding have many drawbacks (Ravinder *et al*., 2014). On one side, indiscriminate use of chemical compounds has a negative impact on human, animal and environment health, on the other conventional plant breeding has a limited scope due to the paucity of genes with interesting traits in the usable gene pools and their time-consuming nature (Jan *et al*., 2010).
Moreover, the increased public concern about the use of chemical compounds in crop disease protection presses in order to search alternatives to protect plants from pathogens. Likewise, during the last years, the research in plant pathology has focused on development of novel molecules with a wide antimicrobial activity spectrum against bacterial and fungal pathogens (Upadhyay *et al.*, 2014). Recent advances in plant biotechnology, including the possibility of gene isolation and characterization, stable transformation and regeneration of transgenic plants in a wide range of species, have driven the development of new strategies and in particular molecular methods have been adopted, which expression in plants of antibacterial proteins of external or endogenous origin (Hou *et al*., 2014). Consequently, genetic engineering and transformation technology offer better tools to test the efficacies of genes and to provide a better understanding of their mechanisms in crop improvement. Therefore, to engineer plants with resistance genes against pathogens is becoming possible and plant transformation *Agrobacterium*-mediated has become a favored approach for many crop species (Barampuram and Zhang, 2011). In fact, this method is most preferred due its accessibility, tendency to transfer low copies of target genes with higher efficiencies, lower cost and with minimal rearrangement of a very large DNA fragments (Shibata and Liu, 2000; Gelvin, 2003). In this scenario, genetic engineering of plants expressing AntiMicrobial Peptides (AMPs) has been developed to create resistant plants and in recent years AMPs have been increasingly identified as candidate for disease protection in plants (Hancock and Lehrer, 2006). Usually, they are peptides of 10-100 amino acids and they are components of innate defense mechanisms in organisms ranging from microbes to plants and animals (Bahar and Ren, 2013; Peters, 2010). A very considerable number of AMPs, more than 5000, have been discovered and reported which have either been identified from natural sources or have been artificially synthesized (Zhao, 2013). For example, the synthetic peptide BP100 was found to be effective at micromolar concentration against *Xanthomonas axopodis* pv. *vesicatoria* in pepper, *Erwinia amylovora* in apple and *Pseudomonas syringae* pv. *syringae* (Badosa *et al.*, 2007, Montesinos and Bardajì, 2008). However, some failures and negative aspects related to this strategy to be mentioned. For example, it was reported that expression of a native cecropin B or a synthetic cecropin analogue in transgenic tobacco and potato showed no enhanced resistance to bacterial infections, presumably due to degradation of the peptides by host proteases present in the intercellular fluid (Hightower *et al.*, 1994; Allefs *et al.*, 1995; Florack *et al.*, 1995; Yevtushenko *et al*., 2005). Most of the AMPs have a common mechanism of action that involves the formation of pores in cell membranes (Sato and Feix, 2006). However,

it was reported that AMPs interfere with cell division, macromolecular synthesis and cell wall formation (Brogden, 2005). For these reasons, it is belived that AMPs are less vulnerable to the resistance development compared to conventional antibiotics (Tan *et al.*, 2000). Althought AMPs possess considerable benefits, their commercial development still have some limitations, such as potential toxicity, susceptibility to proteases, and high cost of peptide production (Jung *et al*., 2014).

Nevertheless, there are some works where the transgenic expression of AMPs has delivered encouraging results in conferring specific or broad spectrum disease resistance in plants such as tobacco, potato, rice, banana, tomato and grapevine (Yevtushenko *et al.*, 2005; Mentag *et al.*, 2003; Vidal *et al.*, 2006; Gao *et al*., 2000; Chakrabarti *et al*., 2003).

In this work, we report the successful transgenic stable transformation *Agrobaterium tumefaciens*-mediated of tobacco plants carrying the anti-virulence peptide AP17. These plants exhibited enhanced disease resistance to the pathogen *Pseudomonas syringae* pv. *tabaci*.

## 3.3 Materials and Methods

### Plant material and bacterial strains

*Nicotiana tabacum* cv Xanthi axenic plants were obtained by germination of seeds on Linsmaier & Skoog Medium (LS) including vitamins (LAB Associates B.V., The Netherlands) after sterilization. Tobacco seeds were surface sterilized as follows: 1 min in 70% (v/v) ethanol, 20 min in a 5% (v/v) hypochlorite containing a drop of Tween 20 and three successive washes of 10 min each in sterile water. Surface sterile seeds were germinated on LS medium containing 30 g/l sucrose and 0.6% agar and further grown at 24±1°C under a 16 h light/8 h dark lighting conditions. Tobacco shoots were maintained *in vitro* by sub-culturing the top part of the shoots on fresh LS medium at intervals of 20 days.

Bacterial strains and plasmids used in this work are described in Table 1. *P. syringae* pv. *tabaci* strain ATCC 11528 (*Pstab*) was cultured and maintained on KB (King *et al.*, 1954) medium at 26°C. Nitrofurantoin when appropriate was added to the medium at the concentration of 50 g/l. *Agrobacterium tumefaciens* strain EH105 was grown and maintained on YEP medium (10 g yeast extract, 10 g bacto peptone, 5 g NaCl, 15 g agar, pH 7, per liter) at 28°C in the dark. Antibiotics were used at the following concentrations: rifampicin at 40 µg/ml, and hygromycin B at 10 µg/ml.

### Plant transformation and molecular analysis of *N. tabacum* transgenic plants

For stable nuclear transformation of *N.tabacum* with DNA coding for the oligopeptide AP17 was inserted into the binary vector pCAMBIA1305.2Δ*gus* (Chapter 2) downstream of the signal peptide GRP (Figure 1) upon removal of the GUSPlus™ gene. The empty vector pCAMBIA1305.2 and the recombinant pCAMBIA::AP17 construct were electroporated into *Agrobacterium tumefaciens* strain EHA105 and a colony of the transformed bacteria, was used to transform leaf explants of *N. tabacum* L. cv Xanthi with the leaf disc infection technique (Horsch *et al*., 1985). Primary transformants were selected using 50 mg/l hygromycin and transformation was confirmed using Phire Plant Direct PCR Kit (ThermoFisher Scientific™) in combination with the CAMBIA_FOR and CAMBIA_REV primers (Table 2), according to the manufacturer's instructions in PCR reaction. $T_0$ transgenic plants were sub-cultured at intervals of 20 days, on fresh LS medium supplemented with the selection agent and 500 mg/l cefotaxime to eliminate *Agrobacterium* cells. Positive independent primary shoots ($T_0$) were transferred to a greenhouse and allowed to self-pollinate at a temperature ranging from 18 to 24±1°C, until $T_1$ seeds production. $T_1$ seeds from each independent line were then surface sterilized and placed in LS medium with 50 mg/l hygromicin and grown at 24±1°C under a 16 h light/8 h dark lighting conditions to obtain $T_1$ transgenic shoots. $T_1$ seedlings were maintained in these conditions through further transfers onto selective fresh medium at growth intervals of 20 days each.

**Table1. Bacterial strains and plasmids used in this study.**

| Strains | Relevant characteristics | Reference/Source^ |
|---|---|---|
| *P. syringae* pv.*tabaci* (11528) | Wild-type | LPVM collection |
| *A.tumefaciens*(EHA105) | C58 pTiBo542; T-region::aph, kan; derivative of EHA101 | Hood *et al.*, 1993 |
| **Plasmids** | | |
| pCAMBIA 1305.2 | nptII, kan, GUSPlus™ , secretion signal peptide | CAMBIALabs, Austrialia |
| pCAMBIA 1305.2*Δgus* | nptII, kan, *Δgus*, secretion signal peptide | (Chapter 2) |
| pCAMBIA1305.2::AP17 | nptII, kan, *Δgus*, AP17 peptide, secretion signal peptide | (Chapter 2) |

^LPVM Laboratorio di Patologia Vegetale Molecolare (University of Florence).

## DNA extraction and PCR analysis

Genomic DNA was extracted from $T_1$ transgenic tobacco plants using the NucleoSpin® Plant II kit (Macherey-Nagel) according to the supplier's instructions. PCR reactions were carried out with primers for the amplification of AP17 peptide expression cassette (CAMBIA_FOR and CAMBIA_REV) and hygromycin resistance gene (HYGRO_FOR/HYGRO_REV) (Table 2). The PCR reaction mixtures contained 200 µM dNTPs (Pharmacia), 0.5 µM each primer, 0.2 U Taq polymerase (Fermentas), 1X PCR buffer and 50 ng genomic DNA. Reactions were carried out in a MJ Research PTC-200 DNA Engine Thermal Cycler set for an initial cycle at 94°C for 5 min followed by 35 cycles at 94°C for 30 s, 56°C for 30 s, 72°C for 40 s and a final extension at 72°C for 10 min.

## RNA isolation, reverse transcription (RT) and qPCR

Total RNA from leaves of 4 selected genotypes of $T_1$ transgenic and wild type tobacco plantlets was extracted following the instructions of the Macherey–Nagel''Nucleospin RNA Plant''kit. RNA concentration was estimated by fluorometry using the Q-bit quantitation platform by Invitrogen and digested with DNAse. RT-PCR for the analysis of transgene expression was performed with the First Strand cDNA Synthesis Kit for RT-PCR (AMV) (Roche Diagnostics, Monza, Italy), following the manufacturer's instructions. PCR amplification of the AP17 transgene was performed on cDNA obtained with oligo (dT) primers, using GRP-FOR and AP17-REV primers (Table 2) to selectively amplify the expressed sequence of the AP17 short oligopeptide comprising the signal peptide. Three µg of RNA from four selected transgenic lines (F, G, L, and N) and wild type *N. tabacum* were used for quantitation of the ectopic expression level of the AP17 sequence.

## Primers for q-PCR

Primers for reference genes Actin (Act 9), Elongation factor (EF-1$\alpha$) and L25 ribosomal protein were designed based on the accession sequences, available in the GenBank® database (X69885, AF120093, L18908). The primers have been designed and tested to assess the amplification efficiency. The sequences are detailed in Table 2. All primers were synthesised by Sigma Aldrich Co., Milan, Italy.

Prior to the assays, serial tenfold dilutions of the line AP17 L c-DNA were amplified to evaluate the amplification efficiency by the comparison of the slope of the regression curves

of transgene regions (AP17) and the reference Actin (Act9), Elongation factor 1$\boldsymbol{\alpha}$ (EF-1$\boldsymbol{\alpha}$), L25 ribosomal protein as previously reported (Biricolti *et al*., 2016). In fact, the use of the $2^{-\Delta\Delta Ct}$ method for relative quantification, a comparative technique in which a target gene is normalised to an endogenous control, requires the PCR efficiencies of target and control genes to be approximately equal.

**Table 2: Primers used in this study.**

| Primer name | Primer sequence (5'-3') | Tm (°C) |
|---|---|---|
| **AP17 qPCR** | For GCTCTTGCCATCCTTGTC<br>Rev CGATTTGGTTGGAAAGGG | 55.0<br>57.0 |
| **Act9 qPCR** | For CCTGAGGTCCTTTTCCAACCA<br>Rev GGATTCCGGCAGCTTCCATT | 62.0<br>64.0 |
| **EF-1$\boldsymbol{\alpha}$ qPCR** | For TGAGATGCACCACGAAGCTC<br>Rev CAACATTGTCACCAGGAAGTG | 60.0<br>61.0 |
| **L25 qPCR** | For CCCCTCACCACAGAGTCTGC<br>RevAAGGGTGTTGTTGTCCTCAATCTT | 61.0<br>60.0 |
| **CAMBIA** | For CTACTACTAAGCATTTGG<br>Rev AACCCATCTCATAAATAAC | 55.0<br>55.0 |
| **HYGRO** | For GCGAAGAATCTCGTGCTTTCAG<br>Rev CCGATGCAAAGTGCCGATAAAC | 63.1<br>63.7 |
| **GRP** | For ATGGCTACTACTAAGCATTT | 57.8 |
| **AP17** | Rev CCCTTTCCAACCAAATCGTT | 58.1 |

**Quantitative PCR procedure**

PCR analyses were performed with a Rotor-Gene 6000 (Corbett Life Science, Mortlake, Australia) in a 15 µl volume containing 3 ng cDNA, 7.5 µl of 2X SsoAdvanced SYBR Green Supermix (Bio-Rad laboratories srl, Hercules, CA, USA) and 250 nM of each primer. PCR conditions were 95°C for 5 min to activate the DNA polymerase, then 40 cycles at 95°C for 13 seconds and 60°C for 40 s for the reference gene and 95 for 13 sec 57 for 13 sec, 60 for 13 sec. The melting curves of the PCR products were acquired by a stepwise increase in the temperature from 50°C to 96°C after PCR amplification, which is a built-in program of the Rotor-Gene® platform. Each c-DNA sample was analyzed in triplicate in separate reactions.

**Relative quantification by the comparative $C_t$ ($2^{-\Delta\Delta Ct}$) method**

The most robust method for the relative quantification in real time PCR of a target gene transcript in comparison to a reference gene transcript is the $C_t$ ($2^{-\Delta\Delta Ct}$) method (Livak and Schimittgen, 2001). If all amplicons amplify with the same efficiency, the difference $\Delta C_t$ between the $C_t$ for the transgene ($Ct_t$: AP17 transcript) and the $C_t$ for the endogenous control ($Ct_r$: Actin or EF or L25) is constant, provided that, independently from the amount, c-DNA is the same for both amplification reactions (transgene and endogenous control):

$\Delta C_t = Ct_t - Ct_r$

In our study, transgene expression is relative to the lowest expressing line (AP17 F) which has been adopted as a calibrator. Thus, in all samples with the same $\Delta C_t$ as the calibrator, $\Delta\Delta C_t$ equals zero and 20 equals one, so that the fold change in gene expression relative to the calibrator equals one, by definition. More generally, the ratio of the expression level of the transgene transcript in the genotype to be tested ($X_s$) to expression level of the transgene transcript in the calibrator ($X_{cal}$) can be calculated as follows:

$X_s/X_{cal} = (1+E)^{\wedge} (-\Delta\Delta C_t)$

where $\Delta\Delta C_t = \Delta Ct_s - \Delta Ct_{cal}$, $\Delta Ct_s = \Delta C_t$ sample, $\Delta Ct_{cal} = \Delta C_t$ calibrator and E=amplification efficiency (varying from 0 to 1).

**Histochemical GUS assay**

Leaf samples were collected and fixed in buffered (phosphate buffer 100 mM) para-formaldehyde 4% for about 15 minutes. Afterwards the samples were washed 5 times with phosphate buffer (100 mM) and put into buffered X-Gluc (phosphate buffer 100 mM; EDTA 10 mM; ferricianyde 2 mM; Triton X-100 0.1%; sodium metabisulphite 2 mM; X-Gluc 1 mM). Then buffered X-Gluc was changed once and the samples were kept in an incubator at 37 °C overnight.

Samples were washed twice with phosphate buffer (100 mM), dehydrated by bathing in an ethanol series, and embedded according to the manufacturer protocol (Historesin). 5 µm thick sections were obtained with a rotary microtome with glass blades.

The sections were examined using a light microscope (Zeiss, Laborlux 12) and staining patterns recorded by photography using Kodak Ektachrome 160T film.

**ELISA assay**

To ascertain the correct expression of AP17 peptide in transformed tobacco leaves an ELISA assay was performed using the apoplastic fluid extracted from wild type and genetically transformed *N. tabacum in vitro* plants with the empty vector pCAMBIA 1305.2 as control or with the four different pCAMBIA1305.2::AP17 lines named AP17 L, G, N, F.

The infiltration-centrifugation technique using vacuum flask was performed and cytoplasmic contamination was verified as previously reported (O'Leary *et al.,* 2014). The fluid recovered after centrifugation was used to perform ELISA assay according to manufacturer's instructions (Bethyl Laboratories Inc., Montgomery, TX, USA). Polyclonal primary antibodies against HrpA protein of *Ptab* were obtained from Primm srl (Milano-Italy) and used together with secondary anti-rabbit horseradish peroxidase conjugate antibodies (Bethyl Laboratories Inc., Montgomery, TX, USA), according to manufacturer's instructions and as reported in Chapter 4. The standard curve was obtained with serial dilution of AP17 peptide synthesised by Primm srl (Milano-Italy). The experiment was performed three times with three replicates for each tobacco lines analysed. The values obtained are calculated according to the following formula:

$$(ng/ml)/(ml_{ext} / ng_{inf})_{unk} - (ml_{ext} / ng_{inf})_{c}$$

Where:

$ml_{ext}$ = leaves fluid extract after infiltration-centrifugation

$ng_{inf}$ = leaves weight after infiltration

unk = sample unknown; c = untransformed plant

**Pathogen assay**

*P. syringae* pv. *tabaci* strain ATCC 11528 (*Ptab*) was grown at 26°C for 1 day in KB medium containing 50 mg/l nitrofurantoin. Cells were then centrifuged and diluted in 0.9% NaCl to a concentration of 108 CFU/ml ($OD_{600}$= 0.5). 1 ml of the diluted suspension culture was then sprayed on the surface of wild type and transgenic plants grown in Wavin flasks (LAB Associates B.V., The Netherlands) containing LS solid medium. Tobacco plants sprayed with *Ptab* were grown *in vitro* up to 20 days. At different days from inoculation, 3, 10 and 20 days, bacterial multiplication into host tissues was evaluated. At each time, a sample of leaves was weighed and then washed in 5 ml sterile 0.9% NaCl (washing solution), to estimate *Ptab* survival on the leaf surface. The leaf sample was sterilised with 1% hypochlorite solution for 5 min and successively washed three times with sterile distilled water. Each sample was, then homogenized in a sterile Eppendorf with a plastic pestle with 1 ml sterile distilled water. 100 µl of washing solution and of the homogenate were serially diluted up to $10^{-7}$/ml cells. Five replications of each dilution were plated on solid KB medium supplemented with 50 mg/l nitrofurantoin. Bacterial growth was scored after two days of incubation of plates at 26°C.

**Statistical analysis**

The analysis of variance between untransformed *N. tabacum* and transgenic plants was conducted using One-way ANOVA ($P < 0.05$). Mean separations were performed using the method of Tukey. For the analysis the PAST program, version 1.89 (Hammer et al. 2001) was used.

## 3.4 Results

### Molecular analysis of transgenic tobacco plants

pCAMBIA1305.2 (http://www.cambia.org/) and pCAMBIA1305.2::AP17 (Figure 1) binary vectors were used to obtain transgenic tobacco plants expressing respectively the GUSPlus™ reporter gene and the short AP17 peptide (17 amino acids) by using EHA105 *Agrobacterium* infections. The short AP17 peptide was cloned downstream of the constitutive CaMV 35S promoter and the GRP signal peptide, this latter addressing the recombinant AP17 peptide to the apoplast. The transformation efficiency in the presence of 50 mg/l of the selection marker ranged from 50% with the pCAMBIA1305.2 compared with 32.05% with the pCAMBIA1305.2::AP17.

**Figure 1. Schematic representation of T-DNA region of pCAMBIA1305.2::AP17 binary vector. LB= Left border; RB= Right border; HYG= hygromycin resistance gene; CaMV35S= cauliflower mosaic virus promoter; GRP= signal peptide; AP17= oligopeptide, 17 aminoacid long; NOS= Nopaline terminator.**

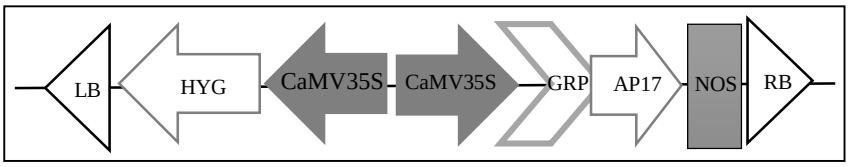


Peptide transgenic shoots able to grow in the presence of 50 mg/l hygromycin were, early scored for the presence of the cassette through the amplification of DNA directly from shoots with the CAMBIA_FOR and CAMBIA_REV primers that amplified a fragment of the expected size including the AP17 peptide (data not shown). Positive plants were allowed to produce self-pollinated seeds that generated hygromycin-resistant progenies. PCR analysis of genomic DNA extracted from positive $T_1$ selfed-lines confirmed the presence of both the hygromycin gene in both pCAMBIA and AP17 transgenic plants and the presence of sequence peptide only in these latter (Figure 2).

**Figure 2. Electrophoretic analysis of PCR carried out with HYGRO_FOR/HYGRO_REV (Left) and CAMBIA_FOR/CAMBIA_REV (Right) primers. 1 kb Plus ladder ThermoFisher (M); *N. tabacum* wild type (1); pCAMBIA1503.2 plants (1-4); pCAMBIA::AP17 plants (5-8); PCR negative control (c-).**

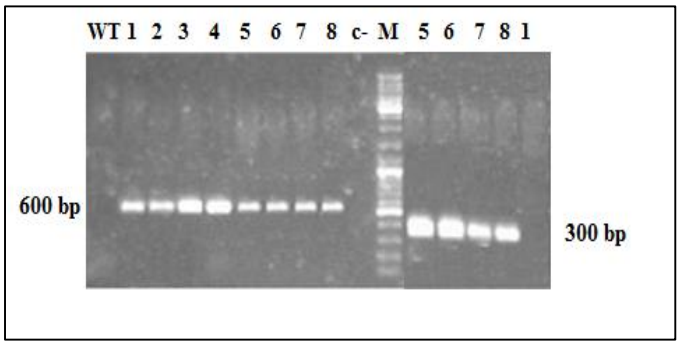

To assess the apoplast localization of the GUSPlus™ protein in pCAMBIA transgenic plants, leaf semithin sections have been made. In Figure 3 the blue color of the X-gluc reaction seems to be localized outside the plasma membrane and often in correspondence of plasmodesma bridging two adjacent cells, indicating that the GUS protein is driven outside the cell cytoplasm.

**Figure 3. Localization of *gus* expression in leaf cells of pCAMBIA1305.2 transgenic plants.**

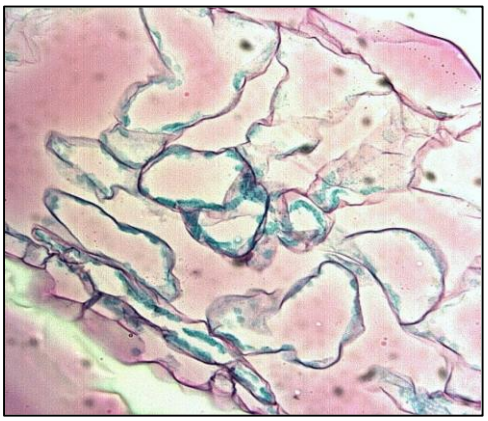

AP17 sequence transcritpion was demonstrated in selected transgenic plants by both RT-PCR and quantitative PCR. In the first case, amplification with RTGRP_FOR e AP17_RTREV primers produced a fragment 70 bp long, corresponding to the transgene coding sequence (Figure 4). The presence of genomic DNA contamination in the RNA samples has been, ruled out by PCR amplification with the same primers carried out on total RNA without RT step (data not shown).

**Figure 4: RT-PCR amplification of the full-length AP17 peptide from cDNAs of four pCAMBIA::AP17 transgenic lines (5-6-7-8), amplification from cDNA of tobacco wild type plant (WT), negative control (c-).**

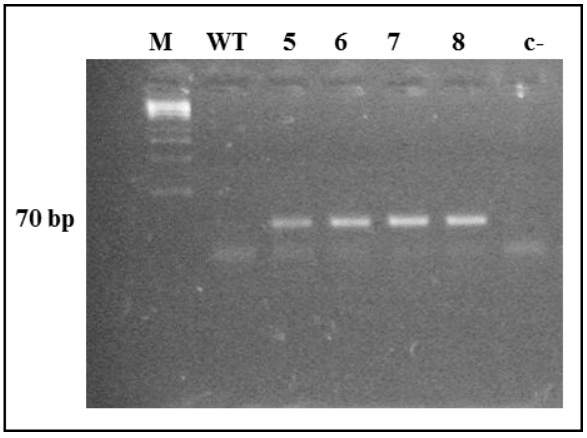

## q-PCR analysis

There is considerable variation among independent transgenic lines obtained under identical conditions using the same DNA construct (Toplak *et al*, 2004). For this reason, in studies of transgenic plants, transgene expression must be assessed in each independent transgenic line. Quantitative PCR was carried out to evaluate the relative level of expression of the AP17 sequence in the leaves of four selected lines of transgenic tobacco. The expression has been normalised with specific housekeeping genes, the highest expression was observed in line AP17 L, which was twice that observed in the two lines AP17 G and AP17 N and 8 times the expression of AP17 observed in line AP17 F (Figure 5).

**Figure 5: Quantitative PCR on cDNA extracted from leaves of four selected lines of transgenic tobacco. Curves of different colour indicate different transgenic lines, in blu (AP17 L), in dark green (AP17 G), in light green (AP17 N) in violet (AP17 F), dark violet lines correspond to the control (sterilised water).**

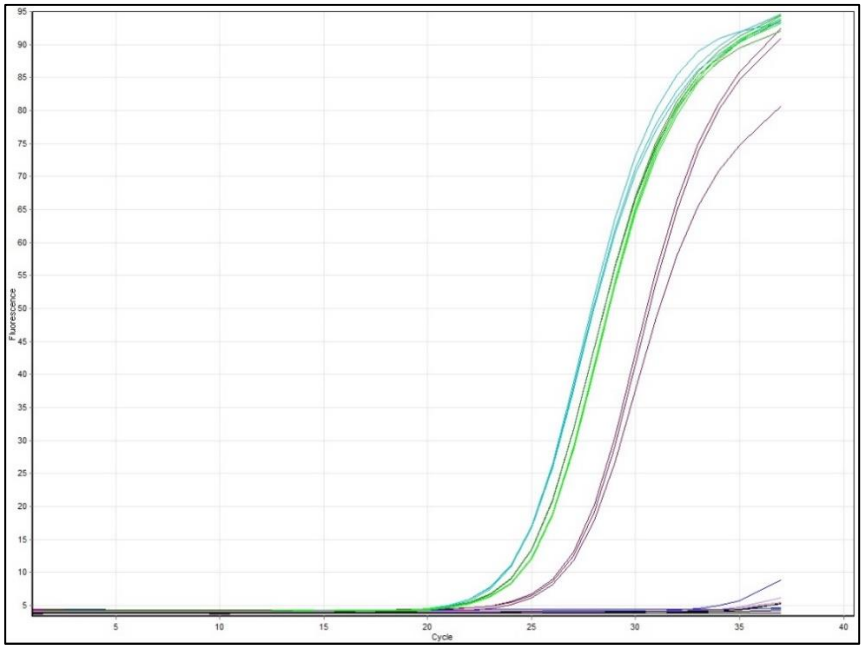


## ELISA analysis

ELISA tests using polyclonal antibody against HrpA, whose sequence includes the one of AP17 peptide (Chapter 2) have been carried out to further confirm the presence and expression of AP17 peptide in transgenic plants as already demonstrated by RT-PCR. To verify the sensitive of ELISA analysis and to exclude that fluid leaves background could change values recorded, we have set up two standard curves. Serial dilution of AP17 synthetic peptide were prepared both in leaves fluid extracts and in phosphate buffer. The two curves are not perfectly overlapping, however, linearity is maintained and the two standard curves are parallele in the range of AP17 concentration testes except for AP17 L (Figure 6A). This line, in fact, expresses this peptide at higher concentrations, above those found within the range of the standard curves linearity. The analysis performed suggest that substances in the fluid leaves extract do not interfere with antibody binding or subsequent reaction in the ELISA

assay. Results obtained and reported in Figure 6B shown a different amount of AP17 peptide deteced by antibody into leaves extracts among the four tobacco lines. The results obtained are consistent with those from qRT-PCR. In particular, low values of AP17 peptide have been recorded for AP17 F, where no statistically differences were recorded in comparison to control (tobacco line C), intermedie values have been reported for AP17 G and N.

**Figure 6: A) Standard curves for AP17 pepetide in phosphate buffer *vs* fluid leaves extract. Standard curves of fluid leaves extract from untransformed tobacco plants added with known concentration of synthesised AP17 peptide (from 500ng/ml to 31,25 ng/ml) [blue line], or diluited in phosphate buffered saline [red line]. Each data point is the mean of three measures ± standard deviation, with the dotted line through the data points representing the linear regression for each curve. B) Detection of AP17 peptide on different fluid leaves samples from *N. tabacum* transformed plants: C; pCAMBIA1305.2 empty vector (used as control); F, L, G, N different lines of tobacco transformed plants). Data obtained and reported in the histogram have been obtained according to the formula reported in Material and Methods. Different letters indicate significant differences among means at $P < 0.05$, according to Tukey's test.**

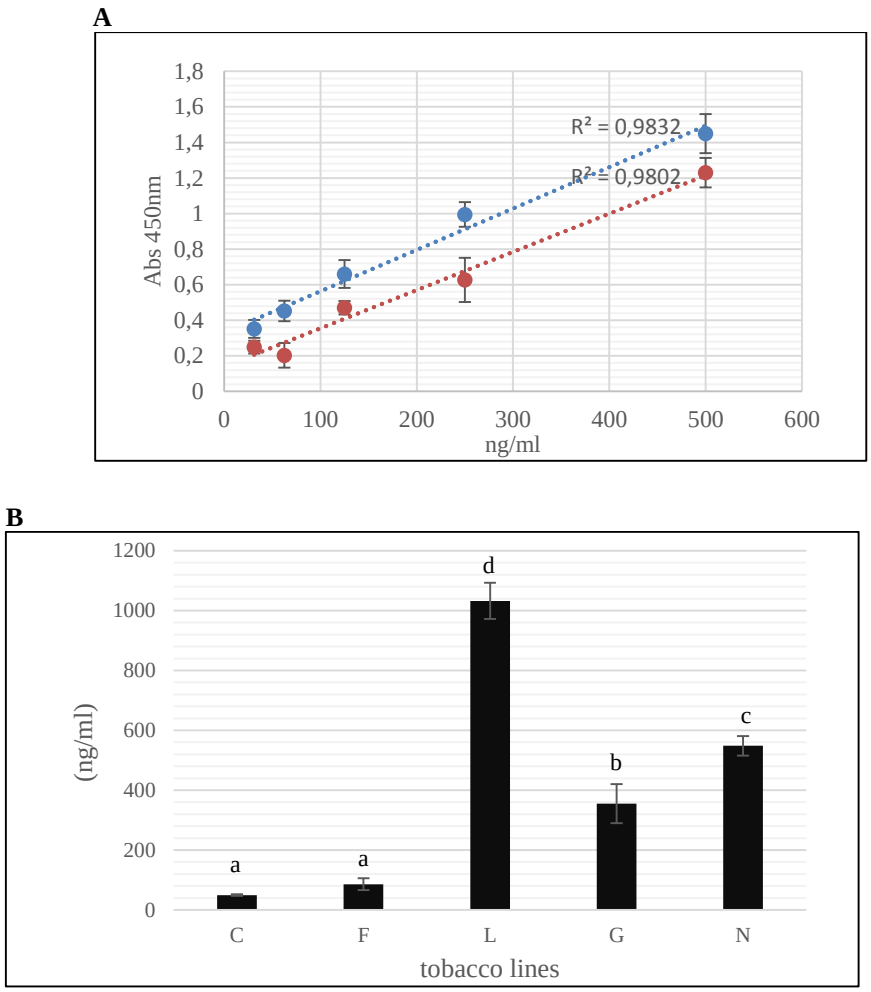


## Tobacco transgenic lines display enhanced resistance to *Ptab*

*In planta* resistance to *P. syringae* pv. *tabaci* inoculation of *in vitro* ten months old $T_0$ plants wild type and genetically transformed with pCAMBIA 1305.2 (as transformed control) or with pCAMBIA::AP17, using the spraying technique (see Materials and Methods), resulted in areas of necrosis on the surface of the exposed leaves only in wild type and

pCAMBIA1305.2 transgenic plants. After 10 days from artificial inoculation, typical *Ptab* symptoms were recorded and evaluated according to an arbitrary disease index (0-5, with 0= no necrotic symptoms and 5= fully necrotized leaves), for a proper comparison among the different symptoms observed in wild type and transgenic tobacco plants (Figure 7).

**Figure 7. Phenotype analysis of tobacco plants before (A, B, C) and after 10 days from bacterial spray inoculation (A1, B1, C1) and disease index on transgenic tobacco plants: *N. tabacum* wild type (A), *N. tabacum* pCAMBIA1305.2 (B) and *N. tabacum* pCAMBIA::AP17 transgenic line L (C).**

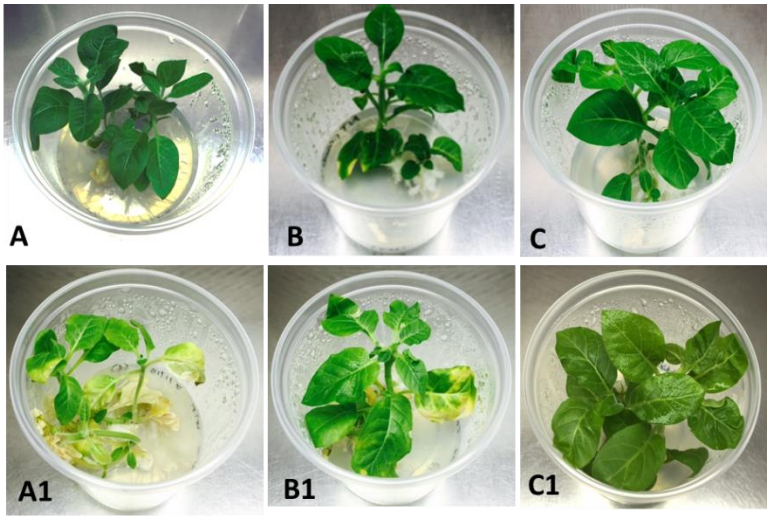


| ***Pseudomonas syringae* pv. *tabaci*** | | |
|---|---|---|
| ***N. tabacum* wild type** | ***N. tabacum* pCambia1305.2** | ***N. tabacum* pCambia::Ap17** |
| **3.31±0.50** | **3.28±0.42** | **0.13±0.02** |

To assess whether the lack of symptoms in peptide transgenic plants was due to bacterial growth inhibition operated by the anti-infective peptide, we repeated the infection with *Ptab* on a panel of three replicates per genotype on two months old plants germinated from $T_1$ selected seeds. Bacterial survival was evaluated both in leaf surface washing solutions and in the host leaf tissue (see Materials and Methods) as CFU/ml/g fresh weight. Data were recorded after 3, 10 and 20 days after spray-inoculation with the bacterial suspensions. The starting concentration of the bacterial inoculum was about $10^8$ cells/ml. After 3 days, the growth data of bacteria present in washing solutions ranged from a maximum of more than $10^{11}$cells/ml in both *N. tabacum* wild type and *N. tabacum* pCAMBIA1305.2 transgenic leaves to a minimum of $10^7$ cells/ml in *N. tabacum* AP17 (Figure 8A). However, no statistical differences were found (*P*= 0,4824), whereas a significant reduction of bacterial growth into AP17 leaf tissues homogenates of each genotype was detected (Figure 8 B). A significant lower number of colonies in comparison with wild type and pCAMBIA1305.2 plants were detected both, in washing solutions and leaf tissues of AP17 plants at 10 days after the inoculation (Figure 8 C, D).

Finally, in Figure 9 we have reported results concerning the growth of bacterial populations present, either on the surface and into leaf tissues of all lines tested, after 20 days of inoculation. In this experiment, a pool of leaves taken from the bottom of the plant (the part of the plant subjected to spraying with bacterial suspension), from each replicate per line, was ground in 1 ml of washing solution. Serial dilutions of the leaf surface washing solutions and leaf homogenates were then plated in KB culture medium to assess the growth of bacteria. By increasing the time after infection, the overall bacterial growth capability was lower for each genotype, but a significant substantial bacterial growth inhibition was still observed in transgenic AP17 plants compared to both wild type and pCAMBIA1305.2 transgenic plants. Based on the results obtained we have hypothesized that these peptides could also act outside the intercellular space, maybe translocated together with plant exudates present on leaf surface.

**Figure 8. Bacterial growth in *N. tabacum* wild type (NtWT), pCAMBIA1305.2 (NtpCa) and pCAMBIA::AP17 (NtAp17) transgenic tobacco plants inoculated with *Ptab*, evaluated at different times after infection. A, C: Colony Forming Units (CFU/ml/g) of bacterial cells present on the surface of the infected leaves; B, D: Colony Forming Units (CFU/ml/g) of bacterial cells present in the infected leaf tissue. Bars indicate standard deviations (n=3). °P< 0,05; ***P<0,001; pair–wise comparisons were determined between NtWT and NtpCa plants (°) and between NtpCa and NtAp17 (***) plants.**

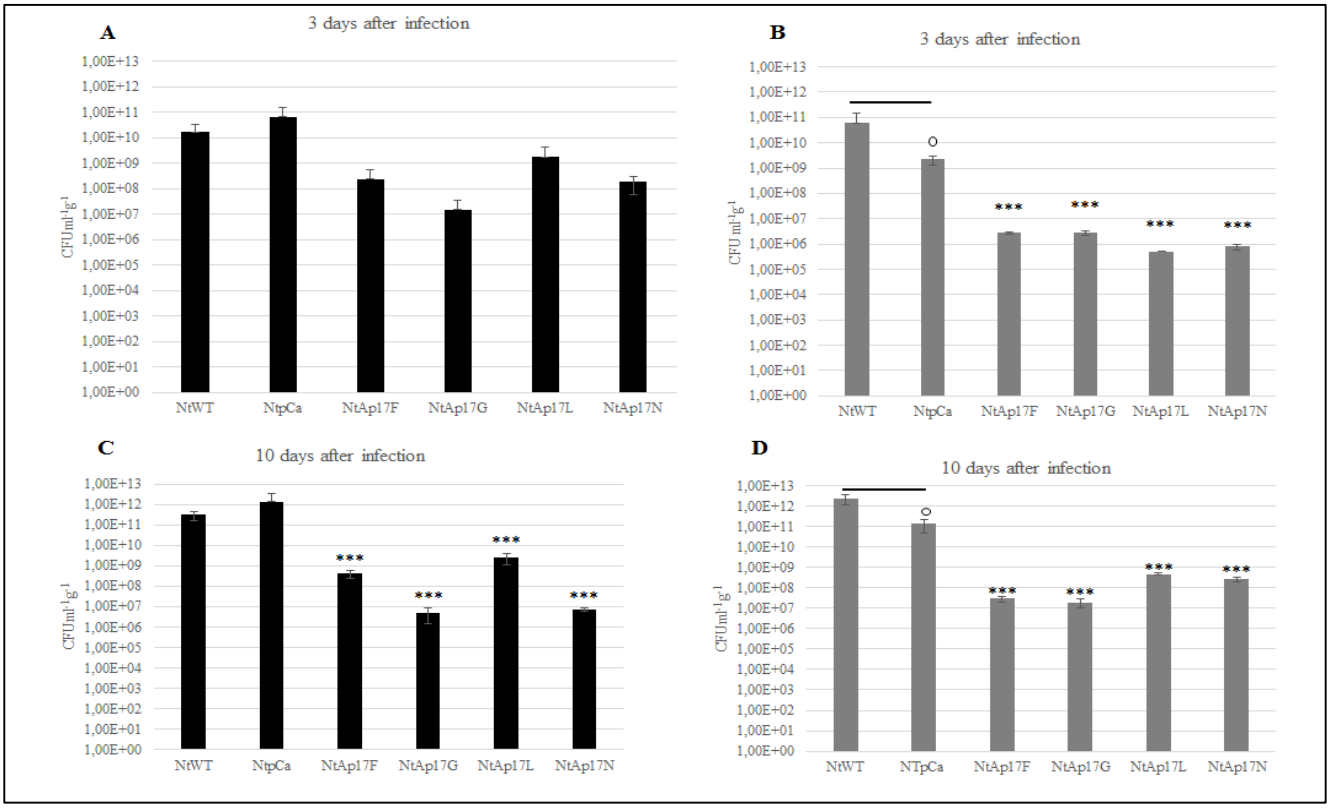

**Figure 9. Bacterial growth in *N. tabacum* wild type (NtWT), pCAMBIA1305.2 (NtpCa) and pCAMBIA::AP17 (NtAp17) transgenic tobacco plants inoculated with *Ptab*, evaluated at 20days after infection. On the left A) tobacco wild type, B) tobacco pCAMBIA1305.2 (control), C) tobacco pCAMBIA::AP17 (transgenic line L) inoculated with *Ptab*. Bars indicate standard deviations (n=3). **P<0,05 ; pair–wise comparisons were determined between NtWT and NtAp17 plants.**

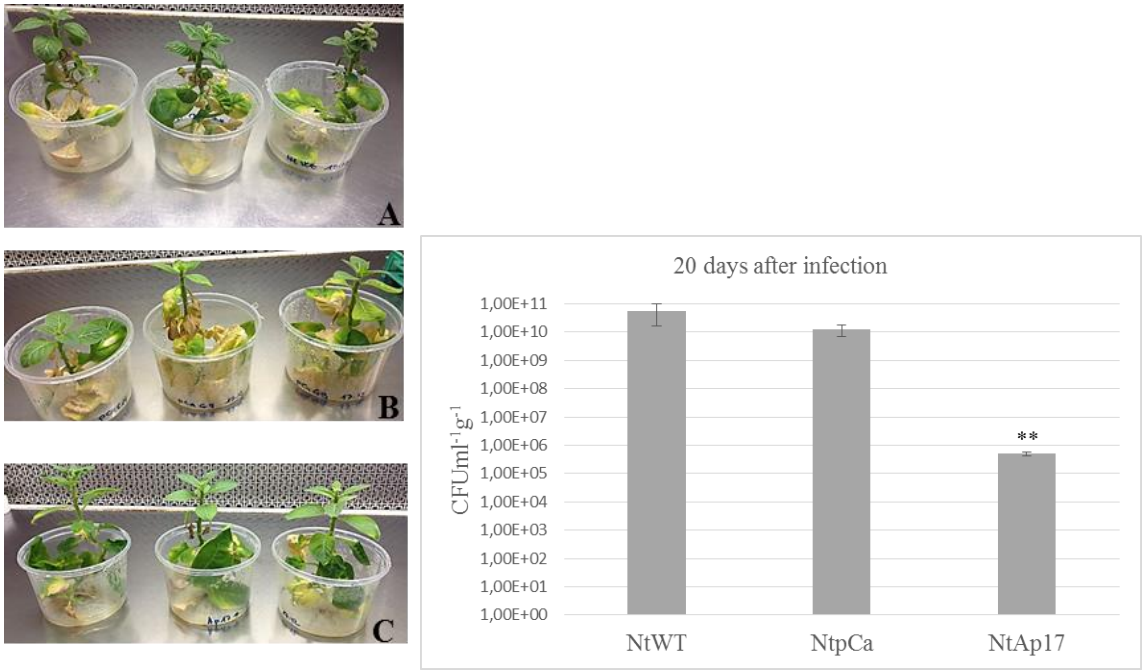

## 3.5 Discussion

The generation of transgenic plants expressing foreign genes of interest is the standard method for verifing and improving resistant against plant pathogen. AntiMicrobial Peptides (AMPs) have been the object of attention as candidates for plant protection products. There are already numerous studies reporting the stable expression of antimicrobial peptide genes in different plant species. This approache mainly aim to enhance the resistance of plants against certain pathogens and to lesser extent to use plants as biophactories to produce high amount of peptides (Ahmad *et al.,* 2010). In the last decade, the succesfull transformation of genetically modified plants expressing resistant genes against a wide range of plant pathogens has greatly increased. For example transgenic plants introduced with defensin genes have been used to control *Alternaria longipes, Verticillium dahliae, Heterobasidium annosum, Phytophthora parasitica, Botrytis cinerea* and *Alternaria solani* (Gao *et al.,* 2000; Elfstrand *et al*., 2001; Park *et al.,* 2002; Schaefer *et al.,* 2005). The hevein Pn-AMP expressed in tobacco protects against *Phytophthora parasitica* (Koo *et al*. 2002), and barley hordothionin expression in tobacco confers protection against *Clavibacter michiganensis* and *Pseudomonas syringae* pv. *tabaci* (Carmona *et al*. 1993). Also, human cathelicidin antimicrobial peptide carried out the substitution Met37Leu in Chinese cabbage and tomato plants significantly inhibited the growth of *Pectobacterium carotovorum* subsp. *carotovorum* on the plant leaves, and it conferred resistance to several fungal pathogens (Jung *et al*. 2012).

In this work, for the first time we described the genetic transformation of *Nicotiana tabacum* L. cv *Xanthi* with the Virulence Inhibiting Peptide AP17, which competes in a highly specific manner with the monomers of not only of *P. savastanoi* pv. *nerii* but also of *P. syringae* pv.*tabaci* HrpA protein by preventing the assembly of the pilus of the Type Three Secretion System (Chapter 2).

We have used herein with succesfull *Agrobacterium*-DNA mediated trasformation with the binary vector pCAMBIA1305.2 characterized by the present of signal peptide upstream of AP17 gene sequence that drives its expression at apoplastic level as ascertained through the histochemical GUS assay. This feature is particular interesting because the peptide AP17 should be expressed in the site where supposedly happens the pilus assembly (Chapter 2).

We have generated four lines of transgenic tobacco plants, which have different levels of AP17 mRNA and different levels of peptide expression as detected in apoplastic fluid by ELISA assay using polyclonal antibodies against the HrpA protein.

The efficacy in both growth bacterial inhibition *in planta* and in symptom development is tightly related to the presence of oligopeptide AP17 in transgenic tobacco plants as confirmed by the results obtained with the control plants transformed with the only pCAMBIA1305.2 vector.

Taken together, the obtained results in the present study are definitely encouraging and unambiguously suggest that the expression of the AP17 peptide provides an exciting approach to verify the effectiveness of this peptide in fighting the plant pathogenic bacteria *P. syringae* pv. *tabaci.* These data suggest that the oligopeptide AP17 has broad application prospects in improving crop disease resistance.

## 3.6 References

**Ravinder K**, Goyal A, Mattoo AK. (2014) Multitasking antimicrobial peptides in plant development and host defense against biotic/abiotic stress. *Plant Sci*. 228:135–149

**Jan PS**, Huang HY, Chen HM. (2010) Expression of a Synthesized Gene Encoding Cationic Peptide Cecropin B in Transgenic Tomato Plants Protects against Bacterial Diseases. *Applied and environmental microbiology*. Feb. 2010, p. 769–775 Vol. 76, No. 3 0099-2240/ doi:10.1128 AEM.00698-09

**Upadhyay A**, Upadhyaya I, Kollanoor-Johny A, Venkitanarayanan K. (2014) Combating Pathogenic Microorganisms Using Plant-Derived Antimicrobials: A Minireview of the Mechanistic Basis. *Biomed Res Int*. 2014; 2014: 761741. doi:10.1155/2014/761741

**Hou H**, Atlihan N, Lu ZX. (2014) New biotechnology enhances the application of cisgenesis in plant breeding. *Front Plant Sci*. 2014; 5: 389. doi:10.3389/fpls.2014.00389

**Barampuram S** and Zhang Z. (2011) Recent advances in plant transformation. *Methods in Molecular Biology* Vol. 701; 1–35 doi: 10.1007/978-1-61737-957-4

**Shibata D** and Liu YG. (2000) *Agrobacterium*-mediated plant transformation with large DNA fragments. *Trends Plant Sci*. 2000 Aug;5(8):354-7

**Gelvin SB**. (2003) *Agrobacterium*-mediated plant transformation: the biology behind the "gene-jockeying" tool. *Microbiol Mol Biol Rev*. 2003 Mar;67(1):16-37

**Hancock REW** and Sahl HG. (2006) Antimicrobial and host-defense peptides as new anti-infective therapeutic strategies. *Nat. Biotechnol.* 24 1551–1557 10.1038/nbt1267

**Bahar AA** and Ren D. (2013) Antimicrobial peptides. *Pharmaceuticals* (Basel). 2013 Dec; 6 (12): 1543–1575. Published online 2013 Nov 28. doi: 10.3390/ph6121543

**Peters BM**, Shirtliff ME, Jabra-Rizk MA. (2010) Antimicrobial peptides: Primeval molecules or future drugs? *PLoS Pathog*. 2010; 6:e1001067

**Zhao X**, Wu H, Lu H, Li G, Huang Q. (2013) Lamp: A database linking antimicrobial peptides. *PLoS One*. 2013;8: e66557. doi: 10.1371/journal.pone.0066557

**Badosa E**, Ferre R, Planas M, Feliu L, Besalu E, Cabrefiga J, Bardajì E, Montesinos E. (2007) A library of linear undecapeptides with bactericidal activity against phytopathogenic bacteria. *Peptides* Volume 28, Issue 12, December 2007, pages 2276–2285

**Montesinos E** and Bardajì. (2008) Synthetic antimicrobial peptides as agricultural pesticides for plant-disease control. *Chem Biodivers*. 2008 Jul;5(7):1225-37. doi: 10.1002/cbdv.200890111

**Hightower R**, Baden C, Penzes E, Dunsmuir P. (1994) The expression of cecropin peptide in transgenic tobacco does not confer resistanse to *Pseudomonas syringae* pv. *tabaci. Plant Cell Reports* 13, 295–299

**Allefs SJHM**, Florack DEA, Hoogendoorn C, Stiekema WJ. (1995) *Erwinia* soft rot resistance of potato cultivars transformed with a gene construct coding for antimicrobial peptide cecropin B is not altered. *American Potato Journal* 72, 437–445

**Florack D**, Allefs S, Bollen R, Bosch D, Visser B, Stiekema W. (1995) Expression of giant silkmoth cecropin B genes in tobacco. *Transgenic Research* 4, 132–141

**Yevtushenko DP**, Romero R, Forward BS, Hancock RE, Kay WW, Misra S. (2005) Pathogen-induced expression of a cecropin A-melittin antimicrobial peptide gene confers antifungal resistance in transgenic tobacco. *Journal of Experimental Botany*, Vol. 56, No. 416, pp. 1685–1695, June 2005 doi:10.1093/jxb/eri165

**Sato H** and Feix B. (2006) Peptide–membrane interactions and mechanisms of membrane destruction by amphipathic α-helical antimicrobial peptides. *Biochimica et Biophysica Acta* 1758 (2006) 1245–1256

**Brogden KA**. (2005) Antimicrobial peptides: pore formers or metabolic inhibitors in bacteria? *Nature Reviews Microbiology* 3, 238-250 (March 2005) doi:10.1038/nrmicro1098

**Tan NS**, Ng MLP, Yau YH, Chong PKW, Ho B, Ding JL. (2000) Definition of endotoxin binding sites in horseshoe crab factor C recombinant sushi proteins and neutralization of endotoxin by sushi peptides. *The FASEB Journal*. 2000;14(12):1801–1813. doi: 10.1096/fj.99-0866com

**Jung YJ**, Kang KK. (2014) Application of Antimicrobial Peptides for Disease Control in Plants. *Plant Breeding and Biotechnology* 2014;2:1-13

**Mentag R**, Luckevich M, Morency MJ, Seguin A. (2003) Bacterial disease resistance of transgenic hybrid poplar expressing the synthetic antimicrobial peptide D4E1. *Tree Physiology*, 23, 405–411

**Vidal JR**, Kikkert JR, Malnoy MA, Wallace PG, Barnard J and Reisch BI. (2006) Evaluation of transgenic 'Chardonnay' (*Vitis vinifera*) containing magainin genes for resistance to crown gall and powdery mildew. *Transgenic research*, 15, 69–82

**Gao AG**, Hakimi SM, Mittanck CA, Wu Y, Woerner B, Stark DM, *et al*. (2000). Fungal pathogen protection in potato by expression of a plant defensin peptide. *Nature Biotechnology*, 18, 1307–1310

**Chakrabarti A**, Ganapathi TR, Mukherjee PK, Bapat VA. (2003) MSI-99, a magainin analogue, imparts enhanced disease resistance in transgenic tobacco and banana. *Planta*, 216, 587–596

**King EO**, Ward MK, Raney DE. (1954) Two simple media for the determination of pyocianine and fluorescein. *J Lab Clin Med*. 1954; 44: 301–307. pmid:13184240

**Horsch R**, Fry J, Hoffmann N, Wallroth M, Eichholtz D, Rogers S, Fraley R. (1985) A simple and general method for transferring genes into plants. *Science* 227: 1229-1231

**Biricolti S**, Bogani P, Cerboneschi M, Gori M. (2016) Inverse PCR and quantitative PCR as alternative methods to Southern blotting analysis to assess trangene copy number and characterize the integration site in transgenic woody plants. *Biochemical Genetics* June 2016, Volume 54, Issue 3, pp 291-305

**O'Leary BM**, Rico A, McCraw S, Fones HN, Preston GM. (2014) The infiltration-centrifugation technique for extraction of apoplastic fluid from plant leaves using *Phaseolus vulgaris* as an example. *J Vis Exp*. 2014 Dec 19;(94). doi: 10.3791/52113

**Biancalani C**, Cerboneschi M, Tadini-Buoninsegni F, Campo M, Scardigli A, Romani A, Tegli S. (2016) Global Analysis of Type Three Secretion System and Quorum Sensing Inhibition of *Pseudomonas savastanoi* by Polyphenols Extracts from Vegetable Residues. *PLoS ONE* 11(9): e0163357. doi:10.1371/journal.pone.0163357

**Toplak N**, Okrslar V, Stani-Racman D, Gruden K, El J. (2004). A High-Throughput Method for Quantifying Transgene Expression in Transformed Plants with Real-Time PCR Analysis. *Plant Molecular Biology Reporter* 22: 237–250, September 2004

**Ahmad A**, Pereira EO, Conley AJ, Richman AS, Menassa R. (2010) Green biofactories: recombinant protein production in plansts. *Recent Pat Biotechnol*. 2010 Nov;4(3):242-59

**Gao AG**, Hakimi SM, Mittanck CA, Wu Y, Woerner B, Stark DM, *et al.* (2000) Fungal pathogen protection in potato by expression of a plant defensin peptide. *Nature Biotechnology*, 18, 1307–1310

**Elfstrand M**, Fossdal C, Swedjemark G, Sitbon F, Clapham D, Olsson O, Sharma P, Lönneborg A, von Arnold S. (2001) Identification of candidate genes for use in molecular breeding – A case study with the Norway spruce defensin-like gene, spi 1. *Silvae Genet. 50*, 75-81

**Park HC**, Kang YH, Chun HJ, Koo JC, Cheong YH, Kim CY, *et al*. (2002) Characterization of a stamen-specific cDNA encoding a novel plant defensin in Chinese cabbage. *Plant Mol. Biol.* 50 57–68 10.1023/A:1016005231852

**Schaefer SC**, Gasic K, Cammue B, Broekaert W, van Damme EJM, Peumans WJ, Korban SS. (2005). Enhanced resistance to early blight in transgenic tomato lines expressing heterologous plant defense genes. *Planta*. 2005; 222:858–866

**Koo JC**, Chun HJ, Park HC, Kim MC, Koo YD, Koo SC, Ok HM, Park SY, Lee SH, Yun DJ, Lim CO, Bahk JD, Lee SY, Cho MJ. (2002) Over-expression of a seed specific hevein-like antimicrobial peptide from Pharbitis nil enhances resistance to a fungal pathogen in transgenic tobacco plants. *Plant Mol Biol.* 2002 Oct; 50(3):441-52

**Carmona MJ**, Molina A, FernBndez JA, Lopez-Fando JJ, Garcia-Olmedo F. (1993) Expression of the a-thionin gene from barley in tobacco confers enhanced resistance to bacterial pathogens. *The Plant Journal* (1993) 3(3), 457-462

**Jung YJ**, Lee SY, Moon YS, Kang KK. (2012) Enhanced resistance to bacterial and fungal pathogens by overexpression of a human cathelicidin antimicrobial peptide (hCAP18/LL-37) in Chinese cabbage. *Plant Biotechnol Rep*. 2012 Jan; 6(1): 39–46. doi: 10.1007/s11816-011-0193-0

# *Chapter 4*

# Global Analysis of Type Three Secretion System and Quorum Sensing Inhibition of *Pseudomonas savastanoi* by Polyphenols Extracts from Vegetable Residues

## 4.1 Abstract

Protection of plants against bacterial diseases still mainly relies on the use of chemical pesticides, which in Europe correspond essentially to copper-based compounds. However, recently plant diseases control is oriented towards a rational use of molecules and extracts, generally with natural origin, with lower intrinsic toxicity and a reduced negative environmental impact. In this work, polyphenolic extracts from vegetable no food/feed residues of typical Mediterranean crops, as *Olea europaea*, *Cynara scolymus*, and *Vitis vinifera* were obtained and their inhibitory activity on the Type Three Secretion System (TTSS) and the Quorum Sensing (QS) of the Gram-negative phytopathogenic bacterium *Pseudomonas savastanoi* pv. *nerii* strain *Psn23* was assessed. Extract from green tea (*Camellia sinensis*) was used as a positive control. Collectively, the data obtained throughgfp-promoter fusion system and real-time PCR show that all the polyphenolic extracts here studied have a high inhibitory activity on both the TTSS and QS of *Psn23*, without any depressing effect on bacterial viability. Extracts from green tea and grape seeds were shown to be the most active. Such activity was confirmed in planta by a strong reduction in the ability of *Psn23* to develop hyperplastic galls on explants from adult oleander plants, as well as to elicit hypersensitive response on tobacco. By using a newly developed Congo red assay and an ELISA test, we demonstrated that the TTSS-targeted activity of these polyphenolic extracts also affects the TTSS pilus assembly. In consideration of the potential application of polyphenolic extracts in plant protection, the absence of any toxicity of these polyphenolic compounds was also assessed. A widely and evolutionary conserved molecular target such as $Ca^{2+}$-ATPase, essential for the survival of any living organism, was used for the toxicity assessment.

**Keywords:** Polyphenolic extracts; anti-virulence compounds; Type Three Secretion System; Quorum Sensing; real time PCR; ELISA assay; $Ca^{2+}$-ATPase

Biancalani C, Cerboneschi M, Tadini-Buoninsegni F, Campo M, Scardigli A, Romani A, Tegli S. (2016) Global Analysis of Type Three Secretion System and Quorum Sensing Inhibition of *Pseudomonas savastanoi* by Polyphenols Extracts from Vegetable Residues. *Manuscript published in* PLoS ONE.

## 4.2 Introduction

Plant pathogenic bacteria cause serious damages and heavy economic loss to the global agricultural production. Although they are less common than phytopathogenic fungi and viruses, bacterial control is a considerable challenge in agricultural practices. According to the first general principle of plant disease management, that is prevention, exclusion of the bacterial phytopathogens from their hosts is the primary control strategy. However, the application of very effective measures such as quarantine and eradication may have also a high economic impact [1]. Furthermore, the conventional control methods for phytopathogenic bacteria essentially still rely on the use of chemicals, mainly copper-based compounds and antibiotics. In Europe, antibiotics are not allowed for plant protection and copper is amongst the very few chemicals still authorized in organic agriculture [2]. Nevertheless, the use of copper was recently restricted as a result of its negative ecotoxicological impact, and for its effect on the increase of antibiotic-resistant bacteria into agroecosystems [3]. While promising alternatives to copper have been proposed against several phytopathogenic fungi, no sustainable options are yet available for phytopathogenic bacteria. Recently, many efforts were made to identify inhibitors which are able to interfere with virulence and pathogenicity bacterial systems and pathways; such efforts have mainly targeted the Quorum Sensing (QS) and the Type Three Secretion System (TTSS). In particular, QS allows bacteria to successfully communicate and thus to adapt their gene expression to biotic and abiotic stimuli [4]. The TTSS is a macromolecular complex essential for causing disease on susceptible plants. Through the TTSS, bacteria directly inject into the cytosol of host cells several pathogenicity and virulence effector proteins [5].

Salicylidene acylhydrazides (SAHs) are amongst the very few synthetic compounds that have been evaluated until now as an alternative to copper. In *Erwinia amylovora*, SAHs were demonstrated to target the TTSS gene expression, the secretion of effectors, and the needle assembly [6]. Similarly, several phenolic compounds were found to possess the ability to specifically alter TTSS gene expression, by acting as inhibitors, such as in *E.amylovora* [7] or as inducers, as for *Dickeya dadantii* [8]. Besides their role as bactericides, some plant phenol-based molecules, such as p-coumaric acid and salicylic acid, have been shown to interfere with the QS of the plant pathogens *Agrobacterium tumefaciens* and*Pectobacterium carotovorum* [9].

Increasing evidence suggests that several extracts from polyphenol rich plants, such as green tea, artichoke, olive tree and grapevine, have high antimicrobial activity [10–13]. For example, epigallocatechin gallate (EGCG) is the most abundant polyphenolic metabolite found in green tea. EGCG was shown to have high anti-virus and anti-bacterial activities against human pathogens. Furthermore, EGCG's copper-like performance was verified against the causal agents of citrus canker and bacterial spot of tomato [10,14]. In this frame, great effort in current research is devoted to the development of anti-virulence compounds, both synthetic or from natural sources, instead of biocides. The control of human, animal, and plant bacterial pathogens would thus affect mechanisms that are not essential for bacterial viability, avoiding the risk of developing resistance, as it occurs with antibiotics and copper [15,16]. In the present study, polyphenolic extracts from *Olea europaea* and *Cynara*

*scolymus* leaves were obtained by a green chemistry approach. Together with extracts from *Vitis vinifera* seeds and green tea (*Camellia sinensis* leaves), they were characterized in their polyphenolic composition, by HPLC/DAD (High-Performance Liquid Chromatography/Diode-Array Detection) and by HPLC/ESI-MS (High-Performance Liquid Chromatography/Electrospray Ionization Mass Spectrometry).

For the first time, these polyphenolic extracts were tested for their inhibitory activity on the TTSS and QS of the Gram-negative phytopathogenic bacterium *Pseudomonas savastanoi*, the causal agent of oleander and olive knot disease. The promoter activity of TTSS and QS on key genes was determined by using specific fusion constructs with the gene coding for the green fluorescent protein (GFP). In addition, inhibition of the TTSS expression and of other virulence and pathogenicity related genes was assessed by quantitative real-time PCR. The ecotoxicological profile of the investigated polyphenolic compounds was also evaluated, in view of their potential application in plant disease control.

## 4.3 Materials and Methods

### Sources of the screened polyphenolic extracts

The extract from *O. europaea* L. (varieties Frantoio and Carboncella) (hereafter denoted as FO) was obtained using green leaves, collected at the Azienda Agricola Frantoio "Il Forbiciaio" (Piancastagnaio, Siena, Italy, 42°51′N 11°41′E) and Vitasafer srl (Montorio Romano, Rieti, Italy, 42°08′16″N 12°48′28″E). The artichoke leaves extract (FC) (cultivars Terom and Violetto) were obtained by Consorzio Carciofo Violetto Brindisino (Mesagne, Brindisi, Italy, 40° 33' 35,28" N, 17° 48' 32,76" E). The grape seeds dry extract (VN) was commercially available and purchased from SOCHIM International S.p.A. (Milano, Italy). The green tea leaves dry extract (TV) was also commercially available, under the name TEAVIGO® (DSM Nutritional Products, Heerlen, Netherlands). At the moment, both extracts are commercialised for cosmetic and nutraceutical purposes.

### Solvents and reagents

All the solvents (HPLC grade) and formic acid (ACS reagent) used for the extraction process were purchased from Aldrich Chemical Company Inc. (Milwaukee, Wisconsin, USA). The standards for tyrosol, luteolin 7-*O*-glucoside, chlorogenic acid, gallic acid, (+) catechin and oleuropein were purchased from Extrasynthèse S.A. (Lyon, Nord-Genay, France). EGCG, epicathechin, cynarin, caffeic acid, hydroxytyrosol and p-coumaric acid were purchased from Sigma-Aldrich Co. (St. Louis, MO, USA). The HPLC-grade water was obtained via double-distillation and purification with a Labconco Water Pro PS polishing station (Labconco Corporation, Kansas City, USA).

### Extraction and fractioning of the polyphenolic extracts

The extraction for FO and FC was performed in a Rapid Extractor Timatic series (Tecnolab S.r.l., Perugia, Italy), using a solid-liquid extraction technology. The extraction was performed with water, in a stainless steel basket at a temperature of 60°C. The working cycle was fully automatic and switched between a dynamic phase, obtained with a set pressure (7–9 Bar), and a static phase necessary for transferring the substance into the extraction solvent. Forced percolation was generated during the stationary phase, which ensures a continuous flow of solvent to the interior of the plant matrix. This avoided over-saturation and the formation of preferential channels, thus ensuring total extraction of the active principles from the vegetal matrix.

### HPLC/DAD and HPLC/ESI-MS analysis

The HPLC/DAD analyses were performed with a HP 1100 liquid chromatograph equipped with a DAD detector (Agilent Technologies, Palo Alto, CA). In detail, the analytical column used for FO and VN was a LiChrosorb RP18 250×4.60 mm, 5µm (LichroCART, Merck Darmstadt, Germany) maintained at 26°C. The eluents were $H_2O$ adjusted to pH 3.2 by HCOOH (A), and $CH_3CN$ (B). For FO, a four-step linear solvent gradient was used starting from 100% A up to 100% B, for an 88-min period at a flow rate of 0.8 ml/min, as previously reported [17]. The VN extract was analyzed after solubilization in 70% EtOH pH 3.2 by

HCOOH. A 7-step linear solvent gradient system, starting from 100% A up to 100% B was applied during a 117-min. period at a flow rate of 0.8 ml/min [18]. For the analysis of the FC and TV, a Luna C18 column 150×3.0 mm, 5µm (Phenomenex, Bologna, Italy) operating at 27°C was used. The eluents were $H_2O$ adjusted to pH 3.2 by HCOOH, and $CH_3CN$. A three-step linear solvent gradient was performed starting from 100% $H_2O$ up to 100% $CH_3CN$, with a flow rate of 0.6 ml/min for a 30-min. period [19]. The HPLC-MS analyses were performed using a HP 1100 liquid chromatograph, equipped with a DAD and a 1100 MS detectors. The interface was an HP 1100 MSD API-electrospray (Agilent Technologies, Santa Clara, United States). Mass spectrometer operating conditions were the following: gas temperature 350°C at a flow rate of 10.0 l/-min, nebulizer pressure 30 psi, quadrupole temperature 30°C and capillary voltage 3500 V. The mass spectrometer operated in positive and negative ionization mode at 80–120 eV.

**Qualitative and quantitative analysis of the polyphenolic extracts**

The phenolic compounds that were present in these extracts were identified by using data from HPLC/DAD and HPLC/MS analyses, by comparing and combining their retention times, UV/Vis and mass spectra with those of several commercial standards. Each compound was quantified by HPLC/DAD, using a five-point regression curve built with the available standards. Calibration curves with $r^2 \geq 0.9998$ were considered. In all cases, the actual concentrations of derivatives were calculated after making corrections for changes in molecular weight. In particular, secoiridoid molecules for FO were calibrated at 280 nm, using oleuropein as a reference; elenolic acid derivatives at 240 nm using oleuropein; hydroxytyrosol, lignans and derivatives were calibrated as tyrosol at 280 nm; verbascoside and other hydroxycinnamic derivatives were calibrated at 330 nm using chlorogenic acid as a reference; flavonoids were calibrated with luteolin 7-*O*-glucoside at 350 nm. For VN, gallic acid was calibrated at 280 nm using gallic acid as reference; catechin, epicatechin and procyanidins were calibrated at 280 nm using (+) catechin as reference. For FC, chlorogenic acid, mono- and di-caffeoylquinic acids were calibrated at 330 nm with chlorogenic acid as a reference; cynarin was calibrated at 330 nm with the pure standard, and flavonoids at 350 nm with luteolin 7-*O*-glucoside. For TV, EGCG and epicatechin gallate (ECG) were calibrated at 280 nm using EGCG as a reference. The evaluation of the polyphenol content was carried out in triplicate. The results were recorded as mean values with the standard deviation.

For each extract, the concentrations (expressed as µmol/g of total polyphenols), as well as the dilutions in water to obtain solutions 100 µM in polyphenols (or any other appropriate concentration according to the tests performed), were calculated by summing the concentrations of the individual polyphenolic compounds here characterized, expressed in µmol/g, according to the HPLC/DAD data and based on the molecular weight of each compound.

**Bacterial strains, media and growth conditions**

The bacterial strains used in this study are listed in Table 1. The bacteria were long-term stored at -80°C, in 40% (v/v) glycerol. Wild type *P. savastanoi* pv. *nerii* strain *Psn23* and its Δ*hrpA* mutant were routinely grown at 26°C, as liquid or solid cultures on King's B medium

(KB) [20], or on hrp-inducing minimal medium (MM) [21] to activate *in vitro* the expression of TTSS genes. *Escherichia coli* strains TOP10 and ER2925 were grown in Luria–Bertani (LB) liquid or agarose medium [22]. According to the experimental purposes and as required for plasmid maintenance, antibiotics were added to the growth medium at the following concentrations: streptomycin 10 µg/ml for *E. coli*, nitrofurantoin 50 µg/ml for *P. savastanoi*, and gentamicin 10 µg/ml in both bacterial species when transformed with the plasmids reported in Table 1. Any bacterial contamination was excluded by periodical monitoring using PCR-based assays specific for *P. savastanoi* [23].

**Table 1. Bacterial strains, mutant and plasmids used in this study.**

| Strain/Plasmid | Relevant characteristics | Reference/Source^ |
|---|---|---|
| **Strain** | | |
| *E. coli* TOP10 | F-, *mcr*A, Δ(*mrr-hsd*RMS-*mcr*BC) Φ80 *lac*ZΔM15 Δ*lac*X74 *rec*A1 *ara*D139 Δ(*araleu*)7697 *gal*U *gal*K *rps*L (StrR) *end*A1 *nup*G | Invitrogen, Carlsbad, USA |
| *E. coli* ER2925 | *ara*-14 *leu*B6 *fhu*A31 *lac*Y1 *tsx*78 *gln*V44 *gal*K2 *gal*T22 *mcr*A *dcm*-6 *his*G4 *rfb*D1 R(*zgb*210::*Tn*10)TetS *end*A1 *rps*L136 *dam*13::*Tn*9 *xyl*A-5 *mtl*-1 *thi*-1 *mcr*B1 *hsd*R2 | NEB, Hertfordshire, UK |
| *P. savastanoi pv. nerii (Psn23)* | Wild type | LPVM collection |
| Δ*hrpA* | *hrpA* in-frame deletion mutant of *Psn23* | [24] |
| **Plasmid** | | |
| pBBR1-MCS5 | broad host range replicating mobilisable vector, $Gm^R$ | [25] |
| pKEN*gfp*mut3 | $Ap^R$ , mutated *gfp* (S6FG, S72A) | [26] |
| pLPVM | $Gm^R$, lacZ, mcs, *gfp* | This study |
| pLPVM_T3A | $Gm^R$, lacZ, mcs, *hrpA* promoter+*gfp* | This study |
| pLPVM_QS | $Gm^R$, lacZ, mcs, *psnI* promoter+*gfp* | This study |

LPVM Laboratorio di Patologia Vegetale Molecolare (University of Florence)
$Gm^R$, gentamicin resistance; $Ap^R$, ampicillin resistance

## Construction of plasmids

Extraction of genomic or plasmid DNA, PCR and general DNA manipulations, such as restriction digestion and ligation, were performed according to standard procedures and in accordance with the manufacturer's instructions [27]. Cloning vector pBBR1-MCS5 was linearized with a double digestion using *KpnI* and *BamHI* enzymes. The primer pair GFP_BamHI_For / GFP_KpnI_Rev was used to amplify *gfp* gene, using the pKEN GFP mut3 plasmid as a template. Afterwards, the *gfp* amplicon was ligated into the linearized pBBR1-MCS5 in order to obtain pLPVM plasmid. A 102 bp fragment containing the promoter region for *hrpA*, and a 630 bp fragment containing the promoter for the *luxI* homologue in *Psn23* (hereafter named *psnI*), were amplified using the primer pair T3_XbaI_For / T3_BamHI_Rev and QS_XbaI_For / QS_BamHI_Rev, respectively (Table 2), which were designed according to the *Psn23* sequences deposited in GeneBank (Accession Number FR717897.2 and FR717654). The amplified fragments were then cloned into the pLPVM plasmid, following their double digestion with *XbaI* and *BamHI*, to drive the expression of the promoter-less *gfp* gene, and to create the promoter-probe constructs pLPVM_T3A and pLPVM_QS. After their sequences were validated, these recombinant plasmids were transferred

into *E. coli* ER2925, and then electroporated into *Psn23* with Gene PulserXCell™ (Bio-Rad Laboratories Inc., Hercules, CA, USA).

**Table 2. Primers used in this study for recombinant plasmids construction.**

| Primer name | Primer sequence (5'→3') | Tm° |
|---|---|---|
| GFP_BamHI_For | AAAGGATCCATGGTGAGCAAGGGCG | 62.1 |
| GFP_KpnI_Rev | AAAGGTACCTTACTTGTACAGCTCGTC | 60.2 |
| T3_XbaI_For | AAATCTAGATTTTTTGCAGAGCGCT | 62.6 |
| T3_BamHI_Rev | AAAGGATCCCTAAATTCAAACAACGTG | 64.0 |
| QS_XbaI_For | AAATCTAGACGACATAGGCACTTCC | 60.0 |
| QS_BamHI_Rev | AAAGGATCCTATAAACTCCACTTCGCA | 62.8 |

## Antibacterial activity test

The antibacterial activity of the polyphenolic extracts VN, TV, FO, and FC was evaluated *in vitro* by monitoring the bacterial growth as optical density at 600 nm ($OD_{600}$), at different times during 24-h incubation with the polyphenolic extracts herein tested using the spectrophotometer Infinite® M200PRO Quad4 Monochromators™-based (TECAN, Switzerland). Moreover, as references for these extracts, catechin, epicatechin, EGCG, oleuropein, caffeic acid, chlorogenic acid, cynarine, and luteolin 7-*O* glucoside, were tested as well. The *Psn23* cells were cultured in KB medium at 26°C overnight, and after two washes in sterile physiological solution (SPS, 0.85% NaCl in distilled water) the bacterial pellet was resuspended adjusting to a final $OD_{600}$ = 0.5 in MM, supplemented or not with the polyphenolic extracts or with other standard molecules, at concentrations ranging from 1 to 100 μM. As control, the antibiotic kanamycin was also used (100 μg/ml).

## Hypersensitive Response assay

Hypersensitive Response (HR) assay was performed on *Nicotiana tabacum* (var. Burley White), grown at 24°C, with a relative humidity of 75% and a photoperiod of 16/8-h light/dark. The polyphenolic extracts VN, TV, FO, and FC were diluted up to 100 μM in sterile distilled water, and a 100 μl aliquot was then co-infiltrated with *Psn23* $OD_{600}$ = 0.5, (approximately $0.5x10^8$ Colony Forming Unit/ml; CFU/ml), by using a needleless syringe into the abaxial mesophyll of fully expanded leaves of three tobacco plants [28]. The development of typical HR necrotic and chlorotic symptoms was monitored, and photographic records of the results were obtained at 24 and 48-h post-inoculation.

## Pathogenicity test

To test any variation in the ability of *Psn23* to cause the typical hyperplastic symptoms on oleander following the treatment with the polyphenolic extracts here studied, a plant model system was developed efficiently mimicking what occurring when using the whole host plant. Explants having a length of about 10 cm were collected from 2-year-old twigs of *Nerium*

*oleander* plants (var. Hardy Red), washed three times under vacuum in sterile water supplemented with Tween®20 (SIGMA-Aldrich Co.), 1% sodium hypochlorite and 10% penconazole, and finally dried on sterile filter paper. These explant were then cut into 3–3.5 cm pieces by carefully removing their ends, weighted and placed on agar-$H_2O$ medium (7 g/l), amended with 10% penconazole, into sterile Magenta™ GA-7 plant culture boxes (bioWORLD, Dublin, Ohio, USA). The upper end of each explant was then inoculated with 10 µl of a bacterial suspension, at a density of $OD_{600}$ = 0.5, mixed or not with each polyphenolic extract (100 µM). The Δ*hrpA* mutant of *Psn23* was used as control. The inoculated oleander explants were then incubated in a growth chamber at 26°C, 75% relative humidity and a photoperiod of 16/8-h of light/dark. Symptoms were recorded at 21 days post-inoculation (dpi). At this time, the explants were weighed, and the weight increment recorded. Nine replicates were used for each treatment, and three independent experiments were performed.

**GFP-based transcriptional screening**

The *Psn23* bacterial cells carrying the promoter-probe plasmids pLPVM_T3A or pLPVM_QS (Table 1) were cultured overnight on KB medium at 26°C. Then their pellet was washed twice with SPS, and inoculated in MM (final $OD_{600}$ = 0.5) supplemented with polyphenolic extracts VN, TV, FO, or FC, or their reference molecules, at concentrations ranging from 1 to 100 µM. Wild type *Psn23* carrying the empty vector was used as control. The experiments were carried out into 24 multiwell plates (BIOFIL®, Guangzhou, China) at different time during 24-h of incubation. The promoter activity of *hrpA* and *psnI* were then analyzed and quantitatively assessed, using the multimode microplate reader Infinite®M200PRO Quad4 Monochromators™-based (TECAN), by simultaneously measuring the GFP intensity and the bacterial growth.

**Quantitative gene expression analysis**

Starter liquid cultures of strain *Psn23* were grown overnight at 26°C on 20 ml KB, with continuous shaking at 100rpm. Cells were washed twice in SPS and used to inoculate MM medium, alone or supplemented with 100 µM of the polyphenolic extracts VN, TV, FO, or FC, to a final concentration $OD_{600}$ = 0.5 (approximately $0.5x10^8$ CFU/ml). The bacterial cultures were then incubated for 24-h at 26°C. Total RNA was purified from bacteria during their stationary phase ($OD_{600}$ = 1), using NucleoSpin® RNA Plus (Macherey-Nagel GmbH and Co. KG, Düren, Germany). Residual genomic DNA was eliminated by a further treatment with NucleoSpin® gDNA Removal Column (Macherey-Nagel GmbH and Co). The RNA quality was evaluated both spectrophotometrically, with NanoDrop™ ND-1000 (NanoDrop Technologies Inc., DE, USA), and visually by standard agarose gel electrophoresis [1% agarose (w/v) in TBE 1×] [27]. About 1 µg of RNA for each treatment was reverse transcribed, using iScript™ Advanced cDNA Synthesis kit (Bio-Rad Laboratories Inc., Hercules, CA, USA), according to the manufacturer's instructions. Diluted cDNA was analysed by real-time PCR, with SsoFast™ EvaGreen®Supermix (Bio-Rad Laboratories Inc.) and using the CFX96 cycler–real-time PCR Detection System and CFX-manager software v1.6 (Bio-Rad Laboratories Inc.). The primer pairs used are listed in S2 Table. The expression of each

monitored gene was normalised with *16S rDNA*, as previously reported [29]. PCR conditions were 95°C for 10s and 60°C for 20s. The melting curves of the PCR products were acquired by a stepwise increase in temperature from 60 to 95°C, with a 0.5°C increase every 5s, at the end of each PCR run to check for aspecific amplifications. The specificity of each primer pairs was confirmed according to the single peak constantly produced in their melting curves, as shown in S1 Fig. To analyze the mRNA levels the comparative Livak ($2^{-\Delta\Delta Ct}$) method was used [30]. The fold induction of the mRNA of each target gene was determined form the threshold cycle values (Ct) of the housekeeping gene, and then for the fold expression of the wild type strain imposed as = 1, to obtain a relative expression data for each gene examined. The use of the $2^{-\Delta\Delta Ct}$ method for relative quantification, a comparative technique in which a target gene is normalized to an endogenous control, requires the PCR efficiencies of target and control genes to be approximately equal. To verify this condition and to avoid significant measurement inaccuracies, ten-fold dilution series of *Psn23* genomic DNA (from 50 ng to 0.5 pg) were amplified to evaluate the amplification efficiency by comparison of the slope of the standard curves of target genes (*hrpA*, *hrpL*, *hrpRS*, *hrpV*, *lon*, *rpoN*, *pssR*, *pssI*) and the reference gene *16S rDNA*. The slope of the linear regression and the correlation coefficient for each curve are reported in S1 Table.

**Congo Red assay**

*Psn23* cells were grown on MM liquid medium ($OD_{600}$ = 0.2), supplemented or not with the polyphenolic extracts here examined (100 μM), and incubated at 18°C for 24-h with continuous shaking (100rpm). After 24-h incubation, the concentration of bacterial cultures was evaluated as $OD_{600}$, and then the dye Congo red (SIGMA-Aldrich Co.) was added (10 μg/ml), followed by a further incubation at 18°C for 1-h, under shaking. Bacterial cells were removed by centrifugation (5000*g* for 10min.), and 1 ml supernatant for each sample was then aliquoted into 24 multiwell plates (BIOFIL®). The absorbance value at 490 nm ($OD_{490}$) was recorded by spectrofluorimetry using Infinite® M200PRO (TECAN). The Congo red binding is directly correlated both to the TTSS pilus assembly and to the bacterial concentration [31]. Therefore, for any treatment the value obtained was calculated as a percentage of the binding ability of the wild type *Psn23* and of its mutant *ΔhrpA*, according to the formula:

$$\frac{(X_{unk} - X_{\Delta hrpA})}{(X_{WT} - X_{\Delta hrpA})} \times 100$$

where $X_{WT}$ and $X_{\Delta hrpA}$ are the ratio $OD_{490}/OD_{600}$ for *Psn23* and *ΔhrpA* respectively, untreated with any polyphenolic extract.

**ELISA assay**

After an overnight growth at 26°C on KB medium, *Psn23* cells were washed twice, and inoculated in MM ($OD_{600}$ = 0.5), supplemented or not with the polyphenolic extracts VN, TV, FO, or FC (100 μM), and grown at 18°C for 24-h under shaking. Cells were removed by centrifugation (8000*g* for 15min., at 4°C). The supernatant was then filtered through a 0.45 μm membrane (Filtropur S., Sarstedt, Nümbrecht, Germany) and 100 μl were then used to

perform ELISA assay. Polyclonal primary antibodies against HrpA protein of *Psn23* were obtained from Primm srl (Milano-Italy), following immunization of two rabbits with recombinant protein HrpA. Secondary anti-rabbit horseradish peroxidase conjugate antibodies were used (Bethyl Laboratories Inc., Montgomery, TX, USA), according to manufacturer's instructions. The standard curve was obtained with serial dilution of HrpA recombinant purified protein. The experiment was performed three times, with two replicates for each treatment.

**Current measurements on a solid supported membrane**

The polyphenolic compounds here examined were investigated for their effects on $Ca^{2+}$-ATPase, taken as a model of the ubiquitous molecular ion pumps P-type ATPases, known to be targets for many toxic compounds. Current measurements were carried out on sarcoplasmic reticulum (SR) vesicles containing $Ca^{2+}$-ATPase adsorbed onto a hybrid alkanethiol/phospholipid bilayer anchored to a gold electrode (the so-called Solid Supported Membrane, SSM) [32]. SR vesicles were adsorbed on the SSM surface during an incubation time of 60min. $Ca^{2+}$-ATPase was then activated by the rapid injection of a solution containing ATP. If at least one electrogenic step, *i.e.* a net charge movement within the protein, is involved in the relaxation process that follows protein activation, a current signal is recorded due to the capacitive coupling between vesicle membrane and SSM. It should be pointed out that the current amplitude is related to the number of adsorbed ATPase molecules that are activated after the ATP concentration jump, and the associated charge, which is obtained by numerical integration of the current signal, corresponds to the overall amount of $Ca^{2+}$ ions translocated by the proteins following their activation [33]. In ATP concentration-jump experiments two buffered solutions were employed, the "non-activating" and the "activating" solution: the non-activating solution contained 100 mM KCl, 25 mM MOPS (pH 7.0), 1 mM $MgCl_2$, 0.25 mM EGTA and 0.25 mM $CaCl_2$ (10 μM free $Ca^{2+}$); in addition, the activating solution contained 100 μM ATP. To investigate the effects of reference polyphenolic compounds on current signals generated by $Ca^{2+}$-ATPase, the required concentration of each compound was added to both the non-activating and activating solutions. The ATP-induced current signal observed in the presence of the polyphenolic compound was compared to the control measurement obtained in the absence of the compound. To prevent $Ca^{2+}$ accumulation into the vesicles, 1 μM calcium ionophore A23187 (calcimycin) was used. The concentration jump experiments were performed by the $SURFE^2R^{One}$ device (Nanion Technologies, Münich, Germany). The temperature was maintained at 22–23°C for all the experiments. To verify the reproducibility of the current signals on the same SSM, each single measurement was repeated six times, and then averaged to improve the signal to noise ratio. Standard deviations did not exceed 5%.

**Statistical analysis**

All the experiments in this study were performed in triplicate and repeated three times, unless otherwise stated. The data were presented as the means ± standard deviation (SD) and subjected to one-way analysis of variance (ANOVA) using PAST software (Version 3.11, Øyvind Hammer, Natural History Museum, University of Oslo). When ANOVA indicated a significant difference ($P < 0.05$), a Tukey-Kramer post-test was performed.

## 4.4 Results and Discussion

### Characterization of polyphenolic extracts from olive, artichoke leaves, grape seeds, and green tea by HPLC/DAD and HPLC/MS

The FO and FC extracts were obtained by an innovative separation process defined as Best Available Technology and recognized by the Environmental Protection Agency [34]. This method consists of an integrated system of several subsequent filtration stages (*i.e.* Micro, Ultra, Nano-filtration), followed by reverse osmosis carried out using ecofriendly materials [35]. Oleuropein is the main phenolic compound (14.92% p/p) present in the FO extract. In this study it was obtained from green olive leaves. Oleuropein consists of a secoiridoid core linked to the structure of hydroxytyrosol. The hydrolysis of oleuropein can yield various compounds, such as hydroxytyrosol, known for its important antioxidant activity, deacetoxy oleuropein and elenolic acid, the latter known as a powerful anti-bacterial molecule [36,37]. The polyphenols content in the FO extract is 240.234 mg/g (512.801 µmol/g polyphenols, 14.92% p/p oleuropein) (Table 3).

**Table 3. Quali-quantitative HPLC/DAD/MS analysis of FO, FC, VN and TV extracts.**

| **Olive leaves extract** | **mg/g[§]** | **µmol/g[§]** |
|---|---|---|
| hydroxytyrosol glycol | 2,352 | 13,834 |
| hydroxytyrosol glucoside | 17,373 | 54,978 |
| hydroxytyrosol | 2,194 | 14,245 |
| tyrosol | 0,319 | 2,313 |
| demethyl elenolic acid glucoside | 7,067 | 18,119 |
| demethyl elenolic acid diglucoside | 13,463 | 24,390 |
| elenolic acid glucoside | 4,605 | 11,399 |
| elenolic acid glucoside derivative | 2,905 | 7,191 |
| caffeic acid derivatives | 0,475 | 2,638 |
| *p*-cumaroyl acid derivatives | 0,422 | 2,571 |
| aesculin | 0,483 | 1,421 |
| verbascoside | 4,726 | 7,573 |
| verbascoside isomer | 1,969 | 3,155 |
| luteolin 7-*O*-glucoside | 1,262 | 2,817 |
| pinoresinol | 5,339 | 14,913 |
| acetoxy pinoresinol | 12,131 | 29,160 |
| oleuropein | 149,158 | 276,219 |
| oleuropein derivative | 13,993 | 25,865 |
| **total polyphenols** | **240,234** | **512,801** |

| **Grape seeds extract** | **mg/g** | **µmol/g** |
|---|---|---|
| gallic acid | 0,004 | 0,024 |
| catechin dimer B3 | 2,217 | 3,836 |
| catechin | 11,073 | 38,183 |
| catechin trimer | 3,213 | 3,710 |
| catechin dimer B6 | 2,614 | 4,522 |
| catechin dimer B2 | 5,374 | 9,297 |
| epicatechin | 13,618 | 46,960 |
| catechin trimer | 3,706 | 4,280 |
| epicatechin gallate | 6,649 | 9,108 |
| epicatechin gallate | 6,098 | 13,796 |
| catechin tetramers | 54,877 | 47,553 |
| epicatechin gallate dimer | 180,647 | 204,816 |
| catechin/epicatechin trimers digallate | 382,968 | 327,323 |
| catechin/epicatechin trimers digallate | 149,655 | 127,910 |
| **total polyphenols** | **822,709** | **841,317** |

| **Green tea leaves extract** | **mg/g** | **µmol/g** |
|---|---|---|
| epigallocatechin gallate | 838,840 | 1831,519 |
| epicatechin gallate | 31,714 | 71,760 |
| **total polyphenols** | **870,554** | **1903,279** |

| **Artichoke leaves extract** | **mg/g** | **µmol/g** |
|---|---|---|
| monocaffeoyl quinic acids | 2,133 | 6,026 |
| dicaffeoyl quinic acids | 4,688 | 9,085 |
| clorogenic acid | 16,350 | 46,188 |
| luteolin derivative | 2,362 | 8,260 |
| **total polyphenols** | **25,534** | **69,559** |

[§] Polyphenolic composition of olive, green te, artichoke leaves and grape seeds extracts. The amount of each polyphenol-based molecule is expressed as mg/g and µg/g.

As for the other extracts, the concentration of total polyphenols expressed as μmol/g was derived by summing the concentrations of each polyphenolic compound, estimated according to their molecular weights and spectrophotometric data. The HPLC/DAD/MS analysis carried out on the FC extract, obtained herein from dried artichoke leaves via a pilot process by hot aqueous extraction, shows the presence of hydroxycinnamic acids (mainly chlorogenic acid and cynarin), and flavones (*e.g*. luteolin 7-*O*-glucoside) for a total polyphenols content of 25.534 mg/g (69.559 μmol/g) (Table 3). Moreover, the presence of mono- and di-caffeoyl esters of the quinic acid and flavonoid glycosides was observed in the phenolic fraction, as previously reported [38].

The VN and TV extracts are particularly rich in condensed tannins, which are monomeric or polymeric polyphenolic compounds with widely variable molecular weights based on flavan-3-olic units, such as catechin or epicatechin. Such molecules may be esterified with one or more gallic acid unit/s (*e.g*. EGCG). Condensed tannins have a higher stability than hydrolyzable tannins, supporting their multifaceted biological properties [39]. The VN studied here includes a variety of condensed tannins with molecular weights ranging from 290Da (*i.e*. catechin and epicatechin) to 1170Da (*i.e*. catechin/epicatechin trimers digallate), as well as free gallic acid. In VN extract, the polyphenols amount is 822.702 mg/g (841.317 μmol/g), consisting entirely of condensed tannins (Table 3). The HPLC/DAD and HPLC/MS analysis of the TV extract shows the presence of 870.554 mg/g (1903.279 μmol/g) polyphenols, represented by EGCG and epicatechin gallate (96% and 4% of the total tannins, respectively) (Table 3).

**Polyphenolic extracts inhibit *hrpA* and *psnI* promoter activity *in vitro* without any antibiotic effect**

To monitor a potential inhibitory activity of these polyphenolic extracts on the TTSS and QS of *Psn23*, we evaluated their effect on the activation of *hrpA* and *psnI* promoters by using the *gfp*-reporter fusion constructs pLPVM_T3A and pLPVM_QS, respectively. As in other bacteria belonging to the *P. syringae* group, the *hrpA* gene encodes the main protein of the TTSS translocating pilus, while *psnI* encodes the *luxI*-homolog lactone synthase of a canonical QS. As reported in Table 4, all the polyphenolic extracts showed, although to a different extent, inhibition of *hrpA* promoter activity when tested at 100 μM.

A reduction of about 48 and 54% was observed for VN and TV, respectively, while a decrease of about 25% was recorded for FO and of 19% for FC. p-coumaric acid (PCA), a plant phenolic compound, was included as positive control at 100 μM as previously reported for the phytopathogenic bacterium *D. dadantii* 3937 [40]. We observed that PCA does not cause any significant decrease in *hrpA* promoter activity of *Psn23*, as well as in QS promoter activity (Table 4).

Furthermore, we found that FC, FO and TV inhibit *psnI* promoter's activity at a different extent (about 43%, 32%, and 21%, respectively), while a slight increase is obtained in the presence of VN. No negative effect on bacterial growth was observed with VN and TV, and a growth increase was recorded after treatment with FO and FC (33 and 45%, respectively). These data indicate that the inhibitory effect of these polyphenolic plant extracts on TTSS and QS may not be a consequence of their negative impact on bacterial growth. Conversely, the

antibiotic kanamycin used as negative control causes both inhibition on bacterial growth, and on TTSS and QS promoter activities (Table 4). Overall, all the extracts tested had a higher inhibitory activity on TTSS rather than on QS. In particular, the extracts VN and TV are the most effective in reducing the *in vitro* activation of the *hrpA* promoter.

**Table 4. Effects on bacterial growth, and on the trans-activation of *hrpA* and *psnI* promoters of the polyphenolic extracts tested in this study and their main constituents. Kanamycin and p-coumaric acid (PCA) were used as negative and positive control, respectively.**

| Extract | Vegetable matrix/ Main molecule | Bacterial growth ($OD_{600}$) | *hrpA* promoter* | *psnI* promoter* |
|---|---|---|---|---|
| **VN** | **Grape seeds** | **1.05 ± 0.30$^{a}$** | **0.52 ± 0.11$^{ab}$** | **1.06 ± 0.17$^{a}$** |
| | Catechin | 1.02 ± 0.22$^{a}$ | 1.08 ± 0.11$^{a}$ | 0.96 ± 0.27$^{a}$ |
| | Epicathechin | 0.99 ± 0.19$^{a}$ | 1.12 ± 0.13$^{a}$ | 1.07 ± 0.32$^{a}$ |
| **TV** | **Green tea leaves** | **1.01 ± 0.16$^{a}$** | **0.46 ± 0.13$^{b}$** | **0.79 ± 0.14$^{ab}$** |
| | Epigallocatechin gallate | 1.00 ± 0.17$^{a}$ | 0.59 ± 0.24$^{ab}$ | 0.94 ± 0.12$^{a}$ |
| **FO** | **Olive leaves** | **1.33 ± 0.16$^{a}$** | **0.75 ± 0.18$^{a}$** | **0.68 ± 0.16$^{ab}$** |
| | Oleuropein | 1.00 ± 0.15$^{a}$ | 1.24 ± 0.18$^{a}$ | 1.01 ± 0.25$^{a}$ |
| | Hydroxytyrosol | 0.98 ± 0.18$^{a}$ | 0.49 ± 0.17$^{b}$ | 0.63 ± 0.16$^{ab}$ |
| | Luteolin 7-*O*-glucoside | 1.32 ± 0.12$^{a}$ | 1.18 ± 0.10$^{a}$ | 0.92 ± 0.18$^{a}$ |
| **FC** | **Artichoke leaves** | **1.45 ± 0.18$^{a}$** | **0.81 ± 0.17$^{a}$** | **0.57 ± 0.13$^{ab}$** |
| | Caffeic acid | 1.16 ± 0.13$^{a}$ | 0.99 ± 0.10$^{a}$ | 0.94 ± 0.17$^{a}$ |
| | Chlorogenic acid | 1.13 ± 0.15$^{a}$ | 1.02 ± 0.12$^{a}$ | 1.08 ± 0.20$^{a}$ |
| | Cynarine | 1.22 ± 0.10$^{a}$ | 1.10 ± 0.32$^{a}$ | 1.03 ± 0.29$^{a}$ |
| | **Kanamycin** | **0.46 ± 0.18$^{b}$** | **0.21 ± 0.18$^{b}$** | **0.23 ± 0.22$^{b}$** |
| | **p-Coumaric acid** | **0.92 ± 0.15$^{a}$** | **1.03 ± 0.22$^{a}$** | **0.98 ± 0.25$^{a}$** |

* $OD_{600}$ was recorded after 24h growth and data are calculated as GFP Abs $_{(Ex.485nm;\ Em.535nm)}$ / Abs $_{(600nm)}$ ± SD, and as normalized fold versus untreated bacterial cultures.
Common letters in correspondence of each chemical compound indicate differences not statistically significant at $p<0.05$ according to Tukey's test.

For comparison, the inhibitory activity against TTSS and QS of the corresponding bioactive molecules for each of the polyphenolic extracts here examined (*i.e.* catechin, epicatechin, EGCG, oleuropein, caffeic acid, chlorogenic acid, cynarine, luteolin 7-O glucoside) was also analyzed. None of these molecules affect bacterial growth, and all but hydroxytyrosol and EGCG (Table 4) show a significant inhibitory effect on *hrpA* and *psnI* promoters. A reduction of *hrpA* and *psnI* promoter activity was found with hydroxytyrosol (51 and 37%, respectively), and with EGCG (41 and 6%, respectively), which represent a considerable fraction of TV and FO extracts. However, both EGCG and hydroxytyrosol had a higher concentration when tested individually than that in TV and FO extracts, respectively.

**Polyphenolic extracts inhibit HR in tobacco and knot development in oleander**

To exclude any phytotoxic effect of the polyphenolic extracts here used, they were infiltrated into the mesophyll of tobacco leaves, without observing any unspecific phytotoxicity (data not shown).

Moreover, when these extracts have been co-infiltrated at 100 µM with *Psn23* wild type cells, a strong reduction in HR symptoms was found when in presence of TV or VN in comparison to the infiltration with *Psn23* alone (Figure 1), and comparable to the results of the non pathogenic Δ*hrpA* mutant [24]. Similarly a reduced HR was obtained in presence of FC or FO, although to a lesser extent than with TV or VN (Figure 1). Therefore, these data further confirm the inhibiting activity of the polyphenolic extracts on the *Psn23* TTSS *in vitro* and *in planta*, where HR elicitation by *Psn23* was suppressed.

**Figure 1. Effect of polyphenolic extracts on HR development on tobacco leaves. Hypersensitive Response assay on tobacco leaves at 48-h after co-infiltration of *Psn23* wild type bacteria (yellow rings), with FO, FC, VN or TV polyphenolic extracts (white rings). As control, sterile physiological solution was used (black ring).**

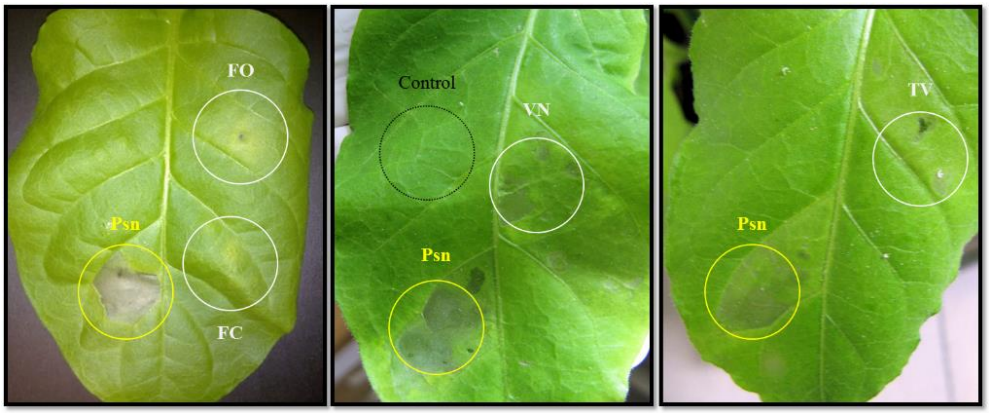


To determine whether these polyphenolic extracts could prevent the development of knot disease symptoms in oleander plants, an *in vitro* plant model system was developed using explants from 2-year old twigs of *N. oleander*.

As shown in Figure 2A, a significant difference in the symptoms development was observed following inoculation of *Psn23* wild type bacteria with VN or TV. In particular, a reduction of more than half of the explant weight increase was obtained for oleander explants inoculated with *Psn23* treated with VN or TV in comparison to those untreated (Figure 2B).

These data were confirmed by monitoring the *in planta* bacterial growth rate at 21 dpi, where a strong decrease of bacterial multiplication was recorded following inoculation of *Psn23* with VN or TV extracts, comparable to the *in planta* growth of Δ*hrpA* mutant (Figure 3).

**Figure 2. Pathogenicity test with *Psn23* on oleander explants, following treatment with polyphenolic extracts VN, TV, FO or FC. Explants from adult oleander plants were inoculated with *P. savastanoi* pv. *nerii* strain *Psn23*, in the presence or absence of the VN, TV, FO or FC extracts (100 µM). As negative control the non pathogenic mutant Δ*hrpA* was used. (A) Development of hyperplastic knots at 21 dpi with (from left to right): *Psn23*, Δ*hrpA*, *Psn23*+VN, *Psn23*+TV, *Psn23*+FO, *Psn23*+FC. The symptoms are detectable as swelling at the inoculated end of oleander explants. (B) Normalized weight increase of oleander explants at 21 dpi inoculated with (from left to right): *Psn23*, Δ*hrpA*, *Psn23*+VN, *Psn23*+TV, *Psn23*+FO, *Psn23*+FC. Values are means ± SD of nine replicates for each treatment. Different letters indicate significant differences among means at $P < 0.05$, according to Tukey's test.**

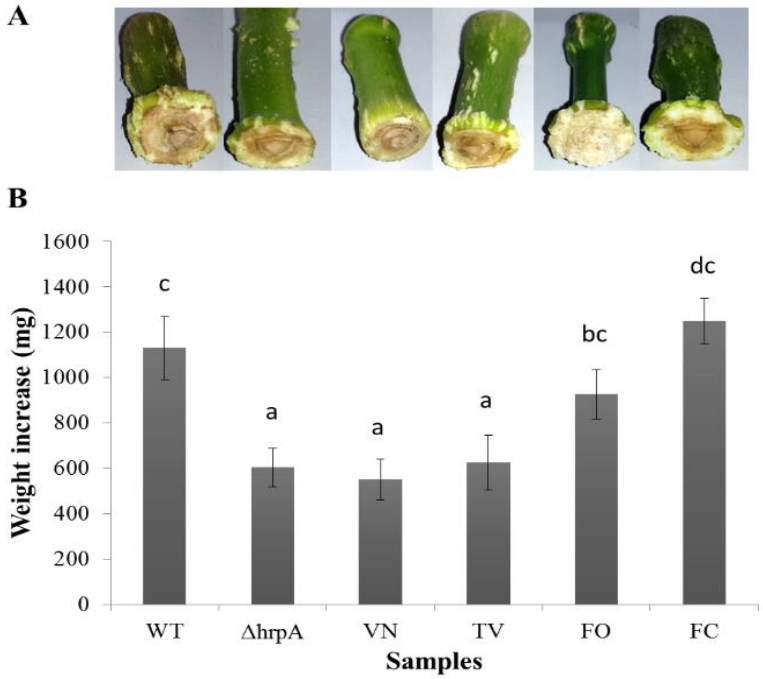


**Figure 3. *In planta* bacterial growth rate of *Psn23* treated with polyphenolic extracts VN, TV, FO or FC. Bacterial multiplication was monitored at 21 dpi. Values are means ± SD of nine replicates for each treatment. Different letters indicate significant differences among means at $P < 0.05$, according to Tukey's test.**

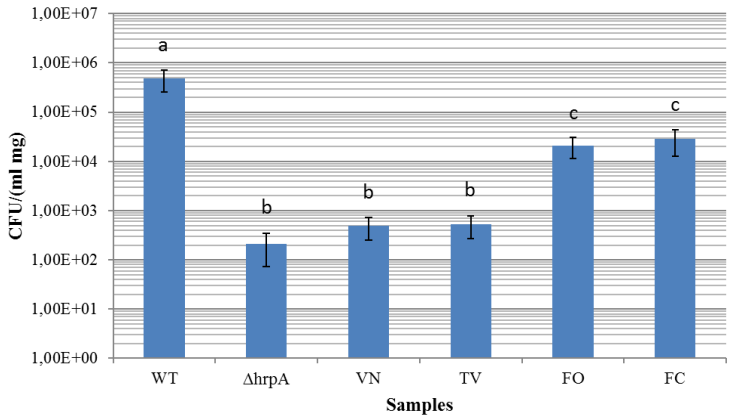

**Polyphenolic extracts alter TTSS and QS gene expression**

To determine the effect of these polyphenolic extracts on the modulation of TTSS and QS pathways of *P. savastanoi* pv. *nerii*, we performed a gene expression analysis by real-time PCR. The whole sequence and organization of the TTSS cluster of *Psn23* has been previously reported [29], and the QS genomic organization is available as well (GenBank Accession Number FR717654). To induce *in vitro* the expression of genes related to the TTSS, *Psn23* was grown on MM, which is considered to mimic plant apoplastic conditions [41]. This medium was supplemented with 100 μM of VN, TV, FO or FC. The expression of the gene *hrpA*, coding for the main component of TTSS pilus, was evaluated as well as that of several genes known to be involved in TTSS regulation, such as *hrpL*, *hrpV*, *hrpRS*, *rpoN* and *lon* [42]. As shown in Figure 4, all the polyphenolic extracts here examined strongly reduce *hrpA* mRNA levels.

**Figure 4. Relative gene expression analysis of key genes correlated to TTSS and QS of *Psn23*. Relative mRNA levels of *hrpA*, *hrpL*, *hrpV*, *hrpRS*, *rpoN*, *lon*, *psnI*, *psnR* genes of *Psn23*, grown in MM supplemented with the polyphenolic extracts TV, VN, FO or FC compared to levels in MM alone (untreated). The expression of each monitored gene was normalised with *16S rDNA*. The data are expressed as the average of three replicates ± SD. Asterisks indicate significant differences compared with the untreated sample at *P* <0.05.**

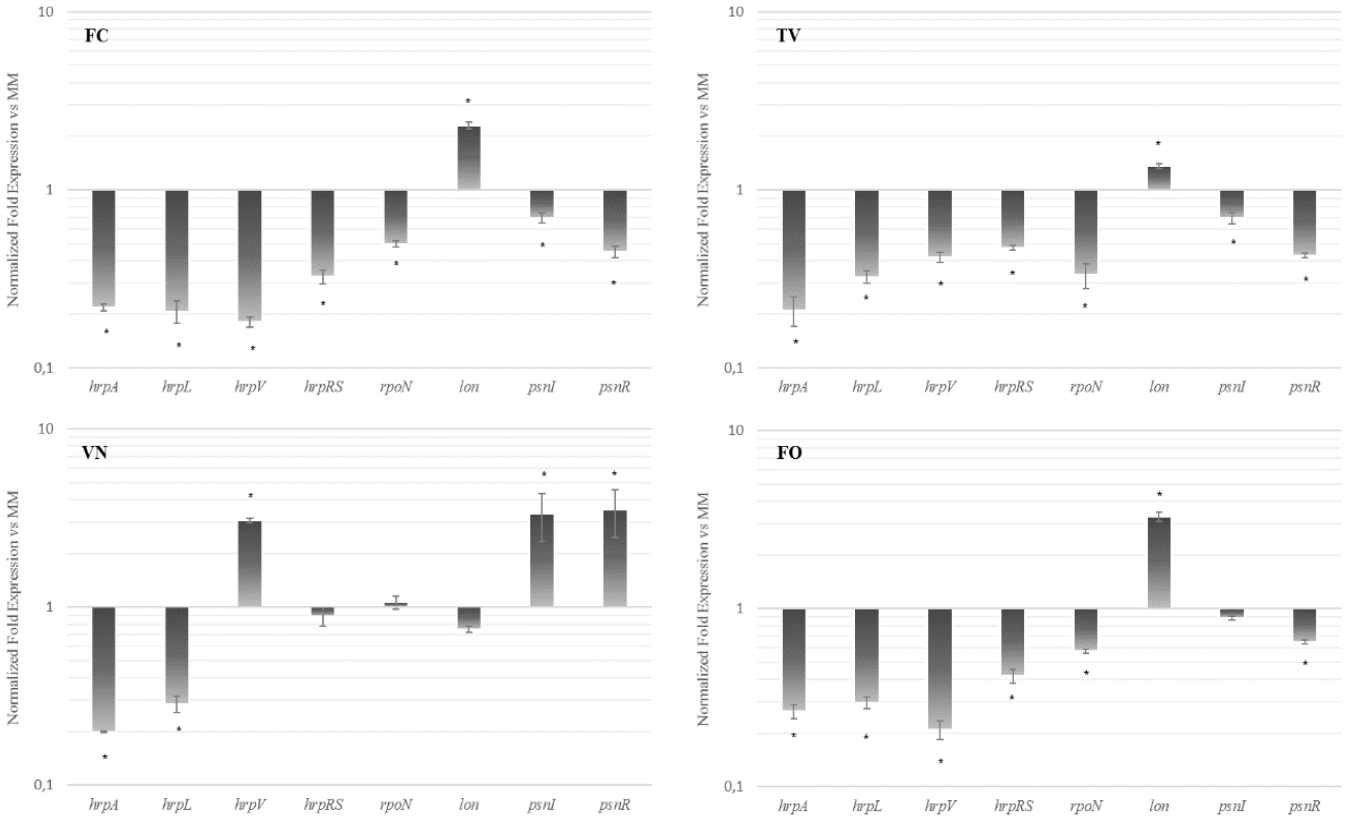


Besides its role in the assembly of the TTSS pilus, HrpA was hypothesised to regulate *hrpRS* gene transcription, in a way that still remains to be determined, presumably through a positive feedback on *hrpRS* [43]. Consistently with these data, *hrpRS* expression is

also negatively affected as well as the *hrpL* mRNA levels (Figure 4). However, it is likely that TV, FO and FC inhibit TTSS expression in the same fashion, while VN impairs TTSS functionality otherwise. The characteristic effects of these polyphenolic extracts on the proper TTSS activation may be attributed to their different impact on the two main regulatory mechanisms that finely control the expression of *hrp* cluster in *P. syringae*, *i.e.* HrpRS and GacS/GacA system [44]. The HrpS/HrpR heterodimer is crucial for the transcriptional activation of *hrpL*, which is also under the positive control of RpoN [45]. The *rpoN* transcription as well as that of *hrpRS* are activated by the GacS/GacA system, although the mechanism through which GacA regulates the expression of *hrpRS* and *rpoN* are still unknown [44]. Concerning negative regulators, HrpV controls *hrp* cascade upstream to HrpRS through a protein-protein interaction between HrpV and HrpS [46], while HrpR is specifically degraded by the Lon protease, and both of them depend on the HrpRS cascade. As shown in Figure 4, we observed a significantly lower amount of *hrpL*, *hrpV* and *hrpRS* mRNA levels in *Psn23*grown in MM supplemented with TV, FO and FC, in comparison to levels found when *Psn23*was grown in MM alone. Moreover, TV, FO and FC promote the decrease of *rpoN* mRNA levels, while the *lon* mRNA levels are almost unaffected, suggesting the involvement of GacA-RpoN-HrpL pathway [47,48]. In contrast, VN appears to compromise *hrp* cascade through the GacA-HrpRS-HrpL pathway, as suggested by the increase of *hrpV* mRNA level, while *rpoN* expression in *Psn23* grown in MM supplemented with VN is not statistically different to the expression level observed in MM alone (Figure 2). Lastly, we investigated the effect of these polyphenolic extracts on the two genes *psnI* and *psnR*, both correlated with QS. In Gram-negative bacteria, the first encodes for an acyl homoserine lactone synthase that belongs in most cases to the LuxI-protein family and produces the most common signal molecule, *i.e.* N-acyl homoserine lactone (AHL). The second encodes for a transcriptional sensor/regulator belonging to the LuxR family that forms a complex with the cognate AHL at threshold (quorum) concentrations, thereby affecting the transcription of target genes [49]. As shown in Figure 4, the data obtained corroborate those previously reported on *psnI* promoter activity. Namely, TV and FC were demonstrated to statistically reduce the transcript levels of both *psnR* and *psnI*, while FO only *psnR*. Conversely, VN strongly enhances both *psnR* and *psnI* expression. Moreover, the data further confirm the involvement of the GacA-HrpRS-HrpL pathway as a putative target of VN, and are in agreement with the tight functional link between TTSS and QS regulation mediated by GacA/GacS as already reported for *P. syringae* pv. *tomato* DC3000 [48].

To the best of our knowledge, this is the first wide gene expression study in which the effects of polyphenolic extracts from grape seeds, green tea, olive, and artichoke have been investigated against a wide set of genes correlated to TTSS and QS in *P. savastanoi* pv. *nerii.*

**Polyphenolic extracts inhibit Type Three Secretion System pilus assembly**

To further demonstrate the highly specific effect of the VN, TV, FO or FC polyphenolic extracts on TTSS machinery, we investigated their impact on the TTSS pilus assembly. To this purpose, we set up and performed a Congo red-based assay on *Psn23*-treated cultures, to quantitatively evaluate any variation in the presence of different types of pili and fimbriae, including the TTSS pilus [50]. Congo red binding has been shown to be associated with the

presence of different types of bacterial appendages, although the basis for this phenomenon is unclear [51]. Furthermore, Congo red staining has been demonstrated to be a fast and economical method for monitoring TTSS assembly also in *P. syringae* pv. *tomato* [31].
The data obtained show that VN and TV cause a reduction of the dye absorption by *Psn23*-treated cells, corresponding to 86% and 96%, respectively (Figure 5). In the case of FO and FC, the Congo red absorption was reduced to about 71% and 52%, respectively (Figure 5). Overall, such a decrease in Congo red binding to *Psn23*-treated cells in comparison to those untreated, indirectly demonstrates that these polyphenolic extracts, although with different effectiveness, compromise the correct assembly of the TTSS pilus.

**Figure 5. Effect of polyphenolic extracts on Congo red dye absorption of *Psn23*bacterial cultures. Percentage of Congo red dye absorption of *Psn23* bacterial cultures, grown in MM amended with the polyphenolic extracts VN, TV, FO or FC. The data were calculated according to the formula: $[(X_{unk}-X_{\Delta hrpA})/(X_{WT}-X_{\Delta hrpA})]*100$ where: $X_{WT}$ and $X_{\Delta hrpA}$ are the ratio $OD_{490}/OD_{600}$ for *Psn23* and *ΔhrpA* respectively. The data represent the means ± SD of three replicates. All treatments are statistically significant (*P* <0.05).**

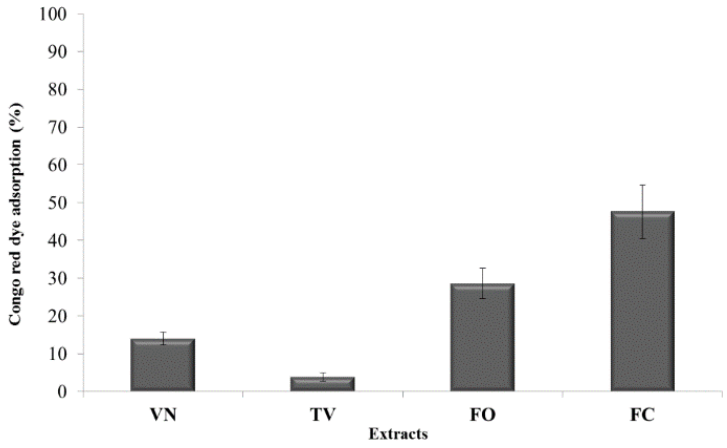


**Figure 6. ELISA assay on *Psn23* bacterial supernatant amended with polyphenolic extracts. Quantification of HrpA protein by ELISA assay on bacterial supernatant of wild type *Psn23* grown on MM, or on MM amended with the polyphenolic extracts VN, TV, FO, or FC. As a negative control the Δ*hrpA* mutant was used. As a reference for quantification, a standard curve was established by a serial dilution of the *Psn23*HrpA recombinant protein (117 pg/ml– 40 ng/ml). The data represent the means ± SD of three replicates. Statistically significant differences are represented by different letters above the bars (ANOVA and Tukey's test, *P* < 0.05).**

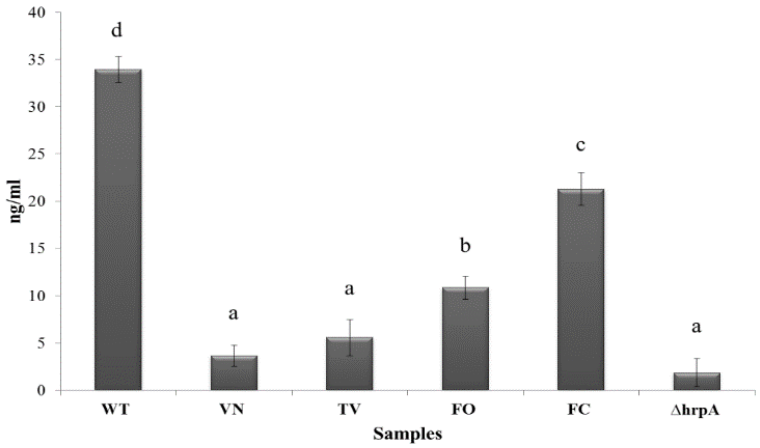

To confirm and directly verify these findings, the amount of HrpA produced by *Psn23* in the supernatant was also quantified by ELISA, following or not treatment with the VN, TV, FO or FC extracts. The results obtained are consistent with those from Congo red assay. In particular, in the supernatants of untreated *Psn23* cells a concentration of 33.93 ng/ml of HrpA protein was detected (Figure 6). In contrast, when TV or VN were supplemented to MM, the HrpA concentrations in the supernatants were 5.58 and 3.68 ng/ml, respectively, thus comparable to the levels detected for the Δ*hrpA* mutant (1.85 ng/ml). Following the treatment with FO or FC, HrpA concentrations of 10.87 and 21.30 ng/ml, respectively, were found (Figure 6). In conclusion, these findings demonstrate that the polyphenolic extracts obtained and tested in our work are able to interfere in a very specific manner with TTSS, as previously indicated by the results on gene expression analysis of this master pathogenicity system.

**Evaluation of toxic effects of polyphenolic compounds at the molecular level**

In view of the potential application of these polyphenolic extracts in plant disease control, we evaluated the toxicity of several polyphenols used here as reference *i.e.* EGCG, catechin, oleuropein, hydroxytyrosol and chlorogenic acid. In particular, these compounds were examined for their effects on the transport activity of SR $Ca^{2+}$-ATPase, which is a crucial molecular target in a variety of physiological processes. SR $Ca^{2+}$-ATPase belongs to the highly-conserved P-type ATPase family. P-type ATPases are a large, ubiquitous and varied family of membrane proteins that are involved in many transport processes in virtually all living organisms [52]. SR $Ca^{2+}$-ATPase couples the hydrolysis of one molecule of ATP to the active transport of two $Ca^{2+}$ ions from the cytoplasm to the lumen of SR. The $Ca^{2+}$-ATPase transport activity plays a major role in cell $Ca^{2+}$ signaling and homeostasis in both eukaryotes and prokaryotes [53,54]. In our study we employed SSM-based electrophysiology to compare the effects of the polyphenolic compounds with the inhibitory action of copper ions ($Cu^{2+}$) towards the SR $Ca^{2+}$-ATPase. In fact, several heavy metal ions, including $Cu^{2+}$, were found to inhibit $Ca^{2+}$-ATPase activity in different types of membranes [55]. Such inhibition typically causes a sudden increase in the cytosolic concentration of calcium ions, endoplasmic reticulum stress, and eventual cell death through apoptosis.

To investigate the interaction of these polyphenolic compounds with SR $Ca^{2+}$-ATPase and its possible inhibition, we performed current measurements on SR vesicles adsorbed on a SSM. The SSM technique allows direct measurements of charge displacements within the transport protein yielding valuable information about the ion transport mechanism [32,56,57]. The technique is also well suited for the analysis of inhibitor interactions with membrane transporters [33,58]. As shown in Figure 7, a current signal was observed following a 100 μM ATP concentration jump in the presence of $CaCl_2$ (10 μM), taken as a control measurement. It is worth mentioning that the charge obtained by numerical integration of the ATP-induced current signal is attributed to an electrogenic event corresponding to translocation and release of bound $Ca^{2+}$, after utilization of ATP [32,33,57].

ATP concentration jump experiments were then performed in the presence of $CaCl_2$ and copper ($Cu^{2+}$) or the polyphenolic compounds at different concentrations. The corresponding ATP-induced current signals were then compared to the control measurement obtained in the absence of these substances. In the case of $CuCl_2$, we found that at 0.1 μM concentration

$Cu^{2+}$ ions suppress almost completely the ATP-induced current signal and the related displaced charge (Figure 7). Therefore, we may conclude that sub-micromolar copper exerts a remarkable inhibitory effect on SR $Ca^{2+}$-ATPase by interfering with ATP-dependent calcium translocation through the enzyme.

On the other hand, the polyphenol-based molecules here studied have minor, if any, effects on the ATP-induced current signal over a concentration range from 1 to 10 µM, with the exception of EGCG (Figure 7). In fact, in the case of EGCG a significant reduction of the current amplitude was recorded at 10 µM EGCG. Such an interference with ATP-dependent $Ca^{2+}$translocation in the presence of a high EGCG concentration has been reported in recent biochemical studies [59,60]. In particular, EGCG was found to inhibit both $Ca^{2+}$ uptake rate and ATPase activity with half-maximal effects observed at ~12 µM [60] and ~16 µM [59]. In these studies, however, no inhibitory effect of EGCG on SR $Ca^{2+}$-ATPase activity was reported in the concentration range between 0.1 and 1 µM.

Therefore, our results indicate that as compared to copper, the polyphenolic compounds here investigated do not affect the SR $Ca^{2+}$-ATPase transport activity in the sub-micromolar concentration range.

**Figure 7. Current measurements on SR vesicles adsorbed on a SSM. Current signals induced by 100 µM ATP concentration jumps in the presence of 10 µM $Ca^{2+}_{free}$ and in the absence (black curve, control measurement) or in the presence of $CuCl_2$ (red curve) or of the polyphenolic compounds EGCG, catechin, oleuropein, hydroxytyrosol and chlorogenic acid (green curves).**

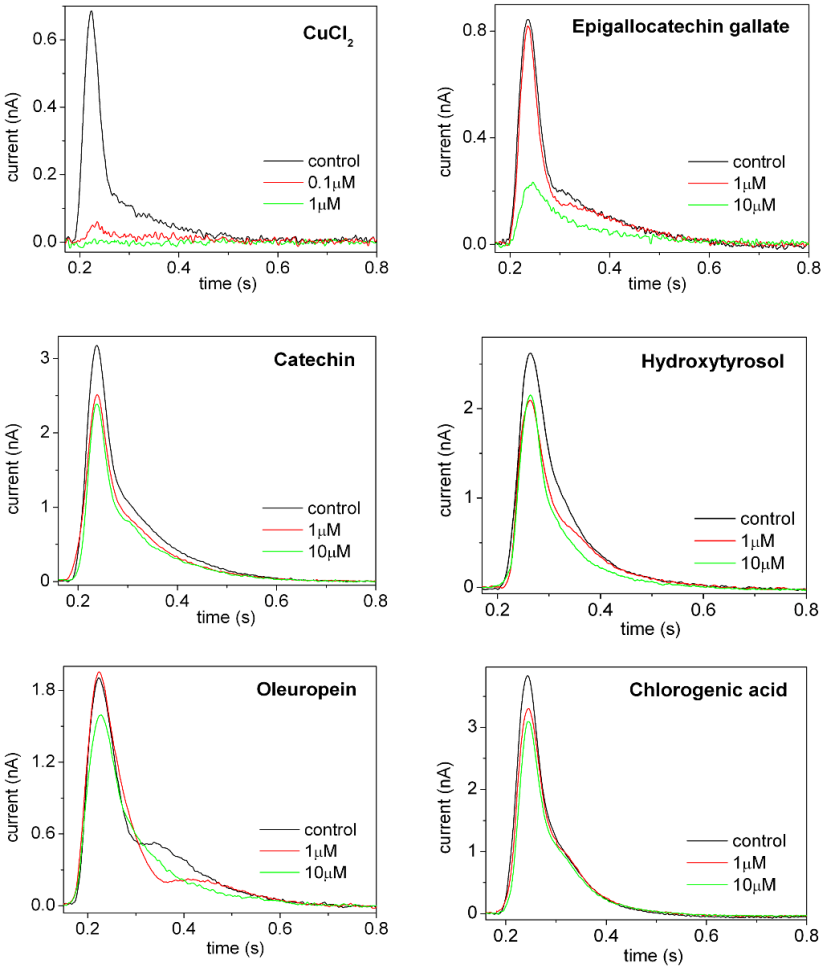

## 4.5 Conclusions

The identification and development of new ecofriendly alternatives for plant protection is becoming increasingly important, especially to reduce the use of copper compounds which are widely employed in agriculture practice, as well as to limit the emergence of copper-resistant strains. Every year the agricultural industry generates billions of metric tons of plant biomass and waste, which can be environmentally polluting if not properly managed.
Currently, several systems for kilo-scale extraction and fractionation of natural active ingredients from plant by-products were proposed [61]. The optimization of industrial closed cycle platforms for the recovery of green chemicals has been so far of interest for innovative applications in feed, food, as well as for cosmetic and nutraceutical industry. The results reported here demonstrated their potential and effective use in plant protection as well, which may lead to the development of sustainable models of circular economy into the agricultural sector.
In this study, we have demonstrated that standardized polyphenolic extracts from *O. europaea*, *C. scolymus* leaves, *V. vinifera* seeds and *C. sinensis* leaves, characterized by HPLC/DAD and HPLC/MS analysis, are able to inhibit specifically the TTSS and partially the QS of *P. savastanoi* strain *Psn23*. A close relationship was found among the data obtained through promoter activation and gene expression analysis, both for TTSS and QS. The *in vitro* anti-microbial activity of olive mill wastewater on the growth of *P. savastanoi* pv. *savastanoi* was already known [62], but in this study for the first time several polyphenolic extracts were successfully examined for their anti-virulence activity against this plant pathogenic bacterium. The additive and synergistic effects of polyphenolic extracts are responsible for their powerful bioactive properties and thus their effectiveness has to be attributed to the complex mixture of phytochemicals present in whole extract. Furthermore, we have shown that these extracts compromise the TTSS pilus assembly in a very specific manner without undermining bacterial viability. Finally, the absence of any significant toxicity on SR $Ca^{2+}$-ATPase supports the potential of this innovative strategy, which aims at employing standardized natural polyphenolic extracts as effective copper substitutes in the control and management of bacterial diseases of plants.

## 4.6 References

**1.** Oerke EC. Crop losses to pests. J Agric Sci. 2006; 144: 31-43.
**2.** Montesinos E, Bardajì E. Synthetic antimicrobial peptides as agricultural pesticides for plant-disease control. Chem Biodivers. 2008; 5: 1225-1237.
**3.** Krishna MP, Varghese R, Mohamed Hatha AA. Heavy metal tolerance and multiple drug resistance of heterotrophic bacterial isolated from metal contaminated soil. SPJNAS. 2011; 30: 58-64.
**4.** Kalia VC. Quorum sensing inhibitors: an overview. Biotechnol Adv. 2013; 31: 224-245.
**5.** Tsou LK, Dossa PD, Hang CH. Small molecules aimed at type III secretion system to inhibit bacterial virulence. Med Chem Commun. 2013; 4: 68-79.
**6**. Yang F, Korban SS, Pusey PL, Elofsson M, Sundin GW, Zhao Y. Small-molecule inhibitors suppress the expression of both type III secretion and amylovoran biosynthesis genes in *Erwinia amylovora*. Mol Plant Pathol. 2014; 15: 44-57.
**7.** Khokhani D, Zhang C, Li Y, Wang Q, Yamazaki A, Hutchins W, et al. Discovery of plant phenolic compounds that act as Type Three Secretion System inhibitors or inducers of the Fire Blight pathogen, *Erwinia amylovora*. Appl Environ Microbiol. 2013; 75: 1223-1228.
**8.** Yang S, Peng Q, San Francisco M, Wang Y, Zeng Q, Yang CH. Type III secretion system genes of *Dickeya dadantii* 3937 are induced by plant phenolic acids. PLoS ONE. 2008; 3: e2973.
**9.** Joshi JR, Burdman S, Lipsky A, Yariv S, Yedida I. Plant phenolic acids affect the virulence of *Pectobacterium aroidearum* and *P. carotovorum* ssp. *brasiliense* via quorum sensing regulation. Mol Plant Pathol. 2015; 17: 487-500.
**10.** Cuia Y, Ohb Y, Lima J, Youna M, Leec I, Pakd H, et al. AFM study of the differential inhibitory effects of the green tea polyphenol (-)-epigallocatechin-3-gallate (EGCG) against Gram-positive and Gram-negative bacteria. Food Microbiol. 2012; 29: 80-87.
**11.** Zhu XF, Zhang HZ, Lo R. Phenolic compounds from the leaf extract of artichoke (*Cynara scolymus* L.) and their antimicrobial activities. J Agric Food Chem. 2004; 52: 7272-7278.
**12.** Pereira AP, Ferreira ICFR, Marcelino F, Valentão P, Andrade PB, Seabra R, et al. Phenolic compounds and antimicrobial activity of Olive (*Olea europaea* L. Cv. Cobrançosa) leaves. Molecules. 2007; 12: 1153-1162.
**13.** Waqar A, Muhammad IK, Muhammad W, Muhammad AK, Akram K, Radia R, et al. *In vitro* antibacterial activity of *Vitis vinifera* leaf extracts against some pathogenic bacterial strains. Advan Biol Res. 2014; 8: 62-67.
**14.** Yin H, Deng Y, Wang H, Liu W, Zhuang X, Chu W. Tea polyphenols as an antivirulence compound disrupt Quorum-Sensing regulated pathogenicity of *Pseudomonas aeruginosa.* Sci Rep. 2015; 5: 16158.
**15.** Strandberg B, Axelsen JA, Pedersen MB, Jensen J, Attrill MJ. Effect of a copper gradient on plant community structure. Environ Toxicol Chem. 2006; 25: 743-753.
**16.** Keyser P, Elofsson M, Rosell S, Wolf-Watz H. Virulence blockers as alternative to antibiotics: type III secretion inhibitors against Gram-negative bacteria. J Int Med. 2008; 264: 17-29.
**17.** Pinelli P, Galardi C, Mulinacci N, Vincieri FF, Cimato A, Romani A. Minor polar compound and fatty acid analyses in monocultivar virgin olive oils from Tuscany. Food Chem. 2003; 80: 331-336.
**18.** Romani A, Baldi A, Mulinacci N, Vincieri FF, Tattini M. Extraction and identification procedures of polyphenolic compounds and carbohydrates in phillyrea (*Phillyrea angustifolia* L.) leaves. Chromatographia. 1996; 42: 571-577.
**19.** Pinelli P, Agostini F, Comino C, Lanteri S, Portis E, Romani, A. Simultaneous quantification of caffeoyl esters and flavonoids in wild and cultivated cardoon leaves. Food Chem. 2007; 105: 1695-1701.
**20.** King EO, Ward MK, Raney DE. Two simple media for the determination of pyocianine and fluorescein. J Lab Clin Med. 1954; 44: 301-307.
**21.** Huynh TV, Dahlbeck D, Staskawicz BJ. Bacterial blight of soybean: Regulation of a pathogen gene determining host cultivar specificity. Science. 1989; 245: 1374-1377.
**22.** Miller H. Experiments in molecular genetics. Cold Spring Harbor Laboratory, Cold Spring Harbor: New York, 1972.

**23.** Tegli S, Cerboneschi M, Marsili Libelli I, Santilli E. Development of a versatile tool for the simultaneous differential detection of *Pseudomonas savastanoi* pathovars by End Point and Real-Time PCR. BMC Microbiol. 2010; 10:156.
**24.** Cerboneschi M, Decorosi F, Biancalani C, Ortenzi MV, Macconi S, Giovannetti L et al. Indole-3-acetic acid in plant-pathogen interactions: a key molecule for *in planta* bacterial virulence and fitness. Res Microbiol. 2016; in press.
**25.** Kovach ME, Elzer PH, Hill DS, Robertson GT, Farris MA, Roop RM, et al. Four new derivatives of the broad-host range cloning vector pBBR1MCS, carrying different antibiotic-resistance cassettes. Gene. 1995; 166: 175-176.
**26.** Cormack BP, Valdivia RH, Falkow S. FACS-optimized mutants of the green fluorescent protein (GFP). Gene. 1996; 173: 33-38.
**27.** Sambrook J, Fritsch EF, Maniatis TA. Molecular Cloning. In *A Laboratory Manual*, edition 3.; Cold Spring Harbor Laboratory Press: New York, 1989.
**28.** Baker CJ, Atkinson MM, Collmer A. Concurrent Loss in Tn5 Mutants of *Pseudomonas syringae* pv. *syringae* of the ability to induce the hypersensitive response and host plasma membrane K+/H+ exchange in Tobacco. Phytopathotogy. 1987; 77: 1268-1272.
**29.** Tegli S, Gori A, Cerboneschi M, Cipriani MG, Sisto A. Type Three Secretion System in *Pseudomonas savastanoi* pathovars: Does timing matter? Genes. 2011; 2: 957-979.
**30.** Livak KJ, Schmittgen TD. Analysis of relative gene expression data using real-time quantitative PCR and the $2^{-\Delta\Delta CT}$ method. Methods. 2001; 25: 402-408.
**31.** Taira S, Tuimala J, Roine, Nurmiaho-Lassila EL, Savilahti H, Romantschuk M. Mutational analysis of the *Pseudomonas syringae* pv. *tomato hrpA* gene encoding Hrp pilus subunit. Mol Microbiol. 1999; 34: 736-744.
**32.** Tadini-Buoninsegni F, Bartolommei G, Moncelli MR, Guidelli R, Inesi G. Pre-steady state electrogenic events of $Ca^{2+/}H^{+}$ exchange and transport by the $Ca^{2+}$-ATPase. J Biol Chem. 2006; 281: 37720-37727.
**33.** Tadini-Buoninsegni F, Bartolommei G, Moncelli MR, Tal DM, Lewis D, Inesi G. Effects of high-affinity inhibitors on partial reactions, charge movements, and conformational states of the $Ca^{2+}$ transport ATPase (sarco-endoplasmic reticulum $Ca^{2+}$ ATPase). Mol Pharmacol. 2008; 73: 1134-1140.
**34.** Pizzichini D, Russo C, Vitagliano M, Pizzichini M, Romani A, Ieri F, et al. Phenofarm S.R.L. (Roma). PCT/IT/2009/09425529 Process for producing concentrated and refined actives from tissues and byproducts of *Olea europaea* with membrane technologies. EP 2338500 (A1), filing date 06/29/2011.
**35.** Pizzichini M, Russo C, Ferrero E, Tuccimei E. Le tecnologie separative mediante membrana. ENEA. Report Ricerca Sistema Elettrico. RSE/2009/19.
**36.** Saija A, Trombetta D, Tomaino A, Lo Cascio R, Princi P, et al. In vitro evaluation of the antioxidant activity and biomembrane interaction of the plant phenols oleuropein and hydroxytyrosol. Int J Pharm. 1998; 166: 123-133.
**37**. Covas MI. Olive oil and cardiovascular system. Pharmacol Res. 2007; 55: 175-186.
**38.** Romani A, Pinelli P, Cantini C, Cimato A, Heimler D. Characterization of Violetto di Toscana a typical Italian variety of artichoke (Cynara scolymus L.). Food Chem. 2006; 95: 221-225.
**39.** Romani A, Ieri F, Turchetti B, Mulinacci N, Vincieri FF, Buzzini P. Analysis of condensed and hydrolyzable tannins from commercial plant extracts. J Pharmaceut Biomed Anal. 2006; 41: 415-420.
**40**. Li Y, Peng Q, Selimi D, Wang Q, Charkowski AO, Chen X, et al. The plant phenolic compound p-coumaric acid represses gene expression in the *Dickeya dadantii* type III secretion system. Appl Environ Microbiol. 2009; 75: 1223-1228.
**41**. Tang X, Xiao Y, Zhou JM. Regulation of the type III secretion system in phytopathogenic bacteria. Mol Plant Microbe Interact. 2006; 19: 1159-1166.
**42**. Ortiz-Martín I, Thwaites R, Macho AP, Mansfield JW, Beuzón CR. Positive regulation of the Hrp type III secretion system in *Pseudomonas syringae* pv. *phaseolicola*. Mol Plant Microbe Interact. 2010; 23: 665-681.
**43**. Wei W, Plovanich-Jones A, Deng WL, Collmer A, Huang HC, He SY. The gene coding for the Hrp pilus structural protein is required for type III secretion of Hrp and Avr proteins in *Pseudomonas syringae* pv. *tomato*. Proc Natl Acad Sci. 2000; 97: 2247-2252.

**44.** Xiao Y, Hutcheson S. A single promoter sequence recognized by a newly identified alternate sigma factor directs expression of pathogenicity and host range determinants in *Pseudomonas syringae.* J Bacteriol. 1994; 176: 3089-3091.
**45.** Hendrickson EL, Guevera P, Ausubel FM. The Alternative Sigma Factor RpoN is required for hrp activity in *Pseudomonas syringae* pv. *maculicola* and acts at the level of hrpL transcription. J Bacteriol. 2000; 182: 3508-3516.
**46.** Jovanovic M, Lawton E, Schumacher J, Buck M. Interplay among *Pseudomonas syringae* HrpR, HrpS and HrpV proteins for regulation of the type III secretion system. FEMS Microbiol Lett. 2014; 356: 201-211.
**47.** Chatterjee A, Cui Y, Yang H, Collmer A, Alfano JR, Chatterjee K. GacA, the response regulator of a two-component system, acts as a master regulator in *Pseudomonas syringae* pv. *tomato* DC3000 by controlling regulatory RNA, transcriptional activators, and alternative sigma factors. Mol Plant Microbe Interact. 2003; 16: 1106-1117.
**48.** Lee JS, Ryu HR, Cha JG, Baik HS. The hrp pathogenicity island of *Pseudomonas syringae* pv. *tomato* DC3000 is induced by plant phenolic acids. J Microbiol. 2015; 53: 725-731.
**49.** Li Z, Nair SK. Quorum sensing: How bacteria can coordinate activity and synchronize their response to external signals? Protein Sci. 2012; 21: 1403-1417.
**50.** Collinson S, Doig P, Doran J, Clouthier S, Trust T, Kay W. Thin, aggregative fimbriae mediate binding of *Salmonella enteritidis* to fibronectin. J Bacteriol. 1993; 175: 12–18.
**51.** Collinson K, Emödy L, Trust T, Kay W. Thin aggregative fimbriae from diarrheagenic *Escherichia coli*. J Bacteriol. 1992; 174: 4490-4495.
**52.** Bublitz M, Morth JP, Nissen P. P-type ATPases at a glance. J Cell Sci. 2011; 124: 2515-2519.
**53.** Brini M, Carafoli E. Calcium pumps in health and disease. Physiol Rev. 2009; 89: 1341-1378.
**54.** Palmgren MG, Nissen P. P-type ATPases. Annu Rev Biophys. 2011; 40: 243-266.
**55.** Gramigni E, Tadini-Buoninsegni F, Bartolommei G, Santini G, Chelazzi G, Moncelli MR. Inhibitory effect of $Pb^{2+}$ on the transport cycle of the $Na^+$, $K^+$-ATPase. Chem Res Toxicol. 2009; 22: 1699-1704.
**56.** Pintschovius J, Fendler K. Charge translocation by the $Na^+$/ $K^+$ - ATPase investigated on solid supported membranes: rapid solution exchange with a new technique. Biophys J. 1999; 76: 814-826.
**57.** Tadini-Buoninsegni F, Moncelli MR, Peruzzi N, Ninham BW, Dei L, Lo Nostro P. Hofmeister effect of anions on calcium translocation by sarcoplasmic reticulum $Ca^{2+}$-ATPase. Sci Rep. 2015; 5: 14282.
**58.** Bartolommei G, Tadini-Buoninsegni F, Moncelli MR, Gemma S, Camodeca C, Butini S, et al. The $Ca^{2+}$-ATPase (SERCA1) is inhibited by 4-aminoquinoline derivatives through interference with catalytic activation by $Ca^{2+}$, whereas the ATPase E2 state remains functional. J Biol Chem. 2011; 286: 38383-38389.
**59.** Kargacin ME, Emmett TL, Kargacin GJ. Epigallocatechin-3-gallate has dual, independent effects on the cardiac sarcoplasmic reticulum/endoplasmic reticulum $Ca^{2+}$ ATPase. J Muscle Res Cell Motil. 2011; 32: 89-98.
**60.** Soler F, Asensio MC, Fernández-Belda F. Inhibition of the intracellular $Ca^{2+}$ transporter SERCA (Sarco-Endoplasmic Reticulum $Ca^{2+}$-ATPase) by the natural polyphenol epigallocatechin-3-gallate. J Bioenerg Biomembr. 2012; 44: 597-605.
**61.** Chemat F, Vian MA, Cravotto G. Green Extraction of Natural Products: Concept and Principles. J Mol Sci. 2012; 13: 8615-8627.
**62.** Krid S, Bouaziz M, Triki MA, Gargouri A, Rhouma A. Inhibition of olive knot disease by polyphenols extracted from olive mill waste water. J Plant Pathol. 2011; 93: 561-568.

## 4.7 Supporting Information

**S1 Figure. qPCR melting curves for each primer pairs tested. Blue scaling color lines correspond to serial dilutions of target gene, red lines correspond to negative control (DNA-free sterile distilled water).**

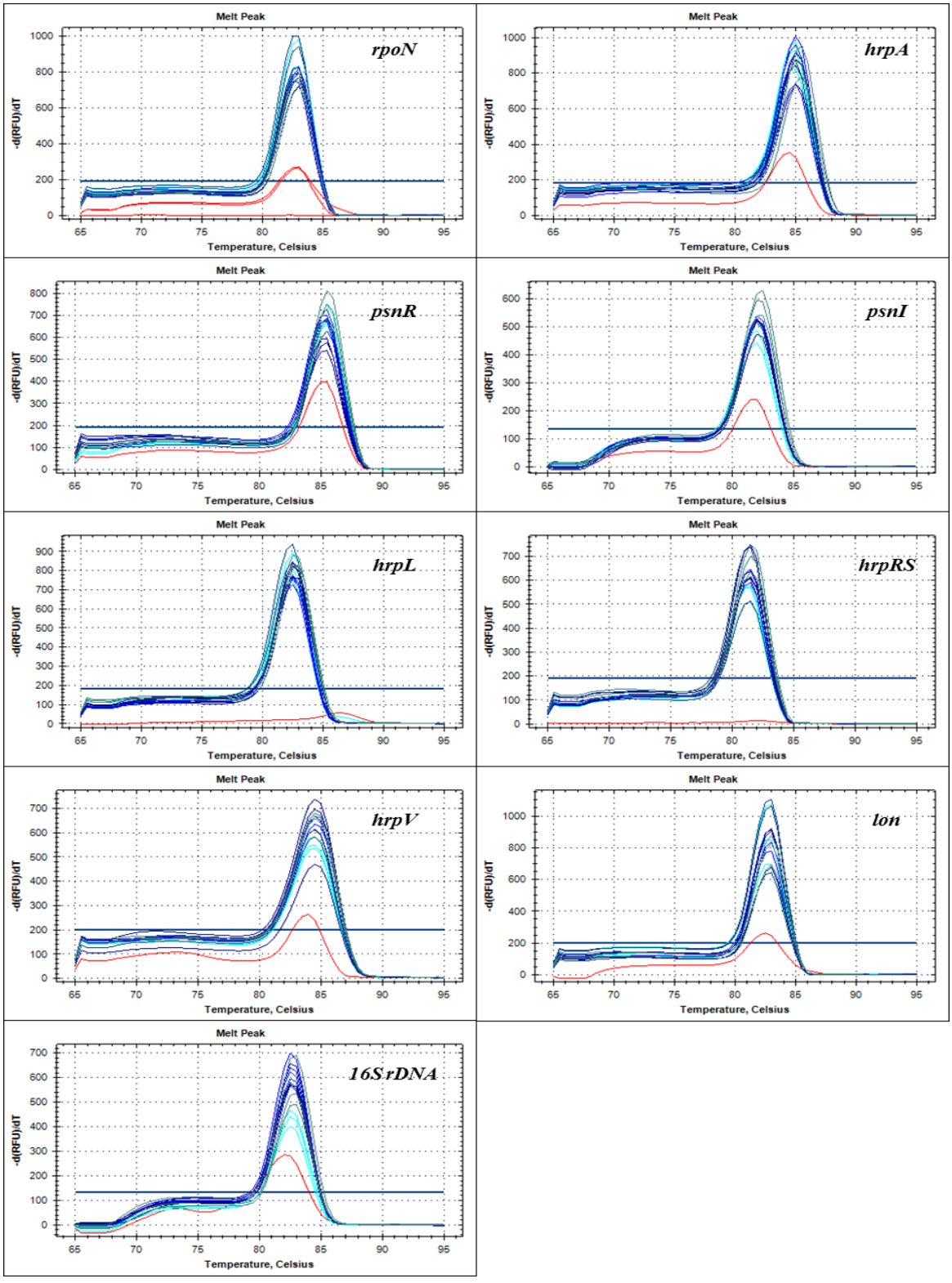

**S2 Table. Sequences, temperature of melting (Tm°), amplicon size (bp), efficiency, $R^2$, slope and Ct values of the primers used in real-time PCR.**

| Gene | Primer name | Tm °C | Primer sequence (5'→3') (bp) | Amplicon size (bp) | Efficiency (%) | $R^2$ | Slope | Ct minor | Ct major |
|---|---|---|---|---|---|---|---|---|---|
| *hrpA* | hrpA_RT_for | 62.7 | GCAGGGTATCAACAGCGTCAAG | 156 | 102.6 | 0.998 | -3.258 | 23.85 | 34.75 |
| | hrpA_RT_rev | 63.0 | CCGTTCTCTTCGTTCGCAGTG | | | | | | |
| *hrpL* | hrpL_RT_for | 59.7 | GTATTGCGTTGAACCTGAT | 126 | 104.6 | 0.994 | -3.216 | 25.83 | 32.56 |
| | hrpL_RT_rev | 59.7 | CGTCTACCTGATGAGTGATA | | | | | | |
| *hrpV* | hrpV_RT_for | 61.3 | GAGCGGTTCCGTAACTAC | 130 | 105.2 | 0.990 | -3.211 | 26.50 | 33.26 |
| | hrpV_RT_rev | 61.6 | CTGCCAGCATCAACTCAT | | | | | | |
| *hrpRS* | hrpRS_RT_for | 61.2 | ACCCGCAGAGTGAAGAAC | 88 | 99.8 | 0.998 | -3.265 | 23.72 | 31.11 |
| | hrpRS_RT_rev | 62.0 | CGCTTGAGTGACTGTTGAATC | | | | | | |
| *rpoN* | rpoN_RT_for | 60.0 | CTACCGTGGATAACCTTGA | 125 | 104.2 | 0.991 | -3.219 | 25.73 | 32.16 |
| | rpoN_RT_rev | 60.3 | GTCATCATCGTTGCTTGG | | | | | | |
| *lon* | lon_RT_for | 61.3 | CCGAGCAGAACCATAACTT | 134 | 103.2 | 0.995 | -3.198 | 25.52 | 34.21 |
| | lon_RT_rev | 61.2 | CAGGCGAATGACTTCCAT | | | | | | |
| *psnI* | pssI_RT_for | 61.0 | ACGGTGGTCAGCAAGGCAATG | 161 | 102.1 | 0.996 | -3.287 | 23.49 | 35.15 |
| | pssI_RT_rev | 61.0 | GCCAACGGAGCAGGTCATCC | | | | | | |
| *psnR* | pssR_RT_for | 61.3 | AATGGCGTAATGCTATGC | 162 | 103.9 | 0.991 | -3.232 | 25.24 | 32.43 |
| | pssR_RT_rev | 60.7 | TGGCGATTTCACTTATGC | | | | | | |
| *16s rDNA* | 16s_RT_for | 63.7 | GGAATCTCGCTGGTAGTGGGG | 157 | 103.7 | 0.998 | -3.289 | 19.31 | 33.49 |
| | 16s_RT_rev | 64.0 | ATCGTCGCCTTGGTGAGCC | | | | | | |

# *Chapter 5*

# Indole-3-acetic acid in plant-pathogen interactions: A key molecule for *in planta* bacterial virulence and fitness

## 5.1 Abstract

The plant pathogenic bacterium *Pseudomonas savastanoi*, the causal agent of olive and oleander knot disease, uses the so called "indole-3-acetamide pathway" to convert tryptophan to indole-3-acetic acid (IAA) via a two-step pathway catalysed by enzymes encoded by the genes in the *iaaM/iaaH* operon. Moreover, pathovar *nerii* of *P. savastanoi* is able to conjugate IAA to lysine to generate the less biologically active compound IAA-Lys, via the enzyme IAA-lysine synthase encoded by the *iaaL* gene. Interestingly, *iaaL* is now known to be widespread in many *P. syringae* pathovars, even in the absence of the *iaaM* and *iaaH* genes for IAA biosynthesis.

Here, two knockout mutants, *ΔiaaL* and *ΔiaaM,* of strain *Psn23* of *P. savastanoi* pv. *nerii* were produced. Pathogenicity tests using the host plant *Nerium oleander* showed that *ΔiaaL* and *ΔiaaM* were hypervirulent and hypovirulent, respectively, and these features appeared to be related to their differential production of free IAA. Using the Phenotype Microarray approach, the chemical sensitivity of these mutants was shown to be comparable to that of the wild-type *Psn23.* The main exception was 8 hydroxyquinoline, a toxic compound that is naturally present in plant exudates and is used as a biocide, which severely impaired the growth of *ΔiaaL* and *ΔiaaM*, as well as the growth of the non-pathogenic mutant *ΔhrpA,* which lacks a functional Type Three Secretion System (TTSS). According to the bioinformatics analysis of the *Psn23* genome, a gene encoding a putative Multidrug And Toxic compound Extrusion (MATE) transporter was found upstream of *iaaL*. Similarly to *iaaL* and *iaaM*, its expression appeared to be TTSS-dependent. Moreover, auxin-responsive elements were identified for the first time in the modular promoters of both the *iaaL* gene and the *iaaM/iaaH* operon of *P. savastanoi*, suggesting their IAA-inducible transcription. The gene expression analysis of several genes related to TTSS, IAA metabolism, and drug resistance confirmed the presence of a concerted regulatory network in this phytopathogen among virulence, fitness and drug efflux.

**Keywords:** *Pseudomonas savastanoi*; Phenotype Microarray; indole-3-acetic acid; IAA-lysine synthase; Type Three Secretion System (TTSS); Multidrug And Toxic compound Extrusion (MATE); drug resistance; plant disease.

Cerboneschi M, Decorosi F, Biancalani C, Ortenzi MV, Macconi S, Giovannetti L, Viti C, Campanella B, Onor M, Bramanti E, Tegli S. (2016) Indole-3-acetic acid in plant-pathogen interactions: a key molecule for *in planta* bacterial virulence and fitness. *Manuscript published in Research Microbiology*.

All figures and tables in this chapter are reproduced from Cerboneschi *et al*., 2016, *Research Microbiology*.

## 5.2 Introduction

Auxins are an essential class of phytohormones that play a crucial role in virtually all aspects of plant development and growth, as well as in the response of plants to environmental stimuli including biotic and abiotic stresses [1-2]. The main naturally occurring auxin in plants is indole-3-acetic acid (IAA), the homeostasis of which guarantees its versatile role in plants mediated by a complex network of processes related to its biosynthesis, catabolism, reversible conjugation, signalling, and transport [3]. IAA is biosynthesized through several pathways from tryptophan (Trp), but Trp-independent routes are also known [4-7]. The free form of IAA is considered to be biologically active. However, in almost every plant tissue, this hormone is mostly conjugated, mainly to amino acids and sugars, and thus it is not more active [8-9]. IAA-conjugating enzymes, such as those encoded by the family of *GH3* plant genes, contribute to the maintenance of cellular IAA homeostasis and bioactivity via an inhibitory feedback loop [8]. The dynamic regulatory role played by IAA, from the whole plant to the cellular level, also relies on rapid and specific alterations of the transcriptional activation of auxin-responsive genes according to the distinct thresholds of IAA, through the so called "auxin response element" (AuxRE), which is always present in their promoters [10-12]. Additionally, the transport and asymmetric distribution of IAA throughout the plant are dynamically modified in response to internal and external stimuli, mainly by the polar active transport (PAT) of IAA from cell to cell, which is mediated by changes in the expression and localization of specific plasma membrane-localised proteins (*i.e.*, PIN, AUX), transporting IAA out of and into the plant cell, respectively [13]. Therefore, local IAA biosynthesis is dynamically integrated across the plant with mechanisms for its active transport, signalling, and perception, the regulation of which results in specific response outputs to nearly any endogenous and environmental input [14].

Recently, several studies have shed light on the molecular basis of the role of IAA in plant-pathogen interactions, particularly on the strategies adopted by phytopathogens to manipulate auxin homeostasis in plants to promote the infection process [15-18]. Basically, the localized increase in IAA during the first stages of their interaction with the host has been shown to be pivotal for plant pathogenic bacteria belonging to the *Pseudomonas syringae* group to promote plant susceptibility to infection [19-22]. In fact, *P. syringae* has also been demonstrated to take advantage of the accumulation in *Arabidopsis*-infected plants of an irreversibly catabolic conjugated form of IAA, IAA-Asp. Although it is less active in the plant than the free form, IAA-Asp has been shown to promote disease development by increasing *P. syringae* progression into the plant following the transcription of its virulence genes, as also observed for the plant pathogenic fungus *Botrytis cinerea* [15, 23]. Several of the *P. syringae* effectors secreted by the Type Three Secretion System (TTSS) have been shown to highjack the host plant systems for auxin biosynthesis, signalling and transport, to suppress active immune responses in susceptible plants [23-25].

Many plant-associated bacteria, including phytopathogens and symbionts, can also synthesize IAA using Trp as the main precursor [9, 26]. This feature was initially incorrectly believed to be restricted to gall-producing bacteria such as *P. savastanoi* and *Pantoea agglomerans*, in which IAA secretion was considered to be the main factor directly supporting the development

of the hyperplastic symptoms on the host [27-28]. However, it soon became evident that a broader distribution of IAA biosynthesis was also present in several non-gall-inducing phytopathogenic bacteria such as *Dickeya dadantii* [29]. The best characterized Trp-dependent pathway in bacteria is the two-step process denoted as the indole-3-acetamide (IAM) pathway, where the enzymes tryptophan-2-monooxygenase (IaaM) and IAM hydrolase (IaaH) are encoded by the *iaaM* and *iaaH* genes, respectively, and sequentially convert Trp to IAM and then to IAA. This is the most common pathway in phytopathogenic bacteria, including *P. savastanoi*, in which the presence of the *iaaL* gene encoding the enzyme that conjugates IAA to the amino acid lysine to give IAA–Lys was first demonstrated [30]. This gene is widely distributed and conserved among *P. syringae sensu lato* species and pathovars, and no significant homology with any plant IAA-conjugating enzyme has been found [31]. Moreover, no plant hydrolases have been discovered to date for the catabolism of IAA–Lys, whereas several plant-associated bacteria have been shown able to hydrolyze plant auxin conjugates such as IAA–Asp **[**8].

In this work, Phenotype Microarray (PM) technology was applied for the first time to *P. savastanoi* to test its chemical sensitivity patterns. Knockout mutants of strain *Psn23* of *P. savastanoi* pv. *nerii*, with impaired IAA synthesis, conjugation or TTSS functionality, were all found to be more sensitive to 8 hydroxyquinoline (8-HQ) than their wild-type counterpart. Overall, the data obtained herein also offer the opportunity to unveil functional links among IAA metabolism, TTSS and drug efflux in *P. savastanoi* pv. *nerii*, and they provide information that could be useful in the near future for the development of alternative strategies for the control of this plant pathogenic bacterium.

## 5.3 Materials and methods

### Bacterial strains and growth conditions

The *P. savastanoi* strain *Psn23* and its mutants used in this study are listed in Table 1. They were routinely grown at 26°C as liquid or solid cultures, in King's B (KB) [32] or in *hrp*-inducing Minimal Medium (MM) [33]. Bacterial growth was monitored by determining the culture optical density at 600 nm ($OD_{600}$) at different times during the incubation, and bacterial concentrations were estimated by serial dilutions and plate counts. For long-term storage, the bacteria were maintained at -20°C and -80°C in 40% (v/v) glycerol. The *Escherichia coli* strains TOP10 and ER2925 were grown in Luria–Bertani (LB) liquid or agarose medium [34]. Antibiotics, when required, were added to the medium at the following concentrations: 20 µg/ml streptomycin, 50 µg/ml nitrofurantoin, 10 µg/ml gentamicin, and 50 µg/ml kanamycin. Any bacterial contamination was excluded by periodical monitoring using PCR-based assays specific for *P. savastanoi* [35-36].

**Table 1: Bacterial strains, mutants and plasmids used in this study.**

| Strain/Plasmid | Relevant characteristics | Reference/Source |
|---|---|---|
| **Strain** | | |
| *E. coli* TOP10 | F-, *mcr*A, Δ(*mrr-hsd*RMS-*mcr*BC) Φ80 *lac*ZΔM15 Δ*lac*X74 *rec*A1 *ara*D139 Δ(*araleu*)7697 *gal*U *gal*K *rps*L (StrR) *end*A1 *nup*G | Invitrogen, Carlsbad, USA |
| *E. coli* ER2925 | *ara*-14 *leu*B6 *fhu*A31 *lac*Y1 *tsx*78 *gln*V44 *gal*K2 *gal*T22 *mcr*A *dcm*-6 *his*G4 *rfb*D1 R(*zgb*210::*Tn*10)TetS *end*A1 *rps*L136 *dam*13::*Tn*9 *xyl*A-5 *mtl*-1 *thi*-1 *mcr*B1 *hsd*R2 | NEB, Hertfordshire, UK |
| *P. savastanoi pv. nerii (Psn23)* | Wild type | This study |
| Δ*hrpA* | *hrpA* in-frame deletion mutant of *Psn23* | This study |
| Δ*iaaM* | *iaaM* in-frame deletion mutant of *Psn23* | This study |
| Δ*iaaL* | *iaaL* in-frame deletion mutant of *Psn23* | This study |
| **Plasmid** | | |
| *pK18mobsacB* | sacB, lacZa, Km, mcs mobilizable vector | Schafer *et al.* 1994 |
| *pK18-*Δ*hrpA* | pK18mobsacB derivative, in-frame deletion of the *hrpA* gene (273 bp) | This study |
| *pK18-*Δ*iaaM* | pK18mobsacB derivative, in-frame deletion of the *iaaM* gene (1101 bp) | This study |
| *pK18-*Δ*iaaL* | pK18mobsacB derivative, in-frame deletion of the *iaaL* gene (561 bp) | This study |

### Molecular techniques

PCR, restriction digestion, ligation, DNA electrophoresis, and transformation were performed according to standard procedure [37]. The plasmids used and those generated in this work are listed in Table 1. Genomic DNA from *P. savastanoi* strains was extracted from single bacterial colonies using thermal lysis [37], or from bacterial cultures ($OD_{600}$=0.8) using the Puregene® Genomic DNA Purification Kit (Gentra Systems Inc., Minneapolis, MN, USA) according to the manufacturers' instructions. The DNA concentration was evaluated both spectrophotometrically with a NanoDrop™ ND-1000 (NanoDrop Technologies Inc., DE, USA) and visually by standard agarose gel electrophoresis [1% agarose (w/v) in TBE 1×] [37]. For plasmid DNA extraction, NucleoSpin® Plasmid (Macherey-Nagel GmbH and Co. KG, Düren, Germany) was used according to the manufacturer's protocol. Amplicons were

purified from the agarose gel using NucleoSpin® Gel and PCR clean-up (Macherey-Nagel GmbH and Co.), and double-strand sequenced at Eurofins Genomics (Ebersberg, Germany). Multiple sequence alignments and comparisons were performed using the computer package CLUSTALW (version 2, http://www.ebi.ac.uk/Tools/clustalw2) [38] and with the Basic Local Alignment Search Tool (BLAST, http://www.ncbi.nlm.nih.gov/blast) [39]. Primers were designed using Beacon Designer 7.7 software (Premier Biosoft International, Palo Alto, CA, USA) (Table 2). The 7,548-bp sequence, containing the genes *iaaL*, *matE*, *iaaM* and *iaaH*, was deposited in GenBank under Accession Number KU351686.

**Table 2: Primers used in this study.**

| Primer name | Primer sequence (5'-3') |
|---|---|
| hrpA_XbaI_For | TTTCTAGAATCTGTACTTTCGCCTTAA |
| hrpA_cross_Rev | CCGGATCCACTAAACTTAAACTCAGAGAACTTATGATGCTC |
| hrpA_cross_For | GTTTAAGTTTAGTGGATCCGGCCAGTTCTGATTTCTTGAATG |
| hrpA_EcoRI_Rev | TTGAATTCAAGTTATCTTCCTTGAGTTCG |
| iaaM_XbaI_For | TTTTCTAGACAAAACCTTTACCGAATG |
| iaaM_cross_Rev | CCGGATCCACTAAACTTAAACTTTTTCAGGTAGTG |
| iaaM_cross_For | AAGTTTAGTGGATCCGGGCAGCGATTGTTTTTTCA |
| iaaM_EcoRI_Rev | TTTGAATTCCTGAGTTGACTGACAATC |
| iaaL_EcoRI_For | AAAGAATTCGTCATTCAGGTTGCTTTT |
| iaaL_cross_Rev | AAAGTTTAAGTTTAGTGGATCCGGGTTCTGAAGTCCTGATAAG |
| iaaL_cross_For | AAACCGGATCCACTAAACTTAAACTGAATACGAGTTTCTGTC |
| iaaL_XbaI_Rev | AAATCTAGAGATTTCGGCTATGATAAC |
| hrpA_ RT_ For | GCAGGGTATCAACAGCGTCAAG |
| hrpA_ RT_ Rev | CCGTTCTCTTCGTTCGCAGTG |
| iaaM_ RT_ For | TTCACTGCCTCACGGATAGCG |
| iaaM_ RT_ Rev | CGACTGGATGGTGGTGGGAAG |
| iaaL_ RT_For | ACCTCAGCAGCGGCGTAAAG |
| iaaL_ RT_ Rev | TCGTCGGTGTGTATGGCAGTTC |
| iaaH_RT_For | TGATGATGCCGATATTGTC |
| iaaH_RT_Rev | AAGGTGGTGATTGATGATG |
| matE_RT_For | CATCGCAGCCATTACG |
| matE_RT_Rev | AGCCTGAAGAACCTGTC |
| hrpL_RT_For | GTATTGCGTTGAACCTGAT |
| hrpL_RT_Rev | CGTCTACCTGATGAGTGATA |
| hopAB1_RT_For | CGCAGGCATAATCATAGT |
| hopAB1_RT_Rev | CGGTTCAAGCGACATT |

## Generation of *Psn23* knockout mutants

The Δ*hrpA*, Δ*iaaM* and Δ*iaaL* mutants were constructed by in-frame deletion of the *hrpA*, *iaaM* and *iaaL* genes, respectively, from the *Psn23* wild-type genome (Table 1), using marker exchange mutagenesis [40]. Knockout constructs were generated by overlap extension PCR using the primers listed in Table 2. The two DNA fragments flanking each in-frame deletion were amplified from *Psn23* genomic DNA as a template with *Pfu* polymerase (Promega Corp.,

Madison, WI, USA). The plasmids generated in this work are based on *pK18mobsacB*, a suicide vector for *P. syringae sensu lato* that allows SacB counterselection [12-13], and they are listed in Table 1. The recombinant vectors were transferred into electrocompetent *Psn23* cells by electroporation with Gene Pulser XCell™ (Bio-Rad Laboratories Inc., Hercules, CA, USA) [41]. $Suc^R$ colonies were screened by PCR, and the marked deletions were then confirmed by sequencing.

**Quantification of bacterial IAA synthesis**

The amount of IAA produced by *P. savastanoi* strains was assessed both by the Salkowski assay [42] and using high-performance liquid chromatography (HPLC). IAA, L-Trp, indole-3-acetamide (IAM), and LC-MS-grade acetonitrile, methanol and formic acid were purchased from Sigma-Aldrich, Inc. (St. Louis, MO, USA). The UniPrep® syringeless filtration device (0.25 µm) was obtained from Agilent Technologies (Santa Clara, CA, USA). Standard stock solutions (1,000 µg/ml) of IAA and IAM were prepared in methanol, while the standard Trp stock solution (1,000 µg/ml) was prepared in ultra-pure Milli-Q water. Working solutions for each standard were prepared by appropriate dilution of the stock solution with 35% MeOH and 0.1% formic acid. Samples were prepared from 0.1 g of lyophilised bacterial supernatant, resuspended in 1 ml of 35% MeOH and 0.1% formic acid, further diluted 1:10 in the same solvent, and filtered using a 0.25-µm Uniprep® syringeless filtration device. The filtrates were analysed by HPLC-DAD/FD or HPLC-MS, with data acquisition and data analysis carried out by the ChromQuest™ 4.2 Chromatography Data System and MassHunter® Workstation Software (B.04.00), respectively.

**Arabidopsis root elongation assay**

Seeds of *A. thaliana* Col-0 were surface-sterilized in 1% bleach, rinsed three times in sterile distilled water, and then stratified at 4°C for 2-4 days to obtain uniform germination. The *Arabidopsis* Col-0 seedlings were then sown on new half-strength MS plates and grown in a vertical orientation. At 4 cm from the root tip, 15 µl of a bacterial suspension ($OD_{600}$=0.5) of *Psn23* or of its mutants were spotted, as previously described [43]. Photographs were obtained after an additional 4 days of vertical growth, and the root length was measured using ImageJ software. The length of newly elongated roots was measured, and the relative root length was calculated. The mean ± standard deviation (SD) for 10 to 15 seedlings was calculated, and each assay was repeated at least three times.

**Pathogenicity tests**

*In vitro* micropropagated oleander *(Nerium oleander* L.) plants with red double flowers (Vitroplant Italia s.r.l., Cesena, Italy) were grown for 3 weeks at 26°C on Murashige-Skoog medium (MS) [44], without the addition of phytohormones and with a photoperiod of 16-h light/8-h dark. The plants were then wounded on the stem at the second internode using a 1-ml syringe needle, and immediately inoculated with 1 µl of a bacterial suspension in sterile physiological solution (SPS, 0.85% NaCl in distilled water), with an $OD_{600}$=0.5 (approximately $0.5\times10^8$ Colony Forming Unit/ml, CFU/ml). Negative control plants were inoculated with SPS alone. The plants were then incubated at 26°C under a 16-h light/8-h dark

photoperiod and periodically monitored for the appearance of symptoms. Photographic records were obtained at 7, 14 and 21 days post-inoculation (dpi). At the same time points, bacterial growth was also estimated as previously described [36, 45]. Three independent experiments were performed, and nine plants for each *P. savastanoi* strain were inoculated in each run.

**Hypersensitive response assays**

As a model plant for the hypersensitive response (HR) assay, *Nicotiana tabacum* var. Burley White was used. The plants were grown at 24°C with a relative humidity of 75% and a photoperiod of 16/8-h light/dark. Bacterial cultures were grown overnight in KB medium at 26°C and resuspended in SPS ($OD_{600}$=0.5). The final bacterial cell concentration was confirmed by the serial dilution agar plating method. Using a 2-ml blunt-end syringe, approximately 100 µl of the bacterial suspension was infiltrated into the abaxial mesophyll of fully expanded leaves of three tobacco plants [46], with six replicates tested per strain in each of the three independent experiments. The development of HR was assessed according to the presence of macroscopic tissue collapse at 24 h post-inoculation. Photographic records of the results were obtained.

**Phenotype Microarray**

*P. savastanoi* strains were tested on chemical sensitivity panels (PM09-PM20) using PM technology (Biolog Inc., Hayward, CA, USA). Overall 1,152 different conditions were tested, including several concentrations of osmolytes (PM09), pH stresses (PM10) and a wide variety of potentially toxic compounds (PM11-20). In the PM11-20 panels, each chemical is dispensed at four increasing concentrations in adjacent wells, from the lowest to the highest. The complete list of compounds assayed can be obtained at http: //www.biolog.com/pdf/pm_lit/PM1-PM10.pdf and http: //www.biolog.com/pdf/pm_lit/PM11-PM20.pdf. PM uses tetrazolium violet reduction as a reporter of active metabolism [47]. Reduction of the dye causes the formation of a purple colour that, recorded every 15 min, provides quantitative and kinetic information about the response of the bacterial cells to each compound [47]. Each strain was grown overnight at 26°C on BUG agar (Biolog, Inc.). Colonies were picked using a sterile cotton swab and suspended in SPS. The cell density was adjusted to 81% transmittance (T) on a turbidimeter (Biolog, Inc.). The bacterial suspension was diluted twelve times in KB medium supplemented with 25 mM L-Trp and 1x dye A (Biolog Inc.). All plates were incubated at 26°C in an Omnilog reader (Biolog, Inc.), and the readings were recorded for 96 h. Kinetic data were analysed using Omnilog-PM software (release OM_PM_109M). For each strain, the area of the kinetic curves detected in PM9-20 was exported and used to calculate the difference between the wild-type and each mutant. Differences greater than 40,000 Arbitrary Omnilog Units (AOU) were considered relevant to identify phenotypic differences between the wild-type and each of its mutants.

**Quantitative gene expression analysis**

Bacterial gene expression was evaluated by real-time PCR. Bacterial cells of wild-type *Psn23* and its mutants were grown overnight in KB (starting concentration $OD_{600}$=0.1), washed twice with SPS, and transferred into MM alone or supplemented with L-Trp (250 µM), IAA (200 µM), 8-HQ (10 µM), or IAA+8-HQ (200 µM and 10 µM, respectively). Cells were collected after 24 h of incubation at 26°C with shaking (100 rpm) and used for RNA extraction performed with a NucleoSpin® RNA Plus (Macherey-Nagel GmbH and Co. KG, Düren, Germany). Residual genomic DNA was removed using a NucleoSpin® gDNA Removal Column (Macherey-Nagel GmbH and Co.). RNA Reverse transcription was performed using the iScript™ Advanced cDNA Synthesis kit (Bio-Rad Laboratories Inc.) with approximately 2 µg of total RNA. Diluted cDNA was analysed with SsoFast™ EvaGreen® Supermix (Bio-Rad Laboratories Inc.), using the CFX96 cycler – Real-Time PCR Detection System and CFX-manager software v1.6 (Bio-Rad, Laboratories Inc.). To normalise the expression of each gene, the 16S rDNA expression level was used as a housekeeping gene. For each sample, three replicates were assessed, and three independent experiments were conducted. The primers used are listed in Table 2.

**Data analysis**

Statistically significant differences among treatments were calculated by one-way ANOVA with Tukey-Kramer post-test ($p<0.05$) with PAST software (Version 3.11, Øyvind Hammer, Natural History Museum, University of Oslo).

## 5.4 Results

### A prokaryotic *AuxRe* identified in the promoters of genes for IAA biosynthesis and conjugation in *P. savastanoi* pv. *nerii*

In the *Psn23* genome, the *iaaM/iaaH* operon for IAA biosynthesis is positioned in close proximity to the gene *iaaL* for IAA conjugation, flanking an insertion sequence of the IS4 family on a 7,548-bp DNA fragment. Moreover, an ORF encoding a putative Multidrug And Toxic compound Extrusion (MATE) efflux transporter is located upstream of *iaaL* (Figure 1A), hereafter denoted as *matE*. According to the *in silico* analysis, the *iaaL* and *matE* genes are divergently transcribed from the *iaaM/iaaH* operon. In the 5' region of the *iaaM/iaaH* operon, as well as upstream of *iaaL* and *matE*, *hrp* box promoter sequences were found, suggesting their TTSS-dependent expression and HrpL-regulated transcription (Figure 1B).

**Figure 1. Diagrams illustrating the physical and functional relationships among IAA metabolism, TTSS and drug efflux in *P. savastanoi* pv. *nerii* strain *Psn23*. (A) Organization of the genomic region containing the *iaaM/iaaH* operon and the *iaaL* and *matE* genes, including the putative promoters and factors regulating their expression. The transcriptional direction of each gene is indicated in orange, yellow, and grey arrows for *iaaL*, *matE*, and the *iaaM/iaaH* operon, respectively. *hrp*-box promoters: black arrows; AuxREs: green arrows; DS element: blue arrow. (B) The *hrp*-box promoter strength evaluated *in silico* for five different loci related to IAA metabolism and TTSS activation. Vertical blue arrows indicate the promoter strength from the bottom (low activation) to the top (high activation). Black bold nucleotides indicate perfect identity with the *hrpA* promoter; red bold nucleotides underline specific mismatches.**

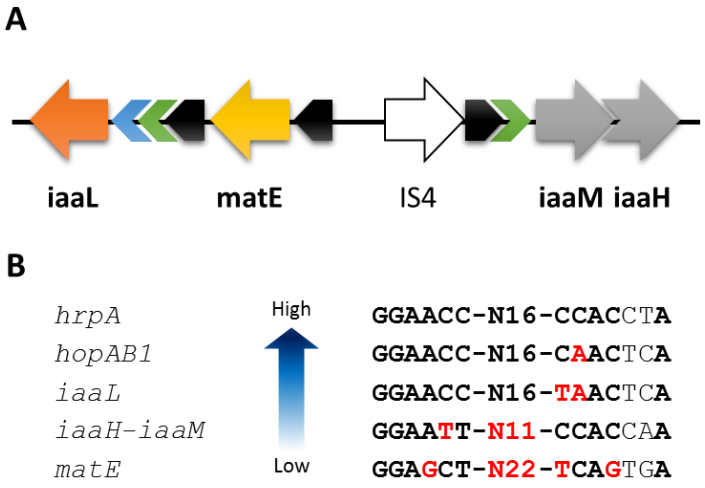


However, several substitutions are present on the first 5 nucleotides of the –35 consensus motif (GGAACC) and the first 4 nucleotides of the –10 motif (CCACNNA) of these promoters in comparison to the canonical *hrp*-box driving *hrpA* transcription in *P. syringae sensu lato* (Figure 1B). Additionally, other regulatory elements were found that have never been identified previously in *P. savastanoi* or in any other *P. syringae sensu lato*. In particular, a putative prokaryotic AuxRe was identified upstream of the *iaaL* gene and the *iaaM/iaaH* operon of *Psn23*. The short sequence (TGTCCA) resembles that located upstream of the *ipdC* gene of *Azospirillum brasiliense*, encoding the key enzyme for Trp-dependent IAA biosynthesis in this bacterium and the only prokaryotic AuxRe identified to date [48]. With

respect to the start codon for *iaaL*, the AuxRe motif is located at positions (–38) to (–33). Moreover, in the *iaaL* promoter, a dyadic sequence (DS) has also been identified between positions (–42) and (–71), characterized by a perfect 8-bp inverted repeat separated by a 14-bp spacer, further supporting the auxin-inducible expression of *iaaL* in *P. savastanoi*. Conversely, no DS was found associated with the putative AuxRe in the promoter of the *iaaM/iaaH* operon (Figure 1A). By an *in silico* analysis of the 5' region of the *iaaL* gene and the *iaaM/iaaH* operon in other *P. syringae* phytopathogens, putative AuxREs were also identified in *P. savastanoi* pv. *nerii* (EW 2009, CFBP5067 and ICMP16943), while a DS sequence was found only in *P. syringae* pv. *tomato* DC3000 (data not shown).

**The increase in free IAA secretion determines the hypervirulence of the Δ*iaaL* mutant**

After 24 and 48 h of growth on MM amended with L-Trp (250 µM), indoles production was evaluated in the culture supernatants of *Psn23* and the mutants *ΔiaaM* and *ΔiaaL*. Given the presence of several *hrp* box motifs in the promoters of the genes for IAA synthesis and conjugation, the mutant *ΔhrpA* was also examined for comparison. The colorimetric Salkowski assay was used for an initial screening because it is able to detect IAA with a high specificity among other indoles (Figure 2). As expected, indole production by *ΔiaaM* was negligible. Conversely, the mutant *ΔiaaL* produced significantly higher amounts of IAA than the wild-type *Psn23*, with approximately 61.3 and 64.5 µg/ml of IAA equivalents after 24 and 48 h of growth, respectively.

**Figure 2. Quantification of IAA production using the Salkowski assay for *Psn23* and its Δ*iaaL*, Δ*iaaM*, and Δ*hrpA* mutant supernatants at 24 (green) and 48 h (blue) post-inoculation on MM supplemented with L-Trp (250 µM). The data are expressed as the average of three replicates ± standard deviation (SD). Statistically significant differences are represented by different letters above the bars (ANOVA and the Tukey test, p<0.05).**

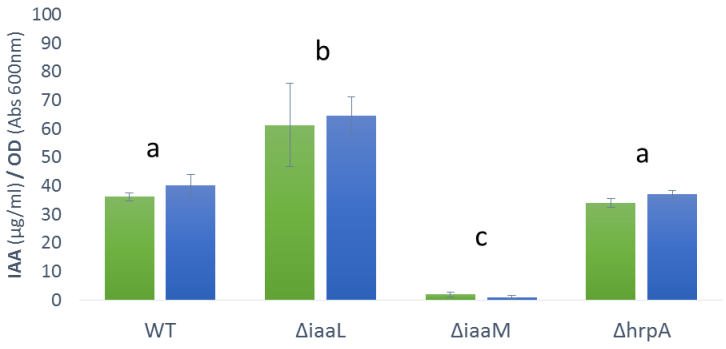


Regarding *ΔhrpA*, IAA biosynthesis was comparable to that of *Psn23* (approximately 40 and 37 µg/ml of IAA equivalents after 24 h and 48 h of growth, respectively). These results were then confirmed using an innovative method developed in this work that is based on liquid chromatography coupled to molecular fluorescence and to tandem mass spectrometry, specifically high resolution QToF. The fluorescence chromatograms at 340 nm ($\lambda_{ex}$=280 nm)

of Trp, IAA and IAM used herein as standards (1 µg/ml) were compared with those from the lyophilised supernatants of *Psn23* and its three mutants *ΔiaaM*, *ΔiaaL* and *ΔhrpA.* In particular, the fluorescence chromatograms for Trp and for IAA displayed a peak with a retention time of 2.68 min and 12.7 min, respectively. As expected, *ΔiaaM* was unable to convert Trp into IAA, and thus the peak at 2.68 min was present while that at 12.7 min was absent (Figure S1). Conversely, the *ΔiaaL* chromatogram showed both peaks for Trp and IAA. Surprisingly, both *Psn23* and its *ΔhrpA* mutant exhibited the peak corresponding to Trp (2.68 min) but not that at 12.7 min for IAA. Moreover, another unexpected signal was a retention time of 3.28 min that was not attributable to any of the standards used herein. Both *Psn23* and *ΔhrpA* have the ability to convert IAA to IAA-Lys, unlike *ΔiaaL.* Thus, it was hypothesized that the peak at 3.28 min corresponded to IAA-Lys. Unfortunately, there is no commercially available standard for IAA-Lys, and thus this analyte requires further characterisation by HPLC-ESI-Q-ToF. Figure S2 shows the mass spectrum, acquired using positive ionization, for this unidentified indolic compound. The presence of m/z 304 ($[M+H]^+$) and 130 ($[NH_2\text{-}(CH_2)_4\text{-}CH\text{-}COOH]^+$) unequivocally confirmed that this compound corresponded to IAA-Lys. The higher content of free IAA in the *ΔiaaL* mutant in comparison to wild-type *Psn23* was also biologically and quantitatively demonstrated by analysing the effect of bacterial IAA on root elongation and lateral root formation in *A. thaliana* seedlings (Figure 3).

**Figure 3. Root elongation and lateral root formation in *A. thaliana* Col-0 seedlings grown on vertical plates in the presence of wild-type *Psn23*, *ΔiaaL*, *ΔiaaM*, and *ΔhrpA* supernatants.**

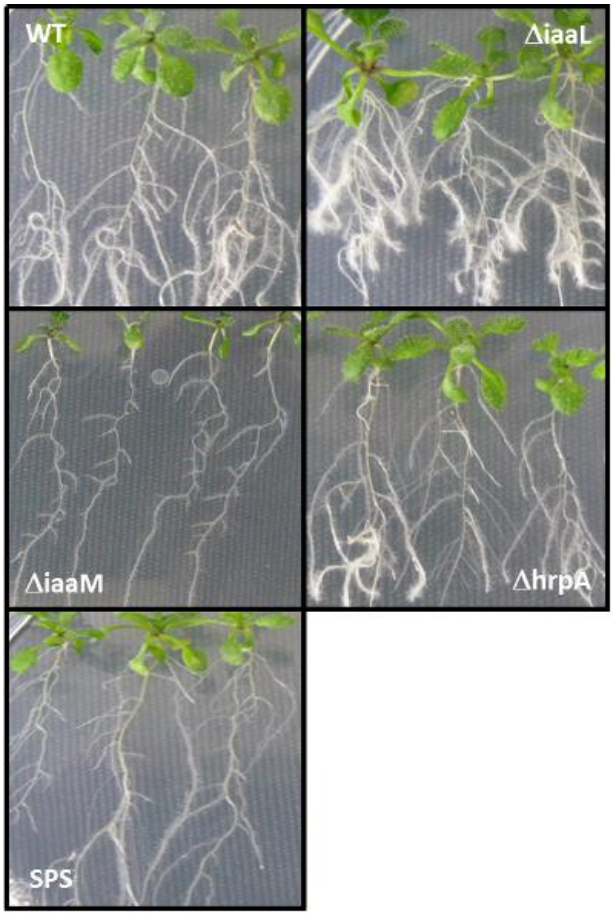

After 14 days, the mean length of the main root in the *ΔiaaM*-treated seedlings was 6.92 ± 0.46 cm, which is comparable to that obtained for untreated seedlings (6.782 ± 0.34). Similarly, the mean root length of the *ΔhrpA*-treated seedlings (5.50 ± 0.46 cm) was longer than that of wild-type *Psn23*-treated seedlings (3.78 ± 0.13 cm). Conversely, the mean length of the roots of *A. thaliana* seedlings treated with *ΔiaaL* were extremely reduced (2.57 ± 0.06 cm). Overall these data biologically confirmed the higher levels of free IAA produced by the *ΔiaaL* mutant in comparison to *Psn23*, inducing a strong inhibition of root elongation. As expected, this effect was not observed in *A. thaliana* seedlings treated with the *ΔiaaM* mutant, which is unable to synthesize IAA. According to the bimodal and opposite effect of the free IAA concentration on the primary root length and local differentiation events, massive lateral root development was also observed following *ΔiaaL* treatment (Figure 3).

Given the high production of free IAA by the *ΔiaaL* mutant, and considering the conflicting results reported to date regarding the role of the *iaaL* gene in the virulence of *P. syringae sensu lato*, pathogenicity trials were subsequently conducted using micropropagated oleander plants. Together with *ΔiaaL*, the wild-type *Psn23* and the mutants *ΔiaaM* and *ΔhrpA* were also used for comparison. The development of hyperplastic symptoms was visually observed and recorded at 7, 14 and 21 dpi (Figure 4A).

**Figure 4**. **Pathogenicity trials of micropropagated oleander plants conducted using on *Psn23* and its mutants *ΔiaaL*, *ΔiaaM*, and *ΔhrpA*. A) Knot development at 21 days post-infection. Black arrows indicate the site of bacterial inoculum. (B) *In planta* bacterial growths at 7 (green), 14 (blue) and 21 (yellow) days post-infection. Values are the mean of 3 independent experiments with 9 replicates for each strain ± standard deviation (SD). ANOVA revealed statistically significant differences ($p<0.05$), comparison using the Tukey post-test are indicated by letters, where different letters indicate statistically significant differences.**

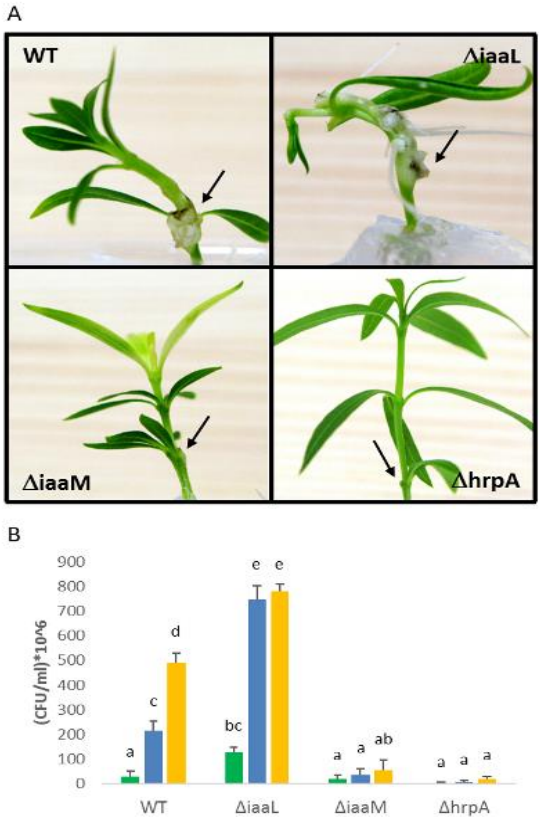

At the same time points, *in planta* bacterial growth was also assessed (Figure 4B). The mutant *ΔiaaL* always induced more extensive hyperplastic lesions than *Psn23*. The symptoms were not restricted to the inoculation site, as observed for *Psn23*, but the upper part of the plant was also affected. Bacterial multiplication *in planta* was significantly correlated to symptoms and disease severity, with *ΔiaaL* achieving higher CFU values than *Psn23* at all the time points considered (Figure 4B). Conversely, hyperplastic symptoms and bacterial growth were drastically reduced or completely abolished in the case of *ΔiaaM* and *ΔhrpA*, respectively, as expected (Figure 4B). Concerning the HR analysis of tobacco, *ΔiaaM* and *ΔiaaL* caused a typical HR, similar to that observed with *Psn23*, while *ΔhrpA* did not. These results confirmed that *ΔhrpA* is not more pathogenic (Figure 5).

**Figure 5. HR assay on tobacco leaves at 48 h post-infiltration. (A) Wild-type *Psn23* (1), *ΔiaaM* (2), *ΔhrpA* (3) and SPS (4) as negative controls. (B) Wild-type *Psn23* (1), *ΔiaaL* (2), *ΔhrpA* (3) and SPS (4) as negative controls.**

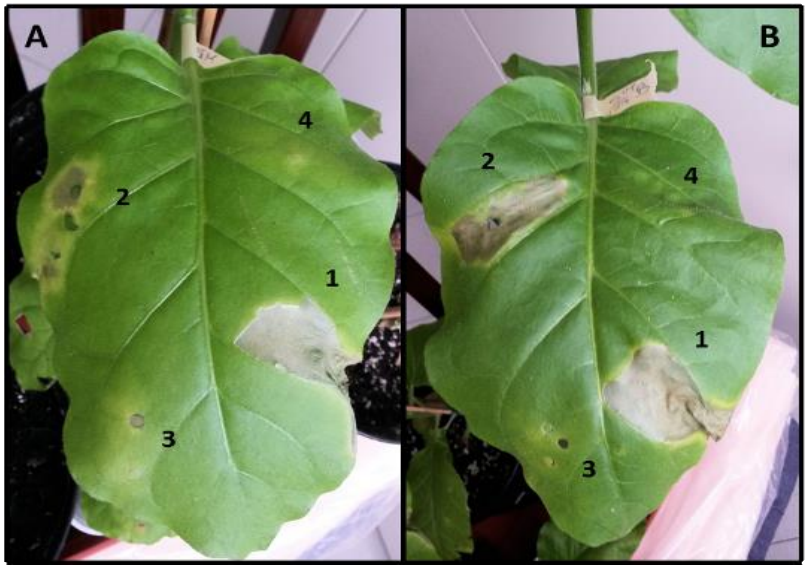


**PM analysis as a tool to unravel the relationship in *P. savastanoi* pv. *nerii* among IAA metabolism, TTSS and resistance to toxic compounds**

Undoubtedly, the fitness *in planta* of a bacterial phytopathogen depends not only on its virulence and its ability to multiply in its hosts, but also on its resistance to a number of toxic and antimicrobial compounds of plant origin that are produced before and during the infection process.

As a result of the unexpected hypervirulence of the *ΔiaaL* mutant, we decided to investigate potential changes in the phenotype of this mutant in comparison to wild-type *Psn23* that could justify its reduced fitness and competitiveness in nature. Moreover, the presence of a gene encoding a putative MATE upstream of *iaaL* further prompted a wide phenotypic screening. PM analysis was applied to strain *Psn23* and to its mutant *ΔiaaL*. The mutants *ΔiaaM* and *ΔhrpA* were also included for comparison.

By using twelve panels (PM9-PM20), their sensitivity to pH, osmolytes and to 240 toxic chemicals, each at four different concentrations, was evaluated. The three mutants showed the same pH and osmolyte sensitivity profiles compared with wild-type *Psn23.* As main characteristics, they tolerated pH values higher than 5.5, as well as NaCl concentrations lower than 4%. Conversely, the sensitivity profiles of the mutant strains to toxic compounds were not completely overlapping those of the wild-type *Psn23* (Table 3). The most noticeable results were those obtained following 8-HQ treatment, in which the three mutants exhibited the same behaviour. In particular, *ΔiaaL*, *ΔiaaM* and *ΔhrpA* showed a significantly higher sensitivity towards 8-HQ than *Psn23*, although to different extents. The most sensitive strain was *ΔiaaL*.

**Table 3. Difference between the areas of the kinetic curve of the wild type and the three mutant strains detected by PM technology.**

| Compound | Dose* | $A_{wildtype} - A_{mutant\ \Delta iaaL}$ | $A_{wildtype} - A_{mutant\ \Delta iaaM}$ | $A_{wildtype} - A_{mutant\ \Delta hrpA}$ |
|---|---|---|---|---|
| **Oxytetracycline** | I | 8350 | 8402 | 5597 |
| | II | 17617 | 7658 | 3834 |
| | III | 18276 | 17675 | 9203 |
| | IV | 33953 | 47479** | 22135 |
| **8-Hydroxyquinoline** | I | 4341 | 1210 | 4582 |
| | II | 5077 | 5214 | 3918 |
| | III | 56283** | 7640 | 22848 |
| | IV | 56771** | 55390** | 54068** |
| **Hydroxylamine** | I | -6994 | 4551 | -15205 |
| | II | 4304 | 334 | -18857 |
| | III | 2638 | -7003 | -27870 |
| | IV | 1130 | -39047 | -76650** |
| **Sodium azide** | I | -24057 | -3998 | -61490** |
| | II | 55 | -199 | -2452 |
| | III | -440 | -1675 | -2577 |
| | IV | 233 | -175 | -2253 |
| **Polymixin B** | I | 10707 | 2512 | -7035 |
| | II | 5561 | 3181 | -6762 |
| | III | 964 | 1262 | 505 |
| | IV | 132 | -872 | -57193** |

* Four increasing doses of the toxic compounds were tested, dose I is the lowest and dose IV is the highest.
** Differences higher than 40,000 AOU were considered relevant to identify phenotypic differences between the mutants and the wild type.

Following these findings, the expression of *matE*, as well as of several genes related to IAA metabolism and to TTSS, was evaluated by real-time PCR and on *Psn23* grown *in vitro* on MM supplemented with 8-HQ. As shown in Figure 6, the transcript levels of *matE* were the only ones to be upregulated in the presence of 8-HQ. Although this increase was quite marginal (1.5-fold), this result could support the hypothesis of 8-HQ efflux in *Psn23* mediated by the hypothetical transporter encoded by *matE.* Moreover, in the presence of 8-HQ, the expression levels of *matE* were generally lower in the mutants compared with *Psn23*, explaining their higher sensitivity to this antimicrobial compound in the PM experiments Figure 7A.

**Figure 6. Differential gene expression of wild-type *Psn23* grown *in vitro* on MM alone or supplemented with L-Trp (250 µM), IAA (200 µM), 8-HQ (10 µM), and IAA+8-HQ (200 µM and 10 µM, respectively). Gene map: *hopAB1* in blue, *hrpL* in orange, *iaaH* in grey, *iaaL* in yellow and *matE* in green. Data are the averages of triplicates ± standard deviation (SD). Asterisks indicate significant differences compared with the untreated sample at p<0.05.**

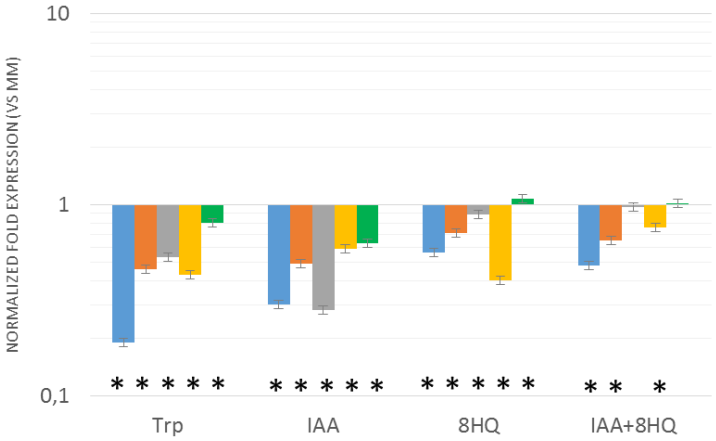


**Figure 7. Relative gene expression analysis of the *ΔiaaM*, *ΔiaaL*, and *ΔiaaA* mutants grown *in vitro* on MM alone or supplemented with (A) 8-HQ (10 µM) and (B) IAA (200 µM) and compared with wild-type *Psn23*. Gene map: *hopAB1* in blue, *hrpL* in orange, *iaaH* in grey, *iaaL* in yellow and *matE* in green. Asterisks indicate significant differences compared with wild-type *Psn23* supplemented with the same treatment at p<0.05.**

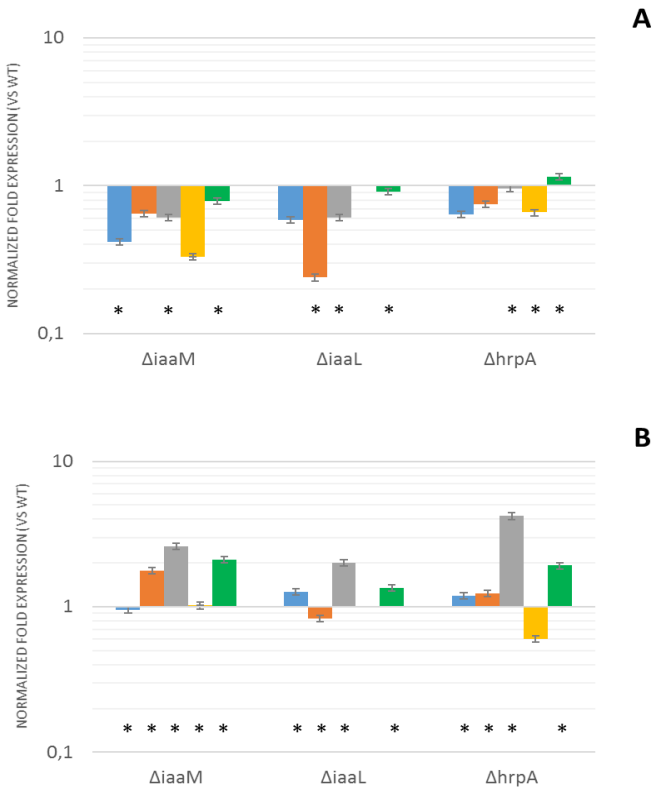

The expression of TTSS genes such as *hrpL* and *hopAB1*, induced by *in vitro* growth on MM, was strongly reduced in wild-type *Psn23* in the presence of IAA (200 µM) (Figure 6). This down-regulation also occurred when MM was supplemented with Trp (250 µM), likely because IAA synthesis was carried out by *Psn23* using Trp as a precursor (Figure 4). Likewise, the expression of genes such as *iaaH*, *iaaL* and *matE* was also reduced in response to IAA or Trp (Figure 6), as expected for the presence of *hrp* box motifs in their promoters (Figure 1B). Surprisingly, the inhibition caused of TTSS-regulated genes by IAA was largely removed when 8-HQ was applied together with IAA. These data could suggest a further role for the putative MATE transporter encoded by *matE*, in addition to conferring resistance to drugs, mediating IAA efflux (Figure 6). In support of this hypothesis, the expression levels of *matE* were upregulated in the *ΔiaaM*, *ΔiaaL* and *ΔhrpA* mutants in comparison to wild-type *Psn23* when IAA was added to the MM (Figure 7B). This result suggested a kind of repressive mechanism directly or indirectly driven by TTSS to activate drug or IAA efflux during specific stages of the infection process when TTSS is downregulated, or even switched off.

## 5.5 Discussion

IAA biosynthesis, as well as of that of many indoles, is widespread among Gram-positive and Gram-negative bacteria, as well as in many fungi, including many pathogens of plants and even humans [49]. Trp is mostly used as a precursor of IAA, essentially by the IAM or IPA pathways [50]. While the pivotal role of this phytohormone for the development of hyperplastic symptoms caused by *Ustilago maydis* and *P. savastanoi* on their hosts [51], or for rhizobia and ectomycorrhizal fungi to support their beneficial interaction with plants is very clear [52], its physiological role in the presence of IAA produced by plant pathogenic necrotrophic fungi such as *Colletotrichum* and *Fusarium* spp. is less intuitive [53-54]. It is even less well understood when IAA biosynthesis occurs in bacteria and yeasts that are pathogenic to mammals, or that belong to different soil and aquatic ecosystems [55]. In fact, in the last few years, accumulating scientific evidence has indicated that IAA is indeed a signalling molecule for bacteria and is essential for the regulation of their physiology, adaption to stress conditions and communication, as well as the mediation of several host-microbe interactions [49]. Although highly speculative, these findings are not surprising when considering that IAA has the same indole-like chemical structure as that of other eukaryotic hormones such as serotonin, melatonin, and epinephrine [56].

Regarding plant-associated bacteria, IAA has been shown to determine changes in bacterial gene expression in the non-gall-forming phytopathogen *D. dadantii* (formerly *E. herbicola*) 3937 [57], in *A. tumefaciens* [58-59], and in the plant growth-stimulating rhizobacterium *A. brasilense* [60], in which its *ipdC* gene has been the only bacterial gene reported to possess an AuxRe in its promoter as observed in the auxin-responsive genes of plants [48]. Similarly, in the yeast *Saccharomyces cerevisiae,* several IAA-inducible genes are regulated at high IAA concentrations by the fungal transcriptional activator YAP-1, which is able to bind to their promoters to induce a switch towards invasive behaviour, together with an arrest of cell growth. Conversely, at lower concentrations, IAA induces *S. cerevisiae* filamentation and adhesion, thus supporting plant infection. This phenotype conversion also involves a family of transporters, and it is noteworthy that YAP-1 is also pivotal for the pleiotropic drug resistance of *S. cerevisiae* [61].

Antibiotic resistance is among the adverse conditions against which IAA increases tolerance in *E. coli*, in which indole has been shown to turn on drug efflux pumps [62-63]. An analogous relationship between IAA/indole biosynthesis and drug resistance has not been reported to date for phytopathogenic bacteria belonging to the *P. syringae* group, whereas IAA production and its increase during the early phases of infection have been shown to be essential for alterations of host auxin signalling, to enhance plant susceptibility and to promote successful infection [15].

In the present study, IAA metabolism, not just its biosynthesis, was found to be an essential virulence determinant for *P. savastanoi.* In fact, the *ΔiaaL* mutant was found to be hypervirulent on its host plant *N. oleander*, where it is able to reach higher *in planta* population densities and cause more extended hyperplastic symptoms than wild-type *Psn23.* This finding was fully coherent with the increased amounts of free IAA produced by *ΔiaaL* in comparison to *Psn23*, as assessed using the Salkowski assay and HPLC MS. Conversely and as expected,

the Δ*iaaM* mutant was found to be hypovirulent. This *ΔiaaL* phenotype contrasted with the data reported thus far for *P. savastanoi* and *P. syringae* pv. *tomato* DC3000 [30, 64-65]. However, the opposite results for *P. savastanoi* could likely be due to downstream transcriptional consequences derived from inactivation of the *iaaL* gene by transposon mutagenesis [30]. Concerning *P. syringae* pv. *tomato* DC3000, previous reports are conflicting, mainly due to substantial differences in the experimental design of the pathogenicity tests applied [64-65]. Moreover, it is reasonable that IAA metabolism has different mechanisms in *P. syringae* pv. *tomato* DC3000 compared with those adopted by a hyperplastic bacterium such as *Psn23.*

According to the data from the phenotypic characterization caused by PM technology, both Δ*iaaL* and Δ*iaaM* were shown to be more sensitive than *Psn23* towards some antibiotics and biocides, with a significant reduced resistance to 8-HQ. This quinoline derivative is produced by plants in nature, generally secreted into their exudates, and used as an antimicrobial agent in agriculture and other industrial sectors during chemical synthesis. Several mechanisms have been proposed to support 8-HQ antibiotic-like activity, such as a lipophilic chelator and an inhibitor of TTSS, of multi-drug efflux pumps and of ribonucleic acid synthesis, although definitive evidence is not yet available [66-67]. Overall the PM data concerning the sensitivity of both Δ*iaaL* and Δ*iaaM* to 8-HQ was also confirmed for *P. savastanoi* pv. *nerii*, as already known for *E. coli*. Thus, IAA has a supplementary role as a fitness cost for the survival of these bacteria under stressful conditions, such as the presence of antimicrobials produced by the antagonists they find in their epiphytic phase and by the host plant during infection. Similarly, most *P. syringae* pathovars produce IAA even in the absence of hyperplastics, and the *iaaL* gene is widespread in *P. syringae sensu lato.* This finding strongly supports the existence of additional roles for IAA besides its involvement in plant-bacterial phytopathogen interactions, to manipulate plant auxin signalling, and even to enhance resistance to antimicrobial and toxic compounds.

Here, we demonstrate that the *ΔhrpA* mutant of *Psn23*, with an impaired TTSS and diminished pathogenicity, is also more sensitive than the wild-type towards 8-HQ. The existence of a physiological link between IAA metabolism and TTSS is already known. In particular, high IAA concentrations (up to 1 mM) have been found to have a strong inhibitory activity on the TTSS functionality of *P. savastanoi* pv. *savastanoi* [29], and further demonstrated herein for *P. savastanoi* pv. *nerii Psn23.* According to this inhibitory activity of IAA on TTSS, the bacterial content of this auxin in its biologically active form must be carefully regulated and modulated in different manners during the various phases of the interaction of phytopathogenic bacterial with their host plants, to guarantee their epiphytic and endophytic survival as well as a successful infection. The tight control of intracellular levels of free IAA, and therefore of IAA metabolism, must be even more stringent for a hyperplastic phytopathogenic bacterium such as *P. savastanoi*, in which the amount of free IAA is pivotal for the development of the typical symptoms.

The *in silico* analysis of the *Psn23* genomic region, including the *iaaM/iaaH* operon and the *iaaL* gene operons, further supports this functional connection between IAA metabolism and TTSS, according to the presence of *hrp* box motifs in their promoters. Moreover, this analysis introduces an additional element to relate these systems that could explain the higher

sensitivity to 8-HQ observed in the PM experiments for the *ΔiaaL*, *ΔiaaM* and *ΔhrpA* mutants in comparison to wild-type *Psn23*. Close to *iaaL*, a gene encoding a putative MATE was found, as also recently reported for *P. syringae* pv. *tomato* DC3000 and *P. savastanoi* pv. *savastanoi* NCPPB3335, and it was very conserved among *P. syringae* bacteria belonging to genomospecies 3 [64, 68]. In the promoter region upstream of the *matE* gene of *Psn23*, an *hrp* box sequence was found, suggesting its HrpL-dependent transcription.

In addition, several other features were identified, which could be considered to simultaneously regulate intracellular IAA levels and TTSS activation, and differentially regulate them during the course of bacterial infection. Here, for the first time, a sequence resembling the AuxRe of IAA-inducible plant promoters was identified in *P. savastanoi*, located at the 5' end of the *iaaM/iaaH* operon, as well as to that of the *iaaL* gene. To date, a similar prokaryotic auxin-responsive element has been reported and found to be active only in the plant growth-promoting rhizobacterium *A. brasilense*, in which the *ipdC* gene is activated by IAA, the end-product of this pathway, via a positive feedback regulation [48]. The AuxRe elements identified herein in *Psn23* are preceded by a conserved *hrp* box motif. This modular architecture resembles that of plant composite AuxREs, in which the TGTCTC element is not sufficient to confer auxin responsiveness to the promoters [69]. In composite AuxREs, the TGTCTC element requires a coupling element that is located close to or overlapping the TGTCTC motif, which confers constitutive expression of the promoter to which it belongs and is not responsive to auxin. Thus, the TGTCTC element acts as a repressor of the expression induced by the constitutive element when auxin levels are low. Conversely, this repression is released in response to high auxin levels, and the expression driven by the composite AuxREs is activated. Basically, we hypothesize that in *P. savastanoi*, IAA synthesis and conjugation are regulated by IAA. The DS element associated with the AuxRe of *iaaL*, but not with that of *iaaM/iaaH* operon, would allow differential IAA-inducible expression of these genes in *P. savastanoi*, as expected based on their function in IAA metabolism. In particular, at high IAA concentrations, the DS element of *iaaL* would guarantee its IAA inducibility by releasing the repression caused by TTSS through HrpL or other unknown TTSS-dependent transcription factors, as observed for the *ipdC* gene of *A. brasilense*. A similar scenario would explain the production of IAA by *P. savastanoi* after successful infection, which is essential to support the development of the hyperplastic knots in which the bacterium resides and thus avoid necrosis of the infected plant tissues. Accordingly, IAA-producing strains of *P. agglomerans*, which are sometimes associated with *P. savastanoi* in hyperplastic knots on olives, have been shown to determine an increase in the size of these knots unless their population is larger than that of *P. savastanoi* (1:100 ratio) at the beginning of the infection process [70]. The inactivation of TTSS expression and functionality after this system has served its purpose is a conserved phenomenon that occurs in other Gram-negative pathogens following successful infection of their hosts [71-73]. The putative MATE transporter encoded by *matE* would further contribute to this picture by mediating IAA efflux, as well as playing a likely role in drug resistance (Fig. 6). This hypothesis is further supported by the higher expression levels of *matE* in the three mutants examined herein in the presence of IAA, to simulate specific stages of the infection process when TTSS is downregulated or even switched off. The hypothetical MATE transporter is

encoded to mediate IAA efflux. Very recently, the MATE transporter Mte1 of the ectomycorrhizal fungus *Tricholoma vaccinum* was shown to export IAA during its compatible interaction with the host, positively regulating ectomycorrhiza formation and morphology [52]. Interestingly, some multidrug resistance-like genes of *Arabidopsis* have also been shown to transport IAA [14]. In *P. savastanoi*, the hypothetical MATE-mediated transport of IAA occurs at a reduced rate when TTSS is switched on by activation of its *hrp* box, and thus IAA levels are low, presumably during the initial steps of infection. Conversely, as the intracellular IAA levels increase, *matE* is further upregulated following transcriptional activation of the downstream gene *iaaL*, as occurs for genes that are part of the same operon. In fact, the pivotal importance of operons in the regulation of bacterial gene networks has been recently demonstrated in *E. coli*, in which the expression of a gene that is part of an operon increases with the length of the operon and according to its distance from the end of the operon during its transcription. By increasing the so called "transcription distance," there is more time for translation to occur during transcription, which will increase the expression of the genes in the operon proportionally to their transcription distances [74]. To confirm this scenario, in *P. syringae* pv. *tomato* DC3000, the *matE* and *iaaL* genes were demonstrated to be transcribed both dependently and independently [64].

To the best of our knowledge, PM technology was applied herein for the first time to *P. savastanoi*, and also used in the *P. syringae* group to assess the chemical sensitivity patterns. Until now, PM has been used to screen the protein-ligand interactions of *P. syringae* pv. *actinidiae* chemoreceptors [75], and a modified phenoarray approach was applied to analyse the apoplast-adapted nutrient assimilation pathways of *P. syringae* pv. *tomato* DC3000 [76]. Although it has not been definitely confirmed that 8-HQ efflux in *Psn23* is mediated directly by the transporter encoded by the *matE* gene, the PM technology approach used herein demonstrated that the impact caused by TTTS and IAA metabolism on the *P. savastanoi* fitness goes beyond its pathogenicity and virulence, and also involves drug and antimicrobial resistance. Moreover, it is reasonable to hypothesize that the same phenomenon also occurs in non-gall-forming phytopathogenic and plant-associated bacteria that are able to synthesize and conjugate IAA. Despite not being the main aim of this study, other relevant and encouraging data were also found that deserve future investigations, such as the higher sensitivity of the *ΔiaaM* mutant to oxytetracycline, and the higher resistance of the *ΔhrpA* mutant to hydroxylamine, sodium azide and polymixin B, in comparison to the wild-type *Psn23*. In conclusion, taken together, these findings provide information for the development of alternative strategies to control pathogenic bacteria through the use of natural products containing indole-based molecules [77].

## 5.6 References

[1] Santner A, Estelle M. Recent advances and emerging trends in plant hormone signaling. Nature 2009; 459:1071-78.
[2] Kieffer M, Neve J, Kepinski S. Defining auxin response contexts in plant development. Curr Opin Plant Biol 2010; 13:12-20.
[3] Ljung K. Auxin metabolism and homeostasis during plant development. Development 2013; 140:943-50.
[4] Normanly J, Cohen JD, Fink GR.*Arabidopsis thaliana* auxotrophs reveal a tryptophan-independent biosynthetic pathway for indole-3-acetic acid. Proc Natl Acad Sci USA1993; 90:10355-9.
[5] Wright AD, Sampson MB, Neuffer MG, Michalczuk L, Slovin JP, Cohen JD.Indole-3-acetic acid biosynthesis in the mutant maize orange pericarp, a tryptophan auxotroph. Science1991;254:998-1000.
[6] Wang B, Chu J, Yu T, Xu Q, Sun X, Yuan J, et al. Tryptophan-independent auxin biosynthesis contributes to early embryogenesis in *Arabidopsis.* Proc Natl Acad Sci USA 2015; 112:4821-26.
[7] Nonhebel HM. Tryptophan-independent indole-3-acetic acid synthesis: Critical evaluation of the evidence. Plant Physiol 2015; 169:1001-5.
[8] Ludwig-Müller J. Auxin conjugates: their role for plant development and in the evolution of land plant. J Exp Bot 2011; 62:1757-73.
[9] Woodward AW, Bartel B. Auxin: regulation, action, and interaction. Ann Bot 2005; 95:707-35.
[10] Dharmasiri N, Dharmasiri S, Weijers D, Lechner E, Yamada M, Hobbie L, et al. Plant development is regulated by a family of auxin receptor F box proteins. Dev Cell 2005; 9:109-19.
[11] Vande Broek A, Lambrecht M, Eggermont K, Vanderleyden J. Auxins upregulate expression of the indole-3-pyruvate decarboxylase gene in *Azospirillum brasilense*. J Bacteriol 1999; 181:1338-42.
[12] Hagen G, Guilfoyle T. Auxin-responsive gene expression: genes, promoters and regulatory factors. Plant Mol Biol 2002; 49:373-85.
[13] Zazímalová E, Krecek P, Skůpa P, Hoyerová K, Petrásek J. Polar transport of the plant hormone auxin – the role of PIN-FORMED (PIN) proteins. Cell Mol Life Sci. 2007; 64:1621-37.
[14] Noh B, Murphy AS, Spalding EP. Multidrug resistance-like genes of *Arabidopsis* required for auxin transport and auxin-mediated development. Plant Cell 2001; 13:2441-54.
[15] Ludwig-Müller J. Bacteria and fungi controlling plant growth by manipulating auxin: balance between development and defense. J Plant Physiol 2015; 172:4-12.
[16] Navarro L, Dunoyer P, Jay F, Arnold B, Dharmasiri N, Estelle M, Voinnet O, Jones JDG. A plant miRNA contributes to antibacterial resistance by repressing auxin signaling. Science 2006; 312:436-43.
[17] Chang X, Riemann M, Liu Q, Nick P. Actin as deathly switch? How auxin can suppress cell-death related defence. PloS One 2015; 10: e0125498.
[18] Spoel SH, Dong X. Making sense of hormone cross-talk during plant immune responses. Cell Host Microbe 2008; 3:348-51.
[19] Fu J, Wang S. Insights into auxin signaling in plant–pathogen interactions. Front Plant Sci 2011; 2:74.
[20] Glickmann E, Gardan L, Jacquet S, Hussain S, Elasri M, Petit A, et al. Auxin production is a common feature of most pathovars of *Pseudomonas syringae*. Mol Plant Microbe In 1998; 11:156-62.
[21] Surico G, Iacobellis NS, Sisto A. Studies on the role of indole-3-acetic acid and cytokinins in the formation of knots on olive and oleander plants by *Pseudomonas syringae* pv. *savastanoi*. Physiol Plant Pathol 1985; 26:309-20.
[22] Patten CL, Blakney AJ, Coulson TJ. Activity, distribution and function of indole-3-acetic acid biosynthetic pathways in bacteria. Crit Rev Microbiol 2013; 39: 395-415.

[23] González-Lamothe R, El Oirdi M, Brisson N, Bouarab K. The conjugated auxin indole-3-acetic acid-aspartic acid promotes plant disease development. Plant Cell 2012; 24:762-77.
[24] Cui F, Wu S, Sun W, Coaker G, Kunkel B, He P, et al. The *Pseudomonas syringae* type III effector AvrRpt2 promotes pathogen virulence via stimulating *Arabidopsis* auxin/indole acetic acid protein turnover. Plant Physiol 2013; 162:1018-29.
[25] Nomura K, Debroy S, Lee YH, Pumplin N, Jones J, He SY. A bacterial virulence protein suppresses host innate immunity to cause plant disease. Science 2006; 313:220-3.
[26] Zhao Y. Auxin biosynthesis and its role on plant development. Annu Rev Plant Biol 2010;61:49-64.
[27] Barash I, Manulis-Sasson S. Virulence mechanisms and host specificity of gall-forming *Pantoea agglomerans*. Trends Microbiol 2007; 15:538-45.
[28] Sisto A, Cipriani MG, Morea M. Knot formation caused by *Pseudomonas syringae* subsp. *savastanoi* on olive plants is Hrp-dependent. Phytopatol 2004, 94:484-9.
[29] Aragon I, Perez-Martinez I, Moreno-Perez A, Cerezo M, Ramos C. New insights into the role of indole-3-acetic acid in the virulence of *Pseudomonas savastanoi* pv. *savastanoi*. FEMS Microbiol Lett 2014; 356:184-92.
[30] Glass NL, Kosuge T. Cloning of the gene for indoleacetic acid-lysine synthetase from *Pseudomonas syringae* subsp. *savastanoi*. J Bacteriol 1986; 166:598-603.
[31] Tiryaki, I, Staswick PE. An Arabidopsis mutant defective in jasmonate response is allelic to the auxin-signaling mutant axr1. Plant Physiol 2002; 130:887-94.
[32] King EO, Ward MK, Raney DE. Two simple media for the determination of pyocianine and fluorescein. J Lab Clin Med 1954; 44:301-7.
[33] Huynh TV, Dahlbeck D, Staskawicz BJ. Bacterial blight of soybean: Regulation of a pathogen gene determining host cultivar specificity. Science 1989; 245:1374-7.
[34] Miller H. Experiments in molecular genetics. Cold Spring Harbor Laboratory, Cold Spring Harbor, N.Y.1972
[35] Sisto A, Cipriani M, Tegli S, Cerboneschi M, Stea G, Santilli E. Genetic characterization by fluorescent AFLP of *Pseudomonas savastanoi* pv. *savastanoi* strains isolated from different host species. Plant Pathol 2007; 56:366-72.
[36] Tegli S, Cerboneschi M, Marsili Libelli I, Santilli E. Development of a versatile tool for the simultaneous differential detection of *Pseudomonas savastanoi* pathovars by End Point and Real-Time PCR. BMC Microbiology 2010; 10:156.
[37] Sambrook J, Fritsch EF, Maniatis TA. Molecular Cloning: A Laboratory Manual, 2nd ed.; Cold Spring Harbor Laboratory Press: New York, NY, USA, 1989.
[38] Thompson JD, Higgins DG, Gibson TJ, CLUSTALW: Improving the sensitivity of progressive multiple sequence alignment through sequence weighting, position-specific gap penalties and weight matrix choice. Nucleic Acids Res 1994; 22: 4673-80.
[39] Altschul SF, Gish W, Miller W, Myers EW, Lipman DJ. Basic local alignment search tool. J Mol Biol 1990; 215:403-10.
[40] Yang CH, Gavilanes-Ruiz M, Okinaka Y, Vedel R, Berthuy I, Boccara M, et al. hrp genes of *Erwinia chrysanthemi* 3937 are important virulence factors. Mol Plant Microbe In 2002; 15:472–80.
[41] Pérez-Martínez I, Rodríguez-Moreno L, Lambertsen L, Matas MI, Murillo J, Tegli S, et al. Fate of a *Pseudomonas savastanoi* pv. *savastanoi* type III secretion system mutant in olive plants (*Olea europaea* L.). App Environ Microbiol 2010; 76:3611-19.
[42] Ehmann A. The Van Urk-Salkowski reagent - A sensitive and specific chromogenic reagent for silica gel thin-layer chromatographic detection and identification of indole derivatives. J Chromatogr 1977; 132:267-76.

[43] Qin G, Gu H, Zhao Y, Ma Z, Shi G, Yang Y, et al. An indole-3-acetic acid carboxyl methyltransferase regulates *Arabidopsis* leaf development. The Plant Cell 2005; 17:2693-704.
[44] Murashige T, SKOOG F. A revised medium for rapid growth and bioassays with tobacco tissue cultures. Physiol Plant 1962; 15:473–97.
[45] Gori A, Cerboneschi M, Tegli S. High-resolution melting analysis as a powerful tool to discriminate and genotype *Pseudomonas savastanoi* pathovars and strains. PlosOne 2012; 7: e30199.
[46] Baker CJ, Atkinson MM, Collmer A. Concurrent loss in Tn5 mutants of *Pseudomonas syringae* pv. *syringae* of the ability to induce the hypersensitive response and host plasma membrane $K+/H^+$ exchange in tobacco. Phytopathol 1987; 77:1268-72.
[47] Bochner BR, Gadzinski P, Panomitros E. Phenotype Microarrays for high-throughput phenotypic testing and assay of gene function. Genome Res 2001; 11:1246-55.
[48] Lambrecht M, Vande Broek A, Dosselaere F, Vanderleyden J. The *ipdC* promoter auxin-responsive element of *Azospirillum brasilense*, a prokaryotic ancestral form of the plant AuxRE? Mol Microbiol 1999; 32: 889–91.
[49] Pandey R, Swamy KV, Khetmalas MB. Indole: A novel signaling molecule and its applications. Indian J Biotechnol 2013; 12:297-310.
[50] Spaepen S, Vanderleyden J. Auxin and plant-microbe interactions. Cold Spring Harb Perspect Biol 2011; 3:a001438.
[51] Mills LJ, Van Staden J. Extraction of cytokinins from maize, smut tumors of maize and Ustilago maydis cultures. Physiol Plant Pathol 1978; 13:73-80.
[52] Krause K, Henke C, Asiimwe T, Ulbricht A, Klemmer S, Schachtschabel S, et al. Biosynthesis and secretion of indole-3-acetic acid and its morphological effects on *Tricholoma vaccinum*-spruce ectomycorrhiza. Appl Environ Microbiol 2015; 81:7003-11.
[53] Maor R, Haskin S, Levi-Kedmi H, Sharon A. In planta production of indole-3-acetic acid by *Colletotrichum gloeosporioides* f. sp. *Aeschynomene*. Appl Environ Microbiol 2004; 70:1852-4.
[54] Tsavkelova E, Oeser B, Oren-Young L, Israeli M, Sasson Y, Tudzynski B, et al. Identification and functional characterization of indole-3-acetamide-mediated IAA biosynthesis in plant-associated *Fusarium* species. Fungal Genet Biol 2012; 49:48-57.
[55] Bommarius B, Anyanful A, Izrayelit Y, Bhatt S, Cartwright E, Wang W, et al. A family of indoles regulate virulence and Shiga toxin production in pathogenic *E. coli*. PLoS One 2013; 8:e54456.
[56] Lee J, Bansal T, Jayaraman A, Bentley WE, Wood TK. Enterohemorrhagic *Escherichia coli* biofilms are inhibited by 7-hydroxyindole and stimulated by isatin. Appl Environ Microbiol 2007; 73:4100-109.
[57] Yang S, Zhang Q, Guo J, Charkowski AO, Glick BR, Ibekwe AM, et al. Global effect of indole-3-acetic acid biosynthesis on multiple virulence factors of *Erwinia chrysanthemi* 3937. Appl Environ Microbiol 2007; 73:1079-88.
[58] Liu P, Nester EW. Indoleacetic acid, a product of transferred DNA, inhibits *vir* gene expression and growth of *Agrobacterium tumefaciens* C58. Proc Natl Acad Sci USA 2006; 103:4658-62.
[59] Yuan ZC, Liu P, Saenkham P, Kerr K, Nester EW. Transcriptome profiling and functional analysis of *Agrobacterium tumefaciens* reveals a general conserved response to acidic conditions (pH 5.5) and a complex acid-mediated signaling involved in *Agrobacterium*-plant interactions. J Bacteriol 2008; 190:494-507.
[60] Malhotra M, Srivastava S. Organization of the *ipdC* region regulates IAA levels in different *Azospirillum brasilense* strains: molecular and functional analysis of *ipdC* in strain SM. Environ Microbiol 2008; 10:1365-73.
[61] Prusty R, Grisafi P, Fink GR. The plant hormone indoleacetic acid induces invasive growth in *Saccharomyces cerevisiae*. Proc Natl Acad Sci USA 2004; 101:4153-7.

[62] Bianco C, Imperlini E, Calogero R, Senatore B, Amoresano A, Carpentieri A, et al. Indole-3-acetic acid improves *Escherichia coli*'s defences to stress. Arch Microbiol 2006; 185:373-82.
[63] Lee HH, Molla MN, Cantor CR, Collins JJ. Bacterial charity work leads to population-wide resistance. Nature 2010; 467:82-5.
[64] Castillo-Lizardo MG, Aragón IM, Carvajal V, Matas IM, Pérez-Bueno ML, Gallegos MT, et al. Contribution of the non-effector members of the HrpL regulon, *iaaL* and *matE*, to the virulence of *Pseudomonas syringae* pv. *tomato* DC3000 in tomato plants. BMC Microbiol 2015; 15:165.
[65] Lam HN, Chakravarthy S, Wei HL, BuiNguyen HC. Stodghill PV, Collmer A, et al. Global Analysis of the HrpL regulon in the plant pathogen *Pseudomonas syringae* pv. *tomato* DC3000 reveals new regulon members with diverse functions. PLoS ONE 2014; 9:e106115.
[66] Fraser RS, Creanor J. The mechanism of inhibition of ribonucleic acid synthesis by 8-hydroxyquinoline and the antibiotic lomofungin. Biochem J 1975; 147:401-10.
[67] Prachayasittikul V, Prachayasittikul S, Ruchirawat S, Prachayasittikul V. 8-Hydroxyquinolines: a review of their metal chelating properties and medicinal applications. Drug Design, Development and Therapy. 2013; 7:1157-1178.
[68] Rodríguez-Palenzuela P, Matas IM, Murillo J, López-Solanilla E, Bardaji L, Pérez-Martínez I, et al. Annotation and overview of the *Pseudomonas savastanoi* pv. *savastanoi* NCPPB 3335 draft genome reveals the virulence gene complement of a tumour-inducing pathogen of woody hosts. Environ Microbiol 2010; 12:1604-20.
[69] Ulmasov T, Murfett J, Hagen G, Guilfoyle TJ. Aux/IAA proteins repress expression of reporter genes containing natural and highly active synthetic auxin response elements. Plant Cell 1997; 9:1963-71.
[70] Marchi G, Sisto A, Cimmino A, Andolfi A, Cipriani MG, Evidente A, et al. Interaction between *Pseudomonas savastanoi* pv. *savastanoi* and *Pantoea agglomerans* in olive knots. Plant Pathol 2006; 55:614-24.
[71] Lucchini S, Liu H, Jin Q, Hinton JC, Yu J. Transcriptional adaptation of *Shigella flexneri* during infection of macrophages and epithelial cells: insights into the strategies of a cytosolic bacterial pathogen. Infect Immun 2005; 73:88-102.
[72] Dahan S, Knutton S, Shaw RK, Crepin VF, Dougan G, Frankel G. Transcriptome of enterohemorrhagic *Escherichia coli* O157 adhering to eukaryotic plasma membranes. Infect Immun 2004; 72:5452-59.
[73] Shen DK, Filopon D, Chaker H, Boullanger S, Derouazi M, Polack B, Toussaint B. High-cell-density regulation of the *Pseudomonas aeruginosa* type III secretion system: implications for tryptophan catabolites. Microbiology 2008; 154:2195-208.
[74] Lim HN, Lee Y, Hussein R. Fundamental relationship between operon organization and gene expression. Proc Natl Acad Sci USA. 2011; 108:10626-31.
[75] McKellar JLO, Minnell JJ, Gerth ML. A high-throughput screen for ligand binding reveals the specificities of three amino acid chemoreceptors from *Pseudomonas syringae* pv. *actinidiae*. Mol Microbiol 2015; 96:694-707.
[76] Rico A, Preston GM. *Pseudomonas syringae* pv. *tomato* DC3000 uses constitutive and apoplast-induced nutrient assimilation pathways to catabolize nutrients that are abundant in the tomato apoplast. Mol Plant Microbe In 2008; 21:269–82.
[77] Melander RJ, Minvielle MJ, Melander C. Controlling bacterial behavior with indole-containing natural products and derivatives. Tetrahedron 2014; 70:6363-72.

## 5.7 Supporting Information

**Fig. S1. Fluorescence chromatograms (HPLC-DAD/FD) at 340 nm ($\lambda_{ex}$=280 nm) obtained from lyophilised supernatants after 48 h of bacterial growth in MM supplemented with 250 µM of L-tryptophan. The retention times specify specific molecules: L-tryptophan (2.68), indole-3-acetic acid or IAA free (12.70) and putative IAA-Lysine (3.28).**

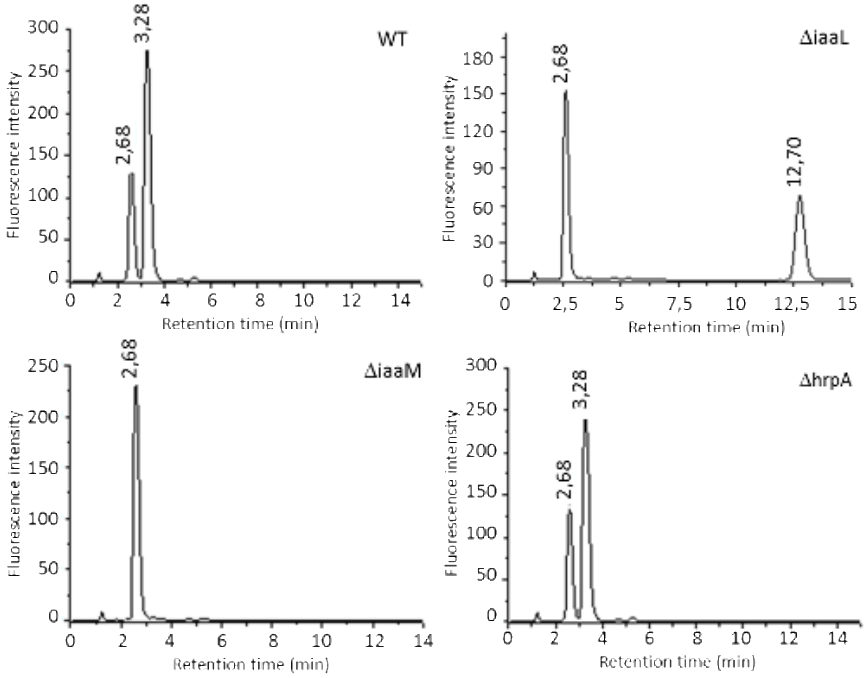


**Fig. S2. Mass spectra acquired during positive ionization of putative IAA-lysine. (A) Mass spectrum of IAA-Lys with the fragmentor potential set at 100 V. (B) Target MS/MS spectrum of m/z 304 of the IAA-Lys mass spectrum with the fragmentor potential set at 100 V and the collision energy at 50 V.**

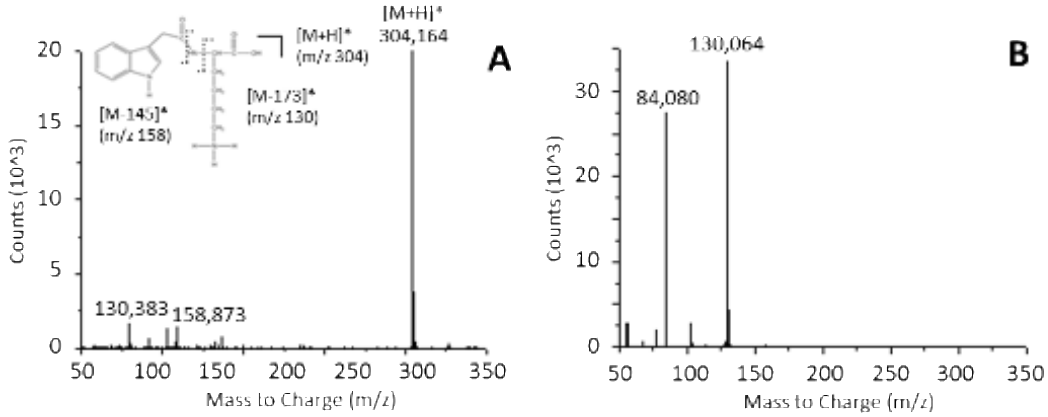

# *Chapter 6*

# Concluding discussion

According to the latest European regulations is now required in all European Union Member countries a drastic reduction in the use of the copper in plant protection against biotic diseases in traditional agriculture, integrated and organic, as part of a broader review process about pesticides and their residues, started with Directive 91/414 / EEC. In fact, copper tends to accumulate in the environment, in particular into the soil, where it is not degraded, and where can contaminate both surface and deep water, causing serious eco-environmental risks and episodes of acute and chronic toxicity towards a wide spectrum of organisms and microorganisms. Recent studies have estimated the consequences of continuous applications of copper salts in the last two hundred years: in agrosystems the concentration of copper in the soil varies between 100 to 1,280 mg / kg soil, against values of 5-20 mg / kg of soil in areas not contaminated by agricultural activities (Mackie *et al*., 2012). Currently, the amount of copper allowed in organic farming is of 6 kg / ha (Regulation (EC) No 889/2008) which should correspond to an accumulation per year of about 5 mg of copper / kg soil in its first 10 cm. Unfortunately, these data are purely theoretical, since it is strongly dependent on many factors, such as the soil composition and its pH. Moreover, in this scenario, the European Union has imposed limits of copper residues on vegetables and fruits (Directive (EC) No 37/2009; Regulation (CE) No 396/2005).

Finally and most importantly, the use of copper salts in agriculture, as fungicides and bactericides, determines in agrosystems an increase of antibiotic-resistant bacteria. In fact, the spread of antibiotic resistance bacteria in environment is also triggered and/or favored by several anthropogenic pollutants, which promote a co-selection process that indirectly selects also for the resistance to antibiotics (Seiler and Berendonk, 2012). Moreover, this phenomenon is dramatically increasing, because the periodic application of copper-based bactericides on crops to control bacterial diseases increases the selection pressure for the development of epiphytic bacterial populations resistant to copper and streptomycin, elevating the risks for transferring of these resistance genes within the plant pathogenic bacterial population and also to other bacteria belonging to the resident microflora. Over the last years, phytopathogenic strains that are resistant to copper treatments have been detected worldwide and are threatening the efficacy of this strategy.

In this context, the limited availability of environmentally-friendly, effective and specific molecules is even more serious considering that climate changes are expanding the distributional areal of some plant pathogenic bacteria even aliens for European Union or exacerbating the incidence and severity of endemic pathogens.

For example, it is worth mentioning the recent spread of two phytopathogenic bacteria *Pseudomonas syringae* pv. *actinidiae* and *Xylella fastidiosa*, responsible for huge economic losses in the Italian country.

The first is the causal agent of bacterial canker of kiwifruit, recently introduced into EPPO (European and Mediterranean Plant Protection Organization) Alert list, due to its massive

spread in the Mediterranean basin and in view of the economic importance of kiwifruit production in Italy. The second is a bacterial pathogen to Olive trees, considered by quarantine for all Europe, which threatens to jeopardize the whole Italian olive sector, as happened in the last two - three years, notably in Apulia, where it has spread with devastating economic and landscape effects.

Unfortunately, to date, there are no effective plant protection products and often the only solution is the eradication of affected plants to contain the spread of the pathogen. This situation makes us think about the urgency to generate innovation in the phytoiatric sector with identification of potential bacterial targets against which to direct alternative molecules with low environmental impact in order to drastically reduce or replace the use of copper. Many different strategies (*e.g.* health seed, antagonistic microorganisms, soil solarization) have been introduced to fight this phenomenon and to gradually decrease the use of chemicals towards a sustainable agriculture.

In this frame, wide space has been given to the development of several defense strategies, including the production of natural AMPs (Zasloff, 2002). The advantage of using antimicrobial peptides as antibacterial agents is that bacteria are less likely to become resistant to these compounds in comparison to antibiotics. However, the peptide availability is one of the major factors that determine the feasibility of their widespread usage as antibiotics and a number of fundamental issues such as mechanisms, efficacy and safety must be addressed. In fact, these new molecules should act against pathogenic and virulence bacterial systems rather than on their viability, in order to reduce the risk of developing resistances as in case of copper and antibiotics.

Among the few examples of currently available targets, it is certainly to worth mentioning the Type Three Secretion System and Quorum Sensing (Yang *et al*., 2014; LaSarre *et al*., 2013). In addition to these targets, scientific evidences indicate as multi drug efflux pumps are relevant elements that contribute both intrinsic and acquired resistance to toxic compounds in several life forms including humans. In fact, in human and animal medicine otherwise in plant protection the potential as ideal targets of proteic membrane pumps for xenobiotic compounds efflux has been explored (Nikaido *et al*., 2008; Poole, 2000). In recent time, it is emerging that microbial efflux pump inhibitors could be other important and theoretically promising therapeutic agents as well, because they would be able to reduce the ability of the bacterial cells to extrude many toxic compounds.

Among these membrane proteins, divided into different classes according to their structure and physiology, the so-called Multidrug and Toxic compound Extrusion (MATE) need to be mentioned, because the putative MATE proteins appeared to be coded in the genomes of all life kingdoms. A gene coding for a putative MATE was recently found in the genomes of the phytopathogenic bacteria such as *P. syringae* pv. *tomato* DC3000 and *P. savastanoi* pv. *savastanoi* (Vargas *et al*., 2011; Castillo-Lizardo *et al*, 2015) and studied and discovered in *P. savastanoi* pv. *nerii* as well (Chapter 5). This protein should be further investigated and evaluated as a new potential target for development of innovative anti-infective inhibitors making bacterial more sensitive to a range of xenobiotic compounds, and thus to be used in the "green" plant pathogens control.

Furthermore, against the canonical targets previously mentioned, the effect and efficacy of alternative molecules such as small peptides (Chapter 2) and polyphenols extracts obtained in a circular economy framework (Chapter 4) have been analysed with very promising results. These molecules do not show neither antibiotic activity nor toxic effect on conserved cellular structures. The production of transgenic plant expressing these peptides, although not marketable in Italy as all GMOs (Genetically Modified Organism), has rapresented not only a perfect tool to assess the VIPs efficacy but also a product that could attract the interest of foreign markets (Chapter 3).

In this work, we have tryed to design and develop peptides, indicated as VIPs, able to overcome some limitations and drawbacks found in the best-known AMPs. Moreover, in view of their possibile applicability in plant protection, their biotechnological synthesis instead chemical one could considerably decrease the cost production and confer a further ecofriendly value.

As far as polyphenol extracts are concerned, these are secondary metabolites present in all plant species and distributed, according to their role, in various plant tissues. Based on their chemical structure these compounds are divided into numerous subclasses with specific functions and localization. In general, polyphenols constitute a support and a barrier against microbial invasion (*e.g.* microorganisms, insects and other animals) and mediate plant response to climate and environmental stress situations. Polyphenols show anti-microbial, antioxidants, anti-inflammatory properties and for these reasons they are exploited in different sector (*e.g* agronomy, animal feed, cosmetics, foods and biomedical), both in traditional and innovative and multifunctional products, in which the synthetic chemical components are partially or totally replaced by natural molecules. Some polyphenols extracts tested in this thesis, for example, are commercilised for cosmetic and nutraceutical purposes.

It is reasonable and desirable to think that these innovative and alternative molecules here analysed and developed might be applied in industrial sector in the foreseeable future. Nevertheless, it is worth to remember that the time this process needs to be completed would necessarily depend on the procedures to be applied, in the frame of the European regulation for the approval of new plant protection products (PPPs) (Regulation EC 1107/2009, repealing Council Directives 79/117/EEC and 91/414/EEC). This Regulation entered into force at the end of 2009, and it became applicable to be used in all EU Member States from June 2011. Basically, to achieve an approval to place a PPP on the EU market, a dossier has to be presented with the basic laboratory, safety and in use data. Field trials have to be carried out in at least two defined geographic zones (in the Country where the first application for approval will be presented and in those Countries where this PPP could be registered in the future). Concerning field trials, there are two main types that have to be performed, residue trials and efficacy trials, whose guidelines are defined by several official EU and international agencies (*e.g.*EPPO), and by EU specific regulations (*e.g* Commission of the European Communities, Directorate General for Agriculture, 7029/VI/95 rev.5, VI BII-1 Appendix B, Genral Recommendations for the Design, Preparation and Realization of Residue Trials).

In conclusion, the results obtained and reported in this PhD thesis demonstrate the potential and effective use of both Virulence Inhibiting Peptides targeting the coiled coil motif of the HrpA protein and the standardized polyphenolic extracts from *O. europaea*, *C. scolymus*

leaves, *V. vinifera* seeds and *C. sinensis* leaves in plant protection. These innovative molecules are able to inhibit specifically the TTSS of bacteria belonging to *P. syringae* complex preventing the pilus assembly and to disarm the pathogenicity and virulence of such bacteria without undermine their viability. Their specific activity against systems not related to bacterial viability and conserved among Gram-negative pathogens, not only of plants but also of humans and animals, suggests that a poor or absent selective pressure may develop in the bacterial population, thus providing a longer efficacy.

## 6.1 References

**Seiler C** and Berendonk TU. (2012) Heavy metal driven co-selection of antibiotic resistance in soil and water bodies impacted by agriculture and aquaculture. *Frontiers in Microbiology*. 2012;3:399. doi:10.3389/fmicb.2012.00399

**Zasloff M**. (2002) Antimicrobial peptides of multicellular organisms. *Nature*. 2002 Jan 24; 415(6870):389-95

**Yang F**, Korban SS, Pusey PL, Elofsson M, Sundin GW, Zhao Y. (2014) Small-molecule inhibitors suppress the expression of both type III secretion and amylovoran biosynthesis genes in *Erwinia amylovora*. *Mol Plant Pathol*. 2014; 15: 44-57

**LaSarre B**, Michael A, Federle J. (2013) Exploiting Quorum Sensing To Confuse Bacterial Pathogens. *Microbiology and Molecular Biology Reviews* 77(1): 73–111

**Nikaido E**, Yamaguchi A, Nishino K.(2008) AcrAB Multidrug Efflux Pump Regulation in *Salmonella enterica* serovar Typhimurium by RamA in Response to Environmental Signals. *J Biol Chem*. 283(35): 24245–24253

**Poole K**. (2000) Efflux-Mediated Resistance to Fluoroquinolones in Gram-Positive Bacteria and the Mycobacteria. *Antimicrob. Agents Chemother*. 44 (10):2595-2599

**Vargas P**, Felipe A, Michan C, Gallegos MT. (2011) Induction of Pseudomonas *syringae pv tomato* DC3000 MexAB-OprM multidrug efflux pump by flavonoids is mediated by the repressor PmeR. *Mol Plant Microbe Interact*. 24(10):1207–19

**Castillo-Lizardo MG**, Aragón IM, Carvajal V, Matas IM, Pérez-Bueno ML, Gallegos MT, Barón M, Ramos C. (2015) Contribution of the non-effector members of the HrpL regulon, *iaaL* and *matE*, to the virulence of *Pseudomonas syringae pv. tomato* DC3000 in tomato plants. *BMC Microbiology* 15:165.

**Directive 2009/37/EC** of 23 April 2009 amending Council Directive 91/414/ EEC to include chlormequat, copper compounds, propaquizafop, quizalofop-P, teflubenzuron and zeta-cypermethrin as active substances.

**Directive 2009/128/EC** of the European Parliament and of the Council of 21 October 2009 establishing a framework for Community action to achieve the sustainable use of pesticides.

**Commission Regulation (EC) N. 889/2008** of 5 September 2008 laying down detailed rules for the implementation of Council Regulation (EC) N. 834/2007 on organic production and labelling of organic products with regard to organic production, labelling and control.

**Regulation (EC) N.1107/2009** of the European Parliament and of the Council of 21 October 2009 concerning the placing of plant protection on the market and repealing Council Directives 79/ 117/EEC and 91/414/ EEC.

**Council Directive 91/414/EEC** of 15 July 1991 concerning the placing of plant protection products on the market.

**Commission Regulation (EU) N. 284/2013** of 1 March 2013 setting out the data requirements for plant protection products, in accordance with Regulation (EC) N. 1107/2009 of the European Parliament and of Council concerning the placing of plant protection products on the market.